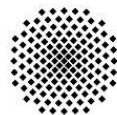




IPREM

Institut des sciences analytiques
et de physico-chimie
pour l'environnement et les matériaux



University of Stuttgart

Institute of
Interfacial Process Engineering
and Plasma Technology

eurecat
Centre Tecnològic de Catalunya



UNIVERSITÉ
DE PAU ET DES
PAYS DE L'ADOUR



escaled

European School on Artificial Leaf: Electrodes and Devices



icvt
Institut für
Chemische
Verfahrenstechnik

In fulfilment of the requirements for the degree of Doctor of Sciences from the

Université de Pau et des Pays de l'Adour

&

Dissertation for the degree of Dr.-Ing. Approved by the

Faculty 4 - Energy-, Process- and Bio-Engineering, University of Stuttgart

**Proton-conducting (blend) membranes based on
sulfonated / phosphonated and basic polymers**

Thesis defended on 14.03.2023 by

Ignasi de Azpiazu Nadal

From Barcelona

Under the supervision of Prof. Günter Tovar, Dr. Stéphanie Reynaud & Dr. Vladimir Atanasov

And a Jury presided by Prof. Dr.-Ing. Ulrich Niekem and Prof. Laurent Billon

Published **2024**



*This Project has received funding from
the European Union's Horizon 2020
research and innovation programme
under grant agreement No. 765376*



Declaration of Authenticity

I herewith declare that I wrote this thesis on my own and did not use any unnamed sources or aid. Thus, to the best of my knowledge and belief, this thesis contains no material previously published or written by another person except where due reference is made by correct citation. This includes any thoughts taken over directly or indirectly from printed books and articles as well as all kinds of online material. It also includes my own translations from sources in a different language.

The work contained in this thesis has not been previously submitted for examination.

Eigenständigkeitserklärung

Hiermit bestätige ich, dass ich die vorliegende Arbeit selbständig verfasst und keine anderen als die angegebenen Hilfsmittel benutzt habe. Die Stellen der Arbeit, die dem Wortlaut oder dem Sinn nach anderen Werken (dazu zählen auch Internetquellen) entnommen sind, wurden unter Angabe der Quelle kenntlich gemacht.

06/10/2022



Abstract

Aiming at new proton-conducting membranes, this thesis deals with the syntheses and characterizations of highly sulfonated poly(arylene sulfides) and other polysulfides for application as polymer electrolytes. The study focuses mainly on the analysis of the polymer structures that would improve the conductivity of current proton conducting membranes while maintaining their mechanical stability.

In a first step, several polymers are obtained from which poly(arylene sulfide)s polymers look more promising for further functionalization. They are obtained by using mild reaction conditions of a polycondensation reaction between 4,4'-thiobisbenzenethiol (TBBT) and decafluorobiphenyl. Optimization of this reaction allows for the obtainment of higher molecular weights than the ones reported in the literature.

In a second step, poly(arylene sulfides) were phosphonated and sulfonated by a nucleophilic aromatic substitution (S_NAr) displacement reaction of the fluorine atoms of the fluorinated polymer sub-units using different agents. Highly sulfonated polymers were obtained when using sodium 3-mercapto-1-propanesulfonate and resulted in water soluble ionomers. Kinetic studies of this reaction were performed and several new sulfonated poly(arylene sulfides) were obtained.

Finally, stable polymer electrolyte membrane (PEM) with enhanced mechanical and chemical stability were obtained by blending these obtained ionomers with polybenzimidazole (PBI/OO). These membranes were further characterized and in the best case a PEM with new sulfonated ionomer showed a conductivity 40 % higher than Nafion 212, used as a golden reference material.

The best performing PEM's obtained were further used in an electrolytic cell being part of eSCALED, a H2020 (MSC-ITN-2017. GA# 765376) European project which aim is to obtain a device that does the artificial photosynthesis in a more efficient way than the current devices.



project ID 765376 — eSCALED — H2020-MSCA-ITN-2017



Keywords: proton-conducting membranes, decafluorobiphenyl, 4,4'-thiobisbenzenethiol, highly sulfonated poly(arylene sulfides), sulfonation, blend polymers, polymer electrolyte membrane (PEM), polybenzimidazole.



Résumé

Visant une nouvelle membrane conductrice de protons, cette thèse rapporte les synthèses et les caractérisations de poly(sulfures d'arylène) hautement sulfonés et d'autres polysulfures pour une application comme électrolytes polymères. L'étude se concentre principalement sur l'analyse des architectures macromoléculaires qui amélioreraient la conductivité des membranes conductrices de protons actuelles tout en maintenant leur intégrité mécanique.

Dans un premier temps, les poly(sulfures d'arylène) semblent les plus prometteurs pour une fonctionnalisation ultérieure. Ils sont obtenus en utilisant les conditions de réaction douces d'une polycondensation entre le 4,4'-thiobisbenzenethiol (TBBT) et le décafluorobiphényle. Plusieurs études visant à optimiser cette réaction permettent d'obtenir des masses molaires plus élevées que celles actuellement observées dans la littérature.

Dans une deuxième étape, les poly(sulfures d'arylène) ont été phosphonés et sulfonés par substitution nucléophile aromatique (S_NAr) des atomes de fluor des unités fluorées en utilisant différents agents. Des polymères hautement sulfonés ont été obtenus en utilisant le 3-mercaptopropanesulfonate de sodium et ont conduit des ionomères solubles dans l'eau. Des études cinétiques de cette réaction ont été réalisées et plusieurs nouveaux poly(sulfures d'arylène) sulfonés ont été obtenus.

Enfin, des membranes électrolytiques polymères (PEM) stables avec une stabilité mécanique et chimique améliorée ont été obtenues en mélangeant ces ionomères obtenus avec du polybenzimidazole (PBI-OO). Ces membranes ont été caractérisées et dans le meilleur cas, une PEM avec un nouvel ionomère sulfoné a montré une conductivité 40 % plus élevée que celle Nafion 212, utilisé comme matériau de référence.

Les meilleures PEMs obtenues ont été utilisées dans une cellule électrolytique faisant partie du projet européen eSCALED (H2020-MSCA-ITN-2017 N765376) dont le but est d'obtenir un dispositif qui réalise la photosynthèse artificielle d'une manière plus efficace que les dispositifs actuels.



Mots clés : membranes conductrices de protons, décafluorobiphényle, 4,4'-thiobisbenzèthiol, poly(sulfures d'arylène) hautement sulfonés, sulfonation, polymères mixtes, membrane électrolytique polymère, polybenzimidazole.



Kurzzusammenfassung

Mit dem Ziel, Grundlagen für eine neue protonenleitende Membran zu erforschen, berichtet diese Arbeit über die Synthese und Charakterisierung von hochsulfonierten Poly(arylsulfiden) und anderen Polysulfiden für die Anwendung als Polymerelektrolyte. Die Studie konzentriert sich hauptsächlich auf die Analyse der Polymerstrukturen, die die Leitfähigkeit der derzeitigen protonenleitenden Membranen verbessern und gleichzeitig ihre mechanische Stabilität aufrechterhalten sollen.

In einem ersten Schritt werden mehrere Polymere dargestellt, von denen insbesondere Poly(arylsulfide) für eine weitere Funktionalisierung vielversprechend erscheinen. Sie wurden unter milden Reaktionsbedingungen durch eine Polykondensationsreaktion zwischen 4,4'-Thiobisbenzol (TBBT) und Decafluorbiphenyl gewonnen. Mehrere Studien zur Optimierung dieser Reaktion haben gezeigt, dass höhere Molekulargewichte als die derzeit in der Literatur beobachteten erzielt werden können.

In einem zweiten Schritt wurden Poly(arylsulfide) durch eine nukleophile aromatische Substitution (S_NAr), Verdrängungsreaktion der Fluoratome der fluorierten Polymereinheiten mit verschiedenen Mitteln phosphoniert und sulfoniert. Bei Verwendung von Natrium-3mercapto-1-propansulfonat wurden hochsulfonierte Polymere erhalten, die zu wasserlöslichen Ionomeren führten. Es wurden kinetische Studien zu dieser Reaktion durchgeführt und mehrere neue sulfonierte Poly(arylsulfide) erhalten.

Schließlich wurden stabile Polymerelektrolytmembranen (PEM) mit verbesserter mechanischer und chemischer Stabilität durch Mischen dieser Ionomere mit Polybenzimidazol (PBI-OO) hergestellt. Diese Membranen wurden weiter charakterisiert, und im besten Fall zeigte eine PEM mit dem neuen sulfonierten Ionomer eine 40 % höhere Leitfähigkeit als das als Referenzmaterial verwendete Nafion.



Die leistungsfähigsten PEM-Membranen wurden in einer elektrolytischen Zelle verwendet, die Teil eines größeren Projekts namens eSCALED ist, dessen Ziel es ist, ein Gerät zu entwickeln, das die künstliche Photosynthese effizienter durchführt als die derzeitigen Geräte.

Schlüsselwörter: protonenleitende Membranen, Dekafuorbiphenyl, 4,4'-Thiobisbenzol, hochsulfonierte Poly(arylsulfide), Sulfonierung, Mischpolymere, Polymerelektrolytmembran, Polybenzimidazol.



project ID 765376 — eSCALED — H2020-MSCA-ITN-2017





General table of Contents

Abstract	2
Résumé	4
Kurzzusammenfassung	6
Acknowledgements	17
Annexes: Lists of figures, tables, and abbreviations	18
Lists of figures	18
Lists of tables and equations	25
List of abbreviations	27
General Introduction	32

Chapter I: Introduction to Proton Exchange Membranes

I. Introduction	36
1. General presentation of the energy issues	36
2. Water electrolysis and Fuel Cell background introduction	42
3. Fuel cells and electrolysers classification and PEM economics and commercial applications.....	46
4. Proton Transport Mechanisms	53
5. Sulphonated and phosphonated polymers	56
II. Project PEM's objective	59
III. Chapter description.....	60
IV. References	61

Chapter II: Synthesis of Polyfluorothioethers

I. Introduction	71
-----------------------	----



1.	Polymer definition and different polymerization reactions	71
2.	Proton-exchange membrane (PEM)	75
3.	Project strategy.....	76
II.	Materials and methods	81
1.	Chemicals and materials	81
2.	Experimental	82
	a) Polycondensation of decafluorobiphenyl and 4,4'-thiobisbenzenethiol.....	82
	(i) Polycondensation by conventional heating method	82
	(ii) Polycondensation by microwave method	83
	b) Polymerization of decafluorobiphenyl and 4,4'-bis(trimethylsilyl)thiobenzene	84
	c) Polymerization of decafluorobiphenyl and Biphenyl-4,4'-dithiol	85
	d) Polymerization of decafluorobiphenyl and hexane-1,6-dithiol	85
	e) Polymerization of phosphonated octafluorobiphenyl and 4,4'-thiobisbenzenethiol.....	86
	(i) Phosphonation of Decafluorobiphenyl monomer.....	86
	(ii) Polycondensation of 4,4'-thiobisbenzenethiol and phosphonated octafluorobiphenyl.....	87
	f) Polymerization of disodium 3,3'-disulfonate-4,4'-difluorodiphenylsulfone and 4,4'- thiobisbenzenethiol	87
3.	Technics	88
	a) Microwave reactor.....	88
	b) IR spectroscopy	88
	c) NMR spectroscopy	89
	d) Size Exclusion Chromatography (SEC)	89
	e) Thermal analysis	89
	f) Elemental Analysis	89



III. Results and discussion	90
1. Polycondensation of decafluorobiphenyl and TBBT.....	90
a) Polymerization optimization	90
b) Characterization	95
(i) SEC analysis.....	95
(ii) NMR analysis	96
(iii) Elemental analysis	98
(iv) Thermogravimetric and FTIR coupled analysis	99
2. Polymerization of decafluorobiphenyl and TMSTB	100
3. Polymerization of decafluorobiphenyl and Biphenyl-4,4'-dithiol	101
4. Polymerization of decafluorobiphenyl and hexane-1,6-dithiol	102
a) Characterization.....	103
(i) NMR analysis	103
(ii) SEC analysis	104
(iii) Thermogravimetric analysis	105
5. Polymerization of TBBT and phosphonated octafluorobiphenyl	106
a) Phosphonation of decafluorobiphenyl monomer	107
b) Polycondensation	109
6. Polymerization of 4,4'-thiobisbenzenethiol and disodium 3,3'-disulfonate-4,4'- difluorodiphenylsulfone	111
IV. Conclusion	112
V. References	114



Chapter III: Postfunctionalization of polyfluorothioether prepolymers

I.	Introduction	121
1.	Phosphonated polymer.....	121
2.	Sulfonated polymers	123
3.	Strategy.....	125
II.	Materials and methods	127
1.	Reagents	127
2.	Experimental.....	128
a.	Phosphonation of fluorinated poly(phenylenesulfide)s	127
(i)	Strategy 1	128
(ii)	Strategy 2	128
(iii)	Strategy 3	129
b.	Phosphonation of fluorinated poly(phenylenesulfone)s	130
b.1.	Oxidation of sulphides to sulphones.....	130
(i)	Strategy 1 (Ox1, Figure II-11)	130
(ii)	Strategy 2 (Ox2, Figure II-11)	131
(iii)	Strategy 3 (Ox3, Figure II-11)	131



b.2. Phosphonation of fluorinated poly(phenylenesulfone)s.....	132
c. Sulfonation of fluorinated poly(phenylenesulfide)s using sodium hydrosulfide.....	133
d. Sulfonation of fluorinated poly(phenylenesulfide)s using sodium sulfide.....	134
(i) Strategy 1	134
(ii) Strategy 2	135
e. Sulfonation of fluorinated poly(phenylenesulfide)s using Lithium sulfide	135
f. Sulfonation of fluorinated poly(phenylenesulfide)s using Sulfuric acid	136
g. Sulfonation of fluorinated poly(phenylenesulfide)s using Sodium 3-Mercaptopropane-1-sulfonate	137
(i) Strategy 1	137
(ii) Strategy 2	138
h. Sulfonation of fluorinated poly(phenylenesulfone)s using Sodium 3-Mercaptopropane-1-sulfonate	138
3. Techniques	139
a. Microwave reactor.....	139
b. IR spectroscopy	139
c. NMR spectroscopy	139
d. Size-Exclusion Chromatography (SEC)	140
e. Thermal analysis	140
f. Elemental Analysis	140
III. Results and discussion	140
1. Phosphonations	140



a.	Phosphonation of fluorinated poly(phenylenesulfide)s	141
	(i) Strategy 1	141
	(ii) Strategy 2	143
	(iii) Strategy 3	144
b.	Phosphonation of fluorinated poly(phenylenesulfone)s : step1, Oxidation of sulfides to sulfones	145
	(i) Strategy 1 (Ox1, Figure II-30)	146
	(ii) Strategy 2 (Ox2, Figure II-30)	146
	(iii) Strategy 3 (Ox3, Figure II-30)	147
	Elemental analysis	147
	Thermogravimetric analysis	148
c.	Phosphonation of fluorinated poly(phenylenesulfone)s : step 2 : functionalization.....	149
d.	Conclusion of phosphonations	151
2.	Sulfonations.....	152
	a. Sulfonation of fluorinated poly(phenylenesulfide)s using sodium hydrosulfide.....	153
	b. Sulfonation of fluorinated poly(phenylenesulfide)s using sodium sulfide	154
	c. Sulfonation of fluorinated poly(phenylenesulfide)s using lithium sulfide	157
	d. Sulfonation of fluorinated poly(phenylenesulfide)s using sulphuric acid	158
	e. Sulfonation of fluorinated poly(phenylenesulfide)s using 3-Mercaptopropane-1-sulfonate	159
	f. Sulfonation of fluorinated poly(phenylenesulfone)s using Sodium 3-Mercaptopropane-1-sulfonate	165
	g. Conclusion of sulfonation.....	170



IV.	Conclusions	171
V.	References	173

Chapter IV: Proton Exchange Membranes (PEMs)of

I.	Introduction.....	179
	1. PEM state of the art	179
	2. PEM process method	180
II.	Materials and methods	181
	1. Reagents.....	181
	2. Experimental.....	182
	a) Phosphonated membranes (P1PM).....	183
	b) Sulfonated membranes (P1SM, P2SM, P4SM and P2SOM)	183
	3. Characterization.....	184
	a) Water uptake	184
	b) IEC	184
	c) Proton Conductivity at room temperature.....	186
	d) Catalyst-coated membrane (CCM)	186
III.	Results and discussion	186
	1. Membrane processing	186
	a) Main issues	187
	b) Phosphonated Membranes	189
	c) Sulfonated Membranes	189



2. PEM's properties.....	191
a) Properties at rt.....	191
b) Conductivity vs. temperature	193
c) Membrane surface.....	194
d) Electrochemical Impedance Spectroscopy (EIS).....	195
IV. Conclusion	199
VI. References.....	202

Chapter V: General Discussion and Conclusions

I. General Discussion	205
II. General Conclusions	210
III. Outlook	211
IV. References	213



Acknowledgements

First of all, I would like to thank Prof. Laurent Billon, Dr. Laia Francesch and Dr. Jochen Kerres who were at the very beginning of my interviews to join the eSCALED project. Secondly and without whom I would not have this thesis I want to thank Dr. Stéphanie Reynaud and Dr. Vladimir Atanasov for all their help this 4 years sharing their knowledge and helping me both in and off the laboratory. I also want to thank Prof. Dr. Günter Tovar who was the last to join this project but a very helpful aide in finishing this thesis.

I want to also thank the team in ICVT in Stuttgart, specially Johannes, Inna and Galina for their help and teaching. The team in Pau, having helped both in the scientific discussions and life in Pau, specially Laia Francesch, Antoine Bousquet and Pierre Marcasuzaa. From Eurecat Mataró I would like to thank Claudia Delgado for my secondment spent there and I would also like to thank all the project supervisors, and anyone involved in the eSCALED project that took the time to provide us with quality training and guidance throughout the PhD.

A big part of the reason I have finished this PhD is also from all the other PhD colleagues involved in the eSCALED project, Andrew Howe, Ludovico Riccardi, Andrew Bagnall, Afridi Zamader, Silvia Pugliese, Domenico Grammatico, Olivera Vukovic, Saeed Sadeghi, Diogo Garcia, Van Nguyen, Robin Dürr, Bruno Branco and Karell Bosson. A big thank you to all of them and especially the ones that have accompanied me whether in Stuttgart or Pau.

On a more personal level I want to thank my family who encouraged me from a very early age to go away and discover new places. To all my friends who have supported me during these years in the distance.

Et pour finir je voudrais remercier Maitia qui m'a toujours poussé pour prendre les bideak les plus compliqués et sans laquelle je ne m'aurais pas embarqué en ce projet.



ANNEXES: LISTS OF FIGURES, TABLES AND ABBREVIATIONS

List of figures

Figure I-1. Matrix of energy conversions. In the cases where more possibilities exist, no more than two leading transformations are identified

Figure I-2. eSCALED project device scheme

Figure I-3. Processes involved in the natural photosynthesis (left), and the artificial photosynthesis (right)

Figure I-4. Prime mover forces evolution through the last 4000 years

Figure I-5. Comparison of the power versus energy density characteristics of different storage media. Stars represent three commercial examples: yellow star-2008 Toyota Prius; green star-BAE bus; red star-A123 F1 race car booster

Figure I-6. Grove's gas voltaic battery (1839)

Figure I-7. Bacon Alkaline fuel cell

Figure I-8. PEMFC in the Gemini 7 spacecraft, 1965. (From Smithsonian Institution, neg. EMP059020, from the Science Service Historical Images Collection, courtesy of NASA)

Figure I-9. PEM electrolysis and PEM Fuel Cell

Figure I-10. Use of PEMFC divided in transport and stationary cells

Figure I-11. Source International Energy Agency (IEA)

Figure I-12. Schematic representation of a Fuel cell electric vehicle (FCEV)

Figure I-13. Nafion structure

Figure I-14. Proton transport mechanisms



Figure I-15. Hydrogen bonds formation among acidic groups

Figure I-16. Membranes conductivity type vs T

Figure II - 1. Poly(ethylene oxide) formula according to Lourenço

Figure II -2. Schematic schemes of step growth (left) and chain growth (right) polymerization processes, ●: monomer, —: covalent bond, I: initiator, X: species present in the reaction system (e.g. monomer, solvent, additives, polymer chains...). The * indicates that the species is activated

Figure II-3. Average \bar{M}_w vs monomer conversion for both chain-growth and step-growth polymerizations

Figure II-4. Hydrolysis of an ester. R1 and R2 being parts of the polymer, ending in two separate molecules when hydrolysis occurs

Figure II-5. Structures of Nafion and Aquivion, two polymers for PEMs

Figure II-6. Decafluorobiphenyl (DFBP) and 4,4'-Thiobisbenzenethiol (TBBT) monomers

Figure II-7. Polymerization of Decafluorobiphenyl (DFBP) and 4,4'-Thiobisbenzenethiol (TBBT)

Figure II-8. Reactions of DFBP with the different dithiols and the resulting copolymers.

Figure II-9. Polymerisation of di-functionalised monomers with TBBT and their polymer structures.

Figure II-10. Polycondensation of DFBP and TBBT.

Figure II-11. Polymerization of decafluorobiphenyl and TMSTB

Figure II-12. Polymerization of decafluorobiphenyl and biphenyl-4,4'-dithiol

Figure II-13. Polymerization of decafluorobiphenyl and Hexane-1,6-dithiol

Figure II-14. Phosphonated octofluorobiphenyl

Figure II-15. Polycondensation of TBBT and decafluorobiphenyl

Figure II-11. Semifluorinated poly(phenylene sulfide)

Figure II-12. Polymerization of decafluorobiphenyl and TMSTB



Figure II-13. Semifluorinated poly(phenylene sulfide)

Figure II-14. Polymerization of decafluorobiphenyl and biphenyl-4,4'-dithiol

Figure II-15. Polymerization of decafluorobiphenyl and Hexane-1,6-dithiol

Figure II-16. Mw vs K_2CO_3 eq./Temperature

Figure II-17. Polymerization under conventional heating at 80 °C using 4 eq. of K_2CO_3 (left picture) and 5 eq. of K_2CO_3 with gel-formation (right picture).

Figure II-18. Polyfluorinated poly(phenylene sulfide)s with polyfluorinated phenyl terminations.

Figure II-19. P6 Fluorinated polythioether polymer precipitation in acidic medium (left) and P6 after drying

Figure II-20. SEC elugram of P6

Figure II-21. 1H NMR of P6

Figure II-22. ^{19}F NMR of P6

Figure III-23. ^{19}F NMR Decafluorobiphenyl

Figure II-24. TGA P6 Polyfluorinated sulphide polymer

Figure II-25. Polymerization of decafluorobiphenyl and TMSTB

Figure II-26. ^{19}F NMR of polymerization of DCFB and TMSTB

Figure II-27. Polymerization of decafluorobiphenyl and biphenyl-4,4'-dithiol

Figure II-28. Polymerization of decafluorobiphenyl and hexane-1,6-dithiol

Figure II-29. 1H NMR polyfluorinated biphenyl hexanesulfide alt-polymer

Figure II-30. ^{19}F NMR polyfluorinated hexanesulfide

Figure II-31. GPC polyfluorinated hexanesulfide



Figure II-32. TGA polyfluorinatedbiphenyl hexanesulfide (red line) and polyfluorinated poly(phenylene sulfide)

Figure II-33. Polymerization of TBBT and 4,4'-phosphonatedoctafluorobiphenyl

Figure II-34. Phosphonation of decafluorobiphenyl monomer

Figure II-35. Phosphonated decafluorobiphenyl monomer

Figure II-36. ^{19}F NMR decafluorobiphenyl, phosphonated octofluorobiphenyl, fluorinated poly(phenylenesulfide)s and biphosphonated hexafluorinated poly(phenylsulfide)s

Figure II-37. ^1H NMR biphosphonated hexafluorinated poly(phenylsulfide)s

Figure II-38. Polymerization of disodium 3,3'-disulfonate-4,4'-difluorodiphenylsulfone and TBBT

Figure II-39. Scheme of polymerizations, in italic, the paragraph number where the experimental protocol is described, above the arrows, the paragraph number where the polymerization is discussed. Plain and dashed arrows for successful and unaccomplished pathways

Figure III-1 Dimethyl phosphonate-4-substituted α,β,β -trifluorostyrene (up-left), PVPA (upright) and PPEEK (down)

Figure III-2. Phosphonic acid anhydride formation

Figure III-3. Some examples of sulfonated polymers presented in J. Ran et al. review of Ion exchange membranes

Figure III-4. Phosphonation paths of poly(phenylesulfide)

Figure III-5. Sulfonation paths of poly(phenylenesulfide)

Figure III-6. Phosphonation of fluorinated poly(phenylenesulfide)s using Tris(trimethylsilyl phosphite)

Figure III-7. Phosphonation of fluorinated poly(phenylenesulfide)s using dimethyl phosphite

Figure III-8. Oxidation of polyfluorinated poly(phenylene sulfide) to polyfluorinated poly(phenylene sulfone)

Figure III-9. Phosphonation of fluorinated poly(phenylenesulfone)s



Figure III-10. Sulfonation of fluorinated poly(phenylenesulfide)s

Figure III-11. Sulfonation of fluorinated poly(phenylenesulfide)s using Na_2S

Figure III-12. Sulfonation of fluorinated poly(phenylenesulfide)s using Li_2S

Figure III-13. Sulfonation of fluorinated poly(phenylenesulfide)s using H_2SO_4

Figure III-14. Sulfonation of fluorinated poly(phenylenesulfone)s using Sodium 3-mercapto-1propanesulfonate

Figure III-15. Sulfonation of fluorinated poly(phenylenesulfide)s using Sodium 3-mercapto-1propanesulfonate

Figure III-16. Phosphonation of fluorinated poly(phenylenesulfide)s

Figure III-17. Phosphonation using strategy 1 (conventional heating)

Figure III-18. ^{19}F NMR phosphonated poly(phenylenesulfide)s

Figure III-19. ^1H NMR phosphonated poly(phenylenesulfide)s

Figure III-20. ^{19}F NMR phosphonated poly(phenylenesulfide)s

Figure III-21. Phosphonation of fluorinated poly(phenylenesulfide)s using dimethyl phosphite

Figure III-22. Oxidation of poly(phenylenesulfide)s scheme

Figure III-23. Proposed Oxidation mechanism following G. kermanshahi and K. Bahrami catalytic mechanism

Figure III-24. Oxidation of P6, from sulfide to sulfone

Figure III-25. TGA fluorinated poly(phenylene sulfone)s. P6_Ox1

Figure III-26. Phosphonation of fluorinated poly(phenylenesulfone)s

Figure III-27. Phosphonation presented by V. Atanasov

Figure III-28. ^{19}F NMR phosphonated poly(phenylenesulfone)s



Figure III-29. Scheme of all phosphonation in *italics*, the paragraph number where the experimental protocol is described, above the arrows, the paragraph number where the polymerization is discussed Figure III-30. Scheme of the sulfonations carried out

Figure III -30. Polymerization and Sulfonation done by S. Takamuku et al. (left), polymerization and sulfonation done in this thesis

Figure III-31. Cross-linking between two sulfonated poly(phenylenesulfide)s

Figure III-32. Sulfonation of fluorinated poly(phenylenesulfide)s using Na_2S

Figure III-33. ^{19}F NMR obtained after attempted sulfonation

Figure III-34. Solution after sulfonating using Na_2S

Figure III-35. Sulfonation of fluorinated poly(phenylenesulfide)s using Li_2S

Figure III-36. Sulfonation of fluorinated poly(phenylenesulfide)s using H_2SO_4

Figure III-37. ^1H NMR of polymer obtained after sulfonation with H_2SO_4

Figure III-38. Sulfonation of fluorinated poly(phenylenesulfone)s using Sodium 3-Mercaptopropane-1-sulfonate

Figure III-39. Dried sulfonated polymer

Figure III-40. Kinetic study of sulfonation (a, left graph), 8eq. used, rt, 72h. Sulfonation eq. vs sulfonation degree (b, right graph), 6h, rt

Figure III-41. ^{19}F NMR polymer with increasing levels of sulfonation

Figure III-42. TGA Backbone polymer/Sulfonated polymer

Figure III-43. FTIR sulfonated polymer

Figure III-44. Sulfonation of fluorinated poly(phenylenesulfide)s using Sodium 3-Mercaptopropane-1-sulfonate



Figure III-45. Figure III-45. Synthesis pathway for the preparation of sulfonated poly(ether ether sulfone) proposed by G. Summers et al.

Figure III-46. ^1H NMR of partially sulfonated poly(phenylenesulfone)s using Sodium 3-Mercaptopropane-1-sulfonate

Figure III-47. ^{19}F NMR of partially sulfonated poly(phenylenesulfone)s using Sodium 3-Mercaptopropane-1-sulfonate

Figure III-48. Cross-linking of two partially sulfonated chains

Figure III-49. Scheme of all sulfonation in *italic*, the paragraph number where the experimental protocol is described, above the arrows, the paragraph number where the polymerization is discussed

Figure III-50. Scheme of phosphonations with final products selected for the membrane elaboration

Figure III-51. Scheme of sulfonations with final products selected for the membrane elaboration

Figure IV-9. First operational PEM, poly(styrenesulfonic acid), PSSA

Figure IV-2. Process from dry polymer (P4S) to membrane (P4SM) obtention after adding PBI-OO (poly-[(1-(4,4'-diphenylether)-5-oxybenzimidazole)-benzimidazole])

Figure IV-3. Scheme of ionically cross-linked acid-base blend membranes

Figure IV-4. P1S and P2S, fluorinated sulfonated poly(phenylenesulfide).

Figure IV-5. No film formation after evaporation of the solvent

Figure IV-6. Film with phase separation after evaporation of the solvent.

Figure IV-7. Swollen film with few ml of H₂O added to keep the membrane hydrated.

Figure IV-8. PBI and PBI-OO chemical formulas.

Figure IV-9. P4SM-a membrane.

Figure IV-10. P2SOM membrane.



Figure IV-11. Membrane Conductivity vs. temperature.

Figure IV-12. Membrane 12x12 cm. P4SMa SEM x 1K, Teflon side (left), Air side (right).

Figure IV-13. Membrane 12x12 cm. P4SM-a SEM x50. P4SM-a SEM x1.5k.

Figure IV-14. Membrane 3x3 cm. P4SM-c_CCM after catalyst deposition.

Figure IV-15. Delamination of the catalyst from the membrane surface in P4SM-c.

Figure IV-16. Electrochemical Impedance Spectroscopy (EIS) comparison.

Figure IV-17. Cell Potential vs Current density.

Figure V-1. Different materials used for PEMs (CNT: carbon nanotubes; FEP: poly(fluoroethylene-co-hexafluoropropylene); GO: graphene oxide; HEP: hexafluoropropylene; NPI: naphthalenic polyimide; P4VP: poly(4-vinylpyrrolidone); PBI: polybenzimidazole; PEI: polyetherimide; PFA: poly(tetrafluoroethylene-co-perfluorovinyl ether); PFCA: perfluorocycloalkene; PFCI: perfluorocarboxylated ionomer; PFSA: perfluorosulfonic acid; PSSA: polystyrene sulfonic acid; PTFE: polytetrafluoroethylene; PVA: polyvinyl alcohol; PVDF: polyvinylidene fluoride; SPAEK: sulfonated poly aryl ether ketone; SPEEK: sulfonated polyether ether ketone; SPPBP: Sulfonated poly(phenoxy benzoyl phenylene); phenylene); and SPSU: sulfonated polysulfone).

Figure V-2. Scheme of polymerizations starting with decafluorobiphenyl.

Figure V-3. Scheme of polymerizations starting with 4,4-thiobisbenzenthiole and functionalized monomers.

Figure V-4. Scheme of all phosphonation in *italics*, the paragraph number where the experimental protocol is described, above the arrows, the paragraph number where the polymerization is discussed

Figure V-5. Scheme of sulfonations

List of tables and equations

Table I-1. Table I-2. Different types of electrolysis and its advantages and disadvantages.



Table I-2. Acidic groups comparison.

Table I-3. Phosponated polymeric membranes.

Table II-3. Evolution of the average degree of polymerization with the evolution of the polymerization.

Table II-2. Parameters tested for the polycondensation, with potassium carbonate as catalyst base and conventional heating process with DCFB:TBBT=1:1 for P1 to P5 and DCFB:TBBT=1.04:1 for P6 to P10, extra 0,04 added after 6h and left for one extra hour. Results: polymer molar mass and dispersity

Table II-3. Elemental analysis comparison

Table III-1. Elemental analysis fluorinated poly(phenylene sulfone)s

Table IV-1 Precursor polymers. First P refers to the poly(phenylenesulfide), the number stands for the degree of sulfonation, S refers to sulfonated, P to phosphonated and O to oxidated sulfides (sulfones). Synthesis of these polymers can be found in chapter 3.

Table IV-2. Membranes with the precursor polymers, the solvents used for the mixture with the additive and the additive to polymer ratio.

Table IV-3. Membranes characterization. First P refers to the poly(phenylenesulfide), number = degree of sulfonation, S refers to sulfonated, P to phosphonated and M to membrane. Finally a, b, c are membranes starting from the same polymer adding different quantities of PBI-OO.

Equation II-1. Definition of the dispersity, \bar{D}

Equation II-2. \bar{M}_n is the number-average molar mass

Equation II-3. \bar{M}_w is the weight-average molar mass

Equation II-4. Degree of polymerisation (p), with \bar{x} = average degree of polymerisation, f = monomer unit functionality (number of functional groups per monomer molecule)

Equation II-5. Monomer functionality average calculation from Carothers



Equation II-6. Degree of polymerisation when all the functionalities of the monomers have reacted

Equation II-7. Degree of the reaction with an A^2B^2 system

Equation II-8. Dispersity (\mathcal{D}) with p being the degree of polymerization, \bar{M}_n the number-average molar mass and \bar{M}_w the weight-average molar mass

Equation II-9. Base equivalents

Equation III-1. Degree of phosphonation

Equation III-2. Number of substitutions

Equation III-3. Degree of sulfonation

Equation IV-1. Water uptake (%) calculation, being W_f = Final weight and W_i = Initial weight

Equation IV-2. Ionic exchange capacity (IEC). Unit MM = Polymer unit Molar Mass.

Equation IV-3. Ionic exchange capacity (IEC). With : $IEC_{Pol.}$ = IEC of the polymer calculated using Equation IV-2, $W_{Pol.}$ = Weight of polymer used for the membrane, IEC_{PBIOO} = IEC of PBI-OO calculated using Equation IV-2, W_{PBIOO} = Weight of PBIOO used for the membrane.

Equation IV-4. Ionic exchange capacity (IEC). $IEC_{Titr.}$ = IEC measured using titration method.

Equation IV-5. Conductivity measurements formula.

List of abbreviations

ADEME Agence de la transition écologique

AFC Alkaline fuel cells

ATP Adenosine 5"-triphosphate

BTR Bridge to Renewables

CAGR Cumulative aggregated growth



CCM	Catalyst coated membrane
CCS	Catalyst coated surface
CNT	Carbon nanotubes
DBU	1,8-Diazabicyclo[5.4.0]undec-7-ene
DFBP	Decafluorobiphenyl
DMAC	N,N-Dimethylacetamide
DMF	N,N-Dimethylformamide
DMFC	Direct methanol fuel cell
DMSO	Dimethylsulfoxide
EIS	Electrochemical Impedance Spectroscopy
EV	Electric vehicle
EW	Equivalent weight
FC	Fuel cell
FCEV	Fuel cell electric vehicles
FEP	poly(fluoroethylene-co-hexafluoropropylene)
FNM	Ferrovie nord milano
FTIR	Fourier-transform infrared spectroscopy
GE	General electric company
GO	Graphene oxide
GPC	Gel permeation chromatography
HEP	Hexafluoropropylene
ICE	Internal combustion engines



ICVT Institut für Chemische Verfahrenstechnik

IEC Ionic exchange capacity

IPREM Institut des Sciences Analytiques et de Physico-Chimie pour l'Environnement et les Matériaux

IR Infrared

IUPAC International union of pure and applied chemistry

MCFC Molten carbonate fuel cells

MM Molar mass

MOF Metal organic framework

NASA National Aeronautics and Space Administration

NMP 1-methyl-2-pyrrolidone

NPI Naphthalenic polyimide

PAFC Phosphoric acid fuel cells

PBI Polybenzimidazole

PBI-OOPoly-[(1-(4,4'-diphenylether)-5-oxybenzimidazole)-benzimidazole]

PEI Polyetherimide

PEFC Polymer electrolyte fuel cell

PEM Proton exchange membrane

PEMFC Proton exchange membrane fuel cell

PES Poly(arylene ether sulfone)s

PFA poly(tetrafluoroethylene-co-perfluorovinyl ether)

PFCA perfluorocycloalkene



PFCI perfluorocarboxylated ionomer

PFTE polytetrafluoroethylene

PFSA Perfluoropolymers with sulfonic acid

POFBP 4,4'-biphosphonatedoctafluorobiphenyl

PPEEK Phosphonated poly(ether ether ketone)

PSSA Poly(styrenesulfonic acid)

PVA Polyvinyl alcohol

PVDF Polyvinylidene fluoride

PVPA Poly(vinyl phosphonic acid)

P4VP Poly(4-vinylpyrrolidone)

SEC Size exclusion chromatography

SEM Scanning electron microscope

SNCF Société nationale de chemins de fer français

SOFC Solid oxide fuel cells

SPAEK sulfonated poly(aryl ether ketone)

SPEEK Sulfonated poly(ether ether ketone)

SPPBP Sulfonated poly(phenoxy benzoil phenylene)

SPSU Sulfonated polysulfone

TBBT 4,4'-Thiobisbenzenethiol

TFA Trifluoroacetic acid

TGA Thermogravimetric analysis

TMSP Tris(trimethylsilyl)-phosphite



project ID 765376 — eSCALED — H2020-MSCA-ITN-2017



TMSTB 4,4'-Bis(trimethylsilyl)thiobenzene

UPPA Université Pau et Pays de l'Adour



General Introduction

With the recent fast raise of the global population and the industrialization in developing nations, the need for energy reaches unprecedented levels. For a sustainable future, the world needs safe, low-carbon, and cheap large-scale energy alternatives to fossil fuels. Fossil energy has taken a heavy toll on the planet, rising levels of greenhouse gases in Earth's atmosphere and is a leading contributor of climate change. It is admitted that it is a race against time, and we need to reduce our dependency on fossil fuels. Innovative technologies are needed and should respond renewable sources of energy, environment friendly, affordable, and globally feasible, a foremost challenge. Fuel cells are gaining attention, hydrogen is environmentally friendly, it emits only water. Fuel cells offer considerable benefits, but the industrial development is still to be improved and international research programs are needed. Photovoltaic systems, on the other hand, convert solar energy into electricity but remain limited by the diurnal cycle and suffers from the lack of efficient and cost-effective energy storage.

Complementarily, artificial photosynthesis converts solar energy into a storable fuel. This is a promising method for providing a carbon-neutral, renewable, and scalable source of energy. In artificial photosynthesis systems, the solar energy is converted and stored as solar fuels (e.g., hydrogen, methanol, available around the clock when needed) via chemical reaction such as water splitting and CO₂ reduction. More than offering storability, artificial photosynthesis also absorbs CO₂ from our environment and release helpful oxygen.

A lot of challenges remain to be solved to obtain efficient and stable artificial devices. The whole device architecture must be assessed. This is the strategy of the European project eSCALED that gathers a network of excellent public and private research entities and industrials. The different sub-components of the artificial photosynthesis device submitted to optimizations by the consortium includes:

- A solar cell to convert sunlight into electricity, to feed two electrodes :



- (i) A cathode for reduction reaction which produces a solar fuel: one carbon molecule ($C_xH_yO_z$) or hydrogen (H_2)
 - (ii) An anode for oxidation reaction of water into oxygen and protons.
- A membrane that enables optimized charge transport.

As a part of eSCALED project, this thesis is dedicated to the proton-conducting membrane that seats in the middle of the device, separating the anode and the cathode. Its function is to allow protons to travel from the anode where the oxidation of water is carried out to the anode where the reduction of H^+ to H_2 or CO_2 to CH_3OH is produced. This work mainly focuses onto new PEMs with (beyond) state-of-the-art (SoA) proton conductivity at elevated temperature and with good mechanical stability. The elaboration method should be carefully studied and implemented to result in PEM with high-molecular molar mass to allow for suitable mechanical properties. Due to the context and the targeted application, special attention should be given to favour environmentally friendly experimental conditions. Different synthesis strategies will be followed: (i) either direct polymerization of functional monomers, and (ii) polymer post-functionalisation by sulfonation or phosphonation. The best promising polymers should be then tested as proton-exchange membranes (PEMs) and their properties characterized and compared to Nafion®212, a golden reference for so-called (low-temperature) PEMFCs. From the different available PEMs, our work was focused on PFSA (perfluorosulfonic acid polymers), which belongs to the class of perfluorinated functional polymers.

The manuscript is organized within 5 chapters:

Chapter 1 is dedicated to the SoA, including a brief overview of the context and the economic and environmental issues the society has to face in terms of energy needs. Then the fuel cells are presented prior to report detail PEM within the literature with their elaboration process and performances. This chapter ends with the polymerization strategies discussed later in chapter 2 and 3 to obtain innovative PEMs in chapter 4.



Chapter 2 starts with the description of the polymerization process to be used to obtain polymer with fluor and sulphur atoms. The goal is to obtain prepolymers with high molar mass and bearing chemical groups able to be subsequently postfunctionalized in a further step.

Another approach is attempted to directly obtain the functionalized polymer.

Chapter 3 is dedicated to the functionalization of the prepolymers obtained within Chapter 2. Again, special attention is given to the characterizations as their molar masses and thermal properties dictate the generation of promising PEMs.

Chapter 4 details the PEM elaboration and performance characterization. Most promising polymers obtained in the previous chapters are tested and compared to Nafion®212.

Chapter 5 ends this thesis manuscript with a general conclusion and outlook on tentative future paths for the research field devoted to PEM.



Chapter 1. Introduction to Proton-Exchange Membranes and objectives

I.	Introduction	36
1.	General presentation of the energy issues	36
2.	Water electrolysis and Fuel Cell background introduction	42
3.	Fuel cells and electrolysers classification and PEM economics and commercial applications.....	46
4.	Proton Transport Mechanisms	53
5.	Sulphonated and phosphonated polymers	56
II.	Project PEM's objective	59
III.	Chapter description.....	60
IV.	References	61



This chapter is an introduction to the questions raised in this thesis. This thesis belongs to a larger project called the eSCALED whose objective is to produce a device capable of artificial photosynthesis. It starts with a general presentation of the energy issues, a fuel cell (FC) background introduction, followed by a description of the different fuel cells existing to the proton-exchange membranes (PEMs) investigated.

The focus and objective of this thesis is to obtain a proton-conducting membrane for its use within a PEMFC and the steps followed are defined in the last part of this introduction where the project is discussed.

I. Introduction

1. General presentation of the energy issues

Energy production, storage and use have been at the centre of human development since its inception in Africa. It was the initial trigger to human expansion in the world and has been since a cornerstone of every civilization. Energy itself has a very vague definition, in physics it is defined as the capacity for doing work and it can exist in several forms (Figure I1). It can also be seen as the natural and most antique form of exchange. People would exchange their physical energy (work) for food (energy stored in comestible goods).



FROM TO	ELECTRO- MAGNETIC	CHEMICAL	NUCLEAR	THERMAL	KINETIC	ELECTRICAL
ELECTRO- MAGNETIC		CHEMILUMINES- CENCE	NUCLEAR BOMBS	THERMAL RADIATION	ACCELERATING CHARGES	ELECTRO- MAGNETIC RADIATION
CHEMICAL	PHOTO- SYNTHESIS	CHEMICAL PROCESSING		BOILING	DISSOCIATION BY RADIOLYSIS	ELECTROLYSIS
NUCLEAR	GAMMA- NEUTRON REACTIONS					
THERMAL	SOLAR ABSORPTION	COMBUSTION	<u>FISSION</u> <u>FUSION</u>	HEAT EXCHANGE	FRICITION	RESISTANCE HEATING
KINETIC	RADIOMETERS	METABOLISM	<u>RADIOACTIVITY</u> <u>NUCLEAR BOMBS</u>	<u>THERMAL EXPANSION</u> <u>INTERNAL COMBUSTION</u>	GEARS	ELECTRIC MOTORS
ELECTRICAL	SOLAR CELLS	<u>FUEL CELLS</u> <u>BATTERIES</u>	NUCLEAR BATTERIES	THERMO- ELECTRICITY	ELECTRICITY GENERATORS	

Figure I-1. Matrix of energy conversions. In the cases where more possibilities exist, no more than two leading transformations are identified.¹

In this figure several transformations that are used in this project are shown. The main energy source received on the planet is the electromagnetic (solar, radiant) energy from the sun which is the product of thermonuclear reactions. The electromagnetic flux is received in a broad spectrum of wavelengths. About 30 % of this massive flow is reflected by clouds and surfaces, another 20% is absorbed by these same clouds and atmosphere and roughly the other half is absorbed by the oceans and continents, converted into thermal energy, and reradiated into space. From all this energy a tiny bit, ca. 0.05 % is transformed by photosynthesis into new stores of chemical energy in plants which is the base of all the other forms of higher life. This project about artificial synthesis aims to replicate this same process in an artificial way, Figure I-2:

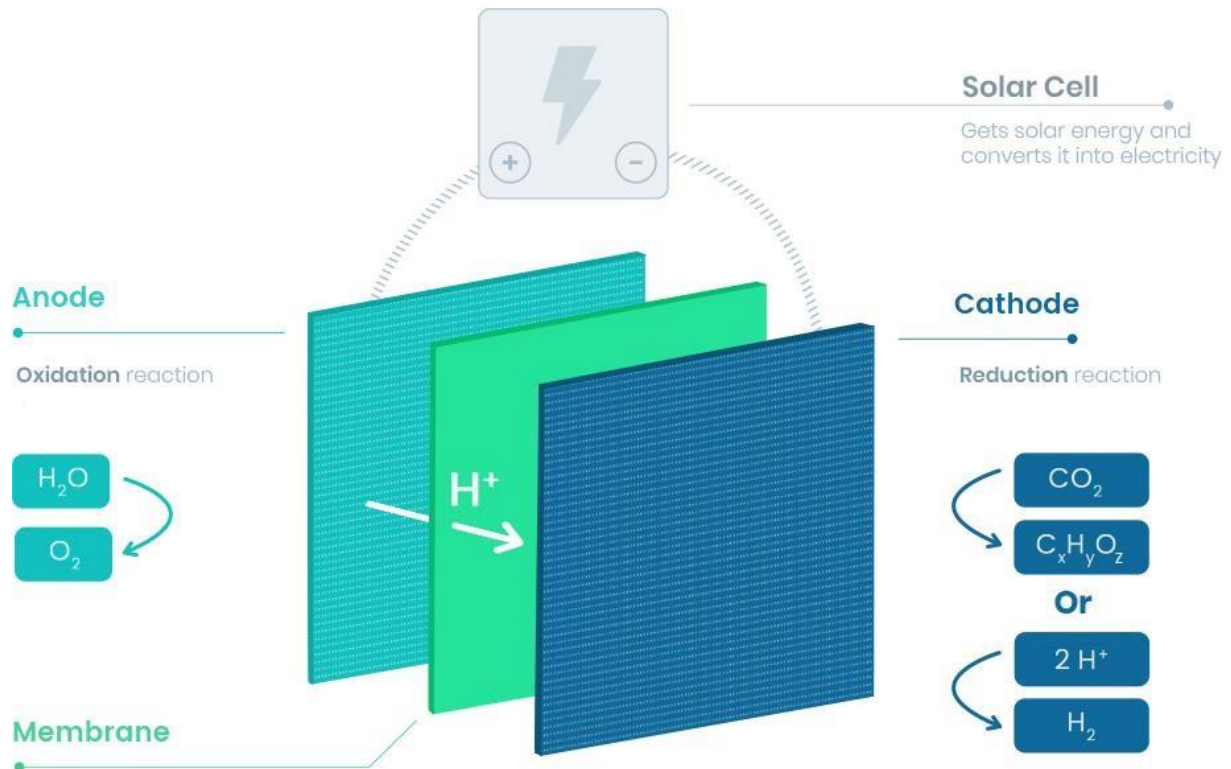


Figure I-2. eSCALED project device scheme.

The eSCALED project is a H2020 MSCA-ITN European project which aims at training 14 early-stage researchers (ESRs) at the European level to elaborate an artificial leaf. A unique device (Figure I-2) will be combined with a solar cell and a bioinspired electrochemical stack where H_2O oxidation and H^+ and/or CO_2 reduction are performed in micro-reactors.

As it can be observed in Figure I-2, the first step of this project is to transform the electromagnetic energy harvested from the sun into electricity. This is the task assigned to the solar cell. This electrical form will be transformed into chemical energy by the electrolysis of water. A further step will be the chemical processing of the protons obtained from the water splitting to be stored as hydrogen or other energetic chemical forms like methanol (CH_3OH) or ethanol ($\text{CH}_3\text{CH}_2\text{OH}$). These could be further used in a fuel cell to transform it back to electricity. These processes are seen and compared with the natural photosynthesis in the following Figure I-3:

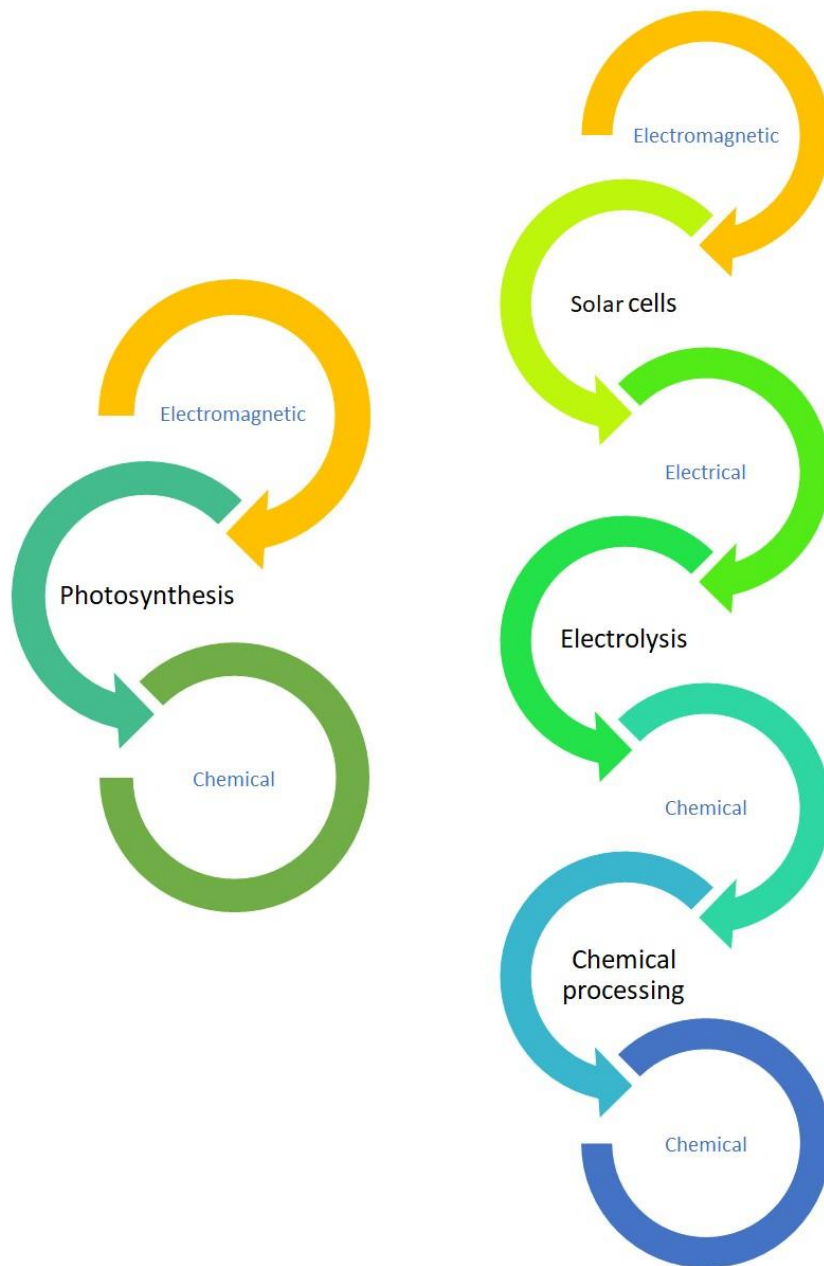


Figure I-3. Processes involved in the natural (left) vs artificial photosynthesis (right) processes, respectively.

Apart from the processes involved in the natural and the artificial photosynthesis, the next use of the chemical energy obtained is completely different. In plants it is used as growth and/or energy storage for further development while in the artificial photosynthesis this chemical energy will be reused in a fuel cell to generate electrical energy.



The principal end-use of energy in history has been its transformation into the kinetic form, meaning that it was used to move things from one place to another. The Figure I-4 shows an evolution of the main source of this energy.

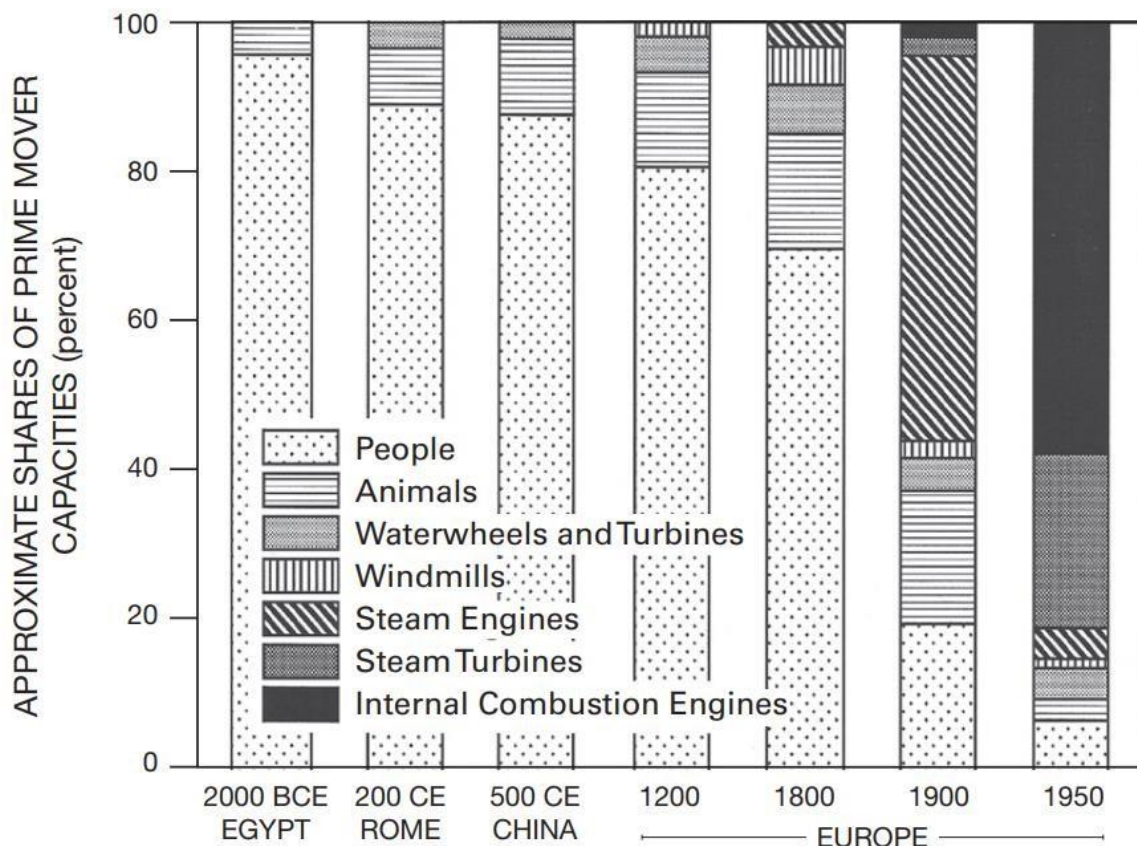


Figure I-4. Prime mover forces evolution through the last 4000 years.²

It can be observed that in roughly just 4000 years, human physical force has decreased from being almost the only one source of this energy to being almost inexistent nowadays. In the next century, fuel cells and batteries are placed in the top positions to substitute internal combustion engines as the main source of energy for mobility.

Fuel cells and batteries offer a high energy density even though their power density is lower than Internal Combustion Engines (ICE) or gasoline. They concentrate a high energy potential but the weight of this energy carrier for the same energy is higher in the fuel cell than in the ICE (Figure I-5).

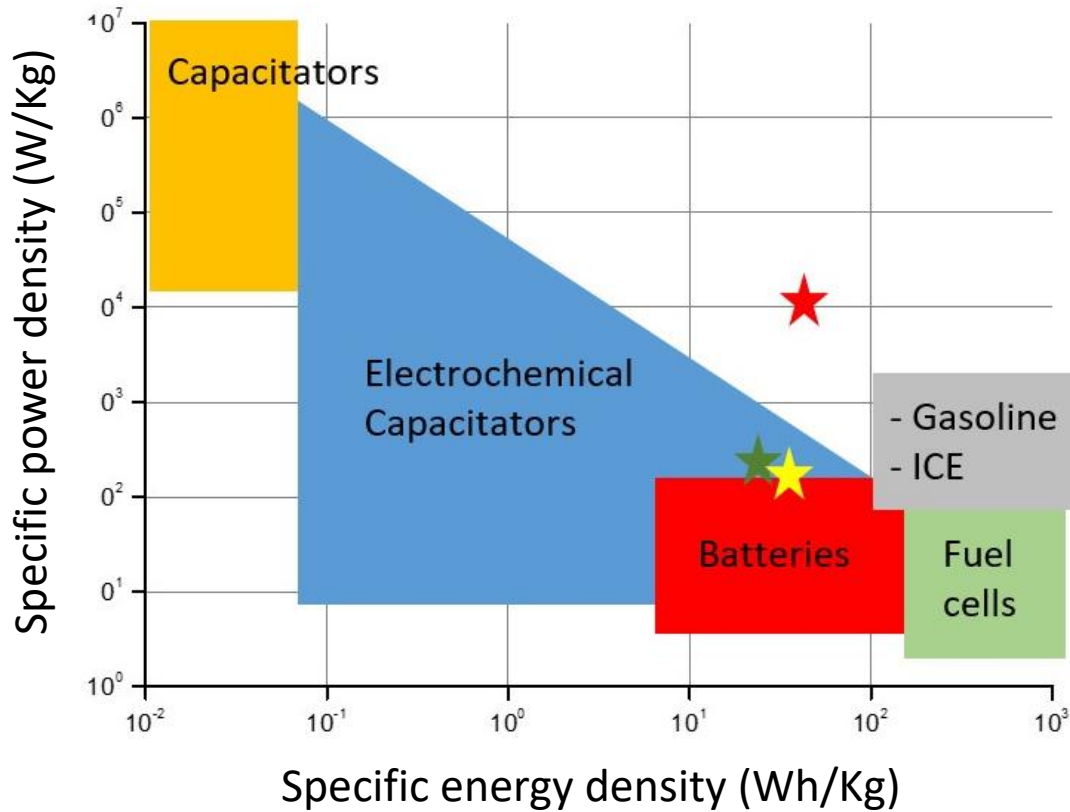


Figure I-5. Ragone Plot: Comparison of the power versus energy density characteristics of different storage media. Stars represent three commercial examples: yellow star-2008 Toyota Prius; green star-BAE bus; red star-A123 F1 race car booster.³

This general view of the energy sources, transformations, uses, and storage devices gives a broad overview of the importance to improve and diversify the generation and storage of energy. The dependence of our civilization in fossil-based fuels cannot last forever and has to be addressed as the demand for energy keeps increasing exponentially and fossil fuel sources keep depleting at a higher rate than the earth can replace them.

To tentatively solve this grand challenge of the 21st century we will focus in this thesis in developing proton-exchange membranes (PEMs) which are both used for the electrochemical water splitting in the electrolyzers, the process by which hydrogen fuel can be produced starting from water, and for the fuel cells by performing the inverse reaction. To understand



the scientific evolution to PEMs, we will start by the very beginning. The water electrolysis discovery and the further batteries development in the next section.

2. *Water electrolysis and fuel cell background introduction*

Water electrolysis was first invented and detailed in 1800 by British scientists Sir Anthony Carlisle and William Nicholson. It was triggered by the discovery of the voltaic pile the same year. The first electrical battery was created by Alessandro Volta by stacking pairs of copper and zinc plates, separated by a cardboard soaked in brine functioning as the electrolyte.⁴ Water electrolysis is considered to be the first chemical reaction using electricity. Therefore, Electrochemistry may be considered as a field of chemistry that started 223 years ago. A special mention must be given to Humphry Davy who developed the first coherent *Electrochemical Theory* published in 1806. He argued that electrochemical decomposition took place at the metal electrodes through which the electricity passed into a compound. Using the voltaic pile, he also discovered a great number of new elements among many other deeds.⁵ However, hydrogen production from water electrolysis never found an industrial application as it can be obtained from fossil fuels. Over 99 % of the presently produced hydrogen is generated from fossil fuels or from electricity produced from fossil fuels.⁶ In the eSCALED project the production of hydrogen is envisioned through the coupling of a photovoltaic solar panel with an electrolyser to produce what is known as green hydrogen (hydrogen obtained from renewable sources). The current efficiency of these systems is actually too low to be economically competitive and several problems are found when commercial applications are attempted (till date).⁷ Due to the surging interests in electrolysers that can produce renewable fuels, the discovery and development of PEMs was done initially and mostly for the inverse reaction, the production of electricity from hydrogen in PEMFCs. Its development is therefore crucial to understand how we arrived to the current SoA PEMs for electrolysers.

The first fuel cell (FC) was invented in the 1830s. Sir William Robert Grove, who invented a device consisting of two platinum electrodes dipped into a sulphuric acid solution having the two other ends sealed in containers of oxygen and hydrogen mixed in water. He assumed that



if in 1801 W. Nicholson and Sir A. Carlisle had been able to split water producing hydrogen and oxygen by the passage of current, the opposite reaction could produce a current. He obtained hydrogen and oxygen and saw that when he disconnected the device, the electrodes were polarized. When linked by an external circuit, a current flow was found. He published this discovery in 1839 in the Philosophical Magazine calling it a gas voltaic battery. Even though it was a promising discovery, he didn't see any practical application to produce electricity through this battery.⁸

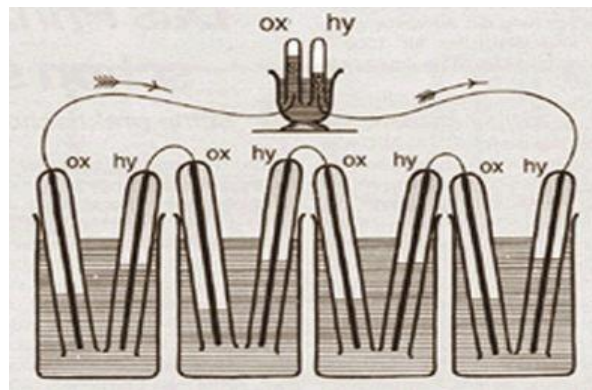


Figure I-6. Grove's gas voltaic battery (1839).

It took fifty years to see substantial improvements to Grove's gas voltaic battery (Figure I-6). The next step was taken by Ludwig Mond and Carl Langer (1889) who used electrodes of platinized platinum (large specific surface area), yielding currents of 2 to 3A at a voltage of 0.73V. Already at this point the two main issues were the high price and the rapid decline in performance (as a bitter-sweet note there are still issues to be improved today). One of the main figures was the 1909 Nobel Prize in Chemistry winner Friedrich Wilhelm Ostwald who wrote "In the future, the production of electrical energy will be electrochemical, and not subject to the limitations of the second law of thermodynamics"; Through his work related to physical and chemical reactions in fuel cells, the interconnections between the different components of the FC were better understood. He foresaw that hydrogen could be used as the source of energy for an Era of Electrochemical Combustion, potentially more efficient than thermodynamic engines.⁹



The first half of the 20th century was mainly dedicated to the electrochemical oxidation of coal and coal gasification products at high temperatures. A basic assumption was that the process could only succeed at high temperatures when coal would burn rapidly. Therefore, first electrolytes used were high temperature molten solids like sodium and potassium carbonates or molten caustic soda, these electrolytes being known as molten carbonate electrolytes and are used for molten carbonate fuel cells (MCFC). They could work at high temperatures; however they were highly corrosive and had numerous practical problems (e.g., ash formation, incomplete oxidation, and the continuous feeding of a solid fuel)¹⁰. These issues brought a lot of new solid electrolyte research, bringing to the use of Zirconia ceramics in 1937 by Baur and Preis¹¹. These new ceramic solid electrolytes formed a new group known as Solid oxide fuel cells (SOFC).¹² In 1947 the first monograph *The Problem of Direct Conversion of the Chemical Energy of Fuels into Electrical Energy*, dedicated to fuel cells was published by soviet researcher O.K. Davtyan.¹³

The second half of the 20th century started with the presentation of Bacon (Figure I-7) alkaline fuel cell (AFC) which used KOH solutions instead of the corrosive acidic solutions to be used as electrolytes. It was the first fuel cell with practical use and the capacity to produce up to 5 kW. One of his fuel cells was used in submarines of the British royal navy during the World War II. The fact that it was feasible for “commercial” use attracted great attention and started the first “fuel cell boom”.

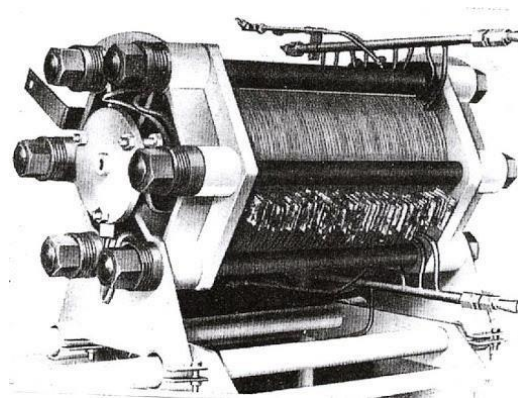


Figure I-7. Bacon Alkaline fuel cell.



The space race between USA and the URSS gave an impulse to the FCs research. In the late 1950s and early 1960s Grubb-Niedrach group working for the General Electric Company (GE) developed FCs using another electrolyte that would open another field inside the FCs, the solid ion-exchange membrane; better known as Proton-exchange Membrane Fuel cell (PEMFC). This technology was used by the NASA for the Gemini project (Figure I-8). It did not just provide energy but also drinking water for the astronauts during their expeditions.

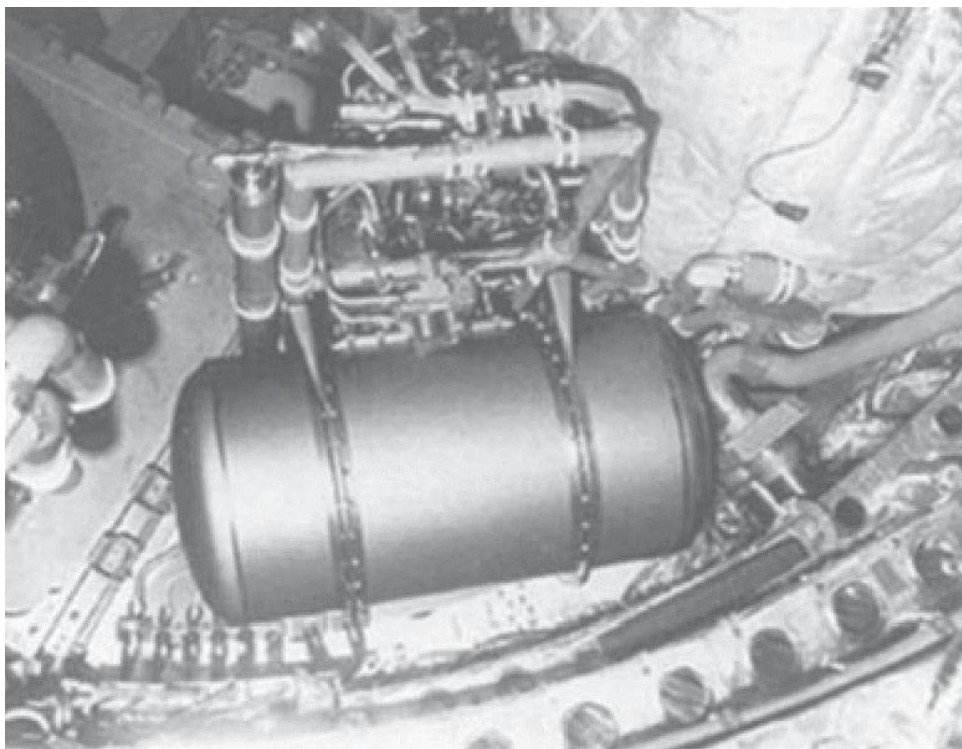


Figure I-8. PEMFC in the Gemini 7 spacecraft, 1965. (From Smithsonian Institution, neg. EMP059020, from the Science Service Historical Images Collection, courtesy of NASA).¹⁴

However, PEMFC technology was still not entirely satisfactory and was not developed further until late 1980s. In the meantime, projects NASA came back to AFCs. Pratt & Whitney, an aircraft engine manufacturer obtained the license of Bacon's patents to build an improved AFC for the Apollo spacecraft that landed onto the Moon.

In these heroic years, a less dashing but also important improvement was the AFC of 15kW that used a mixture of gases as fuel, and cheap potassium hydroxide as the electrolyte for a tractor. New types of FCs were also being investigated in the 1960s. At the University of Amsterdam G.H.J. Broers and J.A.A. Ketelaar were investigating simultaneously the use of



molten salts as electrolytes. These cells had the advantage of using hydrocarbons and carbon monoxide directly as fuel, which generated an international interest. Power plants were built in various countries being able to produce up to 2 MW. Still during the same period, solid oxide fuel cells using transition metals were being developed in several places. The operating models produced were in the range of tens of kW.

The first information on FCs using phosphoric acid can be tracked back to 1961 with the works of Elmore and Tanner who published Intermediate Temperature Fuel Cells. These phosphoric acid fuel cells (PAFCs) had the advantage to run at medium-temperatures with less purified hydrogen, meaning they could tolerate up to 2 % of CO impurities in the anode and air in the cathode. MW plants were built to supply some hotels, hospitals, and city districts.

The cold war and the oil crisis in the 1970 spurred research interests for new energetic resources that would make the principal powers less dependent of oil. These years were characterized by the suppression of diffusion limitations in the electrodes, the reduction of costs and the increase of performance and endurance. The next huge development came out with a collaboration between the Jet propulsion laboratories of the NASA in conjunction with the University of Southern California: a direct methanol fuel cell (DMFC) was developed, needing a fuel liquid (methanol) from where they extract the hydrogen.¹⁵ Here like in the PEMFCs, polymer electrolyte membranes were used.

3. Fuel cells and electrolyzers classification and PEM economics and commercial applications

Following the different discoveries briefly contextualized in the previous section, fuel cells can be mainly classified in six groups according to the nature of the electrolyte used and divided in two groups based on the operating temperature:

- Low operating temperature fuel cells
 - Alkaline Fuel Cell (AFC)
 - Polymer Electrolyte Fuel Cell (PEFC), finding as a subgroup:
 - Proton-exchange Membrane fuel cell (PEMFC)



- Direct Methanol Fuel Cell (DMFC)
- Phosphoric Acid Fuel Cell (PAFC).
- High operating temperature fuel cells
 - Solid Oxide Fuel Cell (SOFC)
 - Molten Carbonate Fuel Cell (MCFC).

In the case of the electrolyzers just three of these types have been developed, Alkaline electrolysis, PEM electrolysis and SOEC electrolysis. The electrolytes used are directly related to the ones used in the AFC, the PEMFC and the SOFC relatively. Their main pros vs cons are defined in the following Table I-1:

Type of electrolysis	Pros	Cons
Alkaline electrolysis	Well established technology Non noble catalysts Long-term stability Relative low cost	Low current densities Crossover of gases (degree of purity) Low partial load range Low dynamics Low operational pressures Corrosive liquid electrolyte
PEM electrolysis	High current densities High voltage efficiency Good partial load range Rapid system response Compact system design High gas purity Dynamic operation	High cost of components Acidic corrosive environment Possibly low durability Commercialization Stacks below MW range



SOEC electrolysis	Efficiency up 100 %;	
	thermoneutral	Laboratory stage
	Efficiency > 100 % w/hot steam	Bulky system design
	Non noble catalysts	Durability (brittle ceramics)
	High pressure operation	No dependable cost information

Table I-1. Different types of electrolysis and its pros and cons.¹⁶

I have focused on PEMs (Proton-exchange membranes) which are used for PEM electrolysis, PEMFC, and DMFC. The relation between PEMFC and PEM electrolysis can be observed in the schematic representation in Figure I-9:

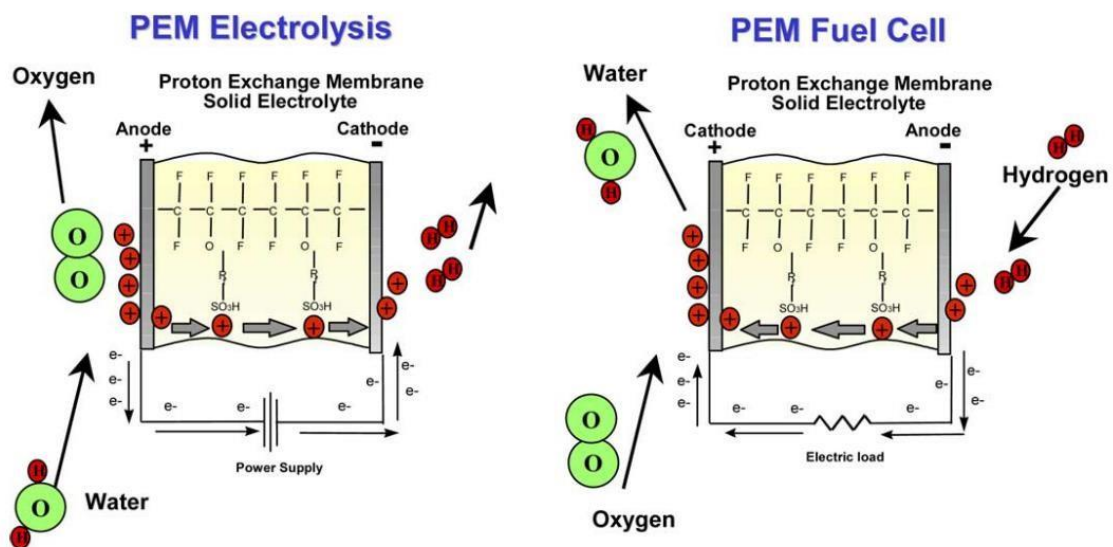


Figure I-9. PEM electrolysis and PEMFC.¹⁷

The global PEMFC market size was worth ca. €1.85 billion in 2021 and according to different market studies, it is expected to reach a value of €22 billion in 2028 meaning it will have CAGR (cumulative aggregated growth) of ca. 40 % in the 2021-2028 period.¹⁸⁻¹⁹ This surge is mainly due to the growth of zero-emission vehicles being sponsored by government initiatives in the search of cleaner and both environmental and health-safe methods for transportation. The only gas the Fuel cell electric vehicles (FCEV) emit is water steam therefore being completely



harmless for health in the cities contrary to diesel/petrol-powered vehicles which emit CO, CO₂, SO_x, NO_x and many other pollutants. PEMFCs are used both in stationary facilities and for transport vehicles, as seen in the following Figure I-10:

Global Proton Exchange Membrane Fuel Cell (PEMFC) Market share, by application, 2020

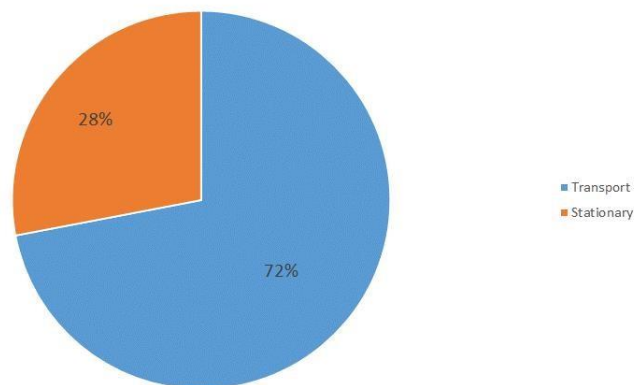


Figure I-10. Use of PEMFC divided in transport and stationary cells.

The FCEVs are still concentrated in a few developed countries which are the largest car manufacturers and have been launching collaborative programs between the automobile industry and both private and public research centres. In the following Figure I-11 the worldwide distribution of FCEVs can be appreciated:



Fuel cell Electric Vehicles Stock (Share in %), by selected Countries, 2020

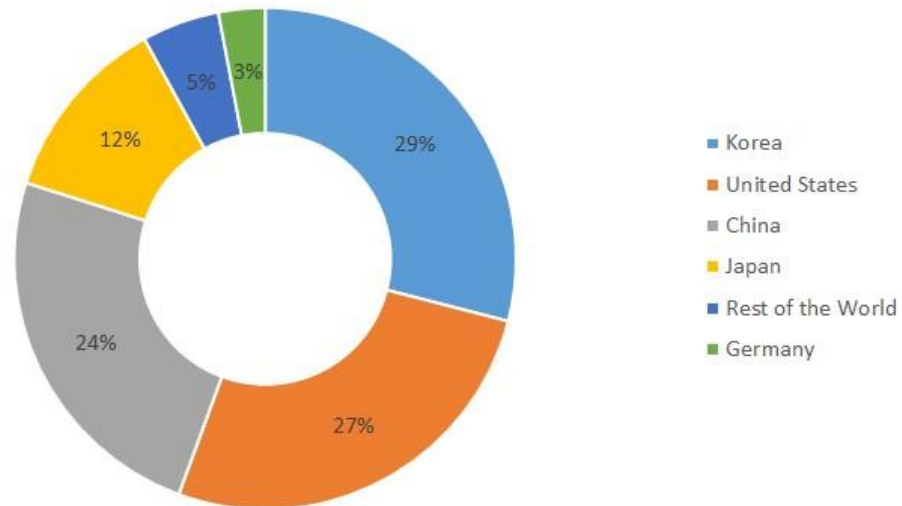


Figure I-11. Source International Energy Agency (IEA).²⁰

One of the main debates is whether PEMFC are feasible for cars from the economic point of view as they need a new supplying hydrogen grid while Electric vehicles (EV) require only an electric charging point, the electric grid being already set-up. T. Larriba et al. pointed out in their study the main advantages of PEMFC based vehicles: a much lower refuelling time, a closer to nowadays refuelling times, and the higher performance under freezing conditions compared to electric batteries-based vehicles.²¹ The two main drawbacks apart from the infrastructure are the high price of the FCEV and the high cost of hydrogen which makes the price per km to be double compared to the EV. In the next Figure I-12 a schematic representation of a FCEV is shown:

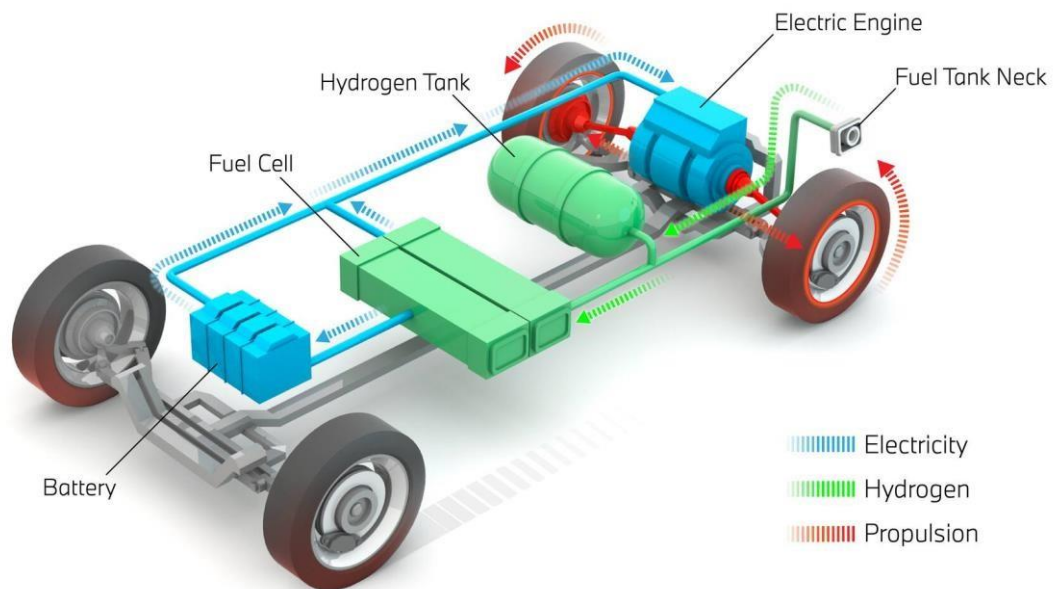


Figure I-12. Schematic representation of a Fuel cell electric vehicle (FCEV)²²

Another high impact drawback is the hydrogen tank as shown within Figure I-12 adding up a lot of volume in the vehicle. Due to this factor and the lack of hydrogen refuelling points nowadays the FCEV is turning its attention to heavy transport vehicles like trucks, buses and trains. In 2018, the world's first hydrogen powered train manufactured by Alstom entered into commercial service in Germany. It has been tested in different European countries and orders have been confirmed by SNCF (Société National de Chemins de Fer Français) in France and FNM (Ferrovie Nord Milano) in Italy.²³ One year later, in 2019, the launch of the first Hydrogen-Powered BRT (Bridge to Renewables) system was introduced in the city of Pau (France), a project cofinanced by the European Union, the ADEME (Agence de la transition écologique) and the Région Nouvelle-Aquitaine.²⁴ It has already been working for three years now producing the hydrogen in the same distribution plant using energy from renewable sources.²⁵ These two examples prove that it is not just a possible source of energy for the future but an actual commercially applied source of energy with operating PEMFCs.

PEMFCs offer some of the most promising advantages over all fuel cells but are still handicapped by their high costs and the low durability. Moreover, PEMFCs require a high purity hydrogen, at least 99.99 %. Typical impurities produced when obtaining H₂ in the



electrolysis of water like CH_4 , O_2 , N_2 , CO_2 and CO usually decrease the efficiency of the cell.²⁶ As seen in Figure I-9, the only waste released after the reaction is water being a completely non-polluting reaction by itself. It is a rising multidisciplinary research field, having attracted researchers with various backgrounds and witnessed a rapid growth and increasing expansion of the field. Ion exchange membrane publications has boomed in the last 20 years, growing from ca. 12,000 to more than 30,000²⁷. Nonetheless the current SoA proton-exchange membrane remains Nafion® which was discovered in the 1960s by Walter Grot who worked for DuPont. Nafion® itself, has a market size in 2022 close to €800 million.²⁸ The Nafion® membrane consists of a poly(tetrafluoroethylene) backbone and regular spaced long perfluorovinyl ether pendant side-chains terminated by a sulfonate ionic group. The chemical formula is shown in Figure I-13:

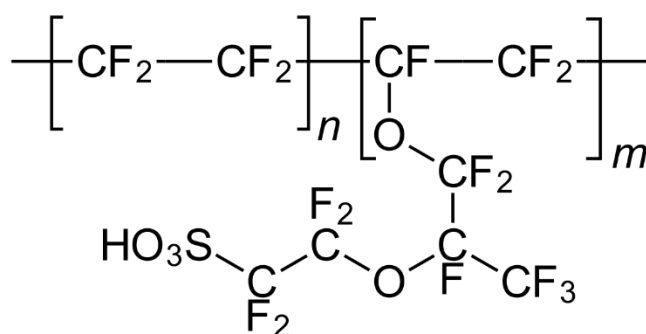


Figure I-13. Nafion structure.

The equivalent weight (EW) of Nafion® would be 1100 g of polymer per equivalent of ionic group ($m=1$, $n \approx 6.5$). Meaning that the molecular weight of one block of this polymer is 1100 g/mol when $n \approx 6.5$. Therefore when $100 < m < 1000$ a rough estimation of the molar mass is usually between 10^5 g/mol and 10^6 g/mol.²⁹ The main disadvantages of this membrane and similar perfluorinated ionomers are³⁰:

- Complicated and environmental-unfriendly production process involving toxic intermediates and waste by-products
- High price
- Strong decrease of proton conductivity when the water content of the membrane is reduced (high temperatures)



- High methanol permeability when operated in DMFC

Even with all these drawbacks, it still dominates the market even though many different research groups are working toward new generation of membranes.

4. Proton Transport Mechanisms

Efficient PEM for water electrolysis starts with an efficient transporting these charge carriers. Proton conductivity and mobility have been extensively studied by (electro)chemists, physicists as well as biologists due to their importance in chemical (like electricity generation in a hydrogen FC), as well as in biological processes (like photosynthesis or adenosine 5'-triphosphate (ATP) production).³¹⁻³²

There are three proposed and studied mechanisms in which the proton moves in a PEM. It is important to point out that they are not exclusive and therefore the final conductivity is a sum of each conductivity mechanism. The three mechanisms are:

- Grotthuss mechanism
- Bulk transport or vehicle mechanism (figure I-14)
- Surface transport mechanism (figure I-14)

Grotthuss mechanism was proposed in 1995 by Noam Agmon who suggested that water molecules have isomerizations of more than one water molecule like $H_9O_4^+$ and $H_5O_2^+$ being the first one the responsible of hydrogen-bond cleavage of a second-shell water and the second one doing the reverse, hydrogen-bond formation. This was discovered due to the abnormal proton mobility in water compared to potassium cations.³³

Bulk transport or vehicle mechanism proposes the idea of the protons attached to different vehicle molecules being phosphonic (or different acidic) species in a solution. G. A. Ludueña et al.³⁴ studied both this vehicle and Grotthuss mechanism making simulations in agreement with experimental observations and found that local proton hopping between adjacent acids occurs frequently but that the net charge transport is due to the Grotthus mechanism, being residual water molecules necessary for the short-distance proton conduction.



The third proposed mechanism is the surface transport mechanism (Figure I-14) in which protons jump from adjacent sulfonic/phosphonic groups creating proton channels inside the membrane. A higher number of channels will increase the proton conductivity (Figure I-14).

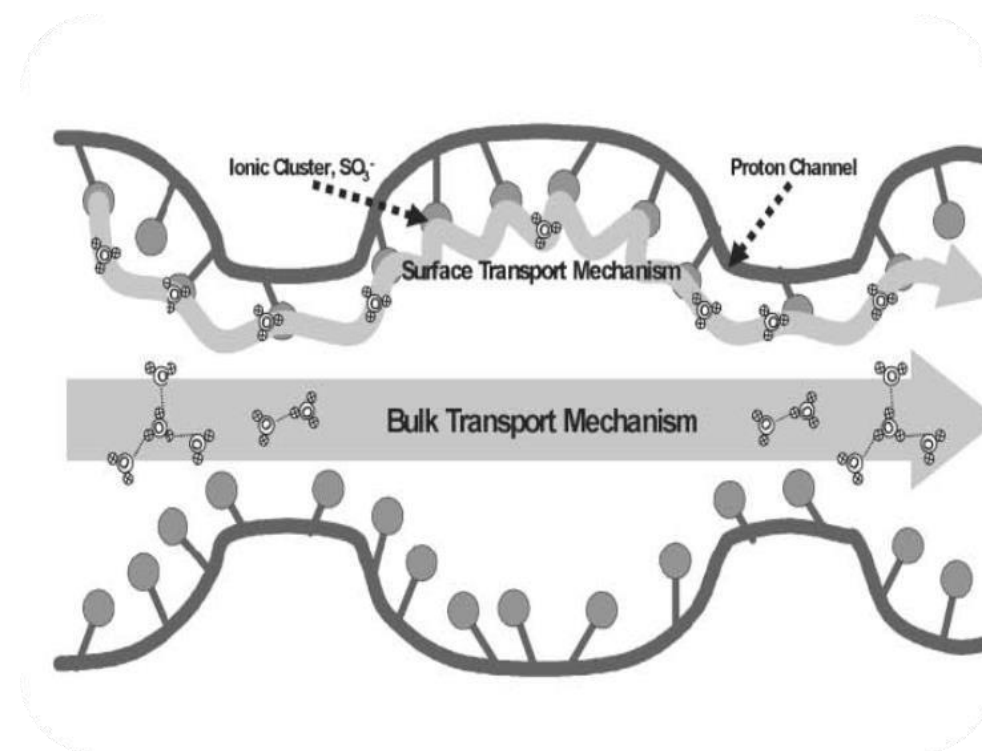


Figure I-14. Proton transport mechanisms.

Other important subjects are the acidity, solubility, and melting point of the attached groups. T. Bock et al. compared the characteristics of these acidic groups attached to a phenyl group in an alkylic chain obtaining the results reported in the Table I-2:

Property	Phenyl-COOH*	Phenyl-SO ₃ H	Phenyl-PO ₃ H ₂
Melting point (°C)**	121	85 ^[20]	170 ^[21]
Boiling point (°C)	249 (ambient pressure)	171 ^[22] (13 mbar)	n.a. (decomposition)
pK _a (in water)	4.2	- 0.7	1.8 / 7.0 ^[23]
Water solubility*** (g)	2.9	93 ^[24]	47 ^[19]

* Anhydrous form, ** per 100 g solution at RT

Table I-2. Acidic groups comparison.³⁵



When compared to the carboxylic acid group, the phosphonic acid moiety is of superior acidic strength; however it possesses a lower dissociation constant (higher pKa) than the sulfonic acid group. This means that the number of available charge carriers will be lower in the case of phosphonic acid derivatives compared to the sulfonic acid compounds. The rise of the melting points in the series is sulfonic < carboxylic < phosphonic acid as an evidence of the increase of polarity and/or hydrogen bonding in the same order. The high melting point of phenylphosphonic acid as well as its low vapor pressure are attributed to its high capacity to form hydrogen bonds (see Figure I-15, c). An additional benefit of hydrogen bond networks of phosphonic acid groups (Figure I-15 c) is the possibility of cooperative proton transport phenomena. Therefore phosphonic acid-containing polymers have found applications as proton conductors in fuel cell membranes.³⁶

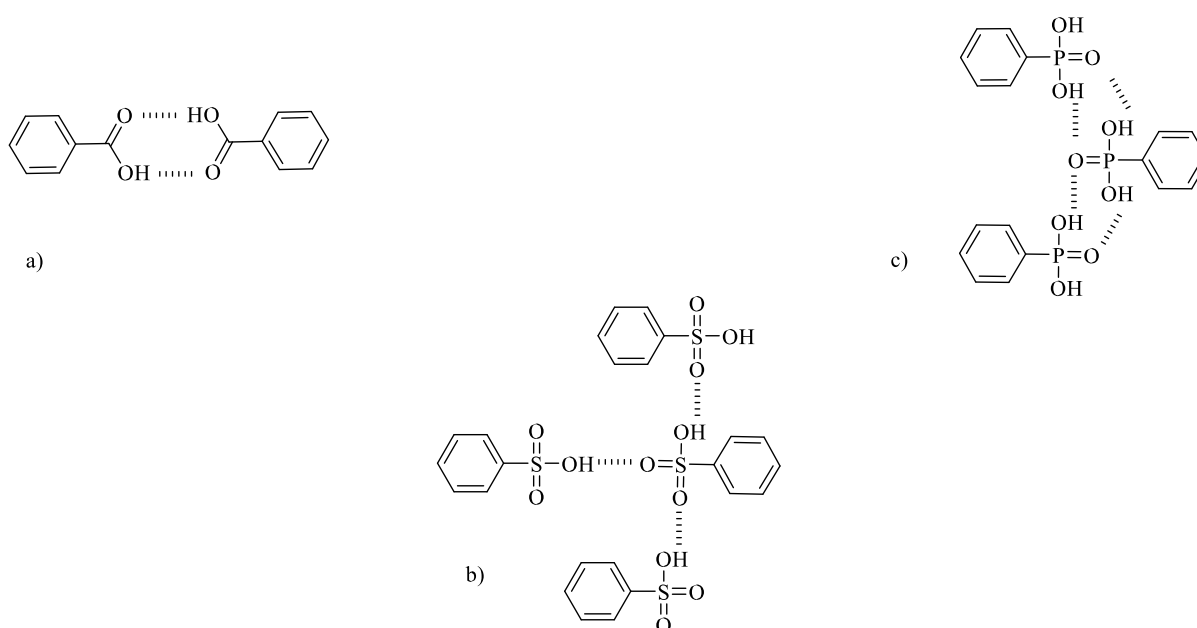


Figure I-15. Hydrogen bonds formation among acidic groups.

S.J. Paddison modeled the proton transport in sulfonic acid-based ionomer (Figure I-15, b) membranes and suggested that the proton dissociates itself from the sulfonate group when the number of water molecules per sulfonic acid group, λ , equals three. It has also been



calculated that in order to have a complete separation between the proton and the sulfonate group, the water content must be higher ($\lambda \geq 6$).³⁷

In the next section a general look into the sulfonated and phosphonated polymers available nowadays and their syntheses will be presented.

5. Sulphonated and phosphonated polymers

Over the last decades research on new sulfonated and phosphonated PEMs has speeded up and several PEMs have been proposed to substitute Nafion® derivatives. Their inconveniences have been already explained in the previous sections and these have been the main drivers of new research. Generally, sulfonated and phosphonated hydrocarbon PEMs can be prepared by:

- (i) post-functionalization (i.e. sulfonation/phosphonation) of prepolymers
- (ii) direct copolymerization of sulfonated/phosphonated monomers and physicochemical modification of the sulfonated/phosphonated polymers
- (iii) A combination of (i) and (ii)³⁸

In chapter 2 and 3, both (i) and (ii) will be discussed in more detail. Among new polymers synthesised in the last decades, aromatic hydrocarbon polymers bearing sulfonic acid groups based on poly(arylene ether)s, poly(arylene ether sulfone)s (PES),^{39,40} poly(arylene sulfide)s, poly(phenyl quinoxaline)s, polybenzimidazoles, polyimides,⁴¹⁻⁴² and poly(ether imides)⁴³⁻⁴⁴ have been reported. Non-fluorinated hydrocarbon has the advantage of being cheaper than perfluorinated ionomers like Nafion® but their acidity and proton conductivity are lower.⁴⁵

When it comes to (i), one of the issues found is that after attaching the first sulfonate group the phenyl ring becomes highly deactivated for further sulfonation. Another important issue is the fact that sulfonic acid groups attached directly to the polymer backbone do not usually show good microphase separation (into hydrophilic/hydrophobic regions) which is important to obtain proton-conducting channels. To overcome this issue C. Wang et al. synthesised a poly(ether sulfone ketone)s which had aryl rings for multiple sulfonation.⁴⁶ They followed the post-polymerization sulfonation method including the synthesis of a non-conductive polymer



prior to its sulfonation. Developing an efficient synthetic methodologies leading to more than one sulfonic acid groups per aromatic rings remains challenging however needed to promote, proton conductivity at low water contents without sacrificing stability.⁴⁷

It is in this regard that the phosphonated polymers seem to have an advantage. Their proton conductivity is less affected by a low water content which means that they can operate at higher temperatures, being less affected by the evaporation of water above 100 °C.

The usual synthetic path to obtain phosphonated polymer membranes is to phosphonate the backbone of a prepolymer using phosphonating agents (e.g. tris(trimethylsilyl)phosphite (TMSP)) followed by an hydrolysis to position phosphonic acid groups onto the polymer backbone.

In the following Table I-3 a summary of different proposed phosphonated polymeric membranes is shown with their proton conductivity and its Ionic Exchange Capacity values (IEC):

Membrane	Conductivity (mS/cm)	IEC (meq/g)	References
Phosphonated polysulfone	12 (100 °C)	3.8	Abu-thabit et al. ⁴⁸
PSU grafted with poly(vinylbenzylphosphonic acid)	4.6 (120 °C)	5.3	Parvole and Jannasch ⁴⁹
Phosphonated peptoid diblock copolymers, poly-N-(2-ethyl) hexylglycine-block-poly-N-phosphonomethyl-glycine	8 (35 °C)	N.A.	Sun et al. ⁵⁰
Chlorotrifluoroethylene (CTFE)-based polymer	0.25 (120 °C)	6.9	Tayouo et al. ⁵¹
Phosphonated poly(arylene ether)s	0.0296 (25 °C)	N.A.	Meng et al. ⁵²



Phosphonated poly(styrene-ethylenebutylene-styrene)	5.8 (140 °C)	0.652	Elumalai et al. ⁵³
Phosphonated Polypentafluorostyrene (PWN)	100 (110 °C)	7.0	V. Atanasov et al. ⁵⁴

Table I-3. Phosphonated polymeric membranes.

Proton conductivity of phosphonated polymers remains significantly lower than the one of sulfonated polymers (ca. 100 mS/cm for $T < 100$ °C). A worth noticing exception is the highly phosphonated polystyrene synthesised by V. Atanasov et al. which resulted in a proton conductivity value on par with the ones of sulfonated polymers. Phosphonated polymers suffers also from deficient durability, acid loss and slow oxygen reduction kinetics.⁵⁵ J. Maier et al. compared sulfonic acid, phosphonic acid and imidazole functionalized model compounds and added proof that phosphonic acid compounds do work better than sulfonic acid compounds in the dry state and at higher temperatures (100 °C $< T < 200$ °C).⁵⁶ A PEM for a fuel cell which includes the advantage of working at ≥ 100 °C was presented by L. Yan et al. by using an acid base composite of phosphonic acid polysulfone and tryazolyl functionalized polysulfone, the membrane showed also a higher proton conductivity (42.71 mS/cm) than most phosphonated acidic membranes.⁵⁷ In a 2021 paper published by P. Jannasch et al. showed new poly(arylene perfluorophenylphosphonic acid) membranes with a high proton conductivity up to 111 mS/cm at 80 °C when fully hydrated which proves that they could be an option, even at temperatures lower than 1000 °C.⁵⁸

In recent reports, the cross-linking of polymer chains is being used as a powerful and simple method to inhibit the methanol permeability and excessive swelling of PEMs. After crosslinking, the polymer matrix forms a network where the macromolecular chains of ionomers are immobilized and compacted.⁵⁹ Nowadays, polymeric materials covering a broad range of temperatures where good PEMs performance have been developed are existing. Figure I-16 show the range at which most common PEMs are used.

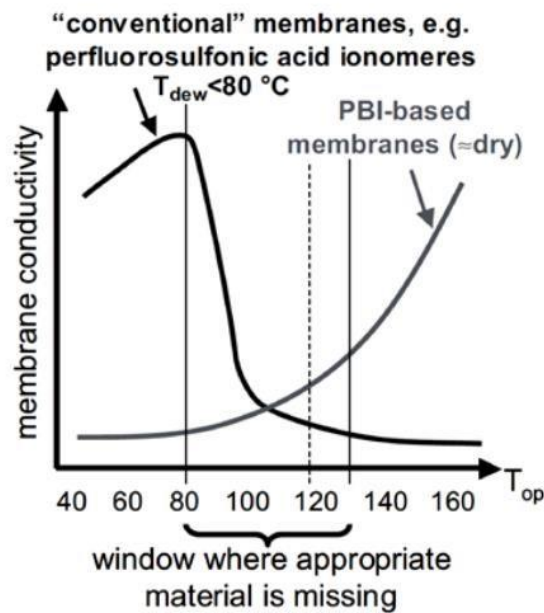


Figure I-16. Membranes conductivity type vs T .⁶⁰

Considering the window where appropriate material is missing, the focus of this work has been to obtain a membrane that would not have a sudden conductivity decrease at Temperatures higher than 80 °C.

II. Project's PEM's objective

This thesis is a part of a larger project whose objective is to obtain artificial photosynthesis devices which can produce either hydrogen or alcohols like methanol or ethanol from sun light using a photovoltaic solar cell. One of the key-enabling sub-components in this device is the proton conducting membrane that is positioned at the heart of the device, separating the anode and the cathode. Its function is to allow protons to be efficiently transferred from the anode where the oxidation of water is taking part to the anode where the reduction of H^+ to H_2 or CO_2 to CH_3OH is produced. My thesis focus is to obtain a new generation of PEM with a proton conductivity of at least 100 mS/cm at 90 °C and a good mechanical stability in an electrolyser. The PEM must be prepared by a single polymer or polymer blends. One of the



objectives concerning the polymer is to have a molar mass of at least 10^5 Da which seems to guarantee a good mechanical stability of a PEM.

Secondary objectives are to minimize energy consumption process (low reaction temperatures) and using as environmentally friendly as possible reactants and solvents. In order to have a high conductivity, proton conducting channels are required in the membrane structure. To obtain these channels, an hydrophobic backbone is needed for stabilizing the PEM bearing sulphonic or phosphonic groups that enhance the protons hopping from one group to another. This so called Grotthuss mechanism allowing for conducting proton being less dependent on the temperature.⁶¹

III. Chapter description

Chapter 2 describes the initial part of the project which was aiming to obtain a high Mw prepolymer to be used for further functionalisation. Decafluorobiphenyl was chosen as the monomer that would be further functionalised, different aromatic and aliphatic sulfides being tested in the initial polymerizations with decafluorobiphenyl. A detailed discussion of the polymerization conditions, the prepolymers obtained and their characterizations is proposed in Chapter 2.

Chapter 3 describes the second part of this project which was focused on post-functionalizing the polymers obtained in chapter 2 so that they could be cast and used to produce a suitable membrane for a PEMFC device. A variety of sulfonation and phosphonation methods are discussed and the functionalized polymers and their characterization is shown in the third chapter. The characterization of the resulting polymers is discussed, and the best ones obtained are further used for the preparation of PEMs.

Chapter 4 describes the membrane preparation. This last part is focused on cross-linking the functionalised polymers with PBI-OO to produce the PEMs. The casting method was used, and



the PEMs were tested and characterized to challenge the hypotheses used for guiding the syntheses route to access the polymers.

Chapter 5 ends the manuscript with a general conclusion and perspectives.

IV. Reference

- ¹ V. Smil, *Energy and civilization: a history*, 2017, Cambridge, MA: the MIT press, p.3-5 [ISBN: 0262035774](#)
- ² V. Smil, *Energy and civilization: a history*, 2017, Cambridge, , MA: the MIT press, p.385-390 [ISBN: 0262035774](#)
- ³ M. Stanley Whittingham, *History, Evolution, and Future status of Energy storage*, 2012, Proceedings of the IEEE, vol.100 DOI:[10.1109/JPROC.2012.2190170](#)
- ⁴ Scharlin, P. & Battino, R. *The Voltaic Pile: A Stimulating General Chemistry Experiment*, 1991, Journal of Chemical Education, 68 (8), p.665-666. DOI:[10.1021/ed068p665](#)
- ⁵ C. A. Russell, *The electrochemical theory of Sir Humphry Davy*, 1963, Annals of Science, 19:4, p.255-271 DOI:[10.1080/0033796300202973](#)
- ⁶ Balat, M. *Potential importance of hydrogen as a future solution to environmental and transportation problems*, 2008, Int. J. Hydrogen Energy, vol. 33, no. 15, p.4013–29. DOI:[10.1016/j.ijhydene.2008.05.047](#)
- ⁷ N.A. Burton, R.V. Padilla, A. Rose, H. Habibullah, *Increasing the efficiency of hydrogen production from solar powered water electrolysis*, 2021, Renewable and Sustainable energy reviews, vol. 135, p.110-255 DOI: [10.1016/j.rser.2020.110255](#)
- ⁸ G. Grimes, *Historical pathways for fuel cells*, 2000, IEEE Aerosp. Electron. Syst. Mag., vol.15, no.12, p.7–10 DOI:[10.1109/62.891972](#)
- ⁹ V. S. Bagotsky, *Fuel Cells: Problems and Solutions, The Long History of Fuel Cells*, 2012, John Wiley & Sons, Inc. p.25–40 DOI:[10.1002/9781118191323](#)
- ¹⁰ M.L. Perry and T.F. Fuller, *A Historical Perspective of Fuel Cell Technology in the 20th Century*, 2002, J. Electrochem. Soc., vol.149, no.7, p.59 DOI:[10.1149/1.1488651](#)



- ¹¹ E. Baur and H. Preis, *Z. Electrochem.*, 43, 1937, p.727-732 [DOI:10.1002/19370430903](https://doi.org/10.1002/19370430903)
- ¹² S.C. Singhal, K. Kendall, *High-temperature Solid Oxide Fuel cells: Fundamentals, design and applications*, 2003, Elsevier, p.29 [ISBN 978-1-85617-387-2](https://doi.org/10.1016/B978-1-85617-387-2)
- ¹³ V. S. Bagotsky, *Fuel Cells: Problems and Solutions, The Long History of Fuel Cells*, 2012, John Wiley & Sons, Inc. p.29 DOI:[10.1002/9781118191323](https://doi.org/10.1002/9781118191323)
- ¹⁴ V. S. Bagotsky, *Fuel Cells: Problems and Solutions, The Long History of Fuel Cells*, 2012, John Wiley & Sons, Inc. p.34 DOI:[10.1002/9781118191323](https://doi.org/10.1002/9781118191323)
- ¹⁵ J. M. Andújar and F. Segura, *Fuel cells: History and updating. A walk along two centuries*, 2009, *Renew. Sustain. Energy Rev.*, vol.13, no.9, p.2309–2322 [DOI: 10.1016/J.RSER.2009.03.015](https://doi.org/10.1016/J.RSER.2009.03.015)
- ¹⁶ M. Carmo, D. L. Fritz, J. Mergel, D. Stolten, *A comprehensive review on PEM water electrolysis*, 2013, *International Journal of Hydrogen energy*, vol.38, p.4901-4934 DOI: [10.1016/j.ijhydene.2013.01.15](https://doi.org/10.1016/j.ijhydene.2013.01.15)
- ¹⁷ F. Barbir, *PEM electrolysis for production of hydrogen from renewable energy sources*, 2005, *Sol. Energy*, vol.78, no.5, p.661–669 <https://doi.org/10.1016/j.solener.2004.09.003>
- ¹⁸ <https://www.fortunebusinessinsights.com/industry-reports/proton-exchange-membrane-fuelcell-pemfc-market-101708>
- ¹⁹ <https://www.globenewswire.com/news-release/2021/04/26/2216819/0/en/Proton-ExchangeMembrane-Fuel-Cell-PEMFC-Market-to-Exhibit-40-6-CAGR-till-2028-Need-to-ReduceCarbon-Emissions-to-Propel-Growth-states-Fortune-Business-Insights.html>
- ²⁰ <https://www.iea.org/data-and-statistics/charts/fuel-cell-electric-vehicles-stock-by-regionand-by-mode-2020>
- ²¹ T. Larriba, R. Garde, and M. Santarelli, *Fuel cell early markets: Techno-economic feasibility study of PEMFC-based drivetrains in materials handling vehicles*, 2013, *Int. J. Hydrogen Energy*, vol.38, no.5, p.2009–2019 DOI:[10.1016/j.ijhydene.2012.11.048](https://doi.org/10.1016/j.ijhydene.2012.11.048)
- ²² <https://www.bmw.com/en/innovation/how-hydrogen-fuel-cell-cars-work.html>
- ²³ <https://www.alstom.com/press-releases-news/2021/9/alstoms-coradia-ilint-hydrogen-trainruns-first-time-france>



- ²⁴https://ec.europa.eu/regional_policy/rest/cms/upload/25092019_104140_Pau_Region_week_presentation_oct19.pdf
- ²⁵ <https://www.idelis.fr/se-deplacer/le-reseau-de-bus/febus-le-bus-zero-emission>
- ²⁶ J. D. Perry, K. Nagai, and W. J. Koros, *Polymer membranes for hydrogen separations*, 2006, MRS Bull., vol.31, no.10, p.745–749 DOI:[10.1557/MRS2006.187](https://doi.org/10.1557/MRS2006.187)
- ²⁷ R. Jin et W. Liang, H. Yubin, Y. Zhengjin, W. Yaoming, J. Chenxiao, G. Liang, B. Erigene, X. Tongwen, *Ion exchange membranes: New developments and applications*, 2017, J. Memb. Sci., vol.522, p.267–291 DOI: [10.1016/j.memsci.2016.09.033](https://doi.org/10.1016/j.memsci.2016.09.033)
- ²⁸ <https://www.marketreportsworld.com/>
- ²⁹ C. Heitner-Wirguin, *Recent advances in perfluorinated ionomer membranes: structure, properties and applications*, 1996, J. Membr. Sci., vol.129, p.1–33 DOI: [10.1016/0376-7388\(96\)00155-X](https://doi.org/10.1016/0376-7388(96)00155-X)
- ³⁰ J. Kerres, A. Katzfuß, K. Krajinovic, A. Chromik, *Preparation and characterization of new Sulfonated partially fluorinated Polyarylenesulfones and their Blends With Polybenzimidazole*, 2010, vol.33, no.1, p. 719–733 DOI:[10.1149/1.3484567](https://doi.org/10.1149/1.3484567)
- ³¹ A. Chernyshev, K. M. Armstrong, S. Cukierman, *Proton transfer in gramicidin channels is modulated by the thickness of monoglyceride bilayers*, Biophys. J. 2003, vol.84, p.238 DOI:[10.1016/S0006-3495\(03\)74845-0](https://doi.org/10.1016/S0006-3495(03)74845-0)
- ³² C. H. Yu, S. Cukierman, R. Pomès, *Theoretical study of the structure and dynamic fluctuations of dioxolane-linked gramicidin channels*, Biophys. J. 2003, vol.84, p.816 DOI:[10.1016/S0006-3495\(03\)74901-7](https://doi.org/10.1016/S0006-3495(03)74901-7)
- ³³ N. Agmon, *The Grotthuss mechanism*, 1995, Chem. Phys. Lett., vol.244, no.5–6, p.456–462 DOI: [10.1016/0009-2614\(95\)00905-J](https://doi.org/10.1016/0009-2614(95)00905-J)
- ³⁴ G.A. Ludueña, T.D. Kühne, and D. Sebastiani, *Mixed Grotthuss and vehicle transport mechanism in proton conducting polymers from Ab initio molecular dynamics simulations*, 2011, Chem. Mater., vol.23, no.6, p.1424–1429 DOI:[10.1021/cm102674u](https://doi.org/10.1021/cm102674u)
- ³⁵ T. Bock, H. Möhwald, R. Mülhaupt, *Arylphosphonic Acid-Functionalized Polyelectrolytes as Fuel Cell Membrane Material*, 2007, Macromol. Chem. Phys., vol. 208, p.1324 DOI: [10.1002/macp.200700193](https://doi.org/10.1002/macp.200700193)



- ³⁶ M. Schuster, T. Rager, A. Noda, K.D. Kreuer, and J. Maier, *About the choice of the protogenic group in PEM separator materials for intermediate temperature, low humidity operation: A critical comparison of sulfonic acid, phosphonic acid and imidazole functionalized model compounds*, 2005, *Fuel Cells*, vol.5, no.3, p.355–365 DOI: [10.1002/fuce.200400059](https://doi.org/10.1002/fuce.200400059)
- ³⁷ S.J. Paddison, *The modeling of molecular structure and ion transport in sulfonic acid based ionomer membranes*. 2001, *Journal of New Materials for Electrochemical Systems* 4:p.197– 207 [ISSN 1480-2422](https://doi.org/10.1002/jnms.1001)
- ³⁸ Z. Wei, S. He, X. Liu, J. Qiao, J. Lin, and L. Zhang, *A novel environment-friendly route to prepare proton exchange membranes for direct methanol fuel cells*, 2013, *Polymer*, vol.54, no.3, p.1243–1250 DOI: [10.1016/j.polymer.2012.12.060](https://doi.org/10.1016/j.polymer.2012.12.060)
- ³⁹ F. Wang, M. Hickner, Q. Ji, W. Harrison, J. Mecham, T.A. Zawodzinski, J.E. McGrath, *Synthesis of Highly Sulfonated Poly(arylene ether sulfone) Random (Statistical) Copolymers via Direct Polymerization*. 2001, *Macromol. Symp.*, vol.175, p.387–396 DOI: [10.1002/1521-3900\(200110\)175:1](https://doi.org/10.1002/1521-3900(200110)175:1)
- ⁴⁰ A. Katzfuß, K. Krajinovic, A. Chromik, J. Kerres, *Partially Fluorinated Sulfonated Poly(arylene sulfone)s blended with Poly- benzimidazole*, 2011, *J. Polym. Sci., Part A: Polym. Chem.*, vol.49, p.1919–1927 DOI: [10.1002/POLA.24624](https://doi.org/10.1002/POLA.24624)
- ⁴¹ N. Asano, M. Aoki, S. Suzuki, K. Miyatake, H. Uchida, M. Watanabe, *Aliphatic/Aromatic Polyimide Ionomers as a Proton Conductive Membrane for Fuel Cell Applications*, 2006, *J. Am. Chem. Soc.*, vol.128, p.1762–1769 DOI: [10.1021/ja0571491](https://doi.org/10.1021/ja0571491)
- ⁴² C. Genies, R. Mercier, B. Sillion, N. Cornet, G. Gebel, M. Pineri, *Soluble Sulfonated Naphthalenic Polyimides as Materials for Proton Exchange Membranes*, 2001, *Polymer*, vol.42, p.359–373 DOI: [10.1016/S0032-3861\(00\)00384-0](https://doi.org/10.1016/S0032-3861(00)00384-0)
- ⁴³ J. Roziere, D.J. Jones, *Non-Fluorinated Polymer Materials for Proton Exchange Membrane Fuel Cells*. 2003, *Annu. Rev. Mater. Res.* vol.33, p.503–555 DOI: [10.1146/annurev.matsci.33.022702.154657](https://doi.org/10.1146/annurev.matsci.33.022702.154657)
- ⁴⁴ M. Rikukawa & K. Sanui, *Proton-Conducting Polymer Electrolyte Membranes based on Hydrocarbon Polymers*, 2000, *Prog. Polym. Sci.* vol.5, p.1463–1502 DOI: [10.1016/S0079-6700\(00\)00032-0](https://doi.org/10.1016/S0079-6700(00)00032-0)
- ⁴⁵ B. Date, H. Junyoung, S. Park, E.J. Park, D. Shin, C.Y. Ryu, C. Bae, *Synthesis and Morphology Study of SEBS Triblock Copolymers Functionalized with Sulfonate and Phosphonate Groups for Proton Exchange Membrane Fuel Cells*, 2018, *Macromolecules*, vol.51, no.3, p.1020–1030 DOI: [10.1021/acs.macromol.7b01848](https://doi.org/10.1021/acs.macromol.7b01848)



- ⁴⁶ C. Wang, Y. Zhou, B. Shen, X. Zhao, J. Li, and Q. Ren, “Proton-conducting poly(ether sulfone ketone)s containing a high density of pendant sulfonic groups by a convenient and mild post-sulfonation, 2018, *Polym. Chem.*, vol.9, n.40, p.4984–4993 DOI: [10.1039/C8PY00996A](https://doi.org/10.1039/C8PY00996A)
- ⁴⁷ S. Takamuku, A. Wohlfarth, A. Manhart, P. Räder, and P. Jannasch, *Hypersulfonated polyelectrolytes: Preparation, stability and conductivity*, 2015, *Polym. Chem.*, vol.6, n.8, p.1267–1274 <https://doi.org/10.1039/c4py01177e>
- ⁴⁸ N.Y. Abu-thabit, S.A. Ali, S.M. Zaidi, *New highly phosphonated polysulfone membranes for PEM fuel cells*, 2010, *J. Memb. Sci.* vol. 360, p.26 doi: [10.1016/j.memsci.2010.04.041](https://doi.org/10.1016/j.memsci.2010.04.041)
- ⁴⁹ J. Parvole, P. Jannasch, *Polysulfones grafted with poly(vinylphosphonic acid) for highly proton conducting fuel cell membranes in the hydrated and nominally dry state*, 2008, *Macromolecules*, vol.27, p.3893 DOI:[10.1021/ma800042m](https://doi.org/10.1021/ma800042m)
- ⁵⁰ J. Sun, X. Jiang, A. Siegmund, M.D. Connolly, K.H. Downing, N.P. Balsara, R.N. Zuckermann, *Morphology and proton transport in humidified phosphonated peptoid block copolymers*, 2016, *Macromolecules*, vol.49, p.3083 DOI:[10.1021/acs.macromol.6b00353](https://doi.org/10.1021/acs.macromol.6b00353)
- ⁵¹ R. Tayouo, G. David, B. Améduri, J. Rozière, S. Roualdès, *New fluorinated polymers bearing pendant phosphonic acid groups, Proton Conducting Membranes for Fuel Cell*, 2010, *Macromolecules*, vol.43, p.5269–5276 DOI: [10.1016/j.eurpolymj.2010.01.011](https://doi.org/10.1016/j.eurpolymj.2010.01.011)
- ⁵² Y.Z. Meng, S.C. Tjong, A.S. Hay, and S.J. Wang, *Synthesis and proton conductivities of phosphonic acid containing poly-(arylene ether)s*, 2001, *Journal of Polymer Science Part A* 39, p.3218–3226. DOI: [10.1002/pola.1304](https://doi.org/10.1002/pola.1304)
- ⁵³ V. Elumalai, R. Annapooranan, M. Ganapathikrishnan, and D. Sangeetha, *A synthesis study of phosphonated PSEBS for high temperature proton exchange membrane fuel cells*, 2018, *J. Appl. Polym. Sci.*, vol.135, n.10, p.1–10 DOI: [10.1002/app.45954](https://doi.org/10.1002/app.45954)
- ⁵⁴ V. Atanasov and J. Kerres, *Highly Phosphonated Polypentafluorostyrene*, 2011, *Macromolecules*, vol. 44, p.6416–6423 DOI: [10.1016/j.eurpolymj.2013.09.002](https://doi.org/10.1016/j.eurpolymj.2013.09.002)
- ⁵⁵ J.S. Wainright, M.H. Litt, R.F. Savinell, *High temperature membranes*, 2003, In: Vielstich, W., Lamm, A., Gasteiger, H.A. (Eds.) *Handbook of Fuel Cells*, Vol. 3, John Wiley & Sons, Inc., New York, pp. 436–346. DOI: [10.1002/9780470974001.f303038](https://doi.org/10.1002/9780470974001.f303038)
- ⁵⁶ M. Schuster, T. Rager, A. Noda, K. D. Kreuer, and J. Maier, *About the choice of the protogenic group in PEM separator materials for intermediate temperature, low humidity operation: A critical comparison of sulfonic acid, phosphonic acid and imidazole functionalized model compounds*, 2005, *Fuel Cells*, vol.5, n.3, p.355–365, DOI: [10.1002/fuce.200400059](https://doi.org/10.1002/fuce.200400059)



- ⁵⁷ B. Yue, G. Zeng, Y. Zhang, S. Tao, X. Zhang, and L. Yan, *Improved performance of acidbase composite of phosphonic acid functionalized polysulfone and triazolyl functionalized polysulfone for PEM fuel cells*, 2017, *Solid State Ionics*, vol.300, p.10–17 DOI:[10.1016/j.ssi.2016.11.011](https://doi.org/10.1016/j.ssi.2016.11.011)
- ⁵⁸ N.R. Kang, T.H. Pham, H. Niderstedt, and P. Jannasch, *Durable and highly proton conducting poly(arylene perfluorophenylphosphonic acid) membranes*, 2021 *J. Memb. Sci.*, vol.623, p.1190-74 DOI:[10.1016/j.memsci.2021.119074](https://doi.org/10.1016/j.memsci.2021.119074)
- ⁵⁹ M.S. Kang, Y.J. Choi, and S.H. Moon, “*Water-swollen cation-exchange membranes prepared using poly(vinyl alcohol) (PVA)/poly(styrene sulfonic acid-co-maleic acid) (PSSA-MA)*”, 2002, *J. Memb. Sci.*, vol.207, n.2, p.157–170 DOI: [10.1016/S0376-7388\(02\)00172-2](https://doi.org/10.1016/S0376-7388(02)00172-2)
- ⁶⁰ X. Sun, S.C. Simonsen, T. Norby, and A. Chatzitakis, *Composite Membranes for High Temperature PEM Fuel Cells and Electrolysers: A Critical Review*, 2019, *Membranes (Basel)*, vol.9, n.7, p.83 DOI:[10.3390/membranes9070083](https://doi.org/10.3390/membranes9070083)
- ⁶¹ N. Agmon, *The Grotthus mechanism*, 1995, *Chemical physics letters* 244, p.456-462 DOI: [10.1016/0009-2614\(95\)00905-J](https://doi.org/10.1016/0009-2614(95)00905-J)



project ID 765376 — eSCALED — H2020-MSCA-ITN-2017





Chapter 2. Synthesis of Polyfluorothioethers

IV. Introduction	71
1. Polymer definition and different polymerization reactions	71
2. Proton-exchange membrane (PEM)	75
3. Project strategy.....	76
V. Materials and methods	81
1. Chemicals and materials	81
2. Experimental	82
g) Polycondensation of decafluorobiphenyl and 4,4'-thiobisbenzenethiol.....	82
(i) Polycondensation by conventional heating method	82
(ii) Polycondensation by microwave method	83
h) Polymerization of decafluorobiphenyl and 4,4'-bis(trimethylsilyl)thiobenzene	84
i) Polymerization of decafluorobiphenyl and Biphenyl-4,4'-dithiol	85
j) Polymerization of decafluorobiphenyl and hexane-1,6-dithiol	85
k) Polymerization of phosphonated octafluorobiphenyl and 4,4'-thiobisbenzenethiol.....	86
(i) Phosphonation of Decafluorobiphenyl monomer.....	86
(ii) Polycondensation of 4,4'-thiobisbenzenethiol and phosphonated octafluorobiphenyl.....	87
l) Polymerization of disodium 3,3'-disulfonate-4,4'-difluorodiphenylsulfone and 4,4'- thiobisbenzenethiol	87



3. Technics	88
g) Microwave reactor.....	88
h) IR spectroscopy	88
i) NMR spectroscopy	89
j) Size Exclusion Chromatography (SEC)	89
k) Thermal analysis	89
l) Elemental Analysis	89
VI. Results and discussion	90
5. Polycondensation of decafluorobiphenyl and TBBT.....	90
c) Polymerization optimization	90
d) Characterization	95
(i) SEC analysis.....	95
(ii) NMR analysis	96
(iii) Elemental analysis	98
(iv) Thermogravimetric analysis	99
6. Polymerization of decafluorobiphenyl and TMSTB	100
7. Polymerization of decafluorobiphenyl and Biphenyl-4,4'-dithiol	101
8. Polymerization of decafluorobiphenyl and hexane-1,6-dithiol	102
b) Characterization.....	103
(iv) NMR analysis	103
(v) SEC analysis	104
(vi) Thermogravimetric analysis	105
7. Polymerization of TBBT and phosphonated octafluorobiphenyl	106
c) Phosphonation of decafluorobiphenyl monomer	107
d) Polycondensation	109



8. Polymerization of 4,4'-thiobisbenzenethiol and disodium 3,3'-disulfonate-4,4'-difluorodiphenylsulfone	111
IV. Conclusion	112
V. References	114



This chapter is dedicated to the synthesis of the prepolymer needed to prepare a proton-exchange Membrane (PEM) for the water electrolysis. After an introduction about electrolytes and membranes of polymers, the polymerization processes are explained. The different polymerizations reactions are discussed and followed by the characterization techniques, and finally, ending with the conclusions.

I. Introduction

1. Polymer definition and different polymerization reactions

The first time the polymer concept appeared was in 1832 when Berzelius wrote *“To distinguish between similar cases of agreement of composition with different properties, I propose to term these substances polymeric”*.¹ This definition was too generic and included cases where no polymer was involved. He studied hydrocarbons, and according to his definition, butylene (C_4H_8) and hexene (C_6H_{12}) were both polymers of ethylene (C_2H_4) as these chemicals exhibit the same chemical composition with different molecular weights. It took almost a century, up to 1920 before the modern concept of polymer (being a macromolecule with giant molecular weights and made up of repeating units) was proposed by Hermann Staudinger².

During this period, discussion of polymer existence was the subject of scientific debates. In 1859 both A.V. Lourenço and C. A. Wurtz reported the first sought polymer synthesis. They synthesised polyethylene glycols following two different synthetic routes. While Lourenço performed the condensation reaction of ethylene glycol with ethylene dyhalide, Wurtz carried out the same reaction using ethylene oxide with water or acetic acid.³ At that time, Lourenço noted two important properties to describe a polymer, the first one is the increase of the viscosity (η) as n (n being the number of ethylene oxide units) increases and the second is the recognition that as n increased to infinity the chemical formula approached the formula of ethylene oxide.⁴ From these works, the following chemical formula for the ethylene oxide was proposed (Figure II- 1):

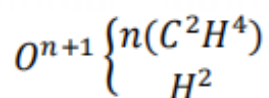


Figure II-1. Poly(ethylene oxide) formula according to Lourenço.⁵

Interestingly, the formula has remained similar for more than 160 years. The International Union of Pure and Applied Chemistry (IUPAC) defines poly(ethylene oxide) as being $HO(C_2H_4O)_nH$. It should be noted that these pioneering works were the beginning of a branch of chemistry that would become of a major importance in the 20th century. However, at that time organic chemists stayed mainly focused on obtaining “pure” substances, and polymers were not considered within this category since an accurate and strict formula could not be obtained. Synthetic polymers remained therefore in oblivion until the beginning of the 20th century.

The polymerization processes were defined by Carothers's in 1929. He distinguished addition from condensation polymerization.⁶ The definitions were based on the chemical composition of monomers, polymers, and on the occurrence of side-products of low molar mass produced during the polymerization process. The last occurs within the condensation polymerization, e.g. with the production of water when acid and alcohol are used as monomers. It should be admitted that Carothers definition remained incomplete as the mechanism was not fully studied and completely understood at that time. In 1953 Paul J. Flory distinguished the step-growth from the chain polymerization processes (Figure II-2, right). In the latter, a polymer is obtained after different steps occurring during the reaction, while in step polymerization, similar and concomitant steps are defined during the process (Figure II-2, left).

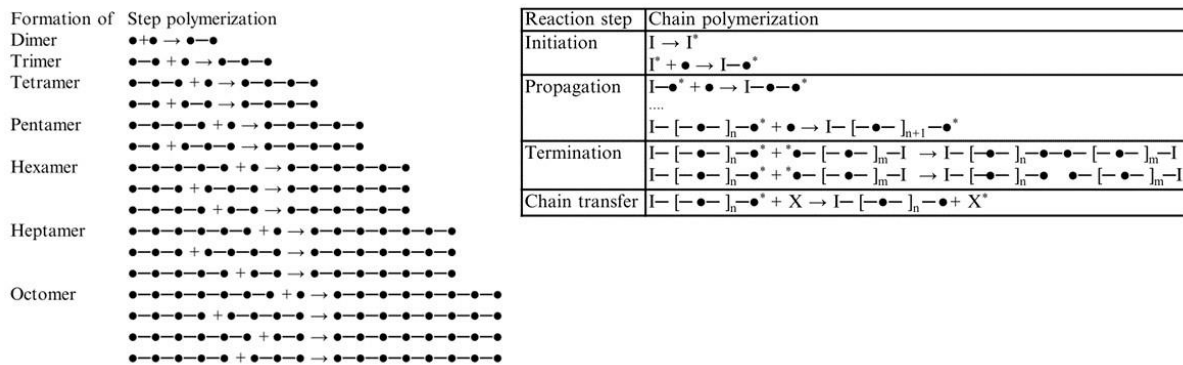


Figure II- 2. Schematic schemes of step growth (left) and chain growth (right) polymerization processes⁷, ●: monomer, -: covalent bond, I: initiator, X: species present in the reaction system (e.g. monomer, solvent, additives, polymer chains...). The * indicates that the species is activated.

Taking a closer look to Figure II-2, it can be seen a large number of chains of different lengths can be found at the end of the reaction. This variability received the name of Dispersity (\mathfrak{D}). It is defined as the ratio of the mass-average molar mass (\bar{M}_w) (Equation II-3) to the number average molar mass (\bar{M}_n) (Equation II-2). It gives an idea of the mass differences of the macromolecules of the polymer sample (Equation II-1).⁸

$$\mathfrak{D} = \frac{\bar{M}_w}{\bar{M}_n}$$

Equation II-1. Definition of the dispersity, \mathfrak{D}

$$\bar{M}_n = \sum_{i=0}^{\infty} \frac{N_i}{\sum N_i} M_i$$

with N_i = Number of molecules i and M_i = Mass of molecules i

Equation II-2. \bar{M}_n is the number-average molar mass

$$\bar{M}_w = \sum_{i=0}^{\infty} \frac{W_i}{\sum W_i} M_i$$

with $W_i = \frac{N_i \times M_i}{\sum N_i \times M_i}$ weight fraction

Equation II-3. \bar{M}_w is the weight-average molar mass



\bar{M}_n (Equation II-2) gives every molecule the same importance no matter its size and results in a lower value than \bar{M}_w (Equation II-3) where high molar masses have a larger influence in the result.⁹

Most polycondensations run through a step-growth polymerization mechanism where high molar mass polymers are obtained at the end. In a polycondensation, the control of the dispersity is harder than in chain-growth polymerization since all the steps defined within the Figure II-2 give a high quantity of N_i with a high range of M_i . At the same time, conversion must reach almost 100 % to obtain a high \bar{M}_w while in a chain-growth mechanism, high \bar{M}_w are reached without the need of a high conversion rate of the monomer (Figure II-3).

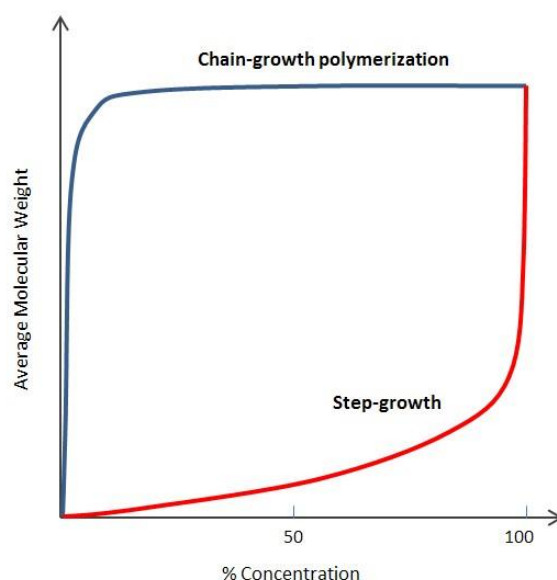


Figure II-3. Average \bar{M}_w vs monomer conversion for both chain-growth and step-growth polymerizations.¹⁰

One of the main drawbacks of polycondensations is the hydrolysis reactions being a backward reaction (Figure II-4). Hydrolysis causes the break of the macromolecular chain therefore decreasing the Mw and changing the properties of the polymer. If hydrolysis is complete, it eventually brings up to the initial monomers.

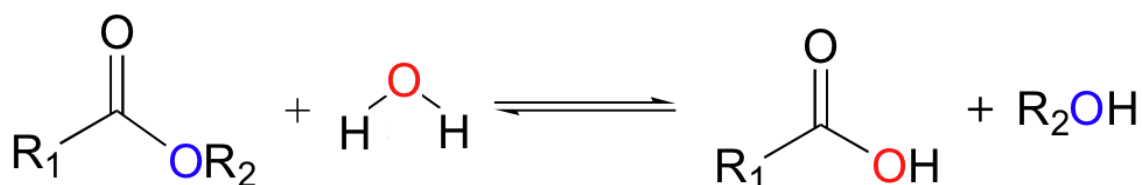




Figure II-4. Hydrolysis of an ester. R1 and R2 being parts of the polymer, ending in two separate molecules when hydrolysis occurs.

In the following part, the proton-exchange membranes (PEM) are defined to describe the specification of the polymer needed to fulfil objectives of that work. Commercially available membranes are also reported and described as reference materials.

2. Proton-exchange membrane (PEM)

Research related to ion exchange membranes can be tracked back to 1925 when Michaelis and Fujita studied homogeneous membranes.¹¹ These studies constitute the foundation for the synthesis of the different membranes that were synthesised in the following decades.

There are many different types of membranes depending on the type of targeted electrochemical applications. As explained in the review of S. Peighambardoust¹², there are mainly two ways of classifying membranes. It can be based (i) on the materials used, i.e. perfluorinated (Nafion®), partially fluorinated and non-fluorinated or based in the process of (ii) the preparation method (acid-base blends, supported composite membrane and poly-AMPS (poly(2-acrylamido-2-methylpropanesulfonic acid))¹³ (to be seen in chapter 4).

Among different commercially available PEMs, my work was focused on PFSA (perfluorosulfonic acid polymers)¹⁴, which belongs to the perfluorinated group. In this group, the commercially available Nafion® from Dupont and Aquivion® from Solvay are the most worldwide-known membranes (see Figure II-5). Within this work, Nafion® has been chosen as reference material due to its availability¹⁵ (see chapter 1) and extended use as golden standard PEM material in scientific reports, papers, and reviews.

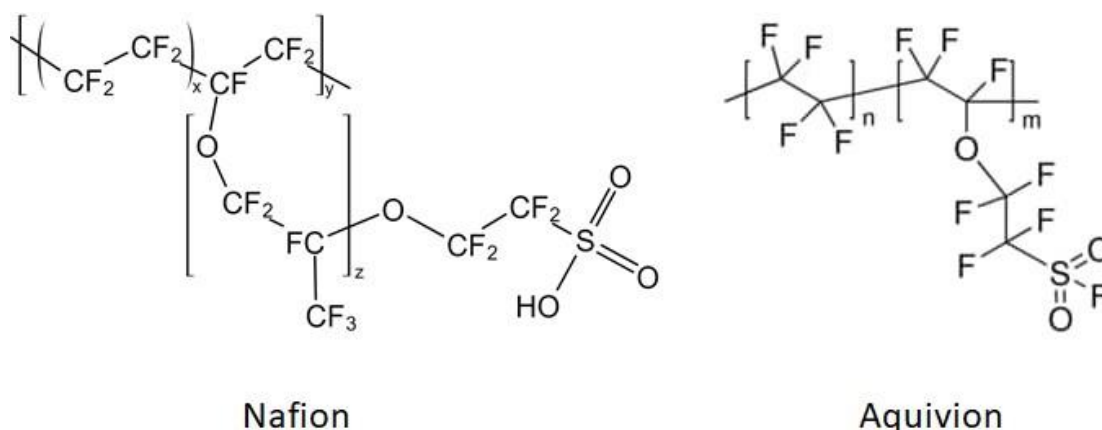


Figure II-5. Structures of Nafion® & Aquivion®, two polymers for PEMs.¹⁶

Both Nafion® & Aquivion® are perfluoropolymers with sulfonic acid groups (PFSA, see Figure II-5) that are responsible of the proton transfer through the membrane (see chapter 1). The combination of perfluorinated polymeric backbones with such acidic groups has been proved to give a high chemical resistance with an appreciable protonic conductivity (of ca. 100-200 mS/cm depending on temperature (T) and relative humidity (RH) values). However, the conductivity remains highly dependent on temperature and humidity. Within this work, my goal was the elaboration of a polymer membrane with chemical and mechanical stability and a target conductivity as high as 200 mS/cm at 90 % RH and at a temperature up to 90 °C.

3. Project strategy

It was decided to choose decafluorobiphenyl as one of the comonomers to perform polycondensation as it offers the possibility of multiple substitutions of its fluorine atoms and at the same time will be the hydrophobic part of the polymer, which is needed to work in an aqueous environment. Additionally, instead of having an ether chemical group like in Nafion® & Aquivion®, the thioether bridge C-S-C is targeted. After the synthesis of these polymers, PEM will be synthesised and their properties compared to those of Nafion® referred as our standard material.

The targeted polymers were chosen from the works developed by the Kerres group in university of Stuttgart¹⁷. The choice of the comonomers was based on the findings from Schuster *et al.* who have proved that the use of arylene ionomers connected by sulfones (-



SO₂- groups) had a high thermooxidative and hydrolytic stability.¹⁸ Following this concept and the work of S. Takamuku about hypersulfonated polyelectrolytes, it was decided to start with the 4,4'-thiobisbenzenethiol (TBBT) and the decafluorobiphenyl (DFBP) substrates for the polycondensation reaction (Figure II-6). TBBT is a bi-functional monomer with two S-H terminal groups, while DFBP has 10 reactive fluorine atoms. It should be mentioned that the fluorines in para positions are expected to be the most reactive ones and lead to a linear polymer.

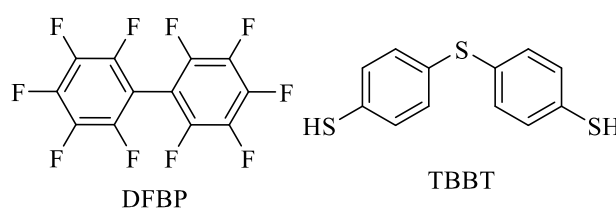


Figure II-6. Decafluorobiphenyl (DFBP) and 4,4'-Thiobisbenzenethiol (TBBT) comonomers.

Within a polycondensation process, the extent of polymerisation (p), is equal to 1 (or 100 %) when all the functional groups of the monomers have reacted. The extent of polymerisation is calculated using equation II-4¹⁹:

$$p = \frac{2}{f} - \frac{2}{x \cdot f}$$

Equation II-4. Extent of polymerization (p), with x = number average value of monomer units in a polymer molecule, f = monomer unit functionality (number of functional groups per monomer molecule).

In this case, if the decafluorobiphenyl monomer unit reacted in all the 10 potential fluorine atoms we would have a A²B¹⁰ system, with A being the TBBT and B the DFBP monomer units. To calculate the monomer functionality of the reaction, an average between the 2 different monomers has to be determined, the formula (equation II-5) proposed by Carothers is the following:

$$f_{av} = \frac{\text{functionality of A unit} \times \text{mol of unit A} + \text{functionality of B unit} \times \text{mol of unit B}}{\text{mol of unit A} + \text{mol of unit B}}$$

Equation II-5. Monomer functionality average calculation from Carothers²⁰



Then in the case where all of fluorine atoms of the decafluorobiphenyl react equation II-5 is equal to:

$$f_{av} = \frac{2 \cdot 5 + 10 \cdot 1}{5 + 1} = 3.3$$

When the average extent of polymerisation is at its maximum and high enough, $\frac{2}{x \cdot f}$ within equation II-4 becomes negligible and the extent of polymerisation turns into equation II-6:

$$p = \frac{2}{f_{av}}$$

Equation II-6. Degree of polymerisation when all the functionalities of the monomers have reacted.

Therefore, having the result of applying f_{av} , $p = \frac{2}{3.3} = 0.6$ meaning that the theoretically limiting yield of the reaction would be 60 %. In other words, gelation (cross-linking) would occur starting at 60 % yield.

If linear (non-crosslinked) and only the para positions (p-position) are now considered, being the most favourable ones to react, the system could be assimilated to an A²B² system.

Equation II-4 turns to equation II-7.

$$p = \frac{2}{f} - \frac{2}{x \cdot f} = \frac{2}{2} - \frac{2}{x \cdot 2} = 1 - \frac{1}{x}$$

Equation II-7. Degree of the reaction with an A²B² system.

In that case $f_{av} = \frac{2 \cdot 1 + 2 \cdot 1}{1 + 1} = 2$, and the extent of the reaction may then be quantitative before gelation phenomenon.

To have a clearer view on how this formula applies, the following Table II-1 gives some number average value of monomer units in a polymer molecule (x) related to the extent of polymerization (p):

P	0	0,25	0,5	0,75	0,9	0,95	0,99	0,999	0,9999
X	1	1,33333333	2	4	10	20	100	1000	10000

Table II-5. Evolution of the average degree of polymerization with the evolution of the polymerization.



In Table II-1 it can be observed the average value of monomer units in a polymer molecule is initially 1 when the extent of the polymerization is 0 (meaning it hasn't started) and how it increases exponentially when high degrees of polymerization are reached.

This simple demonstration highlights the fact that a slight change in the monomer reactivity and/or monomer ratio hugely affects the mass-average molar mass to be obtained (Figure II3, step growth).²¹

(Figure II-7) reports the polycondensation reaction of TBBT and DFBP considering the p-position of decafluorobiphenyl as the only position to react. This higher reactivity of the p-position has been observed in several polycondensation reactions like the ones observed by Tkachenko *et al.*²² or Li *et al.*²³ for the preparation of fluorinated poly(arylene ether)s or Xu *et al.*²⁴ for the synthesis of poly(arylene ether sulfone).

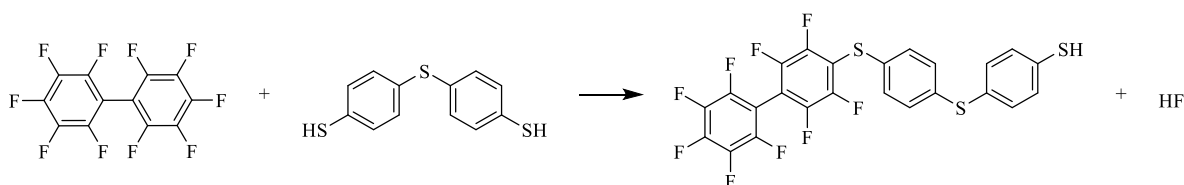


Figure II-7. Polymerization of Decafluorobiphenyl (DFBP) and 4,4'-Thiobisbenzenethiol (TBBT).

Within a polycondensation, the dispersity (\mathcal{D}) is defined as:

$$\mathcal{D} = \frac{\bar{M}_w}{\bar{M}_n} = 1 + p$$

Equation II-8. Dispersity (\mathcal{D}) with p being the degree of polymerization, \bar{M}_n the number-average molar mass and \bar{M}_w the weight-average molar mass.

Therefore, the dispersity (\mathcal{D}) is equal to 2 by quantitative conversion of both monomers.

In the following schemes (Figure II-8 and Figure II-9) a map of our whole strategy for the polymerizations is reported. The next paragraphs will sort out each one of these polymerizations and detail all the steps taken.

Within Figure II-8 the synthesis access to polyfluorothioethers prepolymer is shown, i.e. the polycondensation of decafluorobiphenyl (DFBP) and biphenyl or dialkyl thiol derivatives.



Targeted prepolymers are meant to be used for post-functionalization (see chapter 3) to respond to the PEM requirements.

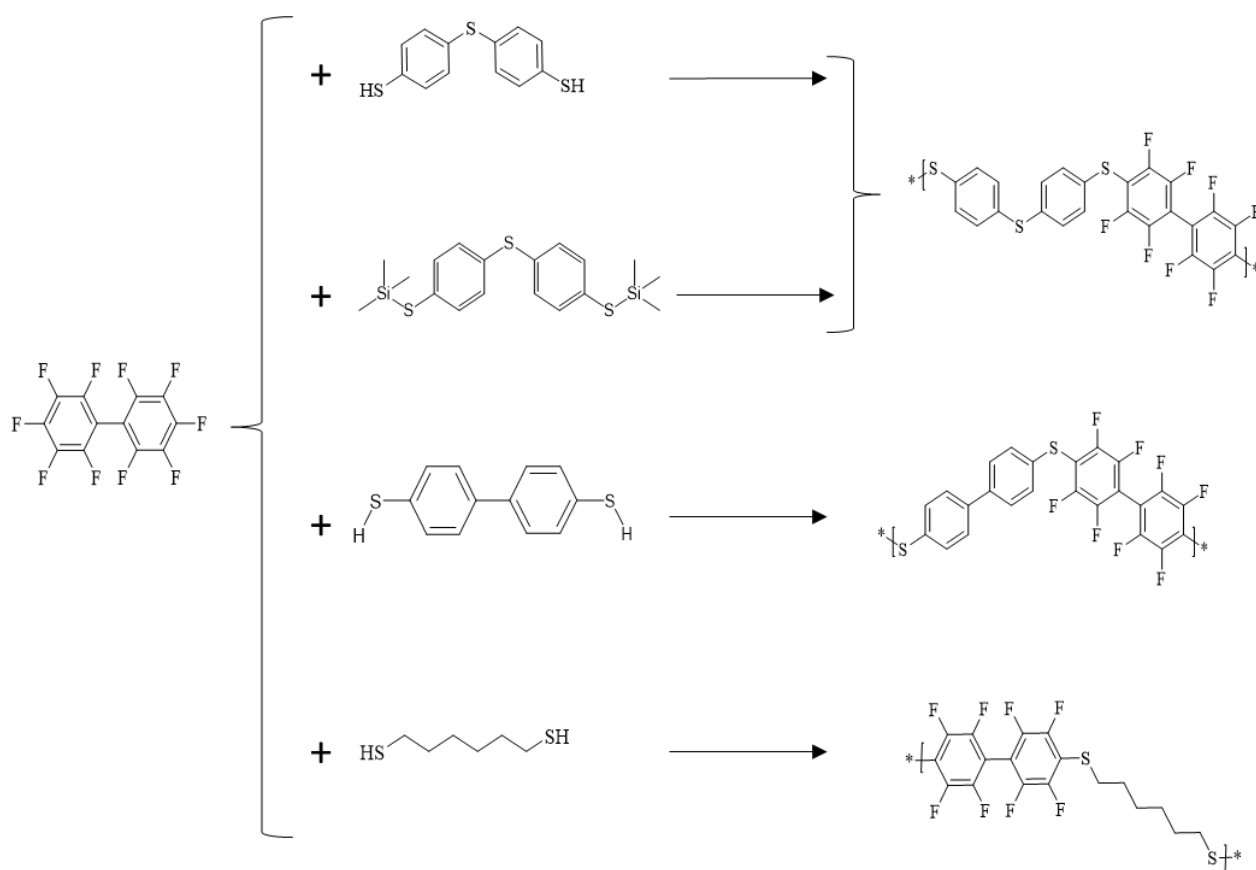


Figure II-8. Reactions of DFBP with the different dithiols and the resulting copolymers.

Within Figure II-9, the synthesis of functionalized polymers is shown, the polycondensation of functionalized monomers are attempted to avoid any further steps of post-reaction onto the fluorine group.

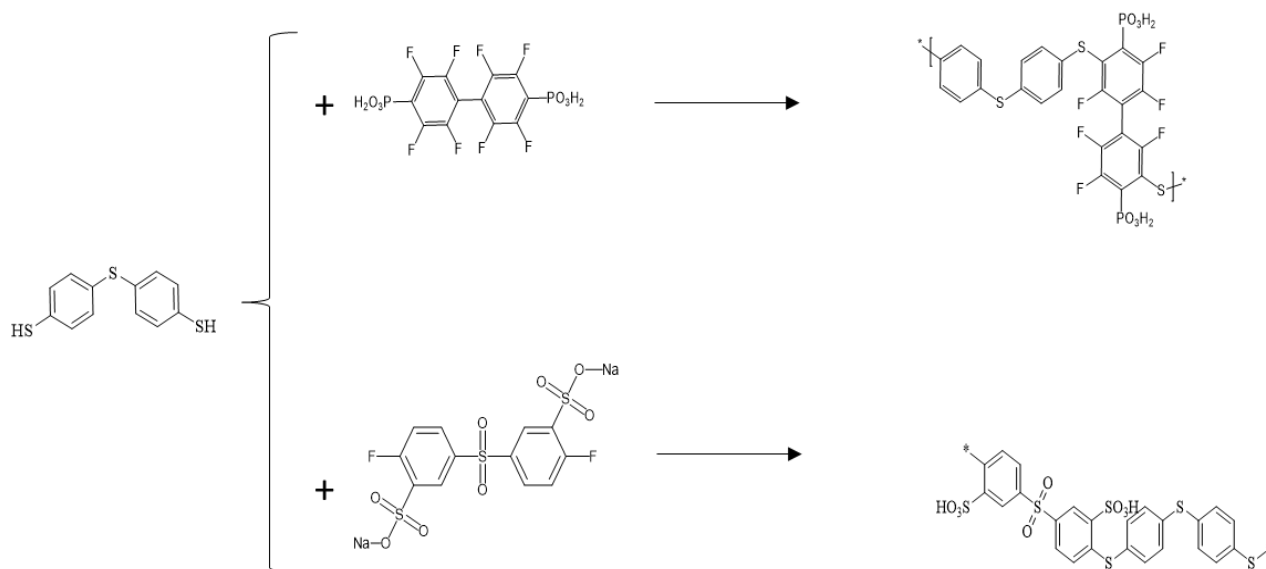


Figure II-9. Polymerisation of di-functionalised monomers with TBBT and their polymer structures.

II. Materials and methods

1. Chemicals and materials

Dimethylsulfoxide (DMSO), N,N-Dimethylacetamide (DMAc) were of “anhydrous” quality (<0.005 % H₂O, 99.5 % purity, Aldrich). 4,4'-Thiobisbenzenethiol (98 %), Decafluorobiphenyl (99 %) and Potassium carbonate (≥99 %) were purchased from Sigma Aldrich. MilliQ water (18.2 μS at 25 °C) and isopropanol (≥70 %, VWR) were used for the purification of the polymer. Hydrogen peroxide (H₂O₂, 34.5–36.5 %, Sigma-Aldrich), acetic acid (CH₃COOH, analytical reagent grade, Fisher Chemical), trifluoroacetic acid (CF₃COOH, ≥99 %, Sigma-Aldrich) and sulfuric acid (H₂SO₄, 95-97 %, Sigma-Aldrich) were used as received. Dialysis tubing cellulose membrane, 12 000 MWCO, Aldrich D9777 was used for dialysis in water.



2. Experimental

a) Polycondensation of decafluorobiphenyl and 4,4'-thiobisbenzenethiol

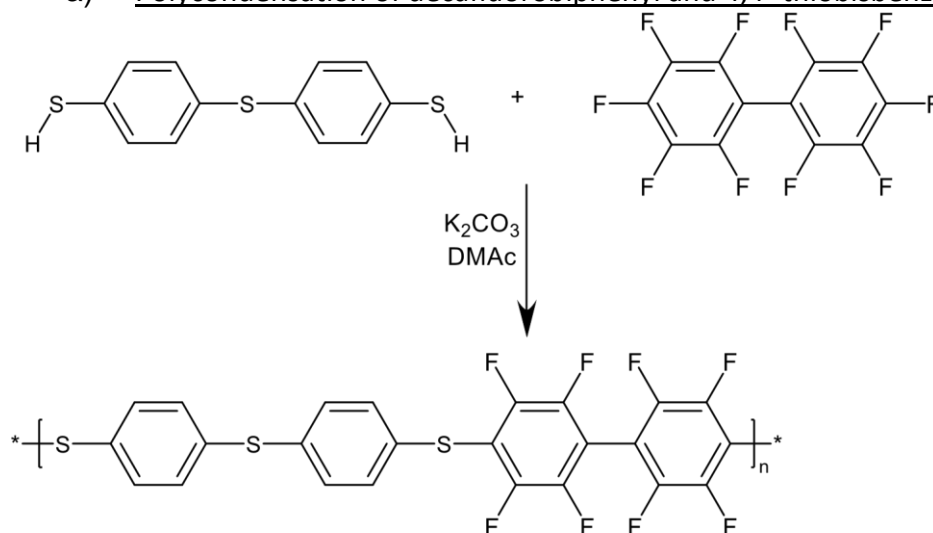


Figure II-10. Polycondensation of DFBP and TBBT

(i) Polycondensation by the “conventional heating” method

Within a typical procedure, the glassware is dried at 100 °C for 1h right before the reaction. 4,4'-Thiobisbenzenethiol (TBBT, 10.22 g, 0.04mol), decafluorobiphenyl (DFBP, 13.50 g, 0.04 mol) and the K_2CO_3 (33.17 g, 0.024 mol) are added in a 250 ml three neck round bottom flask, equipped with a reflux condenser and an argon inlet. The reagents are stirred under argon for 30 min in 100 ml of dimethylacetamide (DMAc) which is slowly added via syringe. Concentrations of TBBT and DFBP are 0.4 M. The reaction mixture is heated up to 100 °C and left 6h for under stirring. During the process, the solution becomes viscous and the solution turned to dark orange. After 6h additional DFBP (0.5 g, 0.002 mol) dissolved in 5 ml of DMAc is added into the reaction mixture and the reaction is left under stirring at 100 °C for one additional hour. The viscous solution is cooled down at room temperature and then poured on 1.5 L of distilled water and 200 ml of 96 % sulfuric acid is slowly added to the medium. The final polymer is left under stirring overnight, filtered out, and washed with distilled water several times until the filtrated water had neutral pH, measured by pH indicator paper-strips. The polymer is then added to 200 ml of isopropanol (>99 %) and left under stirring overnight



before being filtered again and dried at 60 °C under vacuum (2×10^{-3} mbar) (yield >92 %). ^1H NMR δ_{H} (400 MHz; CDCl_3) 7.41 (d, J 8.26 Hz, H_1), 7.29 (d, J 7.79 Hz, H_2); ^{19}F NMR δ_{F} (235 MHz; CDCl_3) -136.8 (F_a), -131.7 (F_b).

(ii) Polycondensation by the “microwave method”

In a typical procedure the microwave tube is dried at 100 °C for 1h right before the reaction. In the microwave tube, a magnetic stirring bar is added with 4,4'-Thiobisbenzenethiol (1.02 g, 0.004 mol), decafluorobiphenyl (1.45 g, 0.004 mol) and 10 ml DMAc. The mixture is degassed with N_2 for 15 min before the addition of K_2CO_3 (3.3 g, 0.024 mol). The microwave tube is equipped with a condenser and installed inside the microwave reactor. The reactive medium is heated up to 100 °C under reflux during 6 h at 100W using a dynamic mode irradiation. After 6h, additional decafluorobiphenyl (0.05 g, 0.2 mmol) dissolved in 3 ml of DMAc is added to the reaction mixture is stirred for one more hour. The viscous solution is then poured into 0.5 L of distilled water. After precipitation, 50 ml of 96 % sulfuric acid is slowly added to the medium. The polymer solution is left under stirring overnight, filtered out, and washed several times with distilled water until the filtrate showed neutral pH. The solid precipitate is added to 200 ml of isopropanol (>99 %) left under stirring overnight before to be filtered out and dried at 60 °C. No F peaks were observed in the ^{19}F NMR. Even though there was a precipitate (1,06 g, 48 %), the NMR didn't confirm that the polymer had been obtained.

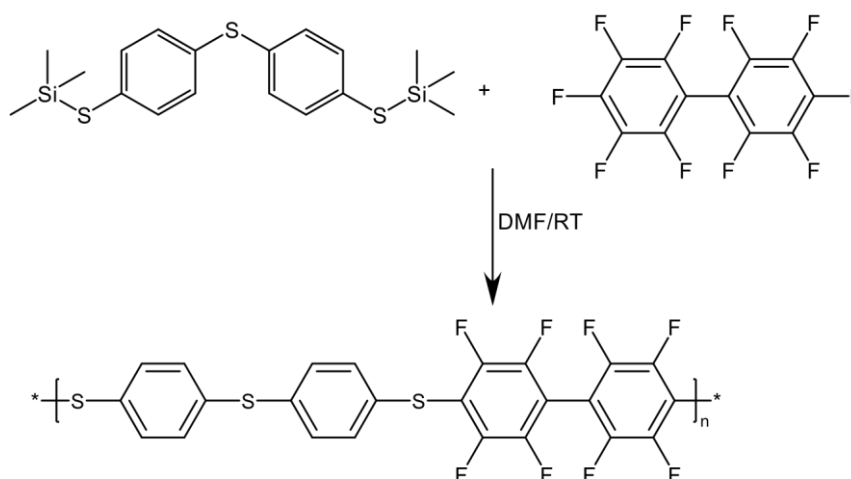
b) Polymerization of decafluorobiphenyl and 4,4'-bis(trimethylsilyl)thiobenzene

Figure II-11. Polymerization of decafluorobiphenyl and TMSTB

In a 100 ml three-necked round bottom flask (equipped with magnetic stirrer, reflux condenser and argon inlet), 4,4'-bis(trimethylsilyl)thiobenzene (TMSTB, 5 g, 12.67 mmol) were introduced. DMF (Dimethylformamide) (50 ml) were then added to the flask under argon. After TMSTB dissolution, decafluorobiphenyl (DFBP, 4.27 g, 12.67 mmol) was added. The mixture was allowed to react for 1 hour at room temperature (20 °C). The viscous solution was then poured into 2 L of distilled water and filtered. The filter residue was stirred overnight in 400 ml of isopropanol, filtered off and dried under vacuum at 60 °C during 24 h and at 90 °C for 2 h under vacuum (2×10^{-3} mbar). (3.9 g, yield = 57 %). $^1\text{H NMR}$ δ_{H} (400 MHz; CDCl_3) 7.31 (d, J 8.26 Hz, H_1), 7.20 (d, J 7.79 Hz, H_2); $^{19}\text{F NMR}$ δ_{F} (235 MHz; CDCl_3) -136.8 (F_a), -131.7 (F_b), 137.0 (F_a'), 149.6 (F_b'), -160.2 (F_c).

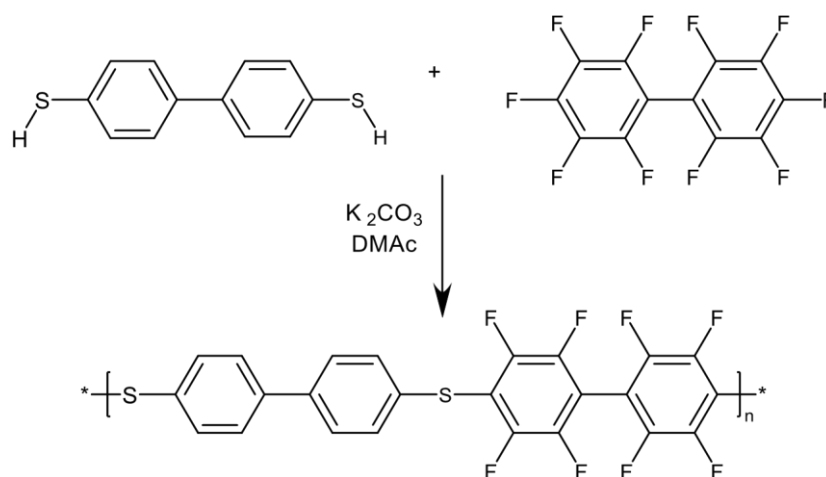
c) Polymerization of decafluorobiphenyl and Biphenyl-4,4'-dithiol

Figure II-12. Polymerization of decafluorobiphenyl and biphenyl-4,4'-dithiol

In a 250 ml three-necked round-bottom flask (equipped with magnetic stirrer, reflux condenser and argon inlet) decafluorobiphenyl (DFBP, 3.38 g, 0.04 mol), [1,1'-biphenyl]-4,4'-dithiol (8.73 g, 0.04 mol) and potassium carbonate K_2CO_3 (33.17 g, 0.24 mol) were mixed together. DMAc (100 ml) were then added to the flask under argon. After monomers were dissolved the temperature was raised up to 100 °C and the reaction medium was left overnight (17 h) under stirring. The solution was poured into 1 L of distilled water, no precipitation was observed.

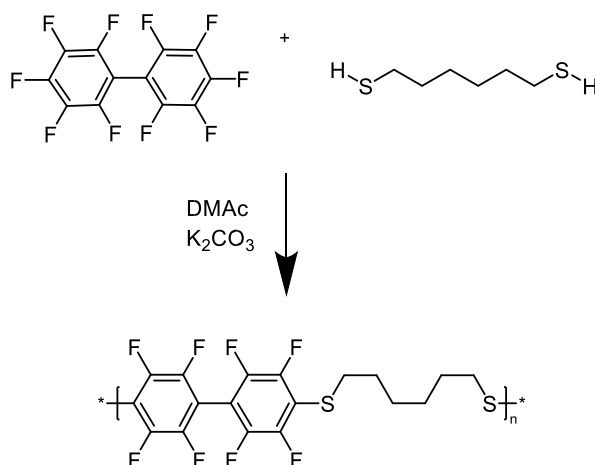
d) Polymerization of decafluorobiphenyl and hexane-1,6-dithiol

Figure II-13. Polymerization of decafluorobiphenyl and Hexane-1,6-dithiol



In a 250 ml three-necked round-bottom flask (equipped with magnetic stirrer, reflux condenser, septum and argon inlet), hexane-1,6-dithiol (6.01 g, 0.04 mol) was weighted directly to the flask before to add potassium carbonate K_2CO_3 (33.17g, 0.24g) and decafluorobiphenyl (DFBP, 13.88 g, 0.04 mol). DMAc (100 ml) is then added to the flask under argon. The temperature is raised to 80 °C and the mixture is allowed to react at this temperature for 6 hours. Thereafter, the viscous solution is poured into 2 L of water, and 200 ml of 20 % sulfuric acid are added until the suspension becomes a pH around 2-3. The acidic solution is stirred at room temperature overnight, filtered and washed with distilled water until the filtrate is of neutral pH. Subsequently, the filter residue is stirred overnight in 400 ml of isopropanol, filtered out and dried at 60 °C for 18h, followed by 2 h at 80 °C under vacuum (2×10^{-3} mbar). 14.416 g obtained (yield = 81 %). 1H NMR δ_H (400 MHz; $CDCl_3$) H_4 (1.59, quintuplet), H_3 (1.41,triplet); ^{19}F NMR δ_F (235 MHz; $CDCl_3$) -138.0 (F_1), -133.5 (F_2).

e) Polymerization of phosphonated octafluorobiphenyl and 4,4'thiobisbenzenethiol

(ii) Phosphonation of Decafluorobiphenyl monomer

In a 50 ml three-necked round bottom flask (equipped with a magnetic stirrer, a reflux condenser, and an argon inlet) is filled with 5 g DFBP (14.97 mmol) and 13.90 g TMSP (46.57 mmol, 3 eq.), the flask is flushed with argon and the reactive medium is let under stirring for 10 min at room temperature before being heated up at 160 °C overnight. At room temperature, 50 ml of water are added prior to heating up the mixture to reflux for 10 min. A solid precipitate is obtained, water is partially evaporated and the solid product is filtered out and dried at 80 °C under vacuum (yield = 68 %). 1H NMR δ_H (400 MHz; $CDCl_3$) 7.31 (d, J 8.26 Hz, H_1), 7.20 (d, J 7.79 Hz, H_2); ^{19}F NMR δ_F (235 MHz; $CDCl_3$) -137.9 (F_a), -132.1 (F_b).

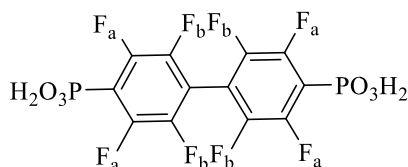


Figure II-14. Phosphonated octafluorobiphenyl



(iii) Polycondensation of 4,4'-thiobisbenzenethiol and phosphonated octafluorobiphenyl

All reactants and materials were dried overnight at 60 °C under vacuum prior to use. In a 100 ml three-necked round bottom flask (equipped with a magnetic stirrer, a reflux condenser, a septum and an N₂ inlet) were weighed TBBT (1.09 g, 0.01 mol), 4,4'-biphosphonated octafluorobiphenyl (POFBP, previously synthesised, chapter 3, II-c) (2 g, 0.01 mol) and 50 ml DMAc. The reaction mixture is degassed using N₂ until complete dissolution of POFBP. Potassium carbonate (6.03 g, 0.1 mol) (in excess) was then added to the flask under N₂ and temperature was heated up to 110 °C and left under stirring for 6h. The solution was poured into distilled water (1 L) and HCl (5 %, 100 ml) were added. A yellow precipitate appeared. It was left under stirring overnight, filtered off, washed three times with 50 ml distilled water until the filtrate is of neutral pH. The precipitate was dialyzed (dialysis tubing cellulose membrane, 12 000 MWCO, Aldrich D9777) in distilled water changing it 3 times per day during 48 h and then the dialyzed polymer was dried under vacuum at 80 °C during 12 h and at 90 °C for 2 h under vacuum (2 x 10⁻³ mbar). A yellow sticky mass was obtained. (0.74 g, yield = 25 %). ¹H NMR δ_H (400 MHz; CDCl₃) 7.55 (Broad peak, H₁ and H₂); ¹⁹F NMR δ_F (235 MHz; CDCl₃) -136.9 (F₄), -132.35(F₃), -131.9 (F₅).

f) Polymerization of disodium 3,3'-disulfonate-4,4'-difluorodiphenylsulfone and 4,4'-thiobisbenzenethiol

Disodium 3,3'-disulfonate-4,4'-difluorodiphenylsulfone (SDFPDPS) and potassium carbonate were first dried overnight at 145 °C in a vacuum oven. The polymerization was conducted in a dried and argon-filled 100 mL round-bottom flask equipped with an argon gas inlet, mechanical stirrer, and a Dean-Stark trap fitted with a condenser. The flask was charged with the disodium 5,5'-sulfonylbis(2-fluorobenzenesulfonate) (4.58 g, 0.01 mol), the 4,4'-thiodibenzenethiol (TBBT) (2.54 g, 0.01 mol) and the anhydrous potassium carbonate (2.90 g, 0.021 mol). This mixture was dried for 2 h at 90 °C under vacuum. Then anhydrous 1-methyl-2-pyrrolidone NMP (30 ml) and dry toluene (12 ml) were added under argon, and the reaction mixture was heated in an oil bath up to 150 °C for 4 h to remove any water via the



Dean-Stark trap. Toluene was then removed by emptying the Dean-Stark trap, and the reaction was allowed to continue for 36 h at 175 °C. After cooling to room temperature, the dark purple reaction mixture was slowly poured into 2-propanol (200 ml) to precipitate the polymer. The purple precipitate was separated by filtration and washed with 2-propanol. The product was redissolved in water (60 mL) and precipitated in 2-propanol (200 ml), filtrated, washed with 2-propanol, and dried at 60 °C. The polymer was finally purified by dialysis in distilled water for 48 h. The water was removed using a rotary evaporator and the product dried at $T=50$ °C in vacuum, yielding the dark-purple polymer. Conversion of the K-form into H-form succeeded by ion exchange with Dowex Marathon C (H-form, Aldrich), yielding a brownish polymer mass after drying at 60 °C in a vacuum oven. (1.62 g, yield = 23 %). No NMR could be done as it was not soluble in any solvent.

3. Technics

a) Microwave reactor

Microwave-assisted polymerization reactions were carried out in standard Pyrex vessels (total capacity of 10 ml) sealed with Teflon septum caps. The temperature profiles of the polymerization reactions were monitored using a calibrated infrared temperature. The reaction parameters (e.g., temperature, irradiation power, air cooling, stirring, etc.) were set using the on-board piloting software reaction parameters. Irradiation power was set up from 100W to 300 W and temperatures from 80 °C up to 120 °C.

b) IR spectroscopy

FTIR spectrometer (Nicolet iS50 FTIR Spectrometer) with a range of 15 to 27,000 cm^{-1} .



c) NMR spectroscopy

^1H , ^{13}C and ^{19}F NMR spectra were recorded on a Bruker Avance 400 spectrometer using deuterated dimethyl sulfoxide (DMSO-d_6) or chloroform (CDCl_3) solvents at RT.

d) Size-Exclusion Chromatography (SEC)

Used in ICVT (University of Stuttgart): An Agilent Technology SEC system (Series 1200) coupled with a viscosity detector (PSS ETA-2010) and a refractive index detector (Shodex RI71). A set of three PSS GRAM columns (30, 3000, 3000 Å) was used and calibrated with a series of polystyrene standards in N,N-dimethylacetamide (DMAc) containing 5 wt.% LiBr. All the samples were filtered by a Whatman syringe filter over a microporous PTFE membrane (1.0 μm , Whatman 6878-2510) before injecting into the column system.

Used in IPREM (UPPA): Molar masses and molar masses distributions were determined by GPC in THF on Waters pump model 515, detectors: RI ERC-101 and UV-VIS Soma S-3702 (254 nm), temperature: 30 °C, standard: polystyrene, concentration: 2 g/l, flow rate: 1.0 ml/min, columns: SDV 106, SDV 104 and SDV 500.

e) Thermal analysis

The thermal stability of the polymers was determined by thermogravimetry (TGA, Netzsch, model STA 449C) with a heating rate of 20 °C /min under an oxygen-enriched atmosphere (65–70 % O_2 , 35–30 % N_2).

f) Elemental Analysis

Elemental analysis was performed in University of Stuttgart at the institute of Organic Chemistry. A Elemental Analyzer Model 1106 from Carlo Erba Strumentazione was used.



III. Results and discussion

1. Polycondensation of decafluorobiphenyl and TBBT

a) Polymerization optimization

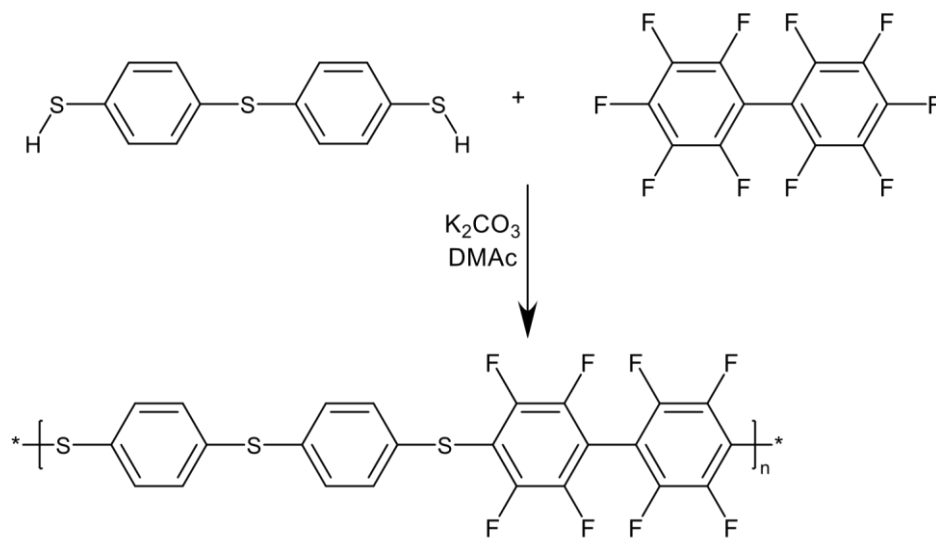


Figure II-15. Polycondensation of TBBT and decafluorobiphenyl

In this first attempt, the polycondensation of the functional monomers decafluorobiphenyl and 4,4'-Thiobisbenzenethiol was tested. Two different energy activation systems were tested for the polymerization, conventional heating and microwave irradiation.



Table II-2 reports the results obtained in conventional heating, with the parameters tested to find optimal conditions.

Name	Time (h)	K ₂ CO ₃ eq.	T (°C)	M _n	M _w	Đ
P1	17	0.75	80	7500	17900	2.4
P2	17	1.5	80	16300	53300	3.3
P3	17	3	80	47800	82300	1.7
P4	17	4	80	43500	113000	2.6
P5	6	3	100	69400	152700	2.2
P6	6+1	3	100	85000	172000	2.0
P7	6+1	3	110	34100	173000	5.1
P8	6+1	3	120	20300	321000	15.8

Table II-2. Parameters tested for the polycondensation, with potassium carbonate as catalyst base and conventional heating process with DCFB:TBBT=1:1 for P1 to P5 and DCFB:TBBT=1.04:1 for P6 to P10, extra 0,04 added after 6h and left for one extra hour. Results: polymer molar mass and dispersity

The first polycondensation (P1) was done following the work of S. Takamuku *et al.*²⁵ In that work they describe the polymerization of decafluorobiphenyl with different thiobisbenzenethiols. The first variable to be tested was the base quantity (K₂CO₃). Takumuku *et al.* used 1.5 eq. of K₂CO₃ (equivalents of base relative to the thiol (S-H) groups in the TBBT, equation II-9).

$$\text{Base equivalents} = \frac{1}{2} \times \frac{\text{mol } k_2CO_3}{\text{mol TBBT}}$$

Equation II-9. Base equivalents

To estimate the effect of the base quantity towards the reaction, 0.75 eq., 1.5 eq., 3 eq., and 4 eq. were tested at 80 °C (P2, P3, and P4 respectively). Then, to estimate the effect of



temperature, the eq. were kept constant at 3eq. and the temperature was tested from 80 °C to 120 °C (P5-P10). The results in terms of M_w are reported within Figure II-16:

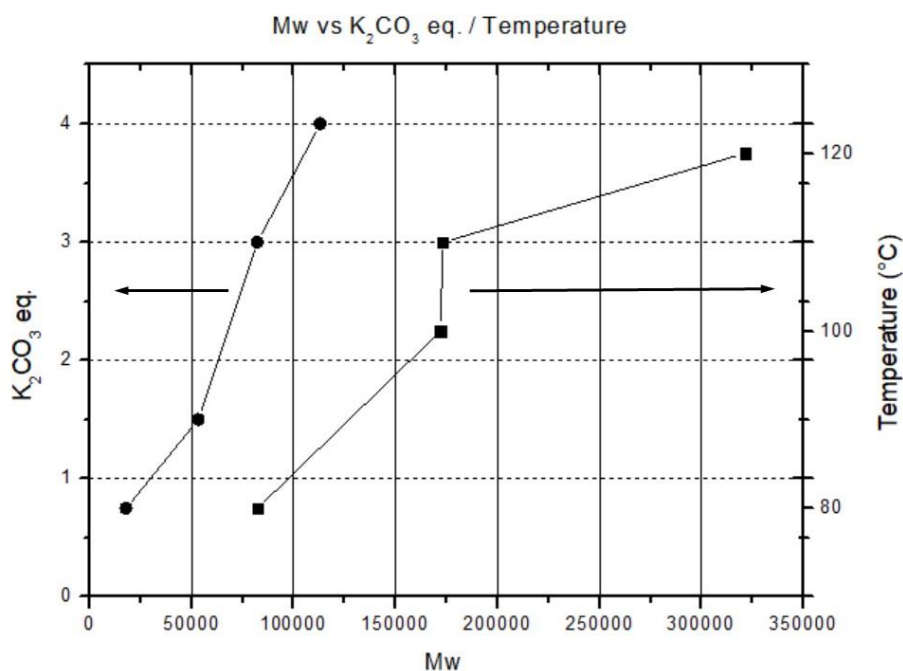


Figure II-16. M_w vs K_2CO_3 eq./Temperature

The effects of the experimental condition parameters may be summarized as follows:

- When the polymerization is performed at 80 °C, the molar mass of the polymer increases from 17,9 kDa with 0.75 eq. (P1) to 113 kDa with 4.0 eq. (P4). At the same time, the dispersity remains between 1.7 and 3.3 (table II-2) which is relatively close to the value of 2.0 which is the expected for a complete polycondensation polymerization. Larger amount of K_2CO_3 (over 4.0 eq.) was not possible due to the fact that this base is insoluble in the solvent of the reaction (DMAc) and the mechanical stirring becomes not efficient enough to ensure the control of the process, and crosslinking and insoluble cross-linked gel was obtained (Figure II-17). Therefore K_2CO_3 was kept at an excess of 3.0 eq.

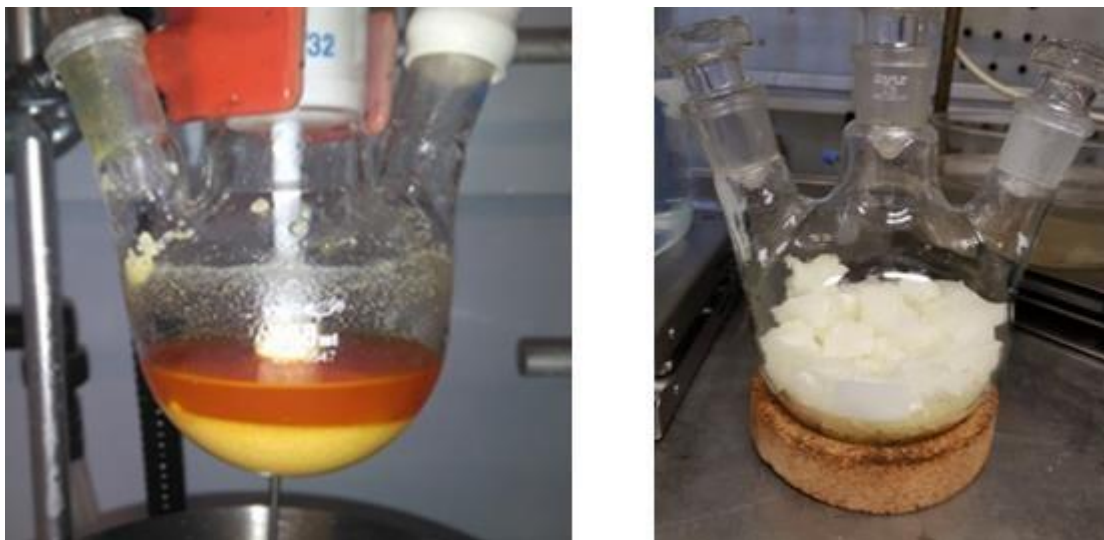


Figure II-17. Polymerization under conventional heating at 80 °C using 4.0 eq. of K_2CO_3 (left picture) and 5.0 eq. of K_2CO_3 with gelformation (right picture).

- P5 kept a $K_2CO_3 = 3.0$ eq, the temperature was raised and the reaction time was decreased at the same time. A total reaction duration was fixed to 6h for several reasons: efficiency with the perspective to be able to run the reaction within the day time and safety reasons, the reaction is left overnight at 100 °C. P5 exhibits a Mw higher than P3` Mw (table II-2), temperature seems to have a much larger impact than time. Dispersity had changed from 1.7 (P3) to 2.2 (P5) which was still in an acceptable range. Therefore all further reaction times of reactions at 100 °C or above were decreased to 6h.
- The molar ratio DCFB:TBBT of the reactions reported within the (Table II-1) was initially equal to DFBP:TBBT=1:1. To target fully end-fluorinated phenyl terminations (figure II-25) and favour further substitution, an extra 4 % (giving a total ratio of DCFB:TBBT=1.04:1) of DFBP at the end of the reaction was added dissolved in DMAc (0,3M) after 6h of polymerization. The reaction was followed by checking the precipitation in water and afterwards the product was characterized by NMR. The reactions were left one more hour at the reaction temperature to give a symmetric telechelic linear polymer with polyfluorinated phenyl terminations. Therefore all further reaction were done at 100 °C for 6+1h and DCFB:TBBT=1.04:1.

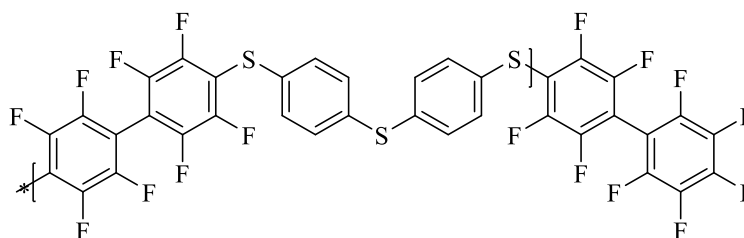


Figure II-18. Polyfluorinated poly(phenylenesulfide) with polyfluorinated phenyl terminations.

- The increase of temperature above 100 °C, P7 and P8 (see table II-2), brought an increase of Mw from 17200 to 321000 but an even higher increase in dispersity (\bar{M}_w/\bar{M}_n) from 2 to 15.8. These polymerizations were harder to control as the temperature was increased and reproducibility experiments showed cross-linking and gelation. Therefore 100 °C was selected as the optimized temperature.

As a conclusion, the optimised conditions to obtain higher quantities (yield 96 %) of the polymer backbone for further use were determined to be 100 °C and 3 eq. of K_2CO_3 during (6+1)h and DCFB:TBBT=1.04:1 (P6 shown in Figure II-19).



Figure II-19. P6 Fluorinated polythioether polymer precipitation in acidic medium (left) and P6 after drying



In a last approach, the reaction was tested under microwave irradiation, with a targeting reaction temperature of 100 °C. In the literature, application of microwave heating for polycondensations reactions has increased in the last 15 years. The main benefits are reduced reaction time and energy consumption as well as an increase of the Mw of polymers.²⁶

A Discover™ microwave equipment was used for the polymerization.²⁷ Whatever the conditions tested (irradiation power (from 100W to 300 W) and the reaction time (from 1h to 6h), no polymer was obtained. Zsuga *et al.* work showed how the dipole moment of the monomers influences greatly in the success of microwave as the heating method to obtain high Mw in short times.²⁸ For a substance to be microwaveable, it must possess an asymmetric molecular structure. However, our comonomers are symmetrical and have no dipole moment, and this is the probable reason of the failure of this strategy. No further attempts were done.

b) Characterizations

While characterization were performed for every final polymers reported in Table II-1, the results and the discussion will take the example of P6 in the following. Note that same treatment analysis and similar results were obtained for all the final polymers in NMR analysis, TGA and elemental analysis

(i) SEC analysis

Figure II-20 reports the results in terms of molar masses and dispersity. The shape of the curve shows a normal distribution having low number of high and low Mw polymers.

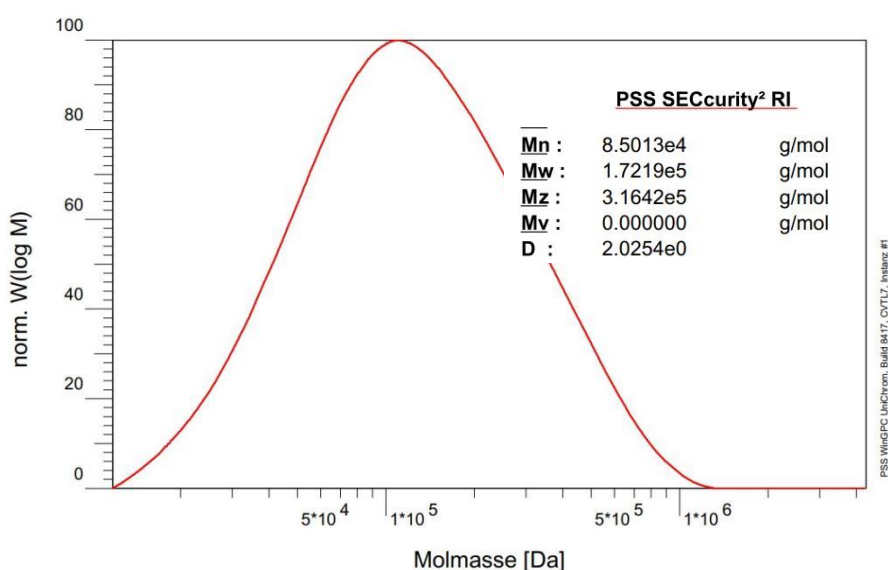


Figure II-20. SEC curve of P6

(ii) NMR analysis

^1H and ^{19}F NMR spectra of P6 obtained are shown in Figures II-28, II-29 respectively.

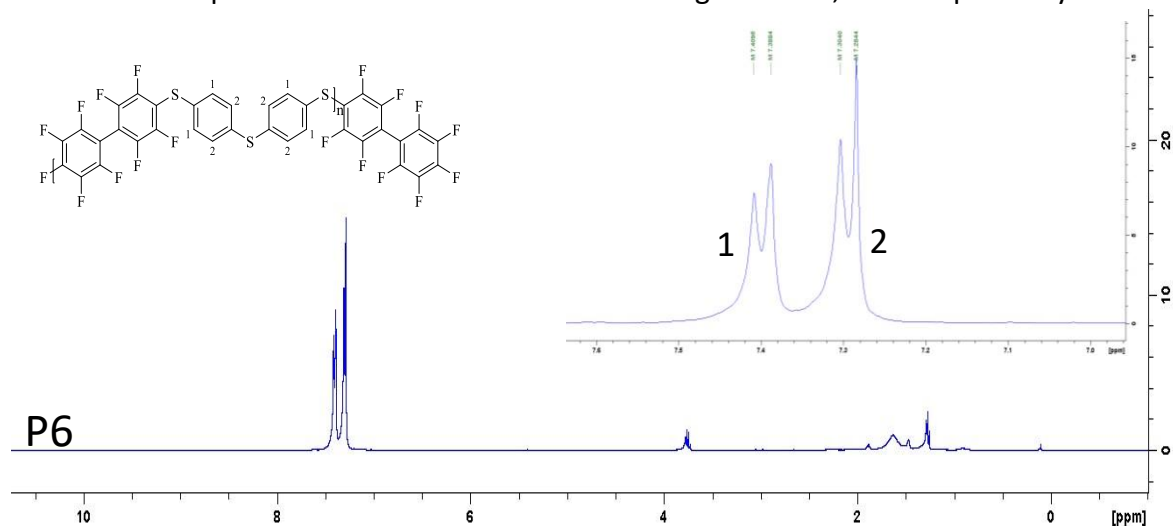


Figure II-21. ^1H NMR P6

In ^1H NMR the doublet peak overlaps with the CDCl_3 (peak 2 in Figure II-21). External protons (1)(H, peak at 7.4ppm) are less shielded as the electronic density around the $-\text{S}-$ bridge (2) the fluorinated tetraphenyl is lower than the internal protons (1) (H_2 , peak at 7.3ppm) which are linked to a more shielded carbon (Figure II-28). In simulated ^1H NMR spectra (performed



with the Chemdraw software), lower values for both proton signals were obtained: 7.27 ppm and 7.14 ppm, instead of 7.40 ppm and 7.30 ppm respectively.

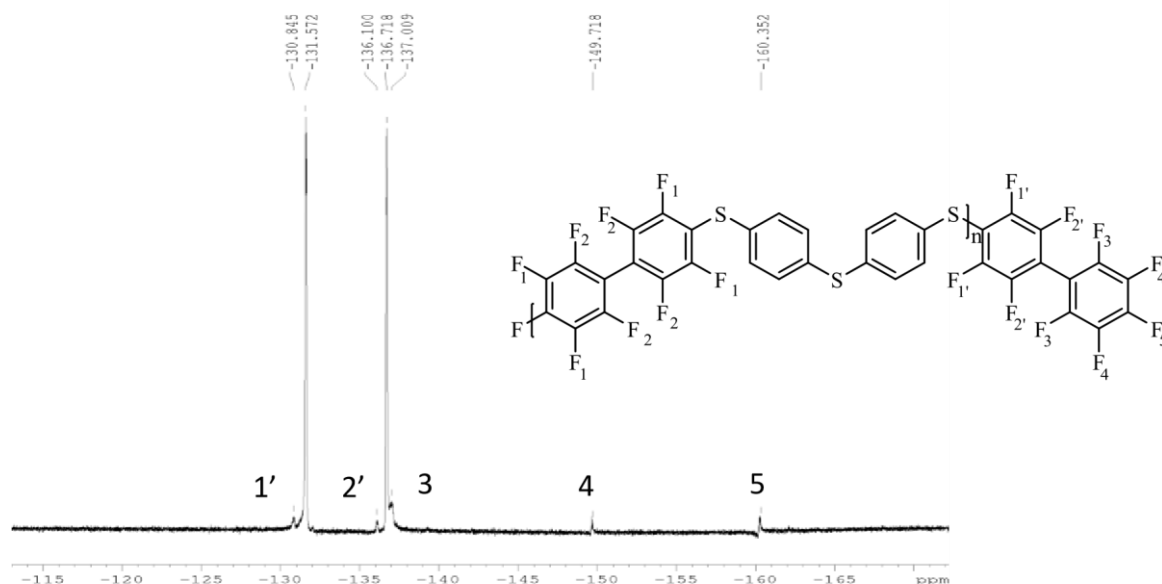


Figure II-22. ^{19}F NMR P6

The ^{19}F NMR is reported within figure II-22. The main ^{19}F NMR peaks at -131.6 ppm and -136.7 ppm correspond to F_2 and F_1 respectively. The smaller peaks at -130.8 ppm and 136.1 ppm next to them correspond to the $\text{F}_{2'}$ and $\text{F}_{1'}$ respectively. F_3 peak is at -137.0 ppm, almost indistinct from $\text{F}_{2'}$ while F_4 and F_5 appear much more shifted at -149.7 ppm and -160.4 ppm respectively. This NMR spectra is in line with the fluorinated polyarylether described by Frank Mercers *et al.*²⁹ and can be also compared to the decafluorobiphenyl molecule ^{19}F NMR (Figure II-23). In that ^{19}F NMR, 2 of the peaks (-150.0 ppm and -160.9 ppm) are almost the same as the ones we observe in the polymer (-149.7 ppm and -160.4) belonging to the end capping group. The fact that the peak at -138.7 ppm (Figure II-23) does not appear in our polymer spectra means that there is no monomer left and confirms we have nonafluorobiphenyl groups as end-capping groups.

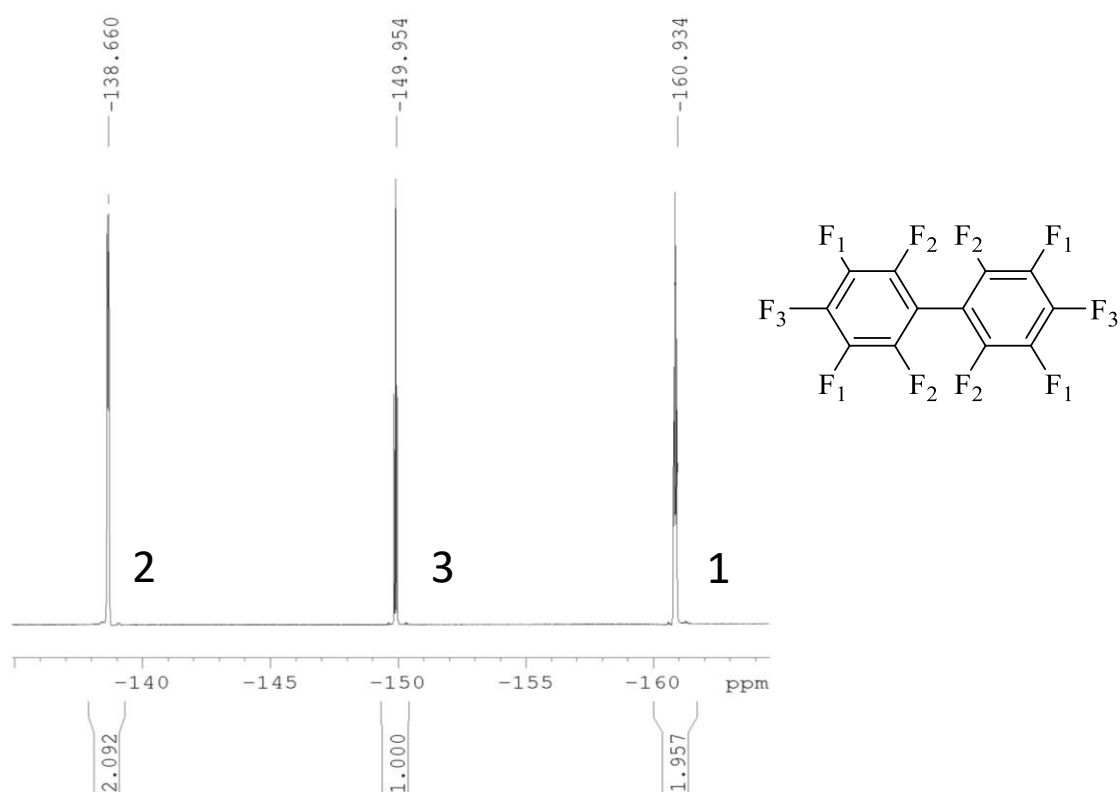


Figure III-23. ¹⁹F NMR Decafluorobiphenyl

(iii) Elemental analysis

Deviation of less than 0.5 % for both C and S compared to the theoretical expected values and a difference of less than 5 % of the theoretical value from H are obtained (Table II-3):

ELEMENT	P6 THEORETICAL	P6 EXPERIMENTAL	DEVIATION IN %
C	52.9	52.68	-0.4
H	1.5	1.43	-4.6
S	17.7	17.68	-0.1

Table-II-3. Elemental analysis comparison



(iv) Thermogravimetric and FTIR coupled analysis

The decomposition gases of the TGA were further examined in a coupled FTIR spectrometer in order to identify the splitting-off temperature of the SO_3 ($T_{\text{SO}_3 \text{ onset}}$) for which the stretching vibration of the S=O group at $1352\text{--}1342\text{ cm}^{-1}$ was used. The results of the thermogravimetric analysis belonging to P6 are reported within figure II-24. Sulphur trioxide (SO_3 , red line) and carbon monoxide (CO, black line) were captured during the thermal decomposition of P6 polymer.

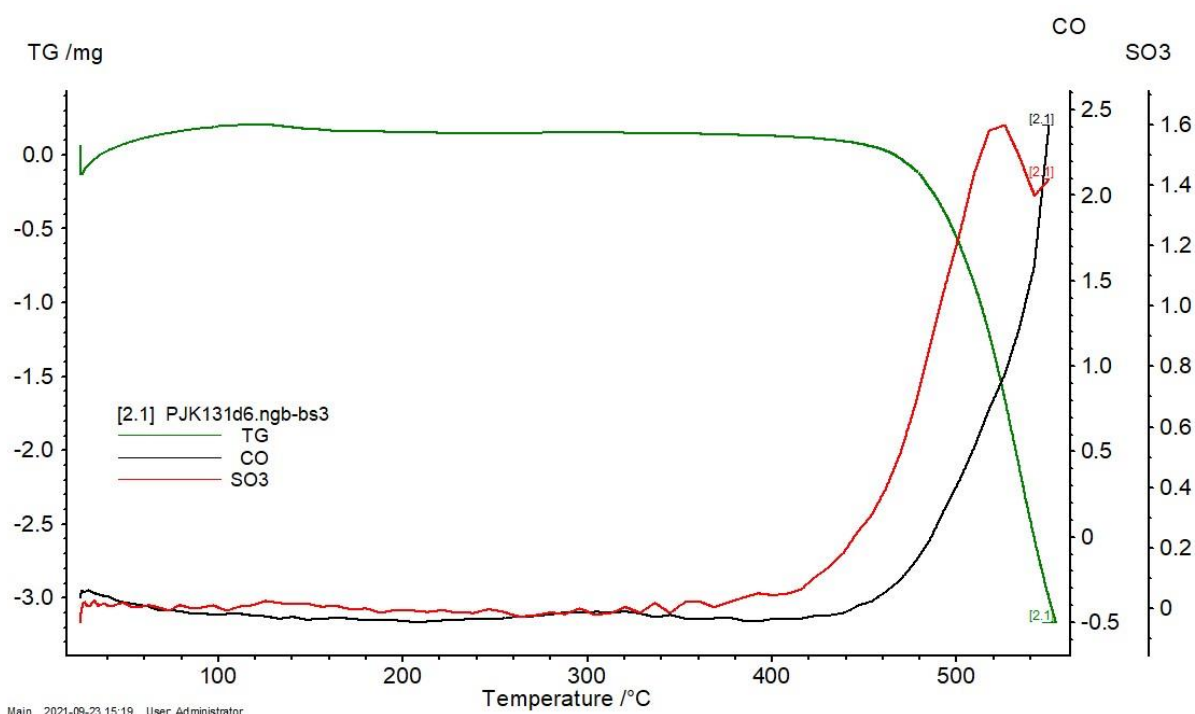


Figure II-24. TGA P6 Polyfluorinated sulphide polymer

The polymer is initially splitting the Ph-S-Ph bonds, due to an oxidation of the thioether and releasing SO_3 . This initial breaking of some thioether bonds starts at $400\text{ }^\circ\text{C}$ while the oxidation of the carbon starts occurring at $450\text{ }^\circ\text{C}$. It confirms that the polymeric backbone is thermally stable up to $400\text{ }^\circ\text{C}$ and therefore suitable for further functionalization and membrane synthesis.

+



2. Polymerization of decafluorobiphenyl and TMSTB

A new synthetic route was applied to obtain polyfluorinated poly(phenylene sulfide) reported previously (figure II-15). In these case bis(4-((trimethylsilyl)thio)phenyl)sulfane (figure II-25) was used instead of TBBT in order to increase reactivity and decrease the temperature of the reaction. The target was to run the reaction at room temperature, due to the bis(4-((trimethylsilyl)thio)phenyl)sulfane being more reactive than the TBBT.

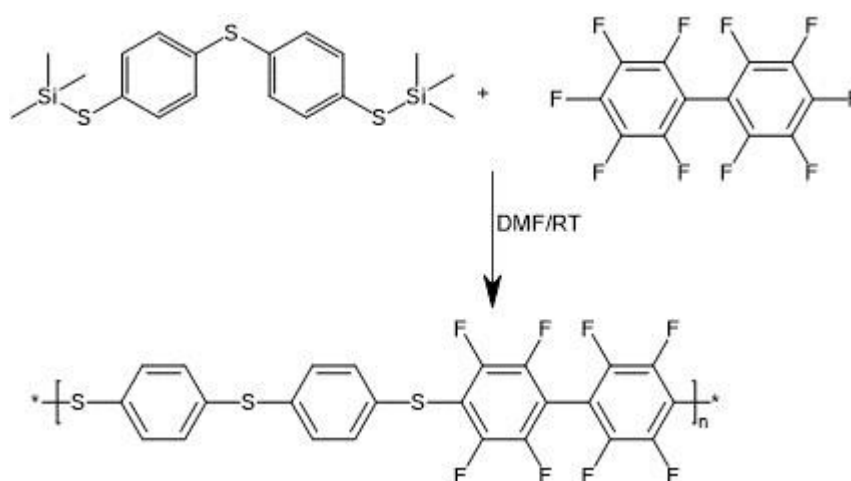


Figure II-25. Polymerization of decafluorobiphenyl and TMSTB to obtain polyfluorinated poly(phenylene sulfide)

The monomers were solubilized in DMF and left to react 1h at room temperature. Afterwards it was purified and a powder obtained and analysed. The integration of the ^{19}F NMR peaks (Figure II-26) showed that only low Mw oligomers were obtained. The peaks at -149.6 (F_5) and 160.2 (F_4) ppm (Figure II-26) belong to nonafluorobiphenyl end-groups, being at a ratio of 3:1 with the peaks of the chain at -136.8 (F_1) and -131.6 (F_2) ppm. It means that the average chain lengths was $n=3$, confirming that only low Mw oligomers were synthesised.



Figure II-26. ^{19}F NMR of polymerization of DCFB and TMSTB

This method leads to too short polymer chains to be suitable for membrane preparation. Because of the poor expected mechanical properties, this polymerization path was not further explored. The purpose of using the TMSTB was to explore if this polymerization could be done at room temperature. Increasing the temperature and time was expected to increase the Mw but in that case it had already been done with TBBT. Therefore, this polymerization path was not further explored.

3. Polymerization of decafluorobiphenyl and Biphenyl-4,4'-dithiol

This approach replaces the TBBT by other dithiol comonomer, targeting a new copolymer with high Mw. This polymerization was hence tested, no literature regarding this polymerization (Figure II-27) being found, to the best of our knowledge. Only self-assembled layers of biphenyl-4,4'-dithiol have been proposed by T. Browser *et al.*³⁰ as a way of having organic thin films.

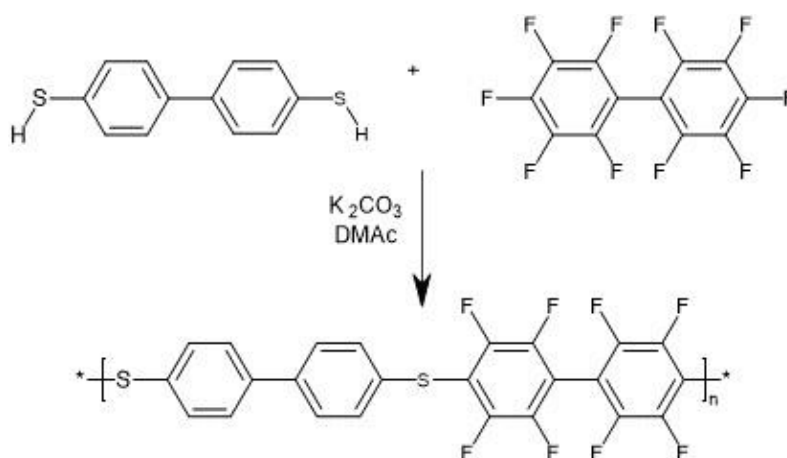


Figure II-27. Polymerization of decafluorobiphenyl and biphenyl-4,4'-dithiol

No polymerization was obtained in the first attempt using potassium carbonate as a base and DMAc as solvent at 100 °C. A second attempt was performed by increasing the temperature up to 180 °C for 6h, but no polymer was obtained. The main hypothesis is that biphenyl-4,4'-dithiol was deactivated by some moisture or that the lack of sulfide group between the phenyls turns the thiol groups less reactive and therefore no polymerization is obtained.

4. Polymerization of decafluorobiphenyl and hexane-1,6-dithiol

In this approach, one of the aromatic comonomers leading to rigid polymers have been replaced by an aliphatic comonomer, aiming at a more flexible and stable polymer. (figure II-28).

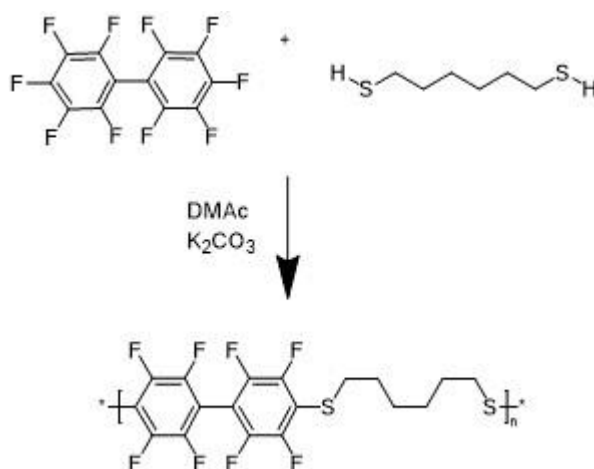


Figure II-28. Polymerization of decafluorobiphenyl and hexane-1,6-dithiol



The reaction was performed for 6h at 80 °C in DMAc with 3.0 eq. of potassium carbonate as a base and the product was obtained with a reaction yield of 81 %. Reactivity of the aliphatic –SH proved to be lower than reactivity of aromatic –SH when comparing the Mw obtained.

a) Characterizations

(i) NMR analysis

^1H NMR (Figure II-29) and ^{19}F NMR (Figure II-30) confirmed the structure of the targeted polymer. In ^1H NMR, two signals were observed in the aliphatic domain, at 1.59 ppm (for $-\text{CH}_2\text{S}$) and 1.41 ppm (for $\text{S}-\text{CH}_2-\text{CH}_2-\text{CH}_2-\text{CH}_2-\text{CH}_2-\text{S}$) with the integral ratio of 1:2.

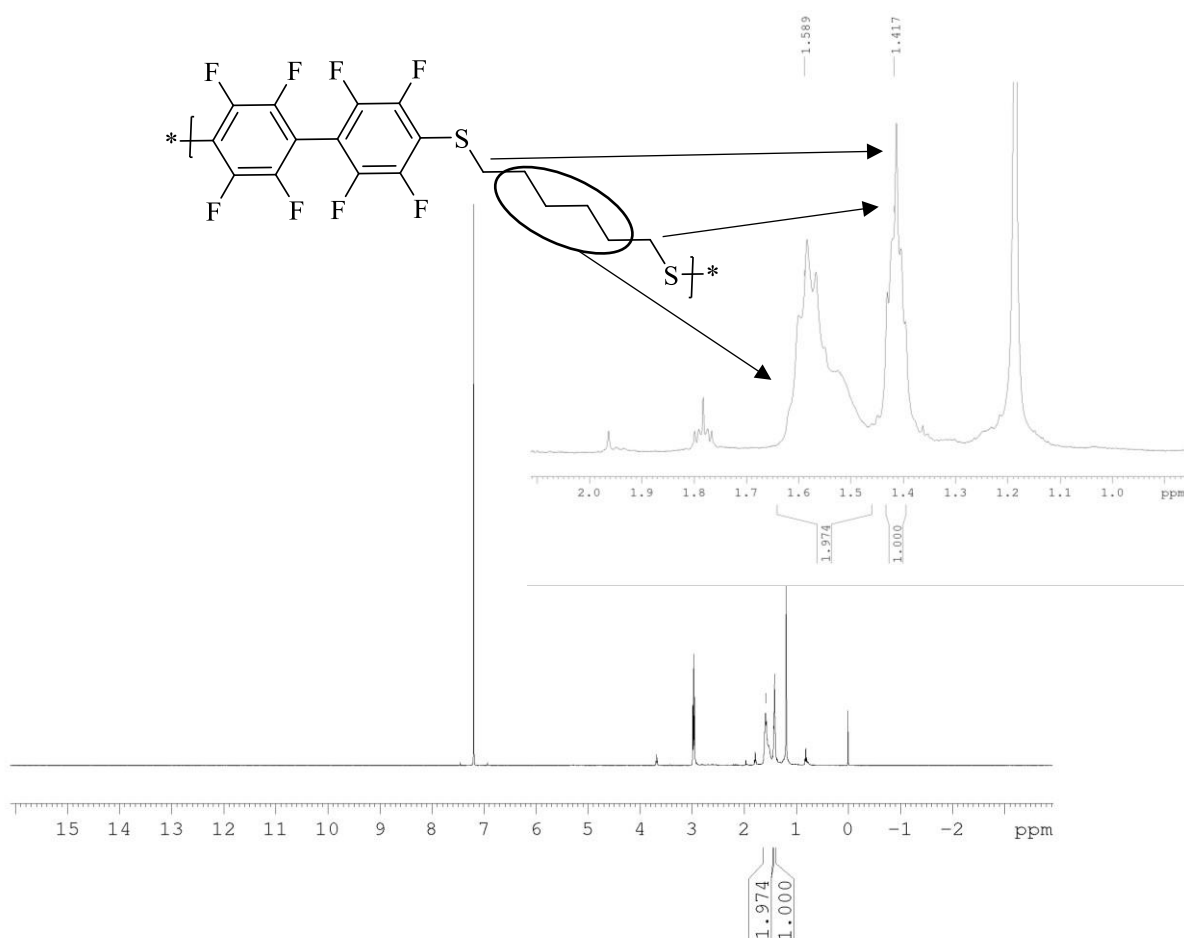


Figure II-29. ^1H NMR polyfluorinated byphenyl hexanesulfide alt-polymer



^{19}F NMR shows the 2 Fluorine signals characteristic of the octafluorobiphenyl at -133.5ppm and -138.0ppm (figure II-30). There is a small shift when compared to the octafluorobiphenyls attached to S-aromatic groups obtained in the previous fluorinated poly(phenylene sulphide)s, peaks were at -131.6ppm and -136.7ppm (figure II-22).

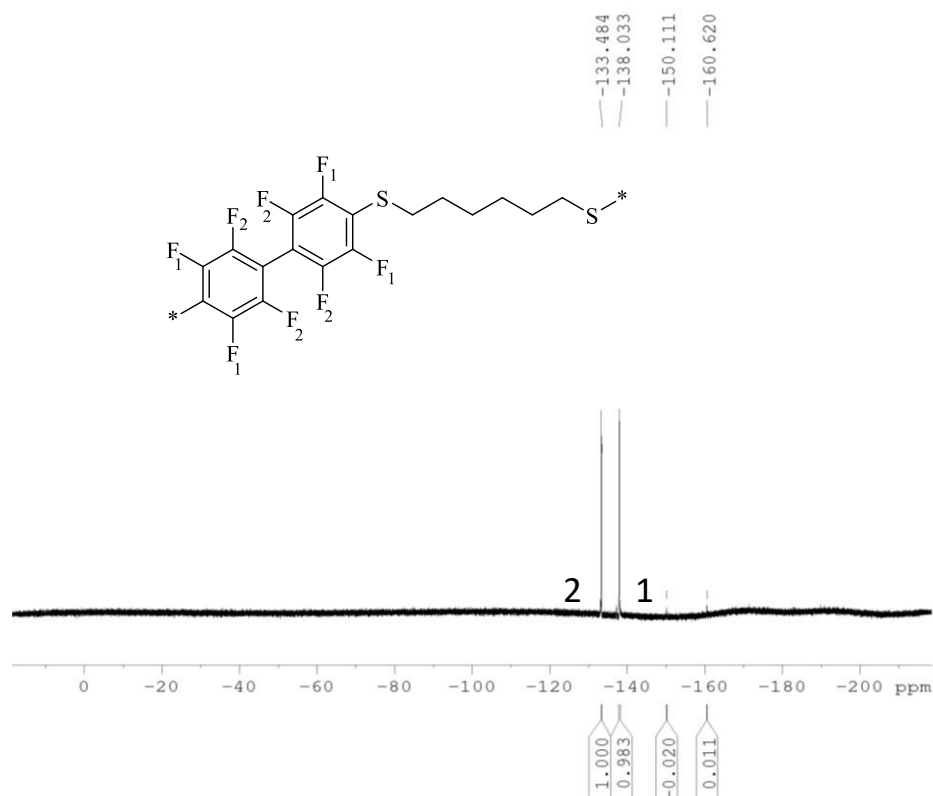


Figure II-30. ^{19}F NMR polyfluorinated hexanesulfide

(ii) SEC analysis

SEC analysis (figure II-31) showed a M_w of less than 10^3 g/mol, a proof of a poor degree of polymerization, i.e. a much lower M_w than the one using the aromatic dithiol (TBBT).

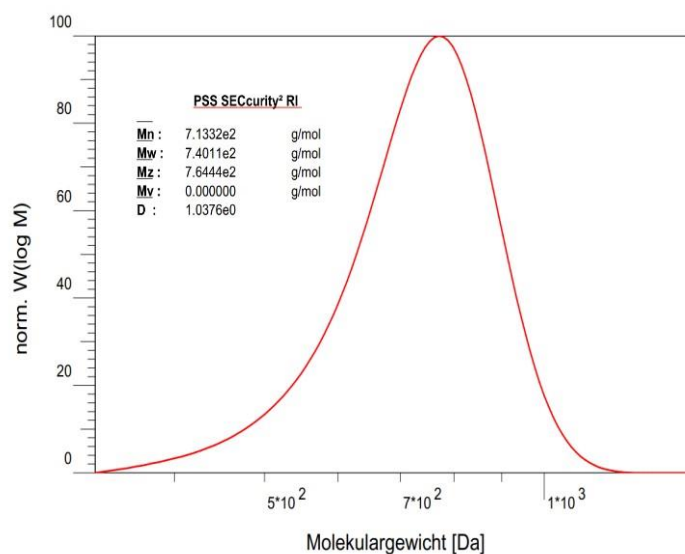


Figure II-31. GPC polyfluorinated hexanesulfide

(iii) Thermogravimetric analysis

Thermal stability was measured through TGA (Figure II-32), leading to a polymer thermostable up to 330 °C (red line, aliphatic). It can be compared with the thermostability of the prepolymer synthesized using the aromatic TBBT comonomer which demonstrated a thermostability up to 450 °C (green line, aromatic).

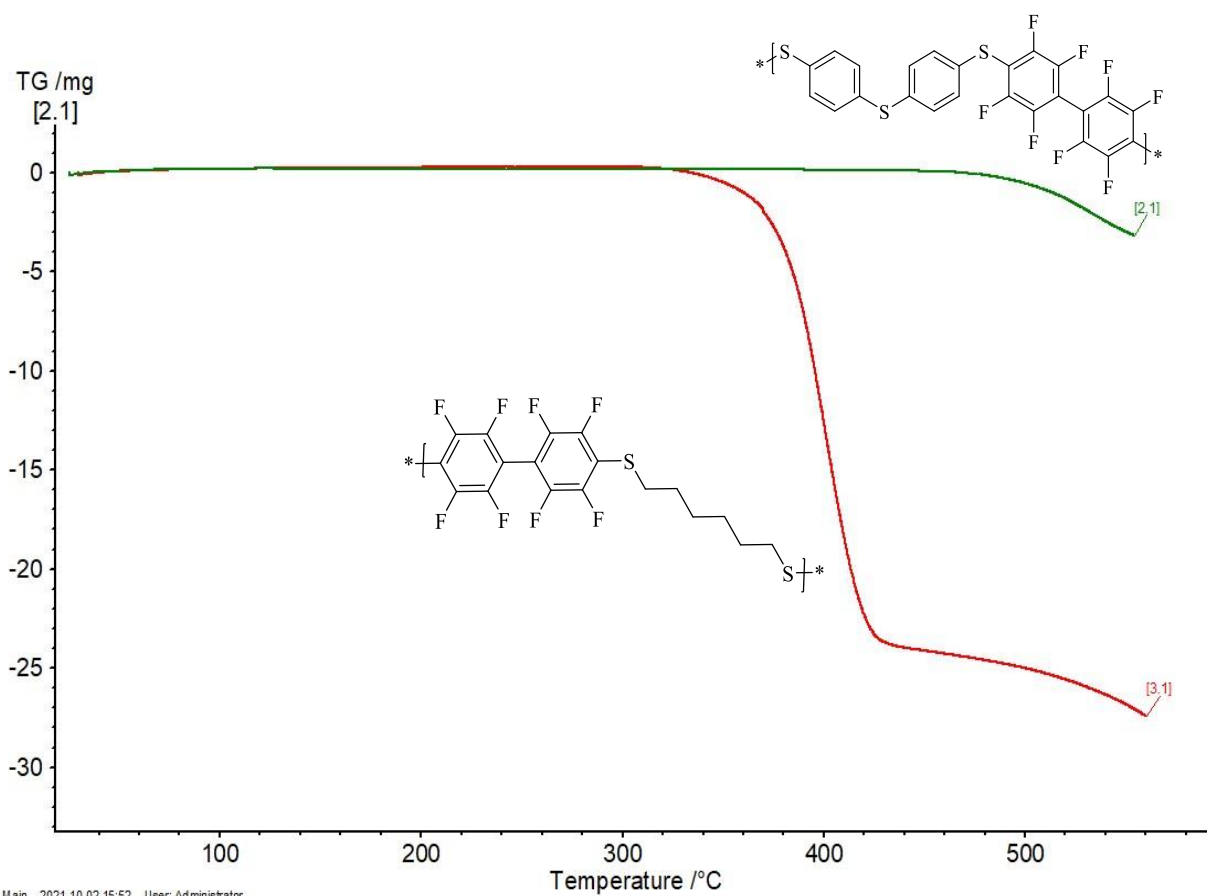


Figure II-32. TGA polyfluorinated byphenyl hexanesulfide (red line) and polyfluorinated poly(phenylene sulfide)

Because of the lower M_w and thermostability it was decided not to further investigate the aliphatic monomers strategy.

Only the first route involving the polycondensation of decafluorobiphenyl and TBBT was successful enough to lead to high quantity of polymer with the targeted M_w with thermostability. This polymer was submitted to sulfonation and phosphonation postfunctionalized are discussed in the next chapters.

The following pathways tested the polycondensation of functionalized monomers, a strategy that would avoid the post-functionalization step.

5. Polymerization of TBBT and phosphonated octafluorobiphenyl

A more direct strategy was pointed out in the elaboration of a functionalized polymer. In this case, a diposphonated hexafluorinated poly(phenyl sulfide) can be used and is shown in figure II-33.



The main advantage of this strategy is that it would avoid a post-phosphonation which requires a more complex set up and higher temperatures. An issue would consist in the obtention of lower Mw values.

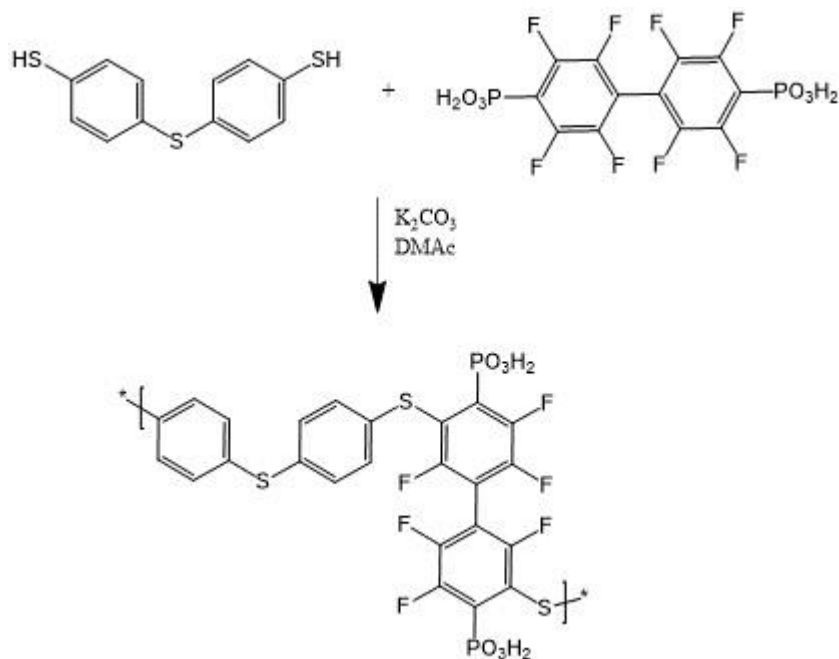


Figure II-33. Polymerization of TBBT and 4,4'-phosphonatedoctafluorobiphenyl

a) Phosphonation of decafluorobiphenyl monomer

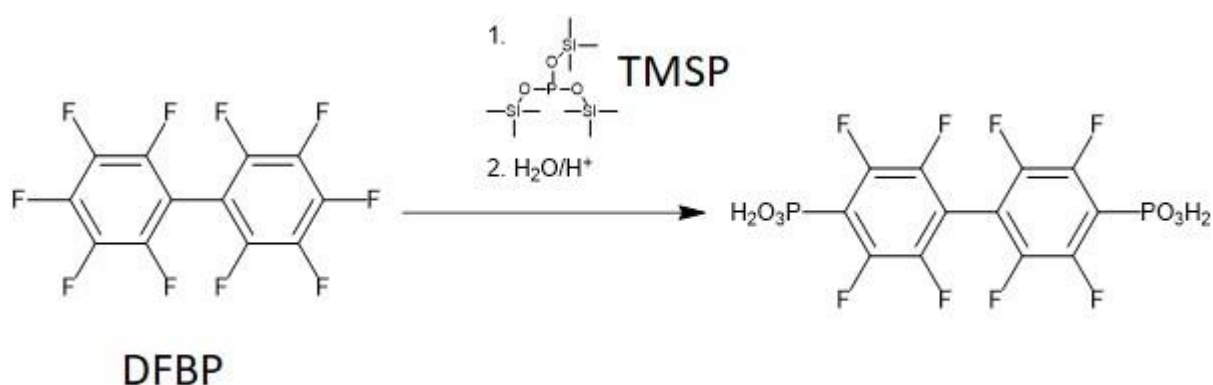


Figure II-34. Phosphonation of decafluorobiphenyl monomer

In this approach, a pre-phosphonated monomer was prepared prior to polymerization. The phosphonation was performed on the decafluorobiphenyl monomer. During the monomer functionalization, a silicon phase was observed corresponding to the $(SiCH_3)_2O$ (Figure II-35)



meaning that the TMS groups had been removed. This silicon phase was removed and the white solution was dried at 80 °C under vacuum giving a white monomer.



Figure II-35. Phosphonated decafluorobiphenyl monomer.

^{19}F NMR (Figure II-36) showed phosphonation in the para-position (4,4'-position) (red spectra) with no residual decafluorobiphenyl (blue spectra) peaks at -138.65 ppm, -149.90 ppm and 160.85 ppm. The peaks of the substituted monomer appear at -132.0 ppm and -137.8 ppm confirming the success of the phosphonation, no Fluoride peak in the para position appeared in the ^{19}F NMR spectrum.

These peaks can also be compared to the ones already seen in our fluorinated polysulfide polymer (P6, green spectra). While the fluorines in meta position ($\text{P}-\text{C}-\text{CF}=\underline{\text{CF}}-\text{C}=\text{C}$) are almost equal ($\text{S}-\text{C}-\text{CF}=\underline{\text{CF}}-\text{C}=\text{C}$) (-131.6 ppm vs -132.0 ppm), the fluorine peaks in orto position ($\text{P}-\text{C}-\underline{\text{CF}}=\text{CF}-\text{C}=\text{C}$) have a higher shift -1.1ppm when compared to P6 ($\text{S}-\text{C}-\underline{\text{CF}}=\text{CF}-\text{C}=\text{C}$). This shift difference is due to the difference in the C-S vs the C-P bond, being the electronegativity of P (2.19) lower than the one of S (2.58). Therefore these fluorines in the aromatic bond are more shielded (higher electron density around) as the P has a higher electron giving effect than the S.



A few smaller peaks (<0.5 %) appeared between -100 ppm and -113 ppm indicating that there are minor substitutions of the Fluorine atoms also in the ortho and meta position in the phosphonated monomer. This phosphonation proves the higher reactivity of the para-position when compared to the attempts of phosphonation in the meta or ortho position of the fluorinated poly(phenylenesulfide)s (P6) polymer. The 4,4-phosphonatedoctafluorobiphenyl monomer obtained was further used for the polymerization with TBBT.

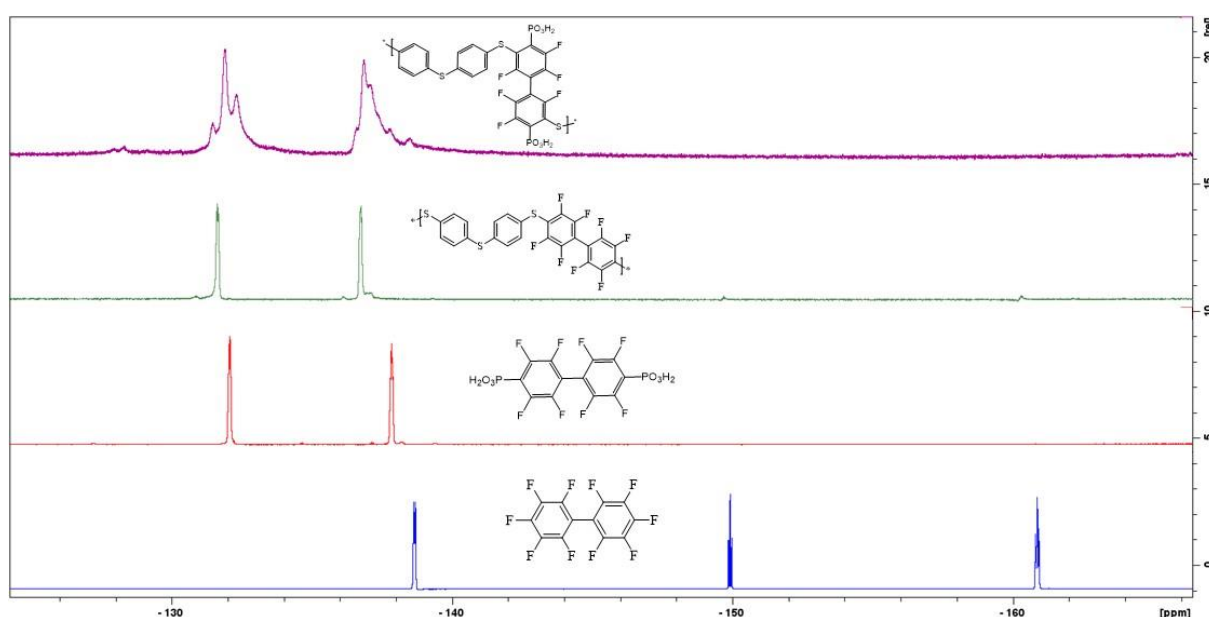


Figure II-36. ^{19}F NMR decafluorobiphenyl, phosphonated octafluorobiphenyl, fluorinated poly(phenylenesulfide)s and biphosphonated hexafluorinated poly(phenylsulfide)s

b) Polycondensation

The 4,4-phosphonatedoctafluorobiphenyl and TBBT were involved within a polymerization to obtain a functionalised polymer for PEM in one step. This reaction was performed at 110 °C for 6h. ^{19}F NMR (see Figure II-36) and ^1H NMR (Figure II-37) of the recovered yellow powder performed to check its structure. ^1H NMR showed a broad peak at 7.5 ppm which englobed all the aromatic peaks and another broad peak at 3.9 ppm corresponding to the phosphonate protons. Compare to the previous strategies, TBBT reacts in ortho position of (4,4'phosphonatedoctafluorobiphenyl), while it reacts in para position of decafluorobiphenyl,



this explains the difference of the NMR peaks observed in Figure II-37. All the protons are around 7.5ppm, forming a broad peak.

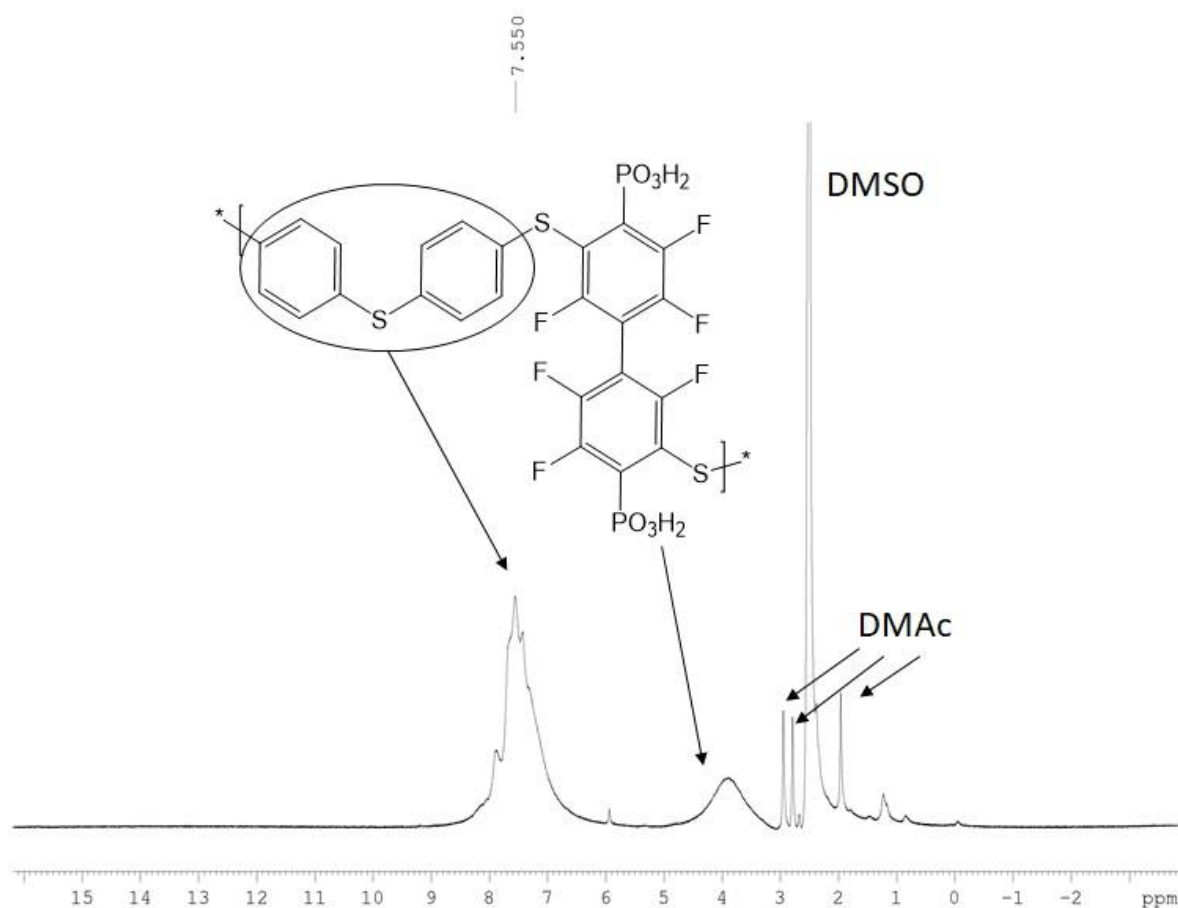


Figure II-37. ^1H NMR biphosphonated hexafluorinated poly(phenylsulfide)s

The H^1 -NMR confirmed that phosphonic protons and phenyl protons are present. However only a low mass was recovered (0.72 g, 25 % yield). Albeit being an interesting one step synthetic route, the observed low yield and mass discarded this strategy to produce a membrane for PEMFCs. The choice was made to not optimize this method and focus on the elaboration of high M_w polymers that could be further postfunctionalized.



6. Polymerization of 4,4'-thiobisbenzenethiol and disodium 3,3'-disulfonate-4,4'-difluorodiphenylsulfone

The motivation for this polymerization was to obtain a polymer with pre-defined sulfonation degree from TBBT and disodium 3,3'-disulfonate-4,4'-difluorodiphenylsulfone (Figure II-38). The synthesis was performed following the procedure published by Schuster *et al.*³¹

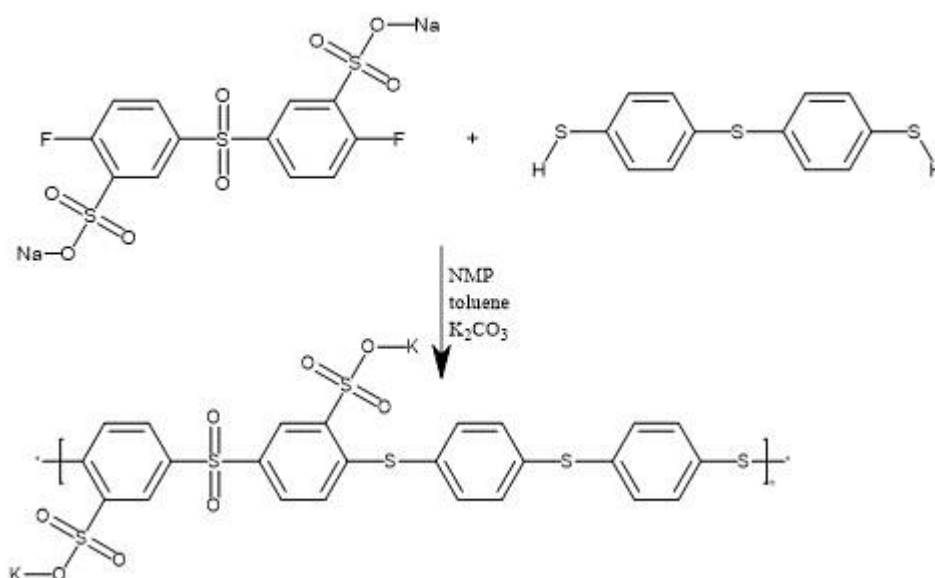


Figure II-38. Polymerization of disodium 3,3'-disulfonate-4,4'-difluorodiphenylsulfone and TBBT

The reaction mixture was heated up to 160 °C and a change in colour in the reaction medium was observed. Brownish insoluble pellets were obtained under which no analyses could be conducted. The main hypothesis is that heating up to 160 °C induce uncontrolled polymerization as well as cross-linking which could cause the insolubility of the obtained polymer. Reaction was not repeated as other paths for further sulfonation starting from a high Mw and limited D prepolymer were explored. Further research should be engaged to assess the viability of this synthetic path.



IV. Conclusion

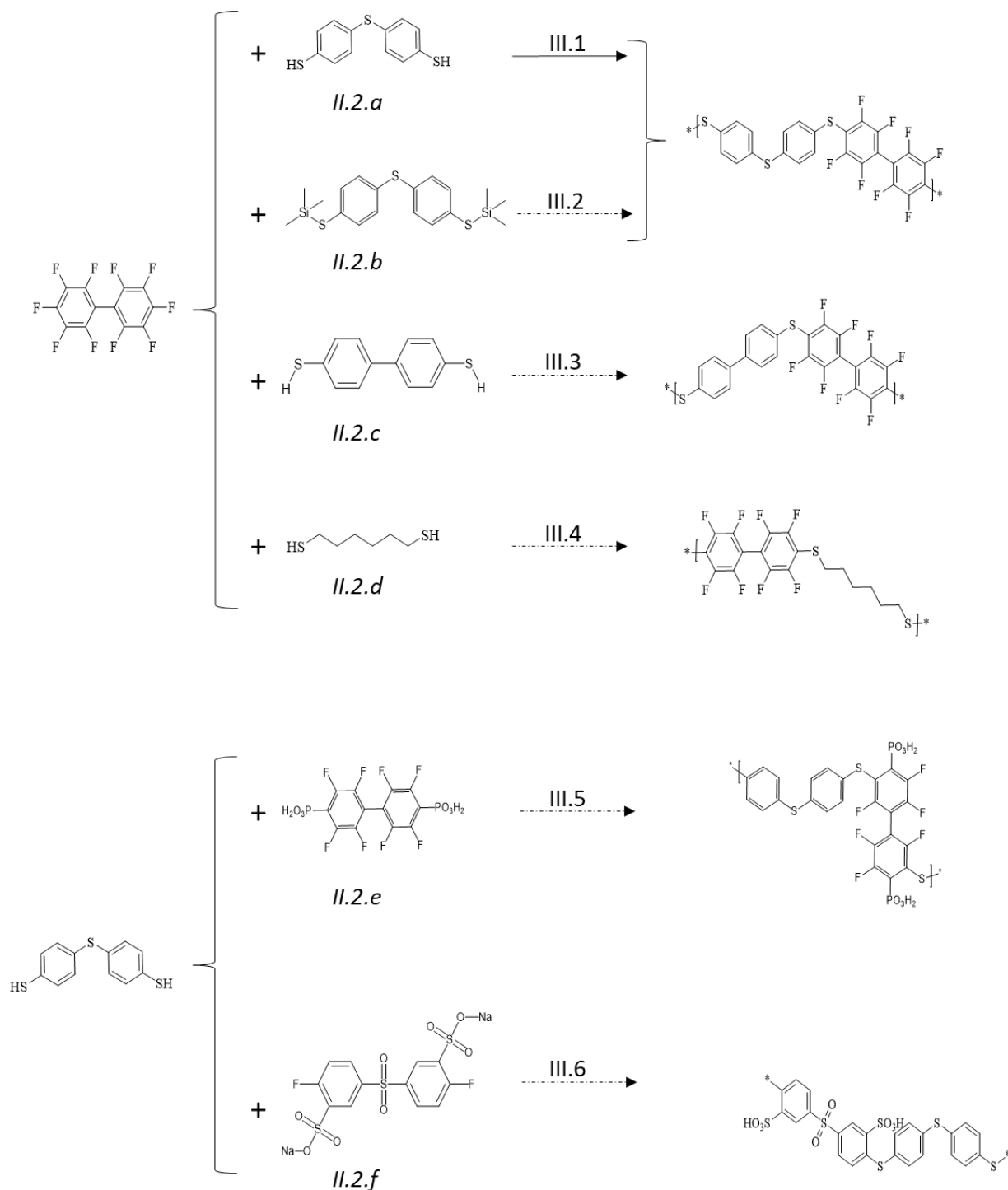


Figure II-39. Scheme of polymerizations, in italic, the paragraph number where the experimental protocol is described, above the arrows, the paragraph number where the polymerization is discussed. Plain and dashed arrows for successful and unaccomplished pathways.



Starting with decafluorobiphenyl, several polymerizations (Figure II-39, upper part) were conducted to obtain a thermostable prepolymer that could be postfunctionalized to insert sulfonic and phosphonic functions. Different dithiols were tested, 4,4-thiobisbenzenthiole (procedure II.2.a, discussion III.1) being the most successful. Another less consuming (no heating) route to obtain polyfluorinated sulfide polymer was tried using trimethylsilylthiobisbenzene (TMSTB) (II.2.b), but only trimers were obtained. Other polymerizations with biphenyl-4,4'-dithiol (II.2.c) were attempted, but no polymer was obtained. An alkyl thiol (1,6-hexanedithiol) (II.2.d) was also tested and the structure analysed by NMR corresponded with what was expected (III.4). However subsequent analyses showed that it was consisting in oligomers with lower thermostability, leading us to discard it for further postfunctionalization as it would result in polymer not showing the targeted mechanical properties suitable for a PEM. The functionalization of the prepolymer obtained following the route II.2.a will be discussed within Chapter 3.

The alternative approach tested, again with the objective to obtain high M_w , chemically and mechanically stable prepolymers; was the polymerization of functionalised monomers. If successful, this approach would have avoided the post-functionalization of the prepolymer that may alter the polymer chain microstructure. However, the use of functionalized monomer might inhibit the polymerization due to steric hindrance and/or lower reactivity.

Polymerizations of already functionalised monomers (Figure II-39, lower part) (phosphonated (II.2.e) and sulfonated (II.2.f) were tested. The reaction yield of the first route (Figure II-39, III.6) was too low to allow any characterizations and clear conclusions. In the case of the phosphonated monomer (Figure II-39, III.5), low M_w product was obtained and did not allow film-forming properties (see chapter 4).

To sum up, the route III.1 was reproducible and gave high quantities (50 g) of a mechanically, chemically and thermally stable (up to 400 °C) with a prepolymer displaying a rather high M_w of up to $3 \cdot 10^5$ g/mol. A polyfluorinated phenylenesulfide polymer was obtained using relatively mild conditions (100 °C) which made it suitable for upscaling and application for proton-



conducting membrane polymer. The postfunctionalization of this prepolymer is described and discussed in the next chapter (Chapter 3).

V. References

- ¹ S. Vysokomol, *Establishing and developing polymer science*, 1982, A24: No. 6, p.1339-1340, p.1523 DOI: [10.1016/0032-3950\(82\)90432-4](https://doi.org/10.1016/0032-3950(82)90432-4)
- ² H. Staudinger, *Über polymerisation*, 1920, Ber. Chem., 53, p.1073–1085 DOI: [10.1002/cber.19200530627](https://doi.org/10.1002/cber.19200530627)
- ³ F.E. Bailey and J.V. Koleske, *Alkylene oxides and their polymers*, 1991, Vol. 35 by Marcel Dekker, Inc., p.27 DOI: [10.1201/9781003066569](https://doi.org/10.1201/9781003066569)
- ⁴ Paul J. Flory, *Principles of Polymer Chemistry*, 1953, p.12 DOI: [10.1126/science.119.3095.555.b](https://doi.org/10.1126/science.119.3095.555.b)
- ⁵ F.E. Bailey, and J.V. Koleske, *Polyethyleneoxide*, 1976, Academic Press, Inc. (London) LTD., preface DOI: [10.1016/B978-0-12-073250-0.X5001-6](https://doi.org/10.1016/B978-0-12-073250-0.X5001-6)
- ⁶ G. Odian, *Principles of Polymerization*, 2004, 4th ed. New Jersey, John Wiley & Sons, Inc., p.2 DOI: [10.1002/047147875X](https://doi.org/10.1002/047147875X)
- ⁷ V. Causin, *Polymers: An Overview. In: Polymers on the Crime Scene*, 2015, Springer DOI: [10.1007/978-3-319-15494-7](https://doi.org/10.1007/978-3-319-15494-7)
- ⁸ IUPAC. *Pure Appl. Chem*, 2012, 84, p.2167–2169 DOI: [10.1351/PAC-REC-10-12-04](https://doi.org/10.1351/PAC-REC-10-12-04)
- ⁹ T.C. Ward, *Molecular Weight and Molecular Weight Distributions in Synthetic Polymers*, 1981, Vol. 58, num. 11, p.867-879 DOI: [10.1021/ED058P867](https://doi.org/10.1021/ED058P867)
- ¹⁰ <http://www.polymerdatabase.com/polymer%20chemistry/Stepgrowth%20Polymerization.html>
- ¹¹ L. Michaelis, A. Fujita. *Über phasengrenzpotentiale*, 1924, Zeitschrift für Physikalische Chemie, p.266-284 DOI: [10-100/978-3-642-90655-8_8](https://doi.org/10.100/978-3-642-90655-8_8)
- ¹² S.J. Peighambardoust, S. Rowshanzamir, and M. Amjadi, *Review of the proton exchange membranes for fuel cell applications*, 2010, vol.35, no.17. Elsevier Ltd. DOI: [10.1016/j.ijhydene.2010.05.017](https://doi.org/10.1016/j.ijhydene.2010.05.017)



- ¹³ B. Smitha, S. Sridhar and A.A. Khan, *Solid polymer electrolyte membranes for fuel cell applications – a review*, 2005, *Journal of Material Science*, vol. 59, p.10-29 DOI: [10.1016/j.memsci.2005.01.035](https://doi.org/10.1016/j.memsci.2005.01.035)
- ¹⁴ M. Carmo & D. L. Fritz, *A comprehensive review on PEM water electrolysis*, 2013, *International journal of hydrogen energy* 38, 8(1), p.4901-4934 DOI: [10.1016/j.ijhydene.2013.01.151](https://doi.org/10.1016/j.ijhydene.2013.01.151)
- ¹⁵ Global Nafion Industry Research Report, Growth Trends and Competitive Analysis 2021-2027, May 2021
- ¹⁶ S. Trabia, K. Choi, Z. Olsen *et al.* *Understanding the thermal properties of precursorionomers to optimize fabrication processes for ionic polymer-metal composites (IPMCs)*, *Materials* 2018, 11, 665 DOI:[10.3390/ma11050665](https://doi.org/10.3390/ma11050665)
- ¹⁷ A. Katzfuss, K. Krajinovic, A. Chromik, J. Kerres, *Preparation and characterization of new sulfonated partially fluorinated polarylenesulfones and their blends with polybenzimidazole*, 2010, *ECS Transactions*, 33 (1) p.719-733 DOI:[10.1149/MA2010-02/10/683](https://doi.org/10.1149/MA2010-02/10/683)
- ¹⁸ M. Schuster, k.-D. Kreuer, H. T. Andersen, J. Maier, *Sulfonated poly(phenylene sulfone) polymers as hydrolytically and thermooxidatively stable proton conducting ionomers*, *Macromolecules*, 2007, 40, p.598-607 DOI:[10.1021/MA062324Z](https://doi.org/10.1021/MA062324Z)
- ¹⁹ Wallace H. Carothers, *Polymers and Polyfunctionality*, *Transactions of the Faraday Society*, 1936, vol. 32 DOI: [10.1039/TF9363200039](https://doi.org/10.1039/TF9363200039)
- ²⁰ Wallace H. Carothers, *Polymerization*, 1931, *Chemical reviews*, Vol. VIII, no. 3 DOI: [10.1021/cr60031a001](https://doi.org/10.1021/cr60031a001)
- ²¹ V.V. Korshak, *Functionality of monomers and structure of polymers obtained by polycondensation*, 1982, *Review Polymer Science U.S.S.R.*, 24(8), p.1783–1797 DOI: [10.1016/0032-3950\(82\)90132-0](https://doi.org/10.1016/0032-3950(82)90132-0)
- ²² I.M. Tkachenko, N.A. Belov, Y. Yakovlev, P.V. Vakuliuk, O.V. Shekera, Y.P. Yampolskii & V.V. Schevchenko, *Synthesis, gas transport and dielectric properties of fluorinated poly(arylene ether)s based on decafluorobiphenyl*, I.M. 2016. AC SC, *Materials Chemistry and Physics* DOI: [10.1016/j.matchemphys.2016.08.028](https://doi.org/10.1016/j.matchemphys.2016.08.028)
- ²³ Q. Li, J.O. Jensen, C. Pan, V. Bandur, M.S. Nilsson, F. Schönberger, N.J. Bjerrum, *Partially fluorinated arylene polyethers and their ternary blends with PBI and H3PO4. Part II. Characterisation and fuel cell tests of the ternary membranes*, 2008, *Fuel Cells*, 8(3–4), p.188–199 DOI: [10.1002/fuce.200890014](https://doi.org/10.1002/fuce.200890014)



- ²⁴ X. Yu, A. Roy, S. Dunn, J. Yang, & J.E. McGrath, *Synthesis and characterization of sulfonated-fluorinated, hydrophilic-hydrophobic multiblock copolymers for proton exchange membranes*, 2006, *Macromolecular Symposia*, 245–246, p.439–449 DOI:[10.1002/MASY.200651363](https://doi.org/10.1002/MASY.200651363)
- ²⁵ S. Takamuku, A. Wohlfarth, A. Manhart, P. Räder & P. Jannasch, *Hypersulfonated polyelectrolytes: Preparation, stability and conductivity*, 2015, *Polymer Chemistry*, 6(8), p.1267–1274 DOI: [10.1039/C4PY01177E](https://doi.org/10.1039/C4PY01177E)
- ²⁶ M. Komorowska-Durka, G. Dimitrakis, D. Bogdał, A.I. Stankiewicz, and G.D. Stefanidis, “A concise review on microwave-assisted polycondensation reactions and curing of polycondensation polymers with focus on the effect of process conditions”, 2015, *Chem. Eng. J.*, vol. 264, p.633–644 DOI:[10.1016/j.cej.2014.11.087](https://doi.org/10.1016/j.cej.2014.11.087)
- ²⁷ A. Loupy, *Microwaves in organic synthesis*, 2006, 2nd edition, Wiley-VCH, p.78 DOI:[10.1002/9783527651313](https://doi.org/10.1002/9783527651313)
- ²⁸ A. Mishra, T. Vats, and J.H. Clark, *RSC Green chemistry: Microwave assisted polymerization*. 2016 DOI:[10.1039/9781782623182](https://doi.org/10.1039/9781782623182)
- ²⁹ F. Mercer, T. Goodman, J. Woitowicz, D. Duff. *Synthesis and Characterization of Fluorinated Aryl Ethers Prepared from Decafluorobiphenyl*, 1992, *Journal of Polymer Science*, Vol. 30, p.1767–1770 DOI: [10.1016/S0032-3861\(96\)00700-8](https://doi.org/10.1016/S0032-3861(96)00700-8)
- ³⁰ T.L. Brower, J.C. Garno, A. Ulman, G. Liu, C. Yan, & A. Go, 2002, *Self-Assembled Multilayers of 4,4'-Dimercaptobiphenyl Formed by Cu (II) Catalyzed Oxidation*, *Society*, 1992 (ii), p.6207–6216. DOI:[10.1021/la020084k](https://doi.org/10.1021/la020084k)
- ³¹ M. Schuster, k.-D. Kreuer, H. T. Andersen, J. Maier, *Sulfonated Poly(phenylene sulfone) Polymers as Hydrolytically and Thermooxidatively Stable Proton Conducting Ionomers*, 2007, *Macromolecules*, vol.40, p.598-607 DOI:[10.1021/ma062324z](https://doi.org/10.1021/ma062324z)

Chapter 3. Postfunctionalization of polyfluorothioether prepolymers

VI.	Introduction	121
1.	Phosphonated polymer.....	121
2.	Sulfonated polymers	124
3.	Strategy.....	125
VII.	Materials and methods	127
1.	Reagents	127
2.	Experimental.....	128
a.	Phosphonation of fluorinated poly(phenylenesulfide)s	128
(i)	Strategy 1	128
(ii)	Strategy 2	128
(iii)	Strategy 3	129
b.	Phosphonation of fluorinated poly(phenylenesulfone)s	130
b.1.	Oxidation of sulphides to sulphones.....	130
(iv)	Strategy 1 (Ox1, Figure II-11)	130
(v)	Strategy 2 (Ox2, Figure II-11)	131
(vi)	Strategy 3 (Ox3, Figure II-11)	131

b.2. Phosphonation of fluorinated poly(phenylenesulfone)s.....	132
c. Sulfonation of fluorinated poly(phenylenesulfide)s using sodium hydrosulfide.....	133
d. Sulfonation of fluorinated poly(phenylenesulfide)s using sodium sulfide.....	134
(iii) Strategy 1	134
(iv) Strategy 2	135
e. Sulfonation of fluorinated poly(phenylenesulfide)s using Lithium sulfide	135
f. Sulfonation of fluorinated poly(phenylenesulfide)s using Sulfuric acid	136
g. Sulfonation of fluorinated poly(phenylenesulfide)s using Sodium 3-Mercaptopropane-1-sulfonate	137
(iii) Strategy 1	137
(iv) Strategy 2	138
h. Sulfonation of fluorinated poly(phenylenesulfone)s using Sodium 3-Mercaptopropane-1-sulfonate	138
3. Techniques	139
a. Microwave reactor.....	139
b. IR spectroscopy	139
c. NMR spectroscopy	139
d. Size-Exclusion Chromatography (SEC)	140
e. Thermal analysis	140
f. Elemental Analysis	140
VIII. Results and discussion	140
1. Phosphonations	140
a. Phosphonation of fluorinated poly(phenylenesulfide)s	141

(i) Strategy 1	141
(ii) Strategy 2	143
(iii) Strategy 3	144
b. Phosphonation of fluorinated poly(phenylenesulfone)s : step1, Oxidation of sulfides to sulfones	145
(iv) Strategy 1 (Ox1, Figure II-30)	146
(v) Strategy 2 (Ox2, Figure II-30)	146
(vi) Strategy 3 (Ox3, Figure II-30)	147
Elemental analysis	147
Thermogravimetric analysis	148
c. Phosphonation of fluorinated poly(phenylenesulfone)s : step 2 : functionalization.....	149
d. Conclusion of phosphonations	151
2. Sulfonations	152
a. Sulfonation of fluorinated poly(phenylenesulfide)s using sodium hydrosulfide.....	153
b. Sulfonation of fluorinated poly(phenylenesulfide)s using sodium sulfide	154
c. Sulfonation of fluorinated poly(phenylenesulfide)s using lithium sulfide	157
d. Sulfonation of fluorinated poly(phenylenesulfide)s using sulphuric acid	158
e. Sulfonation of fluorinated poly(phenylenesulfide)s using 3-Mercaptopropane-1-sulfonate	159
f. Sulfonation of fluorinated poly(phenylenesulfone)s using Sodium 3-Mercaptopropane-1-sulfonate	165
g. Conclusion of sulfonation.....	170
IX. Conclusions	171
X. References	173

This chapter is dedicated to the different synthetic paths to functionalize the polymers synthesised in chapter 2 and make them suitable to be used to produce Proton exchange Membrane (PEM) for fuel cells. After an introduction, the functionalization process is explained. The different functionalization pathways are accomplished with the characterization of the produced functionals obtained before closing this chapter with the conclusions.

I. Introduction

In this chapter, the focus will be on cation-exchange polymers, that are capable to exchange protons. Ionic transport in PEMs is a complex process, which involves three mechanisms describing the transport of protons. These three mechanisms are the (i) Grotthus-type proton transport, (ii) vehicle mechanism and (iii) surface and interface transport where the principle is close to the Grotthus-type, where protons jump from one functionalized proton exchanging group (e.g. $-\text{SO}_3\text{H}$, $-\text{PO}_3\text{H}_2$) to another. As explained in the review of X. Sun et al.¹, the total proton conductivity of a polymer depends on the polymer chain microstructure and dynamics, the concentration acidity, and water content. There are commonly two functional acidic groups used for this purpose, i.e. the sulfonic ($-\text{SO}_3\text{H}$) and phosphonic ($-\text{PO}_3\text{H}_2$) acid groups.

The experimental procedures have proved that it is more challenging to phosphonate than to sulfonate aromatic polymers, due to side-reactions observed in the addition of the phosphonic acid moiety.² In the following sections a deeper look into these questions is proposed.

1. Phosphonated polymers

Phosphoric acid as a proton conductor has been used for fuel cells for a long time as it allows to operate at temperatures ranging from 160 to 220 °C. The first phosphoric acid fuel cells (PAFCs) have been reported by Elmore and Tanner in 1961, where the electrolyte was the phosphoric acid itself.³ Some improvements were done in the following years, and finally, in the late 1990s the interest in PAFCs waned. It was due

to its high cost, its poor reliability and the fact that its proton conductivity depends highly on acid concentration and is better at high temperature; which is an advantage when it comes to catalyst needs but increases the energetic cost.^{4,5} There are definitively scientific and technological interests in synthesizing phosphonated polymers that could work at intermediate temperatures, have a good stability and a high conductivity. For this purpose, several phosphonic groups would need to be grafted onto a thermostable polymeric backbone.

N. Kang *et al.*⁶ described different routes for the phosphonation of fluoroaryl polymers. Among them the one using trimethylsilyl phosphite as the phosphonating agent is worth noticing. Different strategies could be followed to phosphonate a polymer backbone. It could be inspired from the work of Stone *et al.*⁷ with the synthesis of dimethyl phosphonate-4-substituted α,β,β -trifluorostyrene (Figure III-1a), the synthesis of poly(vinyl phosphonic acid) (PVPA) proposed by A. Bozkurt *et al.*⁸ (Figure III-1b) or the synthesis of phosphonated poly(ether ether ketone) (PPEEK) (Figure III-1c) performed by S. Bano *et al.*⁹ These phosphonated polymers can be classified according to polymer chain microstructure being an aliphatic backbone with aromatic phenyls (Figure III-1a), aliphatic (Figure III-1b) or aromatic (Figure III-1c) backbone. It can also be separated according to whether it is fluorinated (Figure III-1a) or non-fluorinated (Figure III-1b,c). Fluorinated polymers offer the advantage of bearing electro-withdrawing F⁻ groups that increase the acidity of the phosphonic acid. Aromatic and aliphatic moieties, on the other hand, influence the mechanical properties of the polymer.

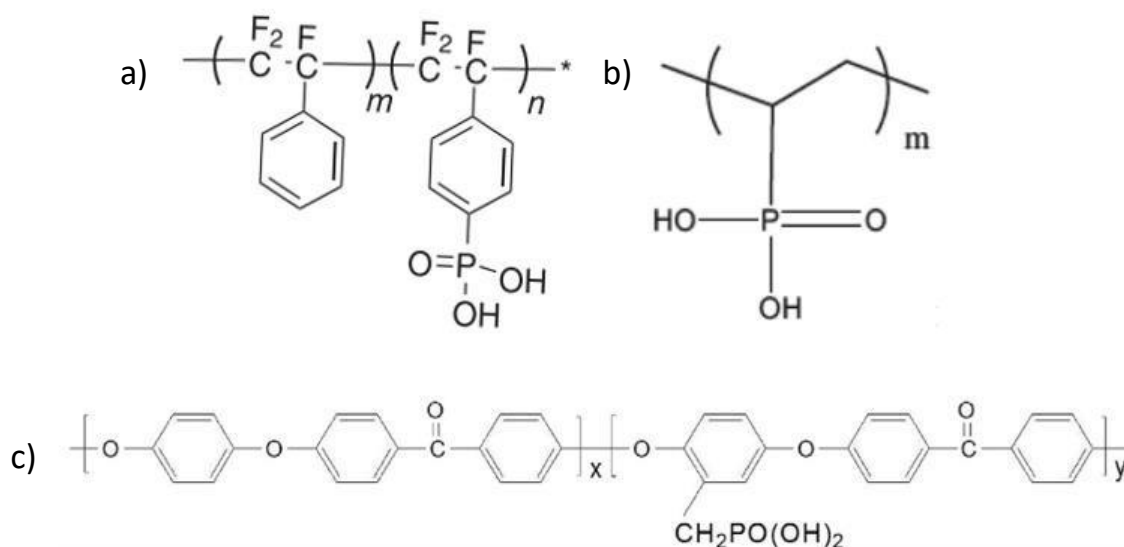


Figure III-1. Dimethyl phosphonate-4-substituted α,β -trifluorostyrene (up-left), PVPA (up-right) and PPEEK (down).

G. Ludueña et al. carried out a research to simulate long-range proton transport of PVPA (figure III-1, c) being a quasi-water-free proton conductor allowing PEMFC operation at temperatures above 100 °C.¹⁰ In a recent publication, V. Atanasov et al. pointed out the challenges of using phosphonated polymers due to their poor mechanical properties and the low anhydrous proton conductivity when phosphonic acid anhydride (figure III-2) is formed between two phosphonic acid groups.¹¹

In my thesis, the phosphonation of poly(phenylenesulfide)s and poly(phenylenesulfide)s is expected to bring the mechanical stability and, at the same time, having the phosphonic acid group with reduced internal anhydride formation.

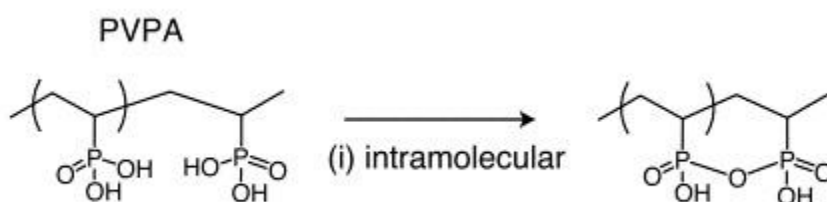


Figure III-2. Phosphonic acid anhydride formation¹².

2. Sulfonated polymers

Sulfonated polymers are the most common and industrially used polymers for PEM. They were firstly used in 1955 by Thomas Grubb for a fuel cell with the use of a sulfonated polystyrene membrane as the electrolyte¹³. The current SoA shows that the most commercially used PEMFCs are perfluorosulfonic acid (PFSA) membranes. This is due to their high proton conductivity and chemical and mechanical stability.¹⁴ In the review of J. Ran et al¹⁵ several sulfonated polyethers and polysulfones have shown these highly seek properties. Sulfonated polymers with increasing levels of structure complexity have been developed in the last decades as reported within figure III-3:

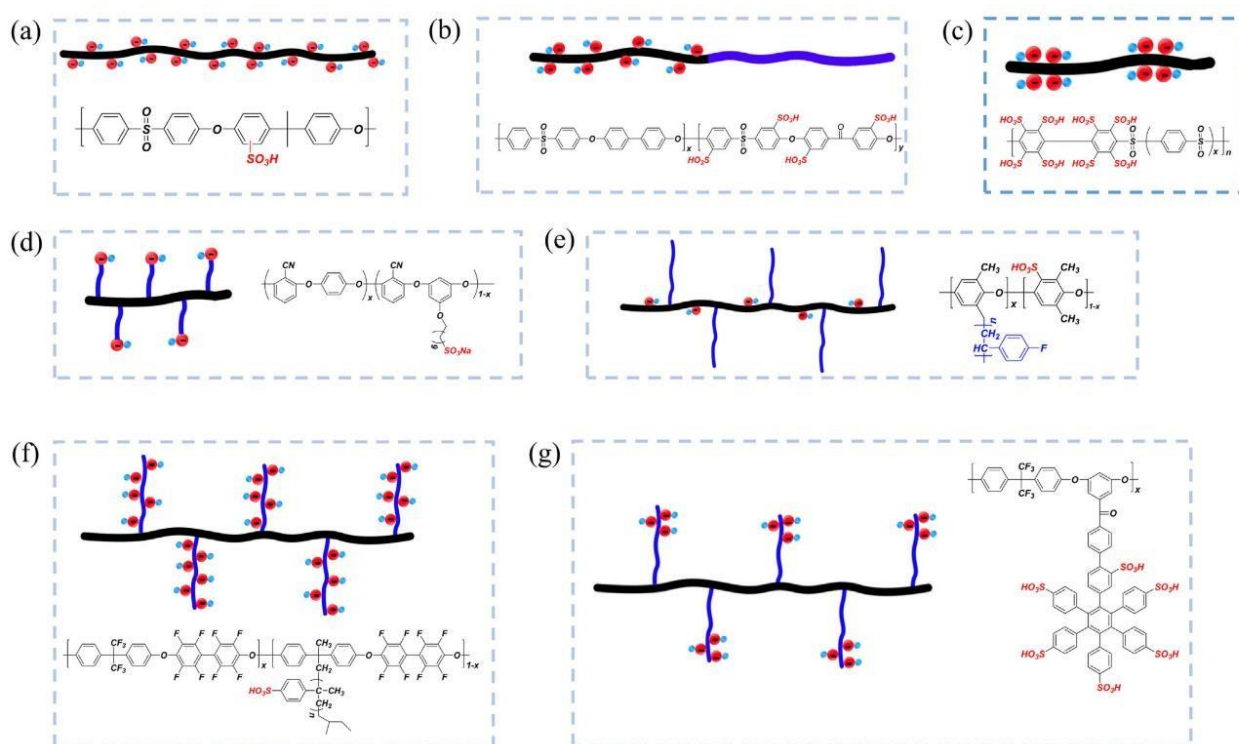


Figure III-3. Some examples of sulfonated polymers presented in J. Ran et al. review of Ion exchange membranes¹⁷.

In Figure III-3, examples of polymer featuring linear and bottlebrush architectures developed in the last decades are reported in Figure III-3. Initially, cationic exchange groups were attached to the polymer backbone (figure III-3, a). However, it was observed however that one of the most effective ways to enhance the proton conductivity is to construct interphases that act as proton-channels. This is the reason

why, the introduction of both hydrophilic and hydrophobic sub-parts in the polymer have been reported block copolymers of different design (figure III-3, f). Initially the sulfonic groups were attached to the backbone polymer (figure III-3, b, c); further developments proved that conductivity could be increased by having the sulfonic groups attached within side-branches grafted onto the polymer backbone (Figure III-3, d, f, g). The sulfonic acid groups attached to a perfluorocarbon backbone have shown a higher proton acidity of the proton in the $-SO_3H$ group compared to non-fluorinated carbon backbone increasing therefore the proton conductivity (figure III-3, f).

In my thesis, the development of new sulfonated polymers was investigated with hydrophobic and hydrophilic monomers. The goal was to improve the properties, efficiency, and reproducibility.

3. Strategy

Two objectives were set in this work.

- The preparation of new phosphonated proton conductive polymers (see Figure III-4), by direct phosphonation of the polymer (the polymerisation of phosphonated monomers were reported within Chapter 2).

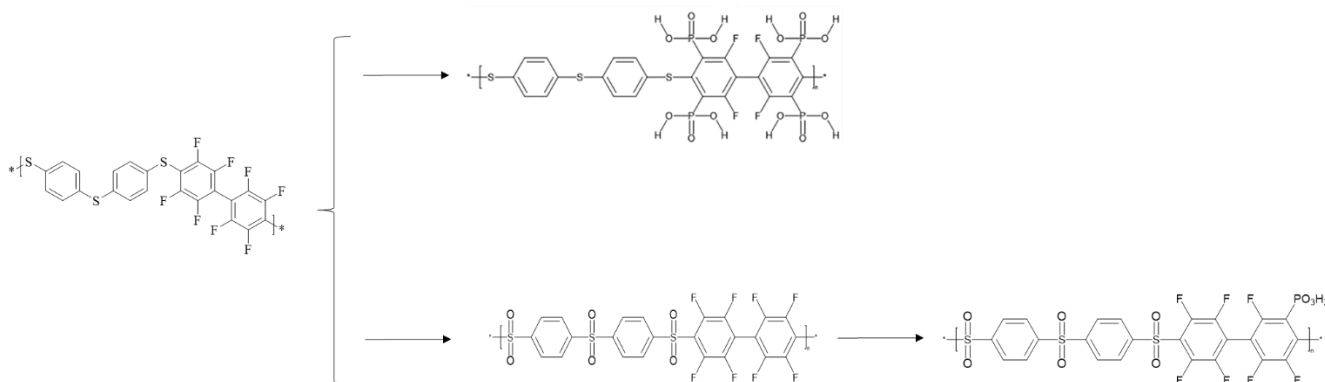


Figure III-4. Phosphonation paths of poly(phenylsulfide).

- The elaboration of new sulfonated proton conductive polymers (see Figure III-5), following two strategies:
 - Direct sulfonation of the polymer backbone
 - Grafting of sidechains ended with a sulfonic acid groups

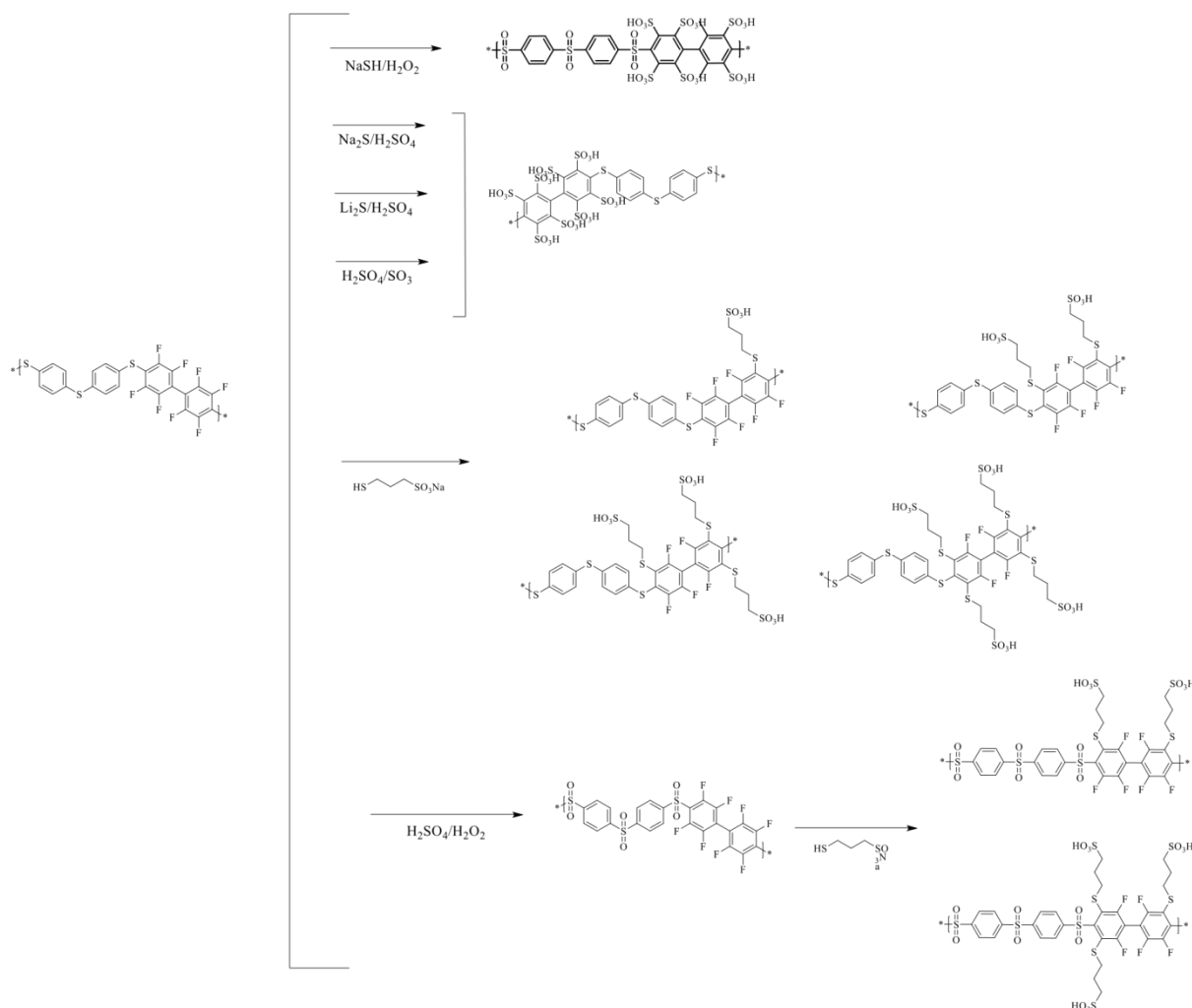


Figure III-5. Sulfonation paths of poly(phenylenesulfide).

Both strategies were explored using different sulfonating/phosphonating agents and fine-tuning the following parameters:

- Type of heating (e.g. conventional or microwave-assisted synthesis)
- Temperature
- Time

The chapter ends with a comparison of both strategies and of the properties of the final polymers toward their application in the fuel cell of the eSCALED H2020 project (MSCA-ITN-2017. GA#765376).

II. Materials and methods

1. Reagents

All glassware and materials were dried at 80 °C in a vacuum oven for 12h prior to use. Each single phosphonation and sulfonation reaction was tested with different polymer quantities, temperature, and functionalizing agents. The solvents used in these reactions (Dimethylsulphoxide DMSO, N,N-Dimethylacetamide DMAc, Dimethylformamide DMF) were of “anhydrous” quality (<0.005 % H₂O, ≥99.5 % purity, Sigma Aldrich).

All the following chemicals have been purchased from Sigma-Aldrich and used as received: sodium hydrosulfide hydrate (NaSH·xH₂O), sodium sulfide (Na₂S), lithium sulfide (Li₂S, 99,98 %), sulphuric acid (H₂SO₄, 95-97 %), sodium 3-mercapto-1-propanesulfonate (90 %), potassium carbonate (K₂CO₃, ≥99 %), lithium carbonate (Li₂CO₃, ≥99 %), lithium Nitrate (LiNO₃, 99.99 %) and 1,8-diazabicyclo [5.4.0]undec-7-ene (DBU, 98 %), decafluorobiphenyl (99 %), tris(trimethylsilyl)-phosphite (TMSP) (≥95 %) and dimethylphosphite (98 %). Distilled water was used for the precipitation and cleaning of the polymer, respectively.

2. Experimental

a. Phosphonation of fluorinated poly(phenylenesulfide)s

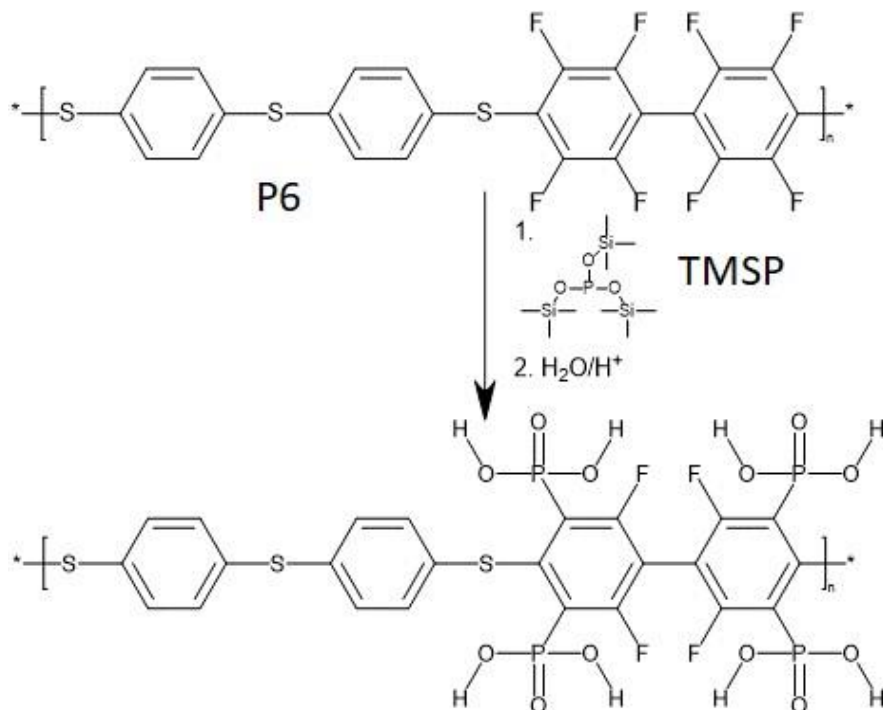


Figure III-6. Phosphonation of fluorinated poly(phenylenesulfide)s using Tris(trimethylsilyl) phosphite).

(i) Strategy 1

In a 50 ml three-necked round bottom flask equipped with a magnetic stirrer, a reflux condenser, and an argon inlet, fluorinated poly(phenylenesulfide)s P6 (2 g, 3.7 mmol) (chapter 2, p.28) and tris(trimethylsilyl)-phosphite (TMSP, 37 mmol, 13.6 ml) are added to the flask under argon and the reaction mixture is heated first, at 100 °C for 10 hours and second, at 150 °C for an additional 6 hour-long period. Temperature was then reduced to 100 °C and 30 ml of water were added to the flask to hydrolyse the silyl ester to yield the targeted phosphonic acid functions. The polymer was then precipitated in 500 ml of distilled water and the oily silicone phase appearing on the top of the solution was removed by decantation. The precipitated polymer gel was filtered and washed with water several times till pH 7 and dried at 90 °C under dynamic vacuum (base pressure of ca. 2×10^{-3} mbar). (yield = 83 %). ^1H NMR δ_{H} (400 MHz;

DMSO-d₆), 7.35 (broad peak), 5.40 (broad peak corresponding to the phosphonic protons); ¹⁹F

NMR δ_F (235 MHz; DMSO-d₆) -137.0, -132.3, -130.6, 128.7, -104.2, -102.9, -95.6. ³¹P NMR δ_P (162 MHz, DMSO-d₆) 2,16 (broad peak).

(ii) Strategy 2

In a 30 ml microwave tube (equipped with a magnetic stirrer and a reflux condenser) were added: fluorinated poly(phenylenesulfide)s P6 (1,84 mmol, 1 g), 5.5 ml of tris(trimethylsilyl)phosphite (TMSP, 8 eq., 14,69 mmol) and DMAc (5 ml). The reaction mixture was stirred under nitrogen till complete dissolution of the solids and then heated up to 130 °C, under pulsed irradiation mode at 300 W for 6 hr. Thereafter, 5 ml of water were added to the tube and heated up at 100 °C using the dynamic mode of irradiation, at 300 W during 30 min under nitrogen. The precipitated polymer was filtered-off and cleaned with distilled water prior to be dried at 60 °C under dynamic vacuum (base pressure of ca. 2 x 10⁻³ mbar). (yield = 49 %). ¹H NMR δ_H (400 MHz; DMSO-d₆), 7.24 (broad peak), 5.40 (broad peak corresponding to the phosphonic protons); ¹⁹F NMR δ_F (235 MHz; DMSO-d₆) 138.40, -137.7, -134.8, -132.3, -104.7, -103.3, -93.0. ³¹P NMR δ_P (162 MHz, DMSO-d₆) 2,10 (broad peak).

(iii) Strategy 3

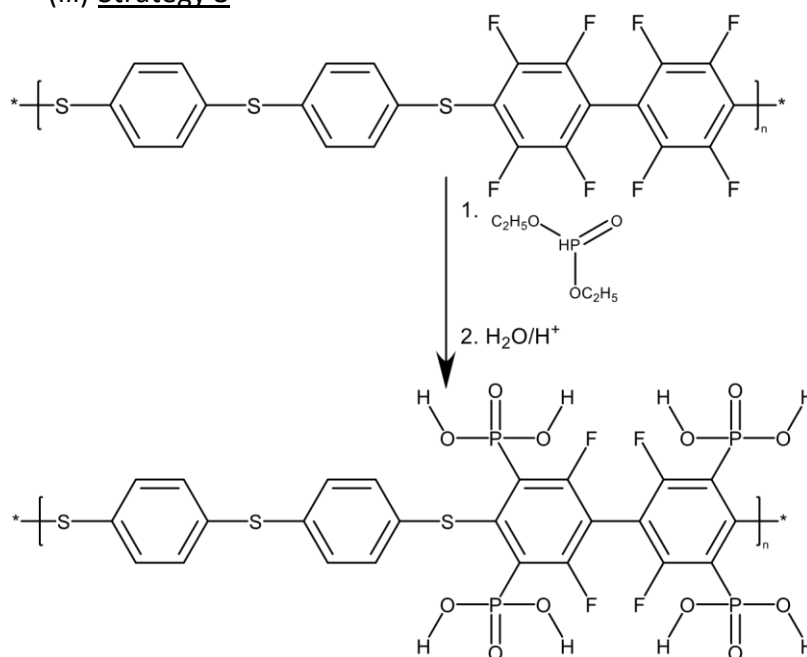


Figure III-7. Phosphonation of fluorinated poly(phenylenesulfide)s using dimethyl phosphite.

In a 50 ml three-necked round bottom flask (equipped with a magnetic stirrer, a reflux condenser and an argon inlet); fluorinated poly(phenylenesulfide)s P6 (0.37 mmol, 0.2 g), diethylphosphite (0.5 ml) and 1 ml DMAc were added under argon, and the reaction mixture was heated to 180 °C for 1 hour under stirring prior to be cooled down to 100 °C and left overnight.

At 100 °C, 2 ml of water was added to the flask to hydrolyse the silyl ester into the phosphonic acid functions. No product could be isolated.

b. Phosphonation of fluorinated poly(phenylenesulfone)s

b.1. Oxidation of sulphides to sulphones

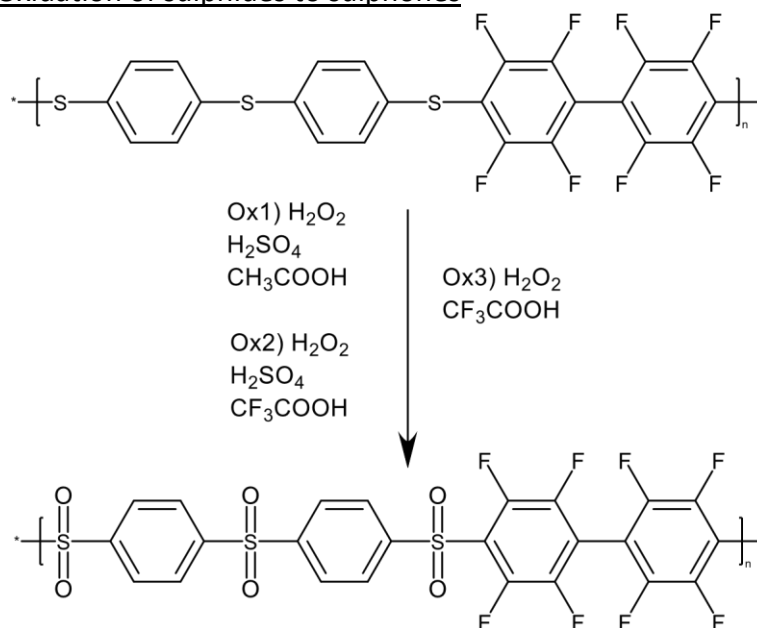


Figure III-8. Oxidation of polyfluorinated poly(phenylene sulfide) to polyfluorinated poly(phenylene sulfone).

(i) Strategy 1 (Ox1)

Oxidation of the sulphides groups of the polyfluorinated poly(phenylenesulfide)s to polyfluorinated poly(phenylenesulfone)s was done following the procedure of S. Takamugu *et al.*¹⁶ Polyfluorinated poly(phenylenesulfide) polymer (1.5 g, 2.75 mmol)

was added to a one neck 100 ml round- bottom flask equipped with a reflux condenser containing H₂O₂ (8 ml, 80 mmol, 34.5–36.5 %), CH₃COOH (30 ml). The flask was cooled down to 0 °C in an ice bath before adding H₂SO₄ (9 ml, 95-97 %, Sigma-Aldrich). The mixture was stirred for 48 hrs at 30 °C prior to be heated up to 100 °C for 1 h. A white milky like dispersion was filtered and the oxidized product was washed three times with 50 ml of deionized water and once with 50 ml 2propanol before to be dried under dynamic vacuum (base pressure of ca. 2×10^{-3} mbar) at 30 °C overnight. (1.6 g obtained, yield = 91 %)

(ii) Strategy 2 (Ox2)

Within this second strategy, the oxidation of the sulphides groups of the polyfluorinated poly(phenylenesulfide)s to polyfluorinated poly(phenylenesulfone)s was conducted using trifluoroacetic acid instead of acetic acid. Fluorinated polythioether polymer (5.5 g, 15 mmol) was added to a 250 mL three-neck round-bottom flask equipped with a reflux condenser containing H₂O₂ (30 ml, 300 mmol, 34.5–36.5 %) and CF₃COOH (110 ml). The flask was cooled down to 0 °C in an ice bath before adding H₂SO₄ (27 ml, 95-97 %, 0.51 mmol). The mixture was stirred for 72 hrs at 30 °C before to be heated up to 100 °C for 1 h. The dispersion was filtered to collect the powder and it was washed three times with 50 ml of deionized water and afterwards with 50 ml of 2-propanol prior to being dried under dynamic vacuum (base pressure of ca. 2×10^{-3} mbar) at 30 °C overnight. (6.28 g, yield = 98 %)

(iii) Strategy 3 (Ox3)

In this third strategy, the oxidation of the sulphides groups of the polyfluorinated poly(phenylenesulfide)s to polyfluorinated poly(phenylenesulfone)s was performed using trifluoroacetic acid and hydrogen peroxide. Fluorinated polythioether polymer (8.25 g, 15 mmol) was added to a 500 mL three-neck round-bottom flask equipped with a reflux condenser containing CF₃COOH (150 ml, ≥ 99 %, Sigma-Aldrich). H₂O₂ (44 ml, 44 mmol) was added via dropping funnel under stirring, at 20 °C. The mixture was stirred for 72 hrs at 30 °C prior to be heated up to 100 °C for 1 h. The dispersion was

filtered to collect the powder and it was washed three times with 50 ml of deionized water and once with 50 ml 2-propanol prior to be dried under dynamic vacuum (base pressure of ca. 2×10^{-3} mbar) at 30 °C overnight. (9.37 g obtained, 97 %)

b.2. Phosphonation of fluorinated poly(phenylenesulfone)s

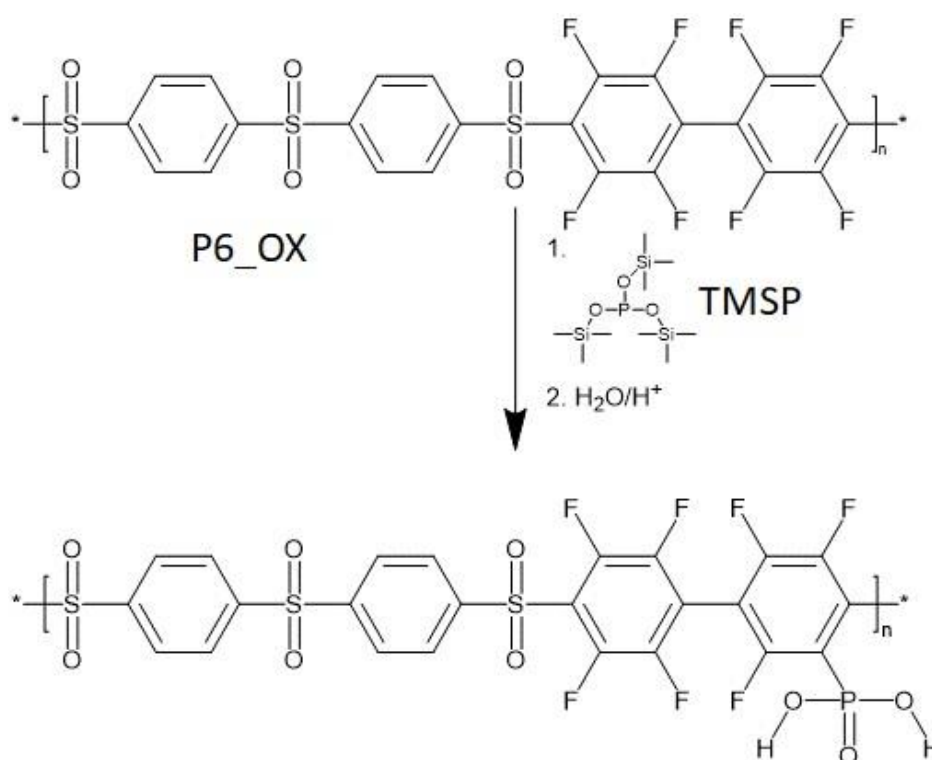


Figure III-9. Phosphonation of fluorinated poly(phenylenesulfone)s.

In a 50 ml three-necked round-bottom flask (equipped with a magnetic stirrer, a reflux condenser, and an argon inlet), 3 g of P6_OX (Chapter 2) (4.69 mmol) and 1.65 ml of tris(trimethylsilyl)-phosphite (TMSP, 4,69 mmol) were added under argon, and the suspension is heated up to 180 °C. After 10 min, 10 ml of DMF was added under argon and the reaction mixture was left at 180 °C under stirring for one hour prior to be cooled down to 100 °C and left for one additional hour under stirring. 5 ml of distilled water were added to the flask at 100 °C to hydrolyse the silyl ester groups into the phosphonic acid functions. The reaction mixture was then left under stirring for one hour at 100 °C. The oily phase was extracted and the aqueous phase was then purified by dialysis (12000 Da tubes) in distilled water (5000 ml) for 48 h changing the water 3 times a day. The product is finally dried at 90 °C (yield=64 %). $^1\text{H NMR}$ δ_{H} (400 MHz;

DMSO-d₆), 7.35 (d, J 59.26 Hz); ¹⁹F NMR δ_F (235 MHz; DMSO-d₆) -137.0, -132.3, -130.6, 128.7, -104.2, 102.9, 95.6.

c. Sulfonation of fluorinated poly(phenylenesulfide)s using sodium hydrosulfide

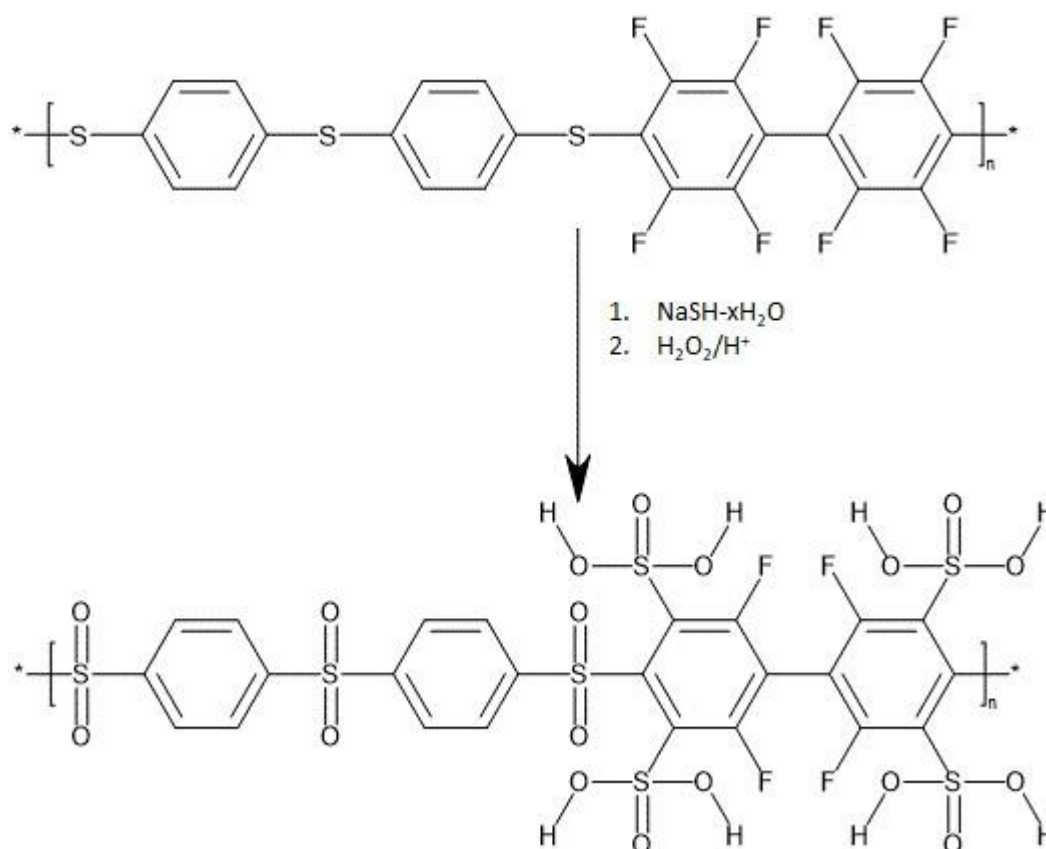


Figure III-10. Sulfonation of fluorinated poly(phenylenesulfide)s.

In a 500 ml three-necked round-bottom flask (equipped with a mechanical stirrer and a deanstark trap); fluorinated poly(phenylenesulfide)s P6 (2 g, 3.8 mmol), NaSH (5.65 g, 60.8 mmol), 60 ml N-methyl-2-Pyrrolidone (NMP) and 120 ml toluene were added. The mixture was degassed by nitrogen bubbling for 10 min prior to adding K₂CO₃ (41.88 g, 30.4 mmol). The temperature was then increased to 160 °C for 4 hours. Thereafter, the solution was poured in diethyl ether and the precipitated solid was then solubilized in 50 ml of acidic water (3 ml, 20 % H₂SO₄). The oxidation of the sulfide groups to sulfonic acid ones was carried out by adding to this acidic solution aq. H₂O₂ (33 mL, 34.5–36.5 %) under stirring for 24 h at 40 °C, followed by 1 h at 110 °C.

Afterwards, the solution was filtered and dialyzed (MWCO: 1000 Da) overnight in deionized water. The polymer obtained was insoluble in DMAc, DMSO, CHCl_3 and H_2O .

d. Sulfonation of fluorinated poly(phenylenesulfide)s using sodium sulfide

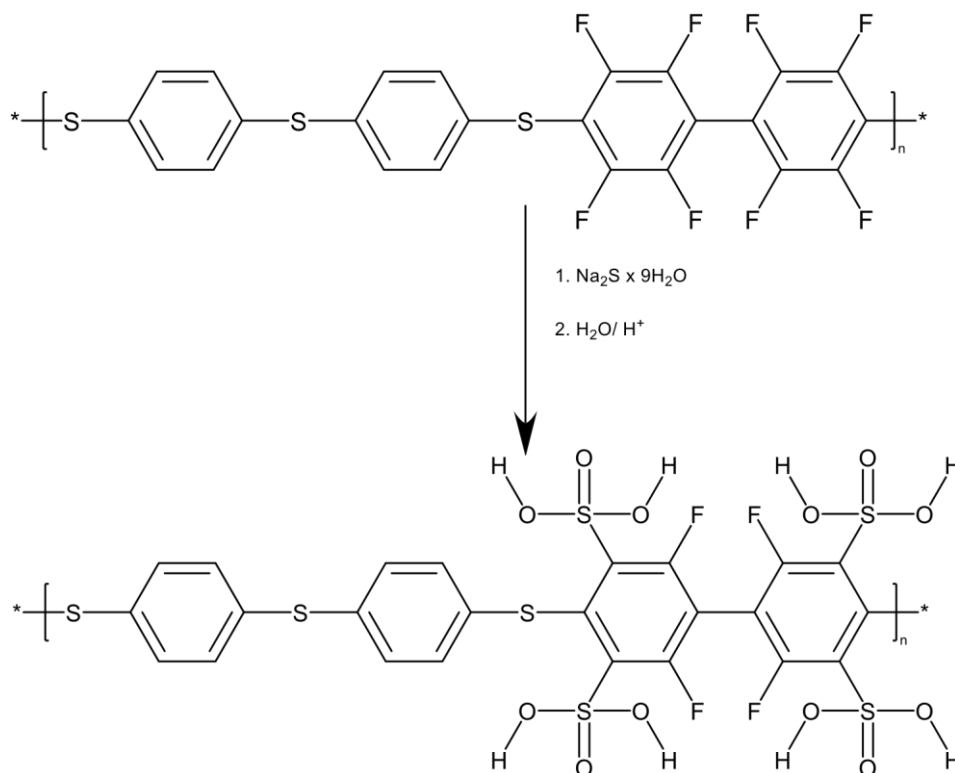


Figure III-11. Sulfonation of fluorinated poly(phenylenesulfide)s using Na_2S .

(i) Strategy 1

In a 50 ml three-necked round-bottom flask (equipped with a mechanical stirrer, a reflux condenser and a dean-stark trap) fluorinated poly(phenylenesulfide)s P6 (1 g, 1.88 mmol), $\text{Na}_2\text{S} \times 9\text{H}_2\text{O}$ (3.6 g, 15mmol) and 15 ml DMAc were added. The reactive medium was degassed for 30 min by bubbling nitrogen before heating up at $150\text{ }^\circ\text{C}$ for 6 h, water being distilled-off with the Dean-stark trap. Thereafter, the solution was cooled down and the mixture was poured in 50 ml of acidic water (10 ml H_2SO_4 , 95-97 %). A yellow precipitate was obtained. It was filtered and washed several times with distilled water. It was finally dried at $60\text{ }^\circ\text{C}$ for 6 h under dynamic vacuum (base pressure of ca. 2×10^{-3} mbar). (1.15 g of product was obtained). No yield can be given as it was not proven that it was the expected product.

(ii) Strategy 2

In a 10 ml microwave vial (equipped with a magnetic bar), fluorinated poly(phenylenesulfide)s P6 (0.2 g, 0.38 mmol), $\text{Na}_2\text{S} \times 9\text{H}_2\text{O}$ (0.9 g, 3.8 mmol) and 5 ml DMAc were added, and the reaction medium was degassed by bubbling with nitrogen for 10 min. It was then heated up under nitrogen at 150 °C for 2 hours, under stirring and using the pulsed irradiation mode at 300 W. Thereafter, an insoluble hard mass is found in the vial. The product is insoluble in 50 ml of acidic water (20 % H_2SO_4), neither in DMAc nor DMSO. (1.08 g of product was obtained). No yield can be given as it was not proven that it was the expected product.

e. Sulfonation of fluorinated poly(phenylenesulfide)s using lithium sulfide

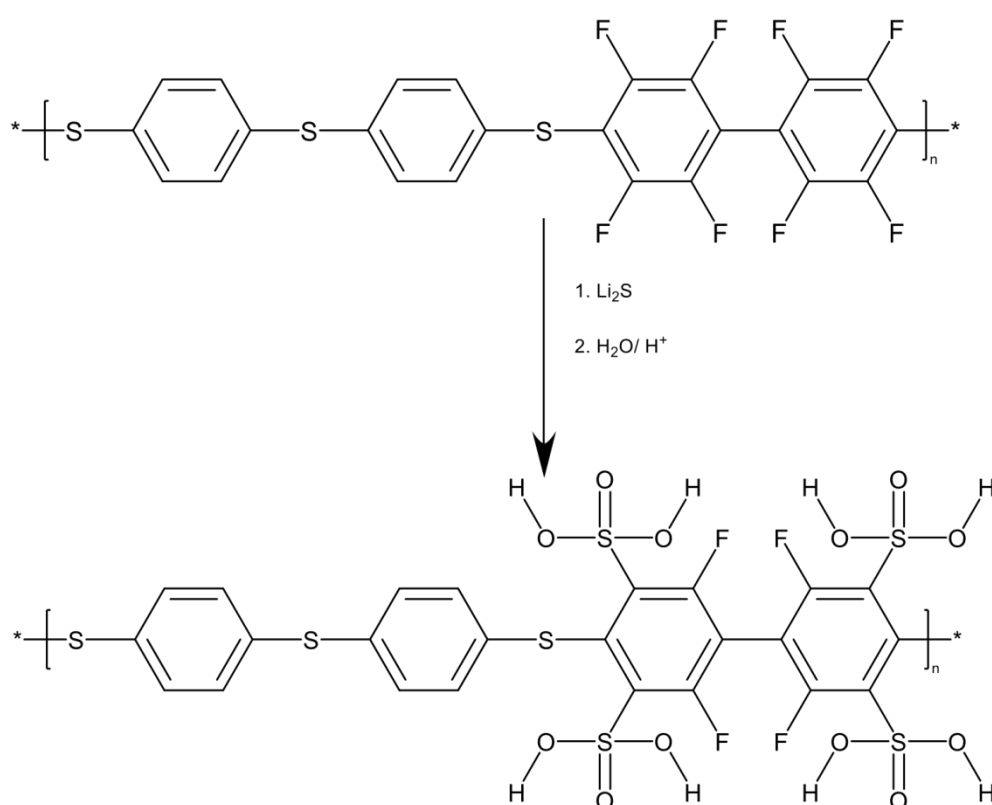


Figure III-12. Sulfonation of fluorinated poly(phenylenesulfide)s using Li_2S .

In a 250 ml three-necked round-bottom flask (equipped with a mechanical stirrer and nitrogen in/outlet), fluorinated poly(phenylenesulfide)s P6 (2 g, 3.6 mmol) (grained prior to use) and 50 ml of DMAc were added. The mixture was degassed under

nitrogen during 1 hr. To the homogenous mixture, Li_2S (0.19 g, 8 mmol, 2.2eq) was then added under inert atmosphere and the reaction mixture was heated up at $60\text{ }^\circ\text{C}$ and left for 72 h before to be heated up to $180\text{ }^\circ\text{C}$ for a period of 6 additional hours. Thereafter, the mixture was added to 500 ml of distilled water and a yellow powder was obtained. It was filtered out and dried at $60\text{ }^\circ\text{C}$ under dynamic vacuum (base pressure of ca. 2×10^{-3} mbar) for 6 h. (0.60 g of product was obtained). No yield can be given as it was not proven that it was the expected product.

f. Sulfonation of fluorinated poly(phenylenesulfide)s using sulfuric acid

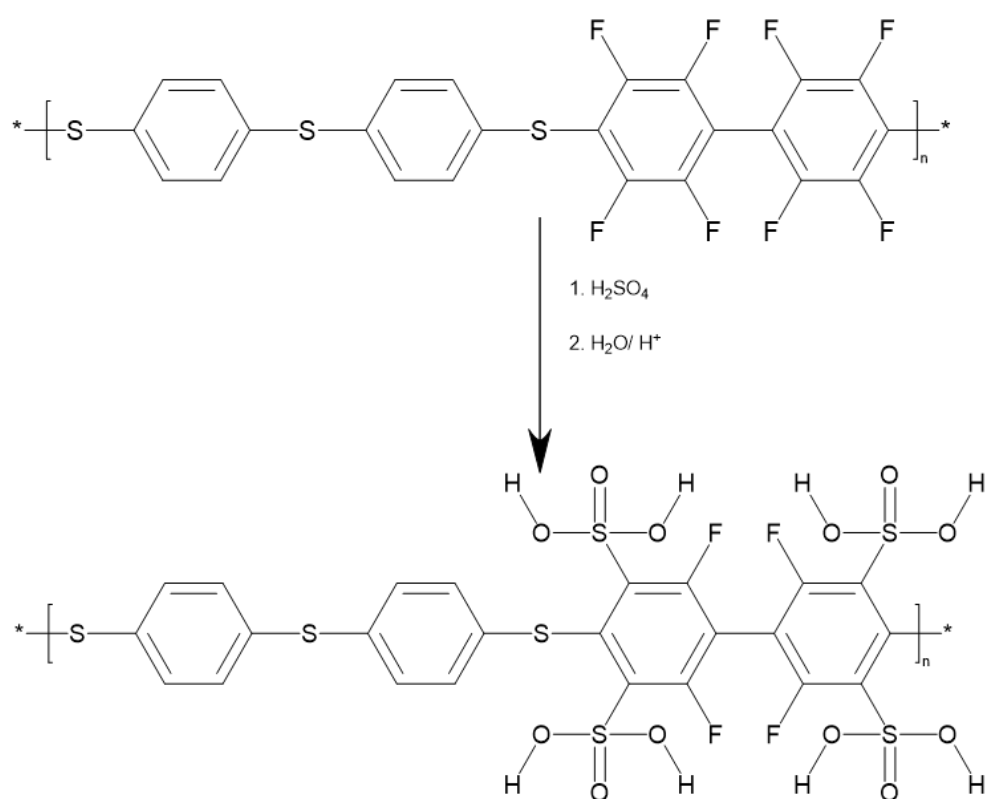


Figure III-13. Sulfonation of fluorinated poly(phenylenesulfide)s using H_2SO_4 .

In a 250 ml three-necked round bottom flask (equipped with magnetic stirrer), fluorinated poly(phenylenesulfide)s P6 (2 g, 3.6 mmol) was added, and the flask was placed in an ice bath. Thereafter, 50 ml of H_2SO_4 (98 %) was slowly added and the solution was left under stirring and nitrogen at room temperature for 48h. The reaction medium turned black. Distilled water (10 ml) was slowly added and the solution turned red. The solution was then filtered-off, leaving a red powder. (1.65 g obtained). No yield can be given as it was not proven that it was the expected product.

g. Sulfonation of fluorinated poly(phenylenesulfide)s using sodium 3-mercapto-1-propanesulfonate

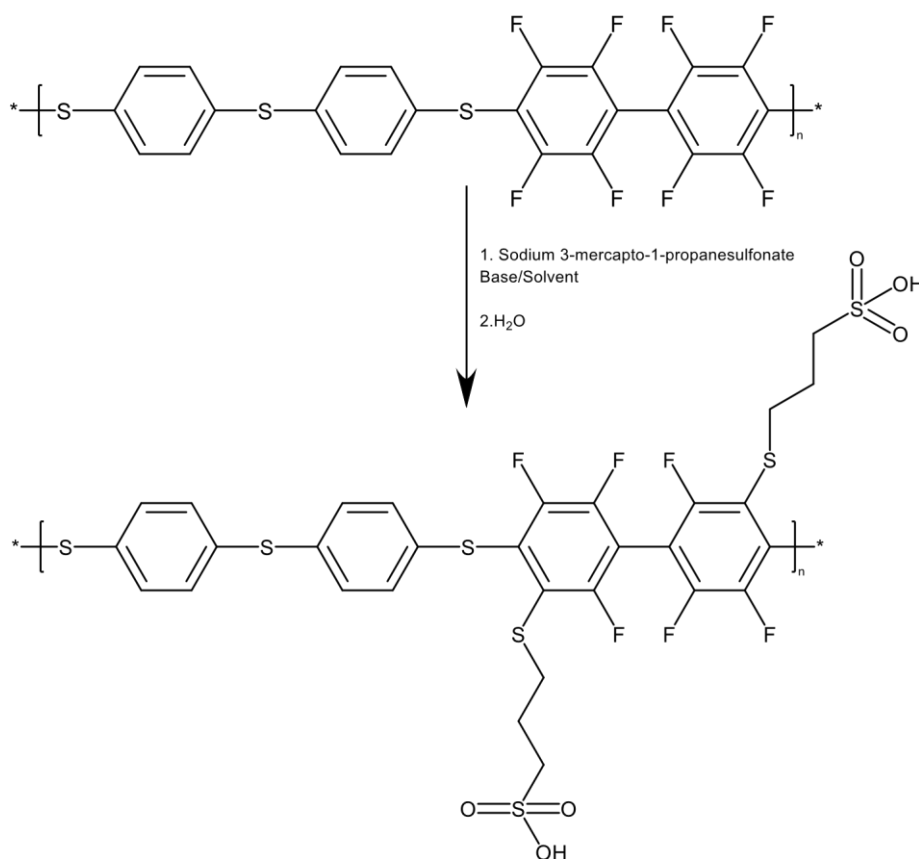


Figure III-14. Sulfonation of fluorinated poly(phenylenesulfide)s using Sodium 3-mercapto-1-propanesulfonate.

(i) Strategy 1

In a 100 ml three-necked round bottom flask (equipped with a magnetic stirrer) fluorinated poly(phenylenesulfide)s P6 (1.50 g, 2.75 mmol), Sodium 3-mercapto-1-propanesulfonate (1.20 g, 6.06 mmol, 2,2 eq.) and 60 ml DMAc were added. The mixture was stirred until it became homogenised. LiNO₃ (0.76 g, 11.02mmol, 4.0 eq.) was then added and the reactive medium was heated up at 60 °C for 6 h. No precipitate was obtained when poured into distilled water. The solution was dialysed and then dried at 80 °C under a dynamic vacuum (base pressure of ca. 2 x 10⁻³ mbar) in the oven (1.37 g obtained). No yield can be given as it was not proven that it was the expected product.

(ii) Strategy 2

In a 100 ml three-necked round-bottom flask (equipped with a magnetic stirrer) fluorinated poly(phenylenesulfide)s P6 (2 g, 3.13 mmol), DBU (0.93 ml, 6.25 mmol, 2 eq.), sodium 3mercapto-1-propanesulfonate (1.36 g, 6.99 mmol, 2.2 eq.) and 40 ml DMAC were added under nitrogen. The reactive mixture was left under nitrogen and stirring at room temperature for 72 h. The solution was then dialyzed during 72 h changing the distilled water 3 times per day and then the dialyzed solution was dried at 80 °C under vacuum (base pressure of ca. 2×10^{-3} mbar) in the oven (1.56 g obtained). No yield can be given as it was not proven that it was the expected product.

h. Sulfonation of fluorinated poly(phenylenesulfone)s using sodium 3-mercapto-1-propanesulfonate

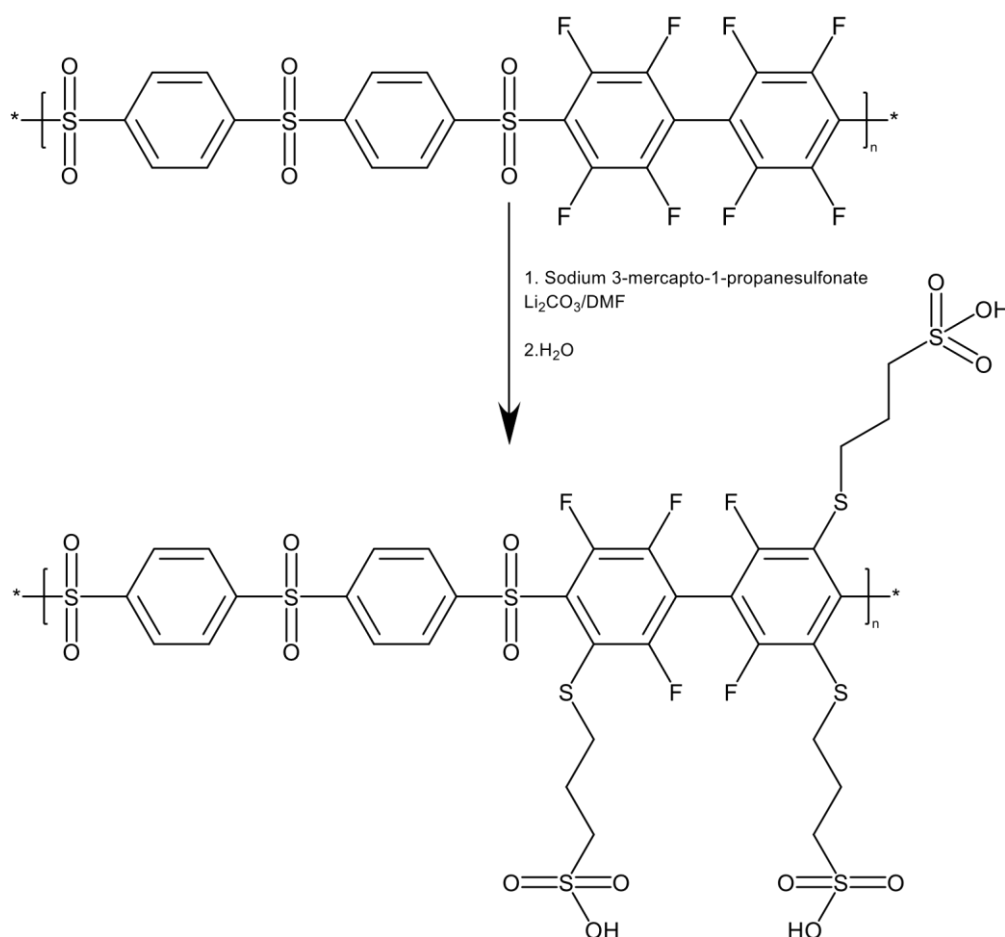


Figure III-15. Sulfonation of fluorinated poly(phenylenesulfone)s using Sodium 3-mercapto-1-propanesulfonate.

In a 100 ml three-necked round-bottom flask (equipped with a magnetic stirrer and reflux condenser) fluorinated poly(phenylenesulfone)s P6_{ox} (2 g, 3.13 mmol)

previously grinded into fine powder, Li_2CO_3 (0.92 g, 9.38 mmol, 3eq.), sodium 3-mercapto-1-propanesulfonate (1.86 g, 9.56mmol, 3 eq.) and 30 ml DMAc were added. The temperature was increased up to 130 °C and the mixture was left under nitrogen and stirring for 6 hr. The solution was cooled down to 100 °C and distilled water was then added. The mixture was kept at 100 °C for 30 min. The product was precipitated in cold acetone, dissolved in distilled water before to be precipitated again in acetone. The product was separated by centrifugation at 2400 rpm and dried at 60 °C (1.45 g obtained). No yield can be given as it was not proven that it was the expected product.

3. Technics

a. Microwave reactor

A Discover™ microwave equipment was used for the reactions.¹⁷ The reaction parameters (e.g.,

temperature, power, cooling, stirring, etc.) were set using the onboard piloting software of the apparatus. The parameters set were the irradiation mode (dynamic or pulsed), the temperature as controlled by the IR sensor, the pre-reaction stirring time (0 s), and the temperature ramp mode (as fast as possible).

b. IR spectroscopy

FTIR spectrometer (Nicolet iS50 FTIR Spectrometer) with a range of 15 to 27,000 cm^{-1} .

c. NMR spectroscopy

^1H , ^{13}C and ^{19}F NMR spectra were recorded on a Bruker Avance 400 spectrometer using deuterated dimethyl sulfoxide (DMSO-d_6) or chloroform (CDCl_3) as solutions.

d. Size-Exclusion Chromatography (SEC)

An Agilent Technology SEC line (Series 1200) coupled with a viscosity detector (PSS ETA2010) and a refractive index detector (Shodex RI71) was used. A set of three PSS GRAM columns (30, 3000, 3000 Å) was used and calibrated with a series of polystyrene standards in N,N-dimethylacetamide (DMAc) containing 5 wt.% LiBr. All the samples were filtered by a Whatman syringe filter over a microporous PTFE membrane (1.0 µm, Whatman 6878-2510) before injection.

Used in IPREM (UPPA): Molar masses and molar mass distributions were determined by SEC in THF on Waters pump model 515, detectors: RI ERC-101 and UV-VIS Soma S-3702 (254 nm), temperature: 30 °C, standard: polystyrene, concentration: 2 g/l, flow rate: 1.0 ml/min, columns: SDV 106, SDV 104 and SDV 500.

e. Thermal analysis

The thermal stability of the polymers was determined by thermogravimetry (TGA, Netzsch, model STA 449C) with a heating rate of 20 °C /min under an oxygen-enriched atmosphere (65– 70 % O₂, 35–30 % N₂).

f. Elemental Analysis

Elemental analysis was performed in the University of Stuttgart at the institute of Organic Chemistry onto an elemental Analyzer Model 1106 from Car.

III. Results and discussion

1. Phosphonations

Two different phosphonations were investigated using phosphonation agents. A phosphonation of fluorinated poly(phenylenesulfide)s (P6) and a phosphonation on a fluorinated poly(phenylenesulfone)s (P6_OX) were carried on. The objective was to obtain a highly phosphonated conducting polymer from which a proton conducting membrane could be processed and used in PEMFC at 100 °C. In the following section, the results of these attempts are discussed.

a. Phosphonation of fluorinated poly(phenylenesulfide)s

(i) Strategy 1

Complete phosphonation of P6 was attempted using an excess of TMSP (10 eq.). The first trials were conducted using conventional heating (Figure III-17), conventional heating having the advantage of being scalable and easier to control when compared to microwave heating.



Figure III-17. Phosphonation using strategy 1 (conventional heating).

The goal was to obtain phosphonation of every single fluorine as it would have a higher proton conductivity with an increased number of substitution. However the results showed a much lower degree of substitution: 3 % calculated from ^{19}F NMR (Figure III-18).

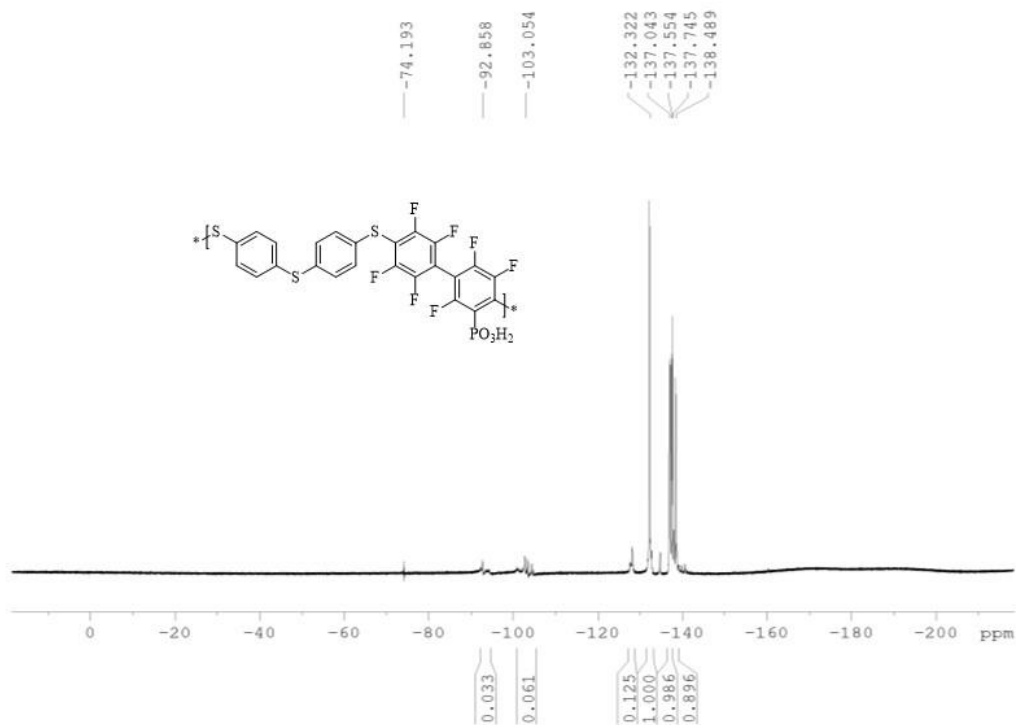


Figure III-18. ^{19}F NMR phosphonated poly(phenylenesulfide)s

^1H NMR (figure III-19) showed a broad peak at 5.45 ppm that corresponds to the acidic protons of the PO_3H_2 . The doublet previously seen in the prepolymer had turned into a broad peak around the same values (7-7.5 ppm).

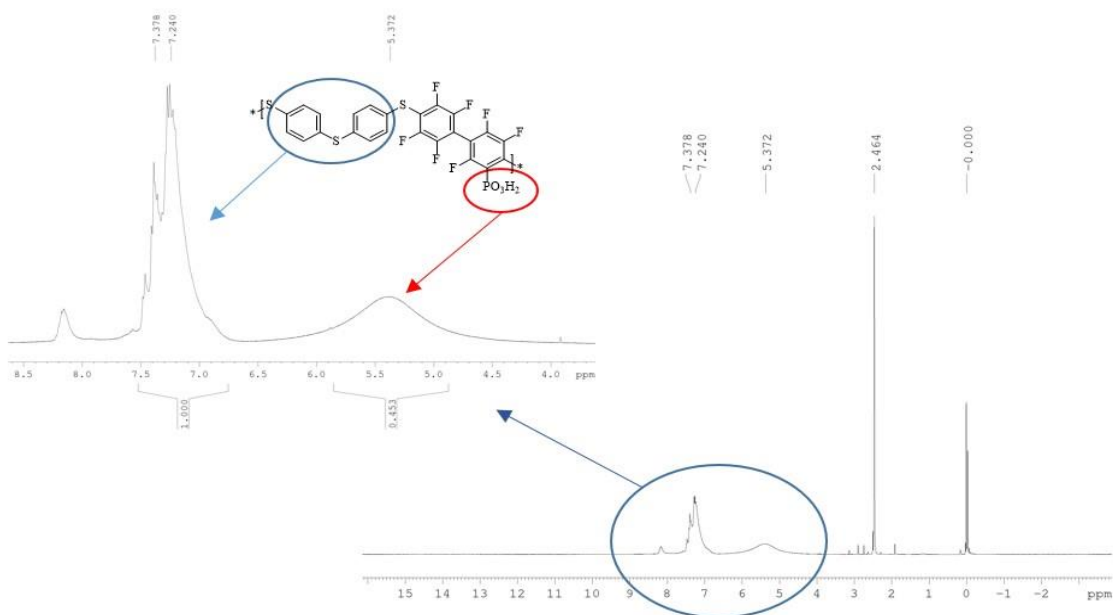


Figure III-19. ^1H NMR phosphonated poly(phenylenesulfide)s.

(ii) Strategy 2

A microwave heating methodology was investigated, for the first time to the best of our knowledge. Microwave was used as the energy providing source to start the reaction. No literature was found referring to this reaction but the use of Microwave for phosphonation of halide aryls has been already successfully demonstrated¹⁸. A heat power of 300 W was used to reach a temperature of 130 °C. TMSP (8 eq.) was tentatively used to try to reach a high degree of phosphonation. However, ¹⁹F NMR (Figure III20) analysis showed that just a 7.4 % of Fluorine atoms were substituted, which indicates that less than one substitution per polyfluorinated biphenyl unit. We are left to propose that once one Fluorine atom is substituted with a phosphonic acid function, the reactivity is decreased, preventing further substitution.

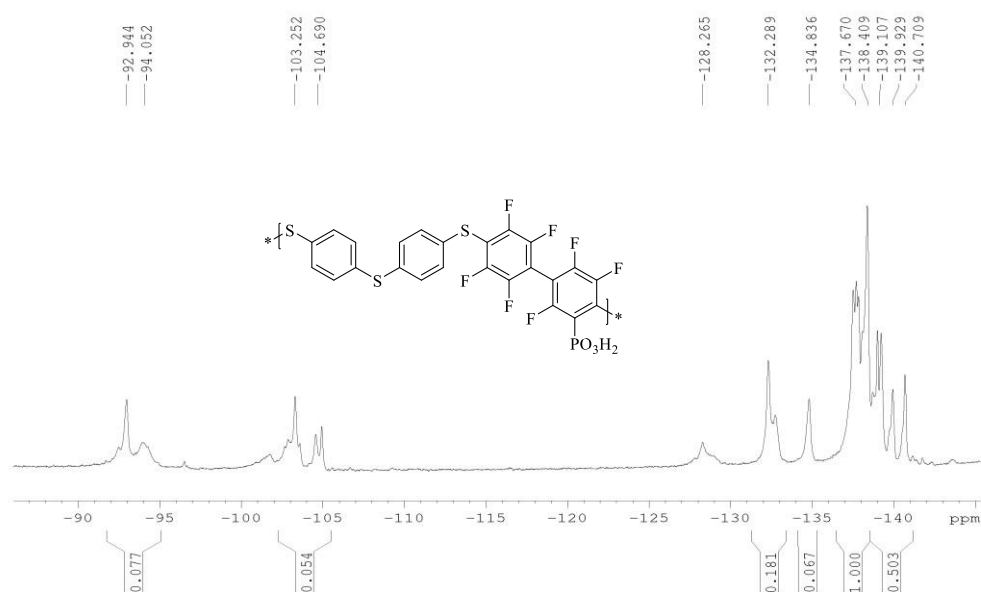


Figure III-20. ¹⁹F NMR phosphonated poly(phenylenesulfide)s.

(iii) Strategy 3

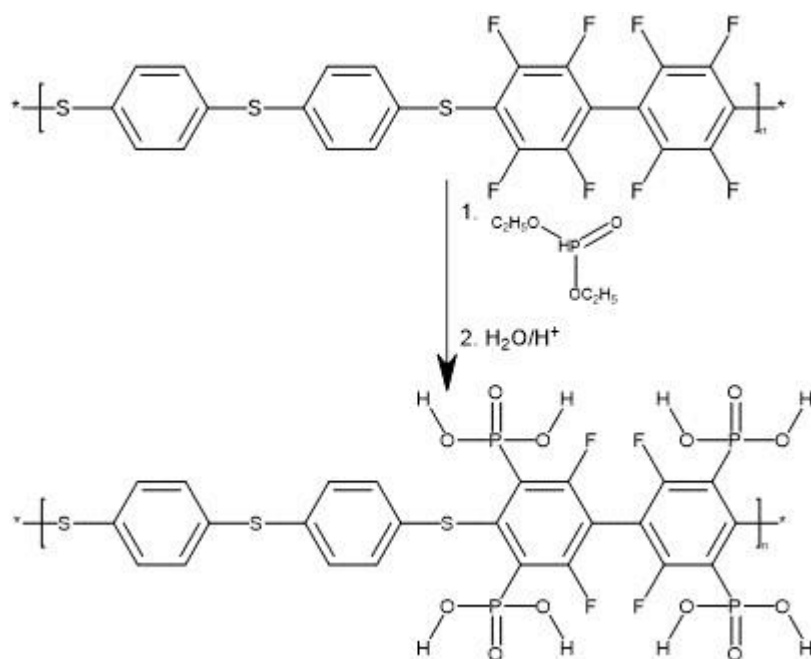


Figure III-21. Phosphonation of fluorinated poly(phenylenesulfide)s using diethyl phosphite.

Another phosphonation agent was tested in this reaction to see if a less sterically hindered phosphonating agent than TMSP would favor the nucleophilic aromatic substitution ($\text{S}_{\text{N}}\text{Ar}$). However, no substitution was obtained suggesting that the electronic effect has a higher importance than the steric one.

Even though some substitutions were observed when TMSP (strategy 1) was used, the efficiency of substitution remains low. The electron-withdrawing effect of the $-\text{SO}_2-$ on the perfluorinated phenyl allows the electrophilic attack of the TMSP on the $\text{C}^{\delta+}$ while having the poly(phenylenesulfide) doesn't have this electron-withdrawing effect. This explains that the main problem in this phosphonation is not the heating method or the phosphonating agent, three strategies were attempted changing these conditions. We are left to conclude that the polymer chain microstructure itself is the main problem.

b. Phosphonation of fluorinated poly(phenylenesulfone)s : step1, Oxidation of sulfides to sulfones

There are many reasons why it was considered oxidation of the sulfide linkages (-S-) to sulfone linkages (-SO₂) before further functionalization. According to the literature, the poly(phenylene sulfone)s show very high thermal, thermooxidative and hydrolytic stabilities, low solubility, and reduced swelling in water when compared to the poly(phenylene sulphide)s.¹⁹ Oxidizing the sulphide bonds will turn the aromatic groups more electron deficient and this can have positive effects for the polymer we are looking for as it would increase its proton mobility. As explained by A. Chromik et al²⁰, an electron-deficient aromatic polymer building block will lead to a higher dissociation degree of a SO₃H group, which is associated with a higher proton conductivity. G. Tivinidze²¹ pointed out how the poly(phenylene sulfone)s preserve its properties in the membrane in the hydrophilic domain leading to a low electro-osmotic water drag. It was expected that having a sulfone instead of a sulfide next to the fluorinated phenyl would allow for an easier substitution in the Fluorine atoms due to the electron density in the fluorinated phenyl.

Three different oxidations routes were followed and are reported within Figure II-22.

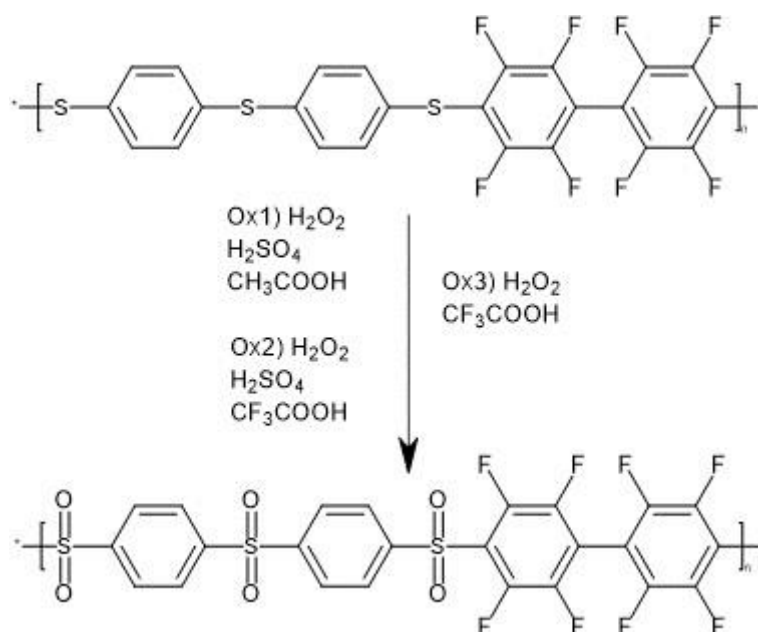


Figure III-22. Oxidation of poly(phenylenesulfide)s scheme.

(i) Strategy 1 (Ox1)

The first route involved sulfuric acid, hydrogen peroxide, and acetic acid (a) as reported by Takamuku et al²². The oxidation mechanism proposed (Figure III-23) is similar to the one proposed by G. Kermanshahi and K. Bahrami²³, but using sulfuric acid as the catalyst instead of Fe₃O₄@BNPs@SiO₂-SO₃H. The sulfuric acid will act as a catalytic proton exchanger with H₂O₂ (see Figure III-23) to allow for the loss of an oxygen atom that will oxidize the sulfide to a sulfoxide (R₁S(=O)R₂) initially and to a sulfone (R₁S(=O)₂R₂) in the second part of this cycle.

The only side-product for this oxidation will be 2 molecules of H₂O.

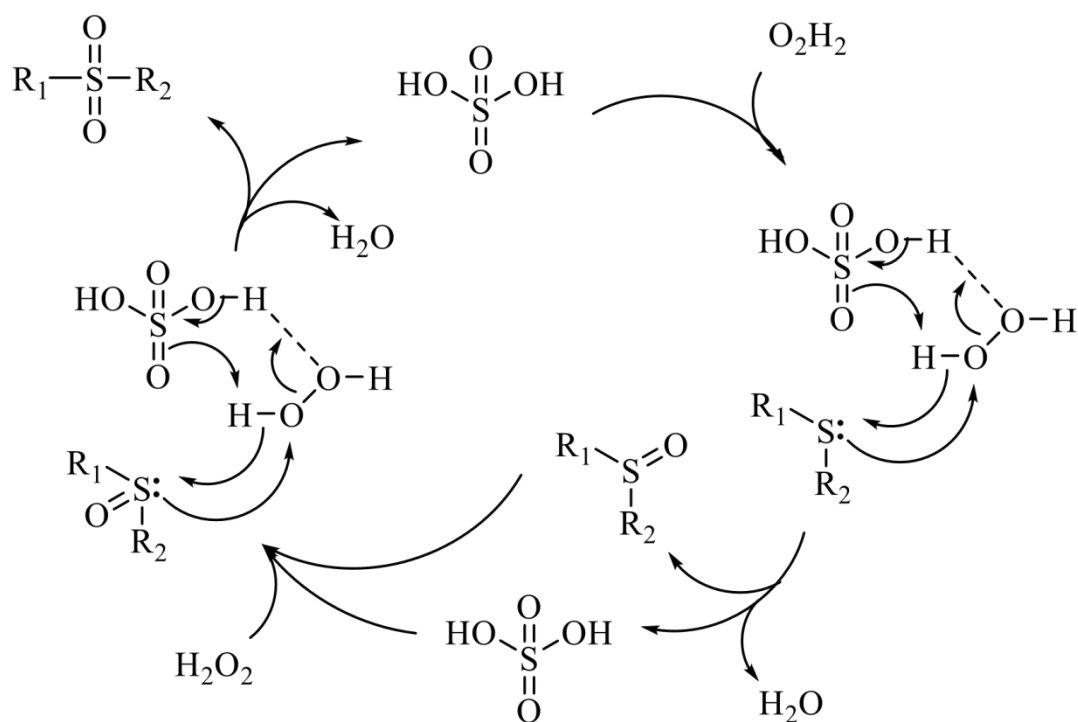


Figure III-23. Proposed Oxidation mechanism following G. Kermanshahi and K. Bahrami catalytic mechanism²⁴.

(ii) Strategy 2 (Ox2)

Oxidation was repeated changing acetic acid for trifluoroacetic acid as a middle step before removing the sulfuric acid from the reaction. The purpose of this reaction was to check if there was any change when using trifluoroacetic acid instead of acetic acid. In Figure III-24, one can notice the polymer product is white after this post-oxidation step.

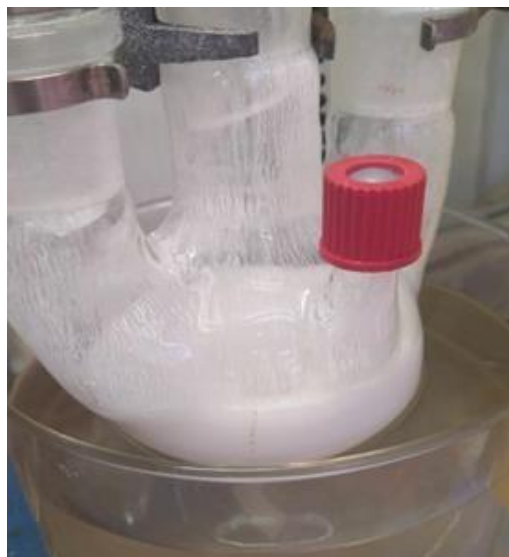


Figure III-24. Oxidation of P6, from sulfide to sulfone.

(iii) Strategy 3 (Ox3)

The oxidation was repeated under less harsh conditions by removing the sulfuric acid. It was anticipated that trifluoroacetic acid (TFA) could play the role of a catalytic proton exchanger with hydrogen peroxide being the oxidant in concordance with the findings of Horvat et al.²⁵ article. In this article, TFA is used in combination with H₂O₂ to oxidise sulphides to sulfoxides at RT. These authors also reported that when the temperature is increased to 60 °C a mix product of sulfoxides and sulfone is obtained. The reaction time is 3h, however in this case the time was decreased to 1h and the temperature was increased to 100 °C to obtain full conversion to sulfone.

In the 3 cases it was found that the polymer obtained was insoluble in DMSO, DMAc, CHCl₃, THF and DMF and therefore NMR analyses could not be undertaken. It should be noted that the fluorinated initial polymer that was initially soluble in DMAc was no longer detected.

Elemental analysis

Elemental analysis were performed to reveal any differences between the 3 strategies (Table II-1).

ELEMENT	ROUTE 1		ROUTE 2	ROUTE 3
	P6_OX THEORETICAL	P6_OX1 EXPERIMENTAL	P6_OX2 EXPERIMENTAL	P6_OX3 EXPERIMENTAL
C	45.0	46.3	46.1	45.8
H	1.3	1.3	1.2	1.3
S	15.0	14.9	15.0	14.8

Table III-1. Elemental analysis fluorinated poly(phenylene sulfone)s.

The results showed less than 5 % deviation between expected and theoretical values. Given its change in solubility and the results in the elemental analysis it can be concluded that the oxidation was successful.

Thermogravimetric coupled with IR analyses

Thermogravimetric analysis of P6-Ox1 is reported in Figure III-25. Sulfur trioxide (SO₃, red line) and carbon monoxide (CO, black line) were captured during the thermal decomposition of the polymer.

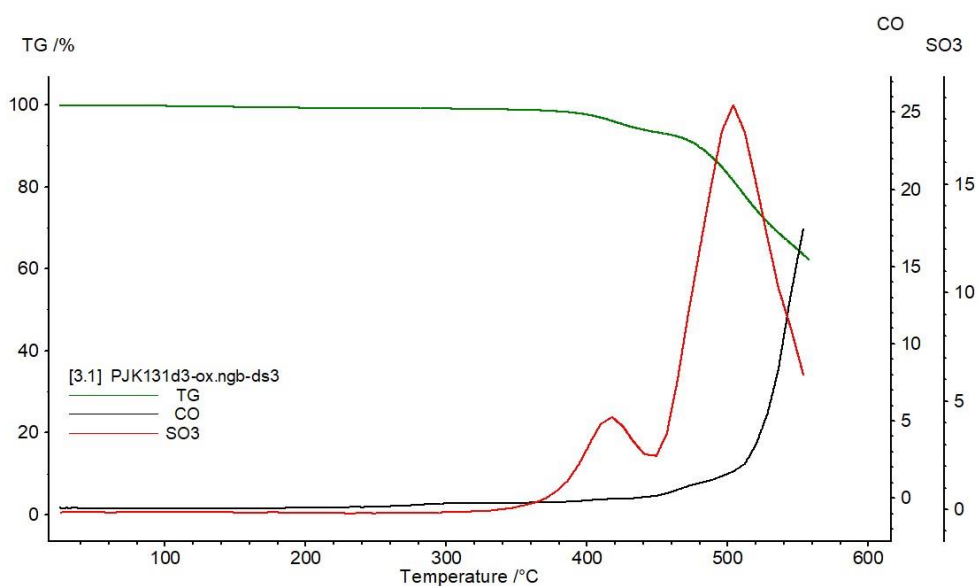


Figure III-25. TGA fluorinated poly(phenylene sulfone)s. P6_Ox1.

The polymer is initially losing Ph-SO₂-Ph fragment, with a sulfone oxydation and SO₃ release. This decomposition begins at 400 °C while the oxidation of the carbon starts at 450 °C. These results coincide with the TG-MS of the sulfonated poly(phenylsulfone) published by takamuku et al.²⁶ It confirms that it is thermally stable up to 400 °C and therefore suitable for further functionalization and membrane preparation.

All three different routes were successful and no significant differences were observed in the elemental analysis or the TGA. However the third route (strategy 3, Ox3) is preferred since it avoids the use of H₂SO₄ and therefore reduces the number of reactants. Up to 10 g of fluorinated poly(phenylene sulfone)s was obtained with yields between 90-96 %. Considering the multistep polymerization and oxidation, the overall yield was 92 %. It will be further used for functionalization (see chapter 3).

c. Phosphonation of fluorinated poly(phenylenesulfone)s : step 2 : functionalization

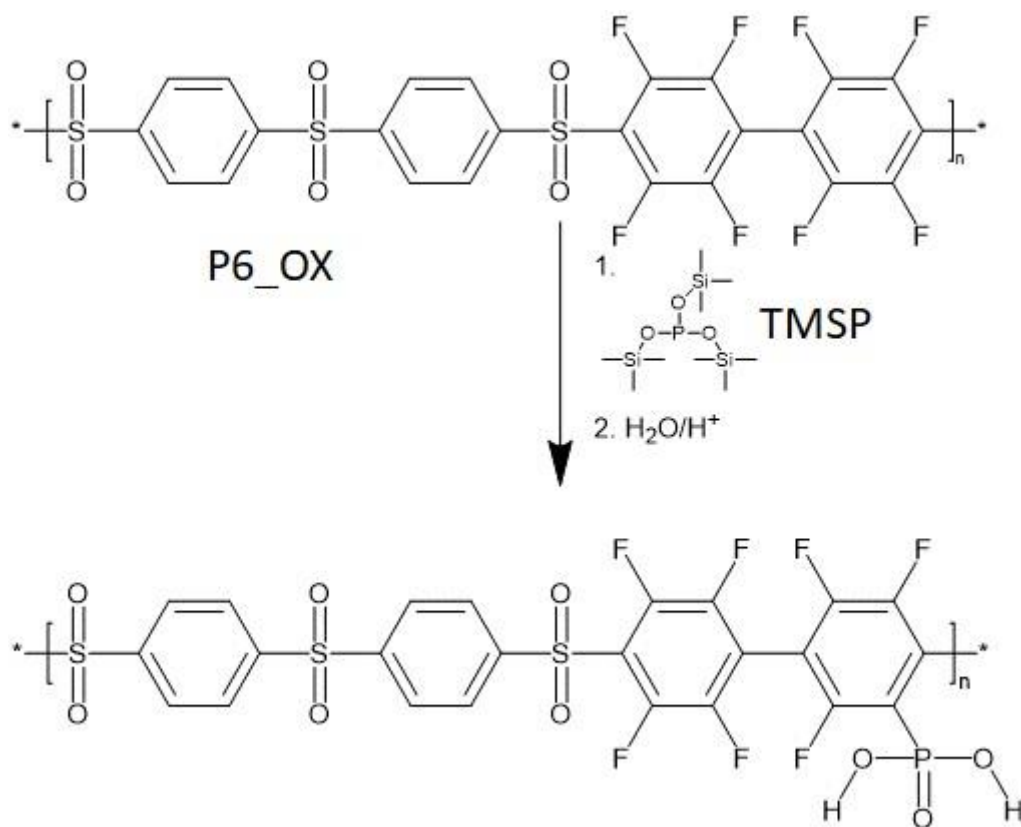


Figure III-26. Phosphonation of fluorinated poly(phenylenesulfone)s.

In this first attempt, the phosphonation of the polyfluorinated sulfone (P6_Ox) was investigated by one equivalent of TMSP to have one substitution, as it would be easier to measure and control. It was done following the procedure reported by V. Atanasov²⁷ et al. (figure III-27) with the phosphonation of poly(2,3,4,5,6-pentafluorostyrene) in the para-position. This is a nucleophilic substitution reaction in the aromatic ring (S_NAr₂) resulting in a gaseous byproduct at room temperature (Me₃SiF). The elimination of a byproduct is pulling the reaction equilibrium towards products.

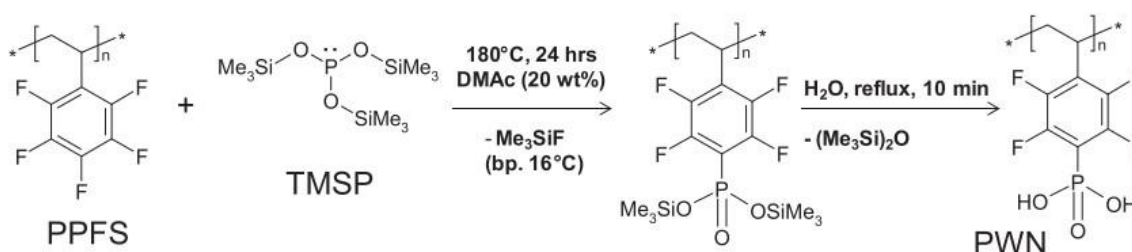


Figure III-27. Phosphonation presented by V. Atanasov.

Atanasov *et al.* have obtained a degree of phosphonation that goes from 17 to 100 % when using different TMSP/polymer ratios.

In my thesis, the use of 1 eq. of TMSP gave an overall degree of phosphonation of 66 % as calculated from equation III-1, applying the values from ¹⁹F NMR (figure III-28).

$$\text{Degree of phosp.} = \frac{\sum \text{Integrals of } ^{19}\text{F NMR peaks next to a phosp. subst.}}{\sum \text{Integrals of initial } ^{19}\text{F NMR peaks}} \times \frac{\text{number of F next to F}}{\text{number of F next to subs.}}$$

Equation III-1. Degree of phosphonation

$$\text{Degree of phosp.} = \frac{0.074 + 0.095 + 0.067}{0.070 + 0.065 + 1.018 + 1.000} \times \frac{6}{1} = 0.66$$

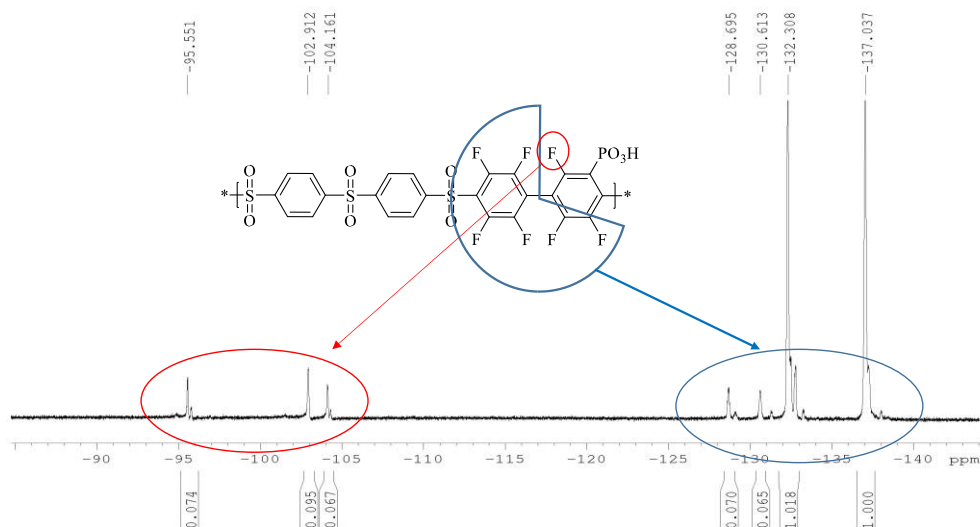


Figure III-28. ^{19}F NMR phosphonated poly(phenylenesulfone)s.

In the ^{19}F NMR spectra several peaks were observed in the zone between -95 and -105 ppm which means that substitution happened both in ortho and meta positions. ^1H NMR analyses were performed and a doublet was observed at 7,30 and 7,45 ppm corresponding to the internal and external phenyl protons, respectively. The polymer obtained was insoluble in DMAc, preventing SEC analyses. Due to its lack of solubility, no further work was done.

d. Conclusion of phosphonations

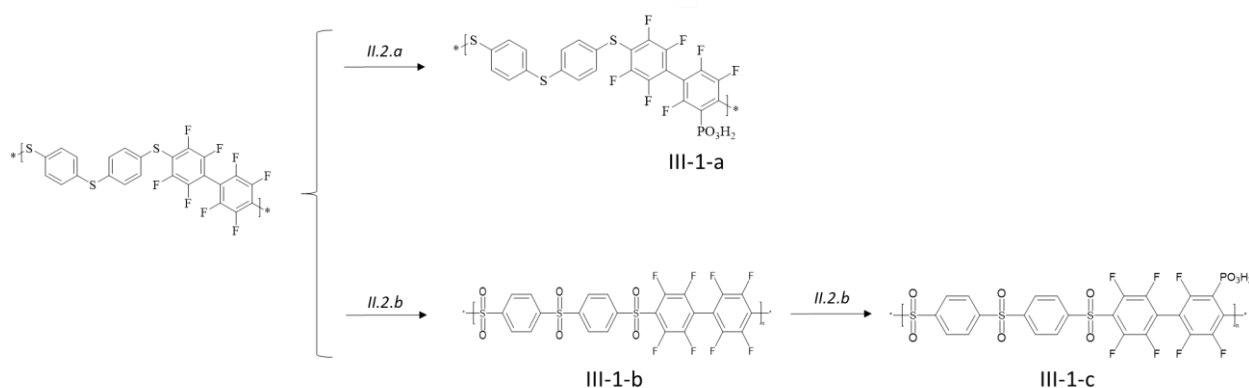


Figure III-29. Scheme of all phosphonation in *italic*, the paragraph number where the experimental protocol is described, above the arrows, the paragraph number where the polymerization is discussed.

The phosphonation of the fluorinated poly(phenylenesulfide)s (III-1-a) yielded a very low degree of phosphonation (<3 %) , it was however kept for the processing of PEM (chapter 4).

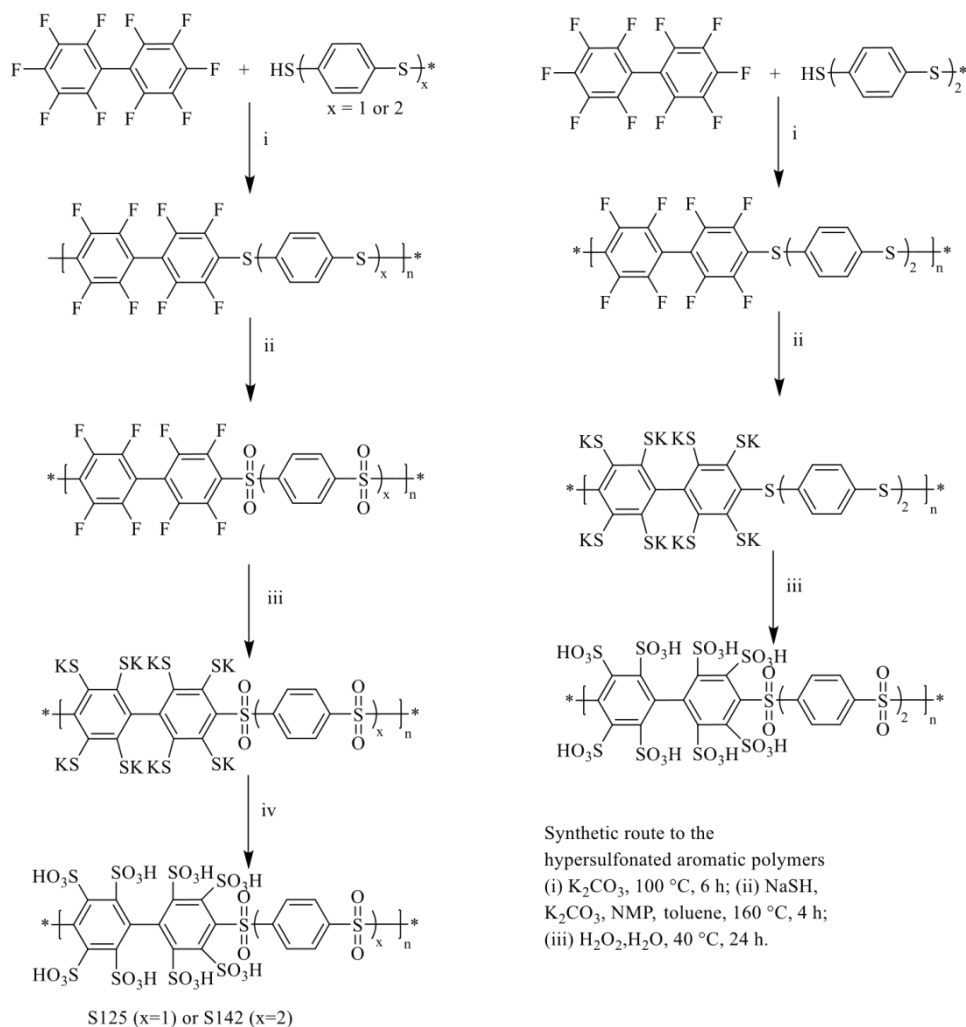
The phosphonation of the fluorinated poly(phenylenesulfone)s (III-1-c) showed a degree of phosphonation of 66 % but the final product had poor solubility in organic solvent and the polymer cannot be used for the membrane elaboration. The main reason we have a higher degree of phosphonation in the poly(phenylenesulfone)s is due to the presence of the sulfone groups which has an electro-withdrawing effect in the fluorinated aromatic rings.

2. Sulfonations

Two main paths were followed with two different starting polymers, fluorinated poly(phenylenesulfide)s (path A) and fluorinated poly(phenylenesulfone)s (path b). Path A was to sulfonate directly on the backbone polymer (fluorinated poly(phenylenesulfide)s), targeting the highest possible substitution of Fluorine atoms by SO₃H functions. For this purpose NaSH/H₂O₂, Na₂S/H₂SO₄, Li₂S/H₂SO₄, and H₂SO₄/SO₃ were used as sulfonating agents. Path B was attempted to position the sulfonate groups away from the polymer backbone and to allow for the generation of proton channels. This path B was also tried with the fluorinated poly(phenylenesulfone)s.

a. Sulfonation of fluorinated poly(phenylenesulfide)s using sodium hydrosulfide

The first attempted sulfonation was inspired by the procedure reported by S. Takamuku et al.²⁸ (figure III-30). Our strategy starts with the sulfonation and is followed by oxidation of the fluorinated polysulfide to fluorinated polysulfone.



Synthetic route to the hypersulfonated aromatic polymers [S125: (i) K_2CO_3 , 80 °C, 17 h; (ii) H_2O_2 , H_2SO_4 , AcOH, 30 °C, 48 h; (iii) NaSH, K_2CO_3 , NMP, toluene, 160 °C, 4 h; (iv) H_2O_2 , H_2O , 40 °C, 24 h. S142: (i) K_2CO_3 , 80 °C, 17 h; (ii) H_2O_2 , H_2SO_4 , AcOH, 30 °C, 48 h; (iii) NaSH, K_2CO_3 , NMP, 205 °C, 20 h; (iv) ion-exchange resin to H^+].

Synthetic route to the hypersulfonated aromatic polymers
 (i) K_2CO_3 , 100 °C, 6 h; (ii) NaSH, K_2CO_3 , NMP, toluene, 160 °C, 4 h;
 (iii) H_2O_2 , H_2O , 40 °C, 24 h.

Figure III-30. Polymerization and Sulfonation done by S. Takamuku et al. (left), polymerization and sulfonation done in this thesis.

The oxidation of the fluorinated poly(phenylenesulfide)s to fluorinated poly(phenylenesulfone)s was done following the step ii in Figure III-30, reported in chapter 3, III-1-b-i. Within this part, it was here decided to do first the sulfonation and afterwards the oxidation in one step of both of the $-SK$ group and the $-S-$ bonds (Figure III-31, right, iii). Hydrogen peroxide was added directly in the reaction vessel after step ii. When adding the water a solid product was observed at the bottom of the flask. The solid product was insoluble in other solvents. The main hypothesis is possible cross-linking reaction resulting in

thio-ether formation (Figure III-31). Based on this result, different sulfonating agents were selected to repeat this reaction.

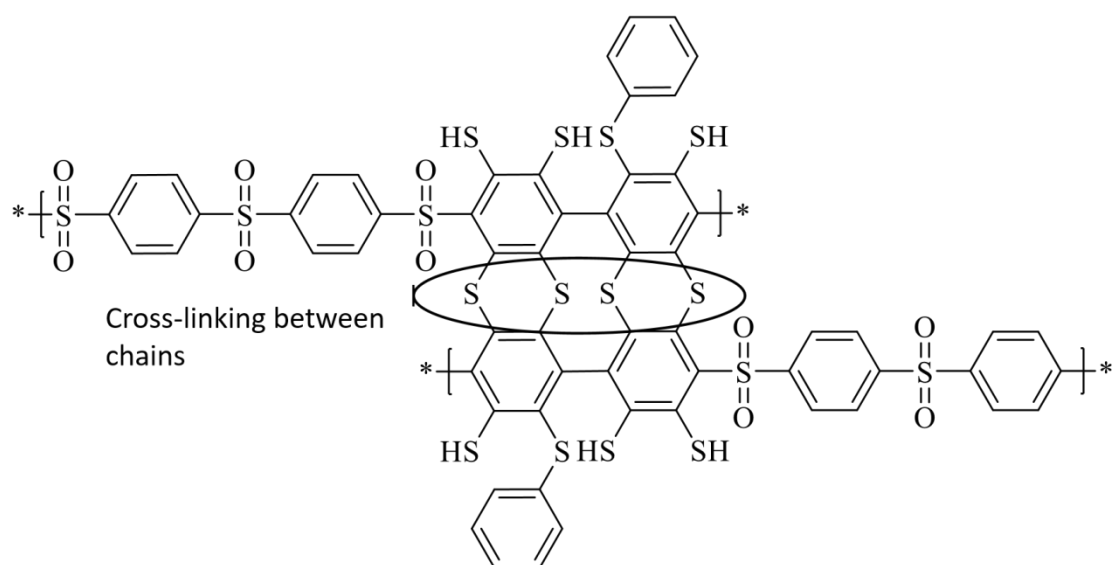


Figure III-31. Cross-linking between two sulfonated poly(phenylenesulfide)s.

b. Sulfonation of fluorinated poly(phenylenesulfide)s using sodium sulfide

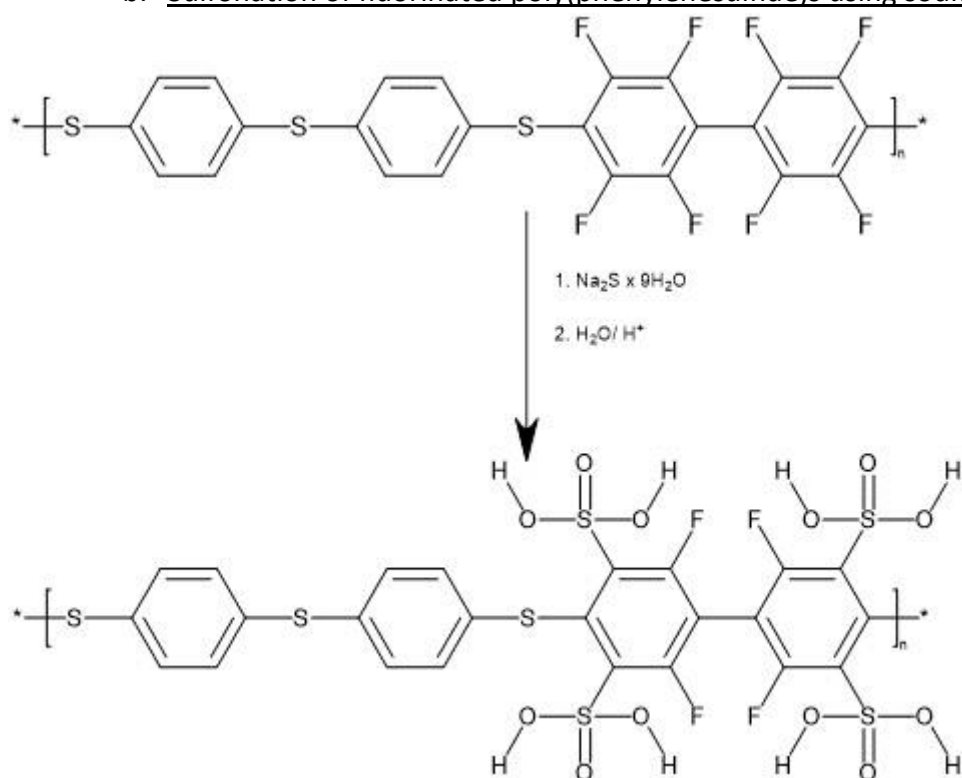


Figure III-32. Sulfonation of fluorinated poly(phenylenesulfide)s using Na_2S .

Reactions between halides and sodium sulphide have been known for more than 100 years as showed by V. Braun²⁹ who used this reaction for a polymerization based on C-S bonds. In

a recent report by T. Taldone³⁰, the reaction between aryl fluorides with sodium sulphide was investigated. It has been shown that a high selective fluoride substitution occurs at room temperature when there are other halides or electron-withdrawing groups attached to the phenyl group. Till date, these reactions have not been attempted during a polymerization reaction. In this case reaction was done at 150 °C for 6h. A colour change was observed from white to red (Figure III-34). No fluorine peaks were observed in the range of -100 ppm to -120 ppm in the ¹⁹F NMR spectrum which indicates the failure of the reaction. However, two new peaks appeared next to the ones from the original polymer which might indicate that there was a cleavage in the C-S bond. It brings to the conclusion that monomeric fluorinated phenyls with sulfonated groups in the para positions were obtained. Due to sulfonic groups being more electron-withdrawing than the thioethers groups, the fluorines are more deshielded than in the original polymer and therefore appear to be in a lower field (higher ppm) (figure III-33).

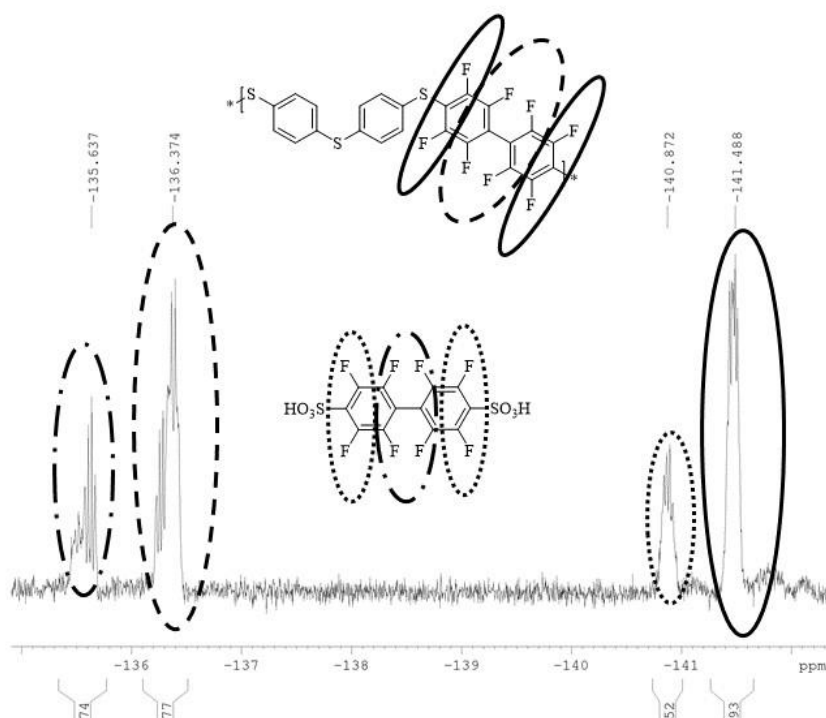


Figure III-33. ¹⁹F NMR spectrum obtained after attempted sulfonation.



Figure III-34. Solution after sulfonating using Na_2S

In order to test different heating methods, microwave heating at 100 °C under reduced power (i.e., 100 W) to avoid breaking the C-S-C bonds. In that case no changes were observed in the ^{19}F NMR spectrum, indicating neither C-S-C bonds cleavage nor new CSO_3 bonds formation. Further analyses are required to optimise this reaction but due to the small amounts that could be used using this heating method and that it could not be further used to produce a membrane it was decided to move to other sulfonating agents that could work better like Li_2S .

c. Sulfonation of fluorinated poly(phenylenesulfide)s using lithium sulfide

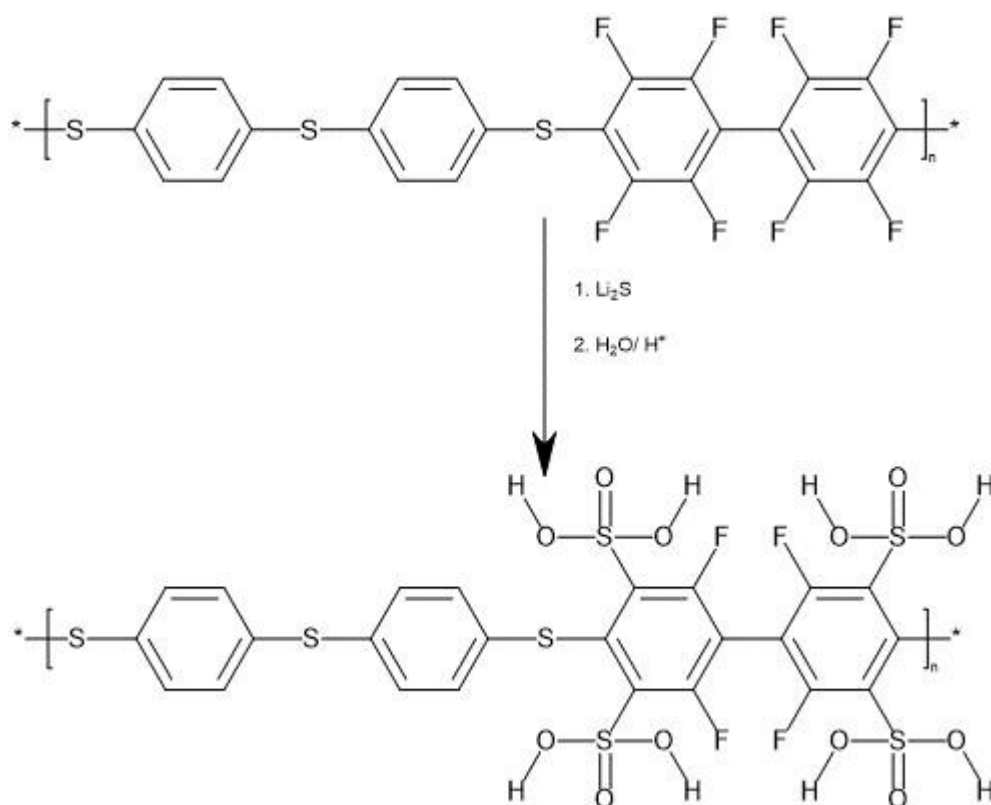


Figure III-35. Sulfonation of fluorinated poly(phenylenesulfide)s using Li_2S .

After the failure of the sulfonation reaction using sodium sulfide, the use of lithium sulfide was attempted, Li^+ being smaller than Na^+ it was expected to polarise the C-F bond favouring a nucleophilic aromatic substitution. Moreover, the LiF is less soluble than NaF and this will pull the reaction equilibrium towards products. The ^{19}F & ^1H NMR spectra did not reveal any changes in the polymer backbone. Both sodium and lithium sulfures did not lead to any product. Therefore, it was decided to use different sulfonation agents like sulfuric acid, which will sulfonate the hydrocarbon part of the polymer.

d. Sulfonation of fluorinated poly(phenylenesulfide)s using sulfuric acid

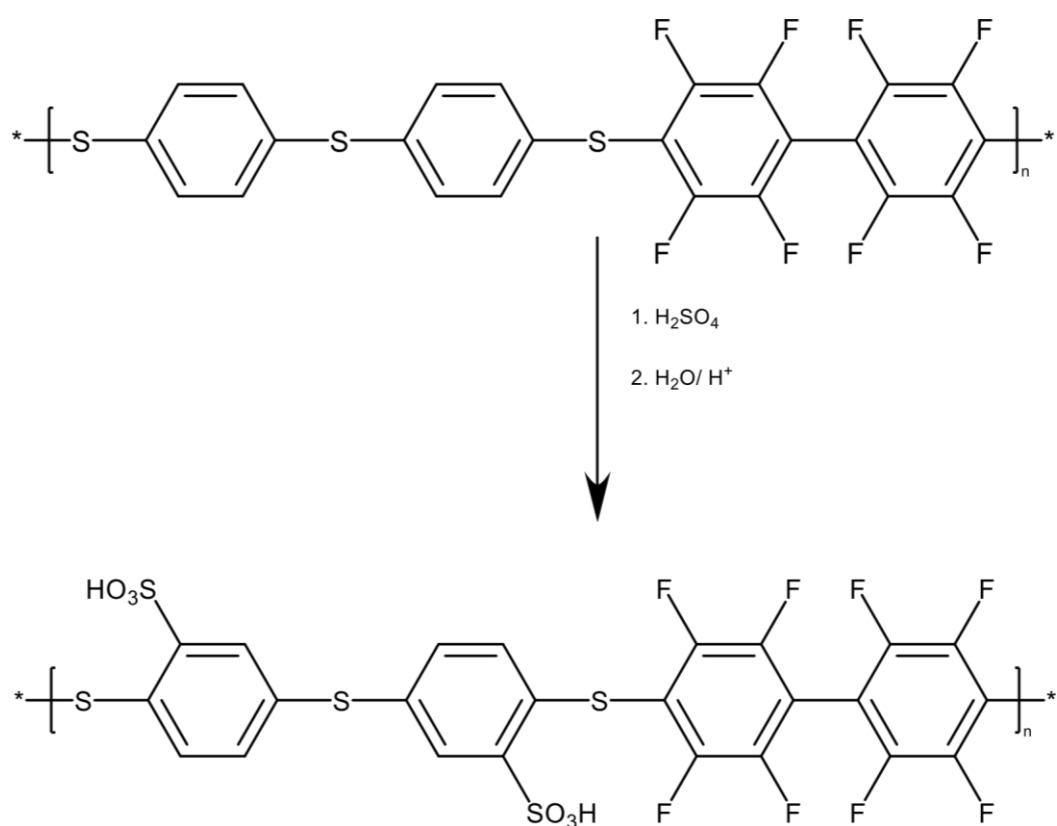


Figure III-36. Sulfonation of fluorinated poly(phenylenesulfide)s using H_2SO_4 .

After the failure of the previous strategies attempted to sulfonate the polymer backbone, a harsher method was tried with fuming sulfuric acid H_2SO_4 (20 % SO_3). The experimental procedure developed by F. Schönberger³¹ for the sulfonation of poly(arylene ether)s was applied. A sulfonation in the fluorinated part of the polymer was expected, however the ^{19}F NMR spectrum showed no change of the fluorinated part of the polymer. ^1H NMR revealed new peaks in the aromatic part (figure III-36) leading to no unambiguous conclusion. This method was not further explored as it was deemed that this sulfonation was hard to control.

Figure III-37. ^1H NMR of polymer obtained after sulfonation with H_2SO_4 .

e. Sulfonation of fluorinated poly(phenylenesulfide)s using 3-mercaptopropane-1-sulfonate

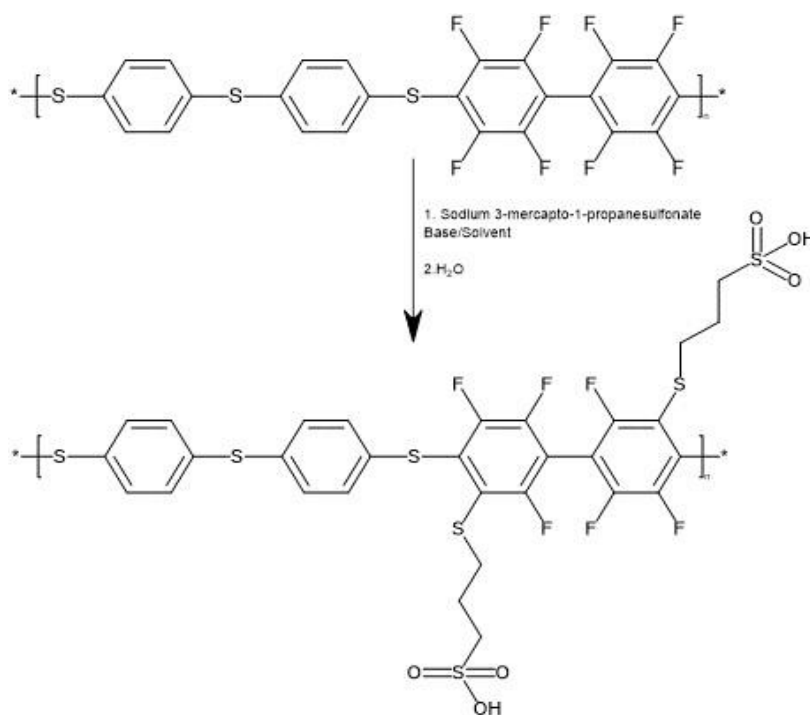


Figure III-38. Sulfonation of fluorinated poly(phenylenesulfide)s using Sodium 3-Mercaptopropane-1-sulfonate.

The fluorinated poly(arylenesulfide)s were sulfonated with sodium 3-mercapto-1-propanesulfonate, in order to introduce flexible side-chains en-terminated by a sulfonic acid function to allow for the generation of a bottle bush macromolecular architecture favouring the generation of proton-conducting channels. LiNO₃ was used initially as the base to deprotonate the thiol group and to trigger the reaction. However LiNO₃ revealed solubility problems and therefore another base was chosen to deprotonate/activate the sodium 3-mercapto-1-propanesulfonate. Looking into the literature³² 1,8 Diazabicyclo[5.4.0]undec-7-ene (DBU) was found to be a good candidate as it has been reported to activate alcohols. Thiol groups being more acidic than alcohols, DBU is expected to successfully deprotonate the sodium 3-mercapto-1-propanesulfonate. This reaction was initially done at room temperature and with an excess of Sodium 3-mercapto-1propanesulfonate. Two studies were done to analyze the effects of time and equivalents of sulfonating agent (Sodium 3-mercapto-1-propanesulfonate).



Figure III-39. Dried sulfonated polymer.

A kinetic study of the functionalization of the 3-mercaptopropene-1-sulfonate onto poly(octofluorobiphenyl-alt-thiobisbenzene) with DBU was carried out. Figure III-40 (a) reports this kinetic study when using 8 eq. and leaving the reaction at room temperature during 72 h. In figure III-40 (b) the results of the addition of different equivalents of sodium 3mercaptopropene-1-sulfonate vs. the degree of sulfonation for 6 hours are shown. There is almost a 50 % degree of sulfonation, meaning that we must double the sodium 3-Mercaptopropene-1-sulfonate eq. to obtain the desired degree of substitution. It can be due to partial deactivation of the sodium 3-Mercaptopropene-1-sulfonate.

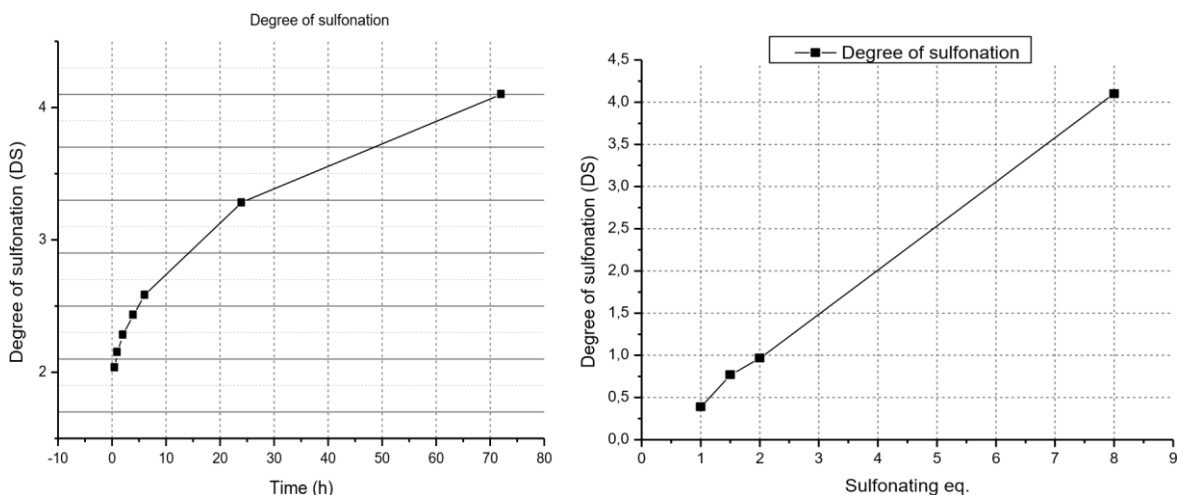


Figure III-40. Kinetic study of sulfonation (a, left graph), 8eq. of DBU used, rt, 72h. Sulfonation eq. vs sulfonation degree (b, right graph), 6h, rt.

The kinetic study shows how the first 2 substitutions (one in each fluorinated phenyl group) happens almost instantly while it takes 15 h hours to reach 3 substitutions and 70 h to reach 4 substitutions. The curve shows a logarithmic function, increasing very fast up to 2 substitutions and slowing down up to 4 substitutions. This kinetic study is showing that the addition of substitution groups doesn't deter further substitution, but it slows it down.

Samples were analysed by ^1H NMR and ^{19}F NMR spectroscopies. In the kinetic study, 8 eq. of DBU at room temperature during 72h (a, Figure III-40) the first substitution in

every tetrafluorophenylene sub-unit happened in the first half an hour. Further substitution is less favoured as the electronic density in the substituted phenyl is increasing with the substitution degree and therefore has less proclivity to a further nucleophilic attack. The highest degree of substitution obtained after 72h was 4,1 (a, Figure III-40) which corresponded to approx. 2 substituted groups in every phenyl group.

Another study was carried on by checking the degree of substitution vs the eq. of sodium 3-mercaptopropane-1-sulfonate. In that case the time was 6 hours at room temperature and the degree of substitution was calculated based on the integrals of the ^{19}F NMR spectrum. It was observed that an excess of sodium 3-mercaptopropane-1-sulfonate must be added as it might have deactivation of some thiol groups in the sodium 3-mercaptopropane-1-sulfonate.

The ^{19}F NMR spectrum shows the evolution of the peaks in line with the increase in the sulfonation (Figure III-41). In the first spectra (a) two peaks are observed corresponding to the Fluorine atoms in the polymer backbone before any functionalization. With the first sulfonation (b) new peaks appeared drifting 4ppm from the original peaks and the emergence of new peaks between 95 and -105 ppm is observed. As the sulfonation degree increases to 2-3 (c) a decrease in the initial peaks is observed. When the degree of sulphonation reaches 4 (d), no more F-C_{ar}-C_{ar}-F is left and therefore no more peaks below -105 ppm are observed.

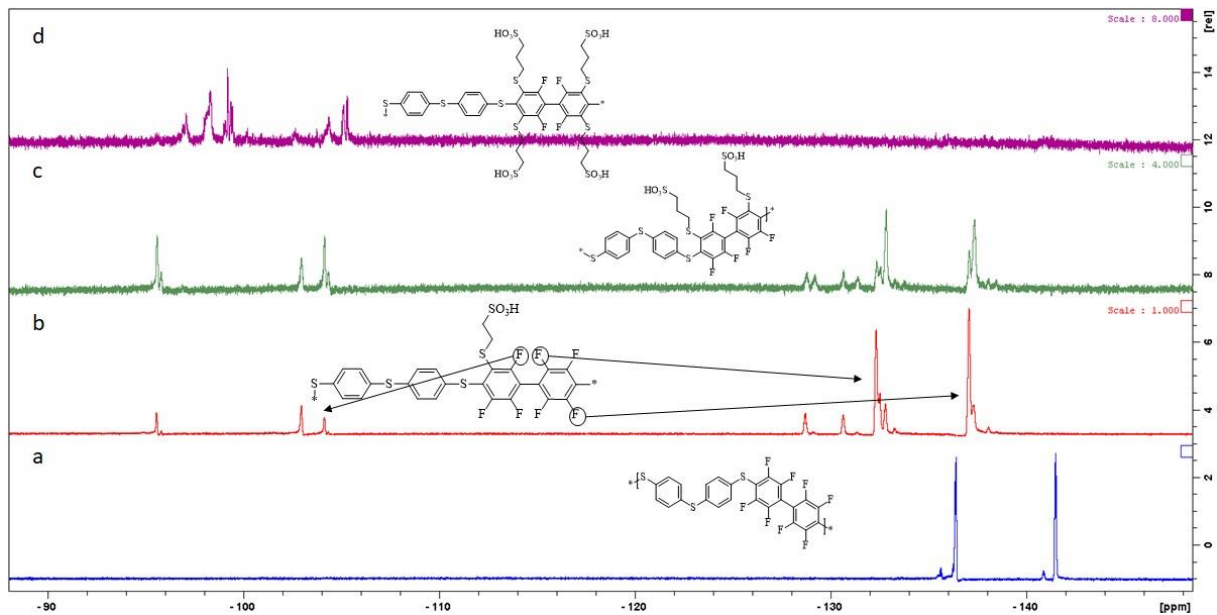


Figure III-41. ^{19}F NMR polymer with increasing levels of sulfonation.

SEC analyses was used to calculate the molar mass of the sulfonated product. A molar mass decrease was observed during the sulfonation step, from $3,2 \cdot 10^5$ Da to $2,5 \cdot 10^4$ Da. This decrease can be due to the cleavage of some of the C-S bonds, nevertheless, the molar masses of the substituted polymer were still high enough to obtain stable films when mixed with PBI (chapter 4).

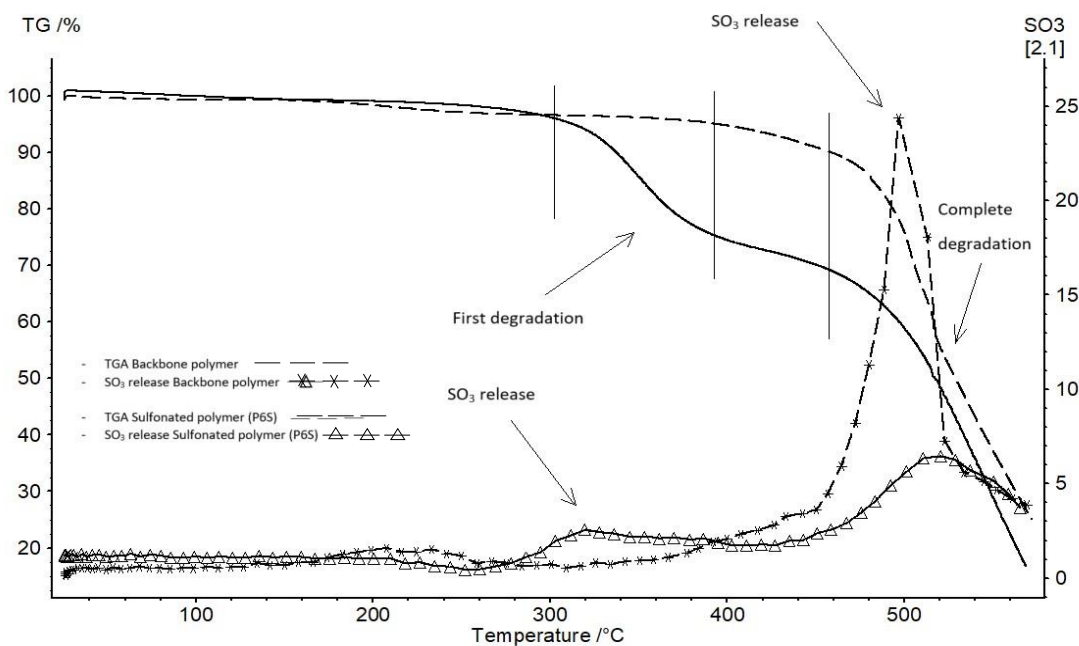


Figure III-42. TGA Backbone polymer/Sulfonated polymer.

The thermal stability was analysed before and after sulfonation (see Figure III-42). The first loss of the sulfonic groups in the sulfonated polymer was observed from 300 °C onwards. A decrease of 30 % was observed in the first mass loss, sulfonic groups have a molecular weight of 323.84 g·mol⁻¹, while the whole polymer has a Mw of 1100 g·mol⁻¹ calculated from the theoretical formula of this polymer. The sulfonic groups Mw corresponds to a 1/3 of the Mw of the total weight which coincides with the weight loss observed on the TGA thermograms. To confirm this hypothesis the gases were analysed by FTIR (Figure III-43) finding the characteristic SO₃ peaks at 1065 cm⁻¹ and 1390 cm⁻¹. CO₂ peak was found around 2150 cm⁻¹. In Figure III-43 it can be observed that SO₃ is first lost after 18min and while the CO₂ IR fingerprint is observed after 25min.

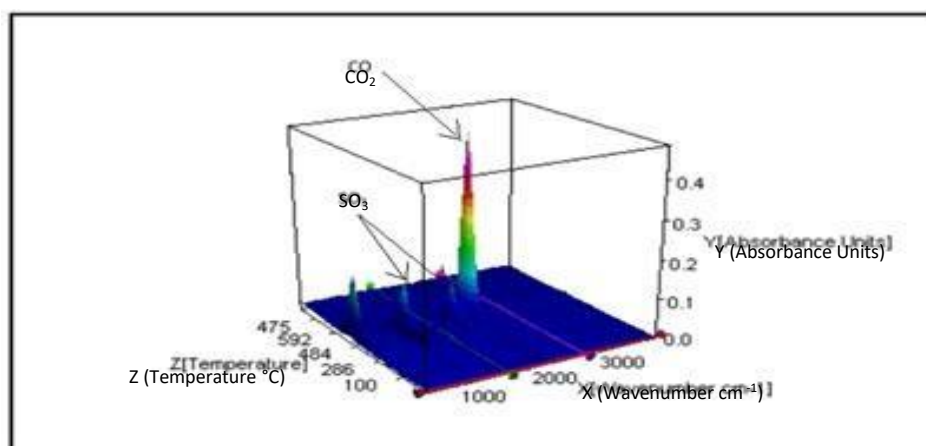


Figure III-43. FTIR sulfonated polymer.

In conclusion, different sulfonated polymers were synthesised and characterized by FTIR and ¹H & ¹⁹F NMR spectroscopies. While direct sulfonation was not successful, the attachment of 3-mercaptopropane-1-sulfonate proved to work at room temperature and obtaining a high degree of sulfonation. This synthetic path offers a relatively simple and with very soft conditions, no high temperature, nor strong acids used to obtain a proton-conducting polymer.

f. Sulfonation of fluorinated poly(phenylenesulfone)s using sodium 3-mercaptopropane-1-sulfonate

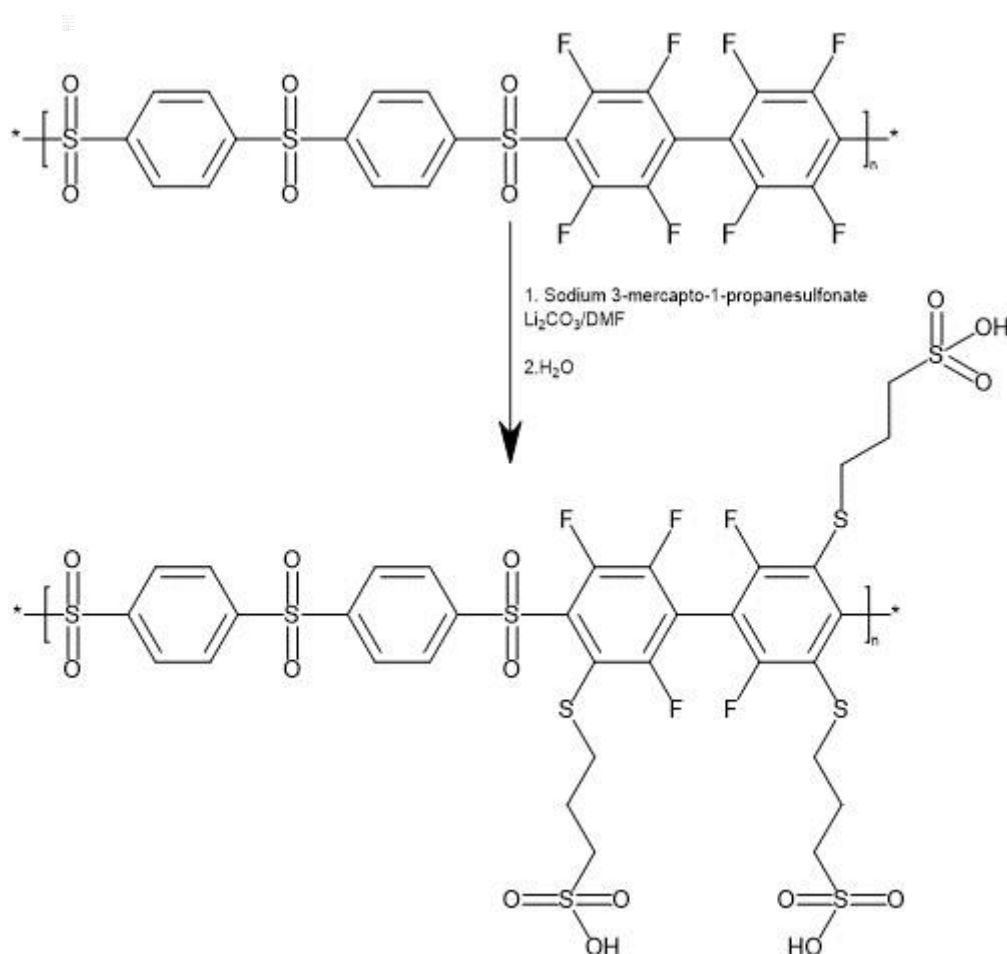


Figure III-44. Sulfonation of fluorinated poly(phenylenesulfone)s using Sodium 3-Mercaptopropane-1-sulfonate

The inspiration for a polymer with sulfonated groups at the end of aliphatic side-chains came from a paper published by G. Summers et al. in 2016³³. In this paper poly(arylene ether sulfone) (PAES) are sulfonated with sodium 3-mercaptopropane-1-sulfonate (SMPS) at 75 °C during 5 days (Figure III-45). Our approach is quite different as we expect to obtain a much higher number of sulfonated chains coming out from the phenyl groups.

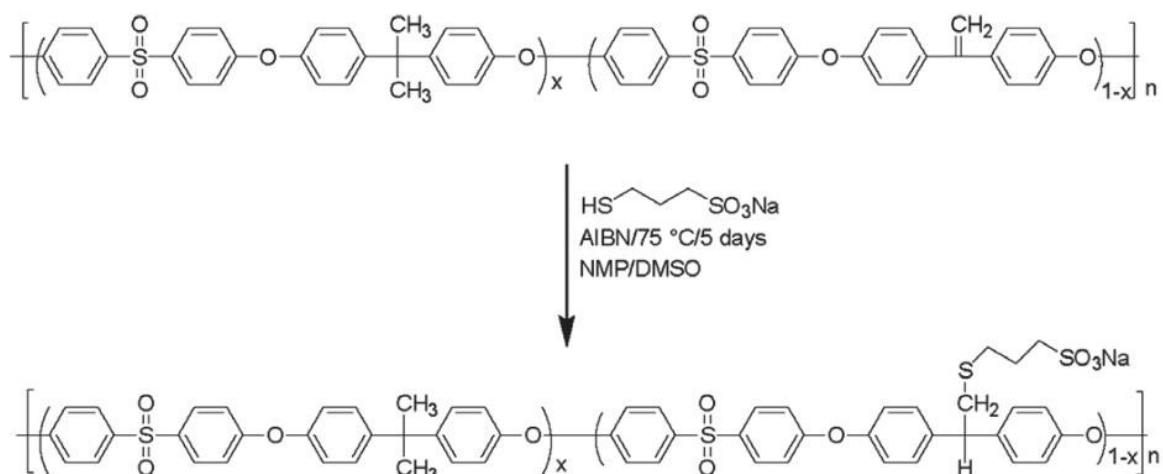


Figure III-45. Synthesis pathway for the preparation of sulfonated poly(ether ether sulfone) proposed by G. Summers et al.

Having the sulfonic groups positioned away from the polymeric backbone is favouring the generation of proton-conducting channels in a much easier way than when the sulfonic groups are directly attached onto the polymeric backbone conductivity. In the first attempt at 130 °C during 6 hours, 3.0 eq. were used to guarantee a degree of substitution of 2.

¹H NMR (figure III-46) analyses was performed to observe whether sulfonation had occurred. By calculating the aromatic protons and the aliphatic propane protons and comparing the integrals one to another, a substitution number can be extracted using the following equations (eq. III-2).

$$\text{Number of substitutions} = \frac{\sum \text{Int. of aliphatic peaks}}{\sum \text{Int. of aromatic peaks}} \times \frac{\text{N. of aromatic H per polymer unit}}{\text{N. of aliphatic H per sulfonic propane unit}}$$

Equation III-2. Number of substitutions

$$\text{Number of substitutions} = \frac{0.522 + 0.535 + 0.496}{1.00} \times \frac{8}{6} = 2.07$$

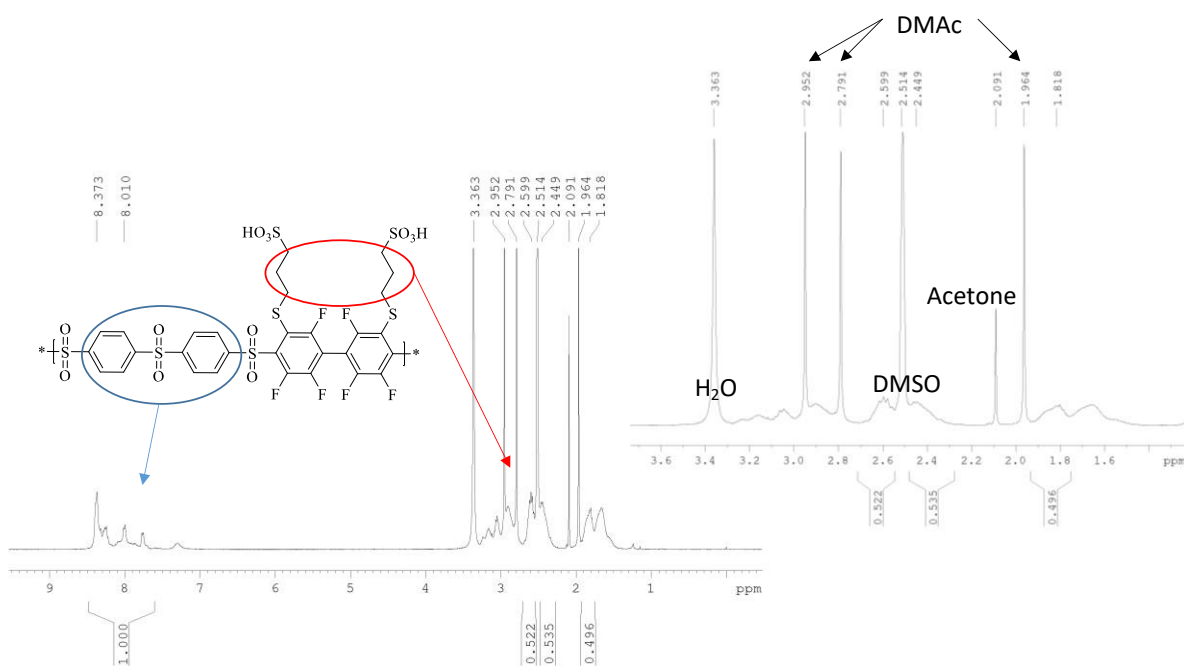


Figure III-46. ¹H NMR spectrum of partially sulfonated poly(phenylenesulfone)s using Sodium 3-Mercaptopropane-1-sulfonate.

According to this ¹H NMR spectroscopic analyses a slightly higher amount than two substitutions is obtained. It should be noticed here that protons of the aliphatic peaks of the mercapto-propane groups are overlapped with some of the solvent which might interfere with the correct result.

Using equation III-3 and ¹⁹F NMR spectrum, the theoretical Degree of sulfonation should be 1 when having a 100 % sulfonation (3 substituted groups in this case using 3 eq.). When the ¹⁹F NMR (figure III-47) results are used in equation III-3 a degree of sulfonation of 1,38 is obtained which can only be explained by the fact that there has been some interchain crosslinking between chains (figure III-48), reducing the number of Fluorines adjacent to other Fluorines.

$$\text{Degree of sulfonation} = \frac{\sum \text{Int. of Fluorines next to mercaptopropane groups}}{\sum \text{Int. of Fluorines next to other fluorines}} \times \frac{N. \text{ of } F \text{ next to other } F \text{ per polymer unit}}{N. \text{ of } F \text{ next to other mercaptopropane groups per polymer unit}}$$

Equation III-3. Degree of sulfonation

$$\text{Degree of sulfonation} = \frac{1.37 + 0.90 + 1.52 + 0.32}{1.00 + 0.99} \times \frac{2}{3} = 1.38$$

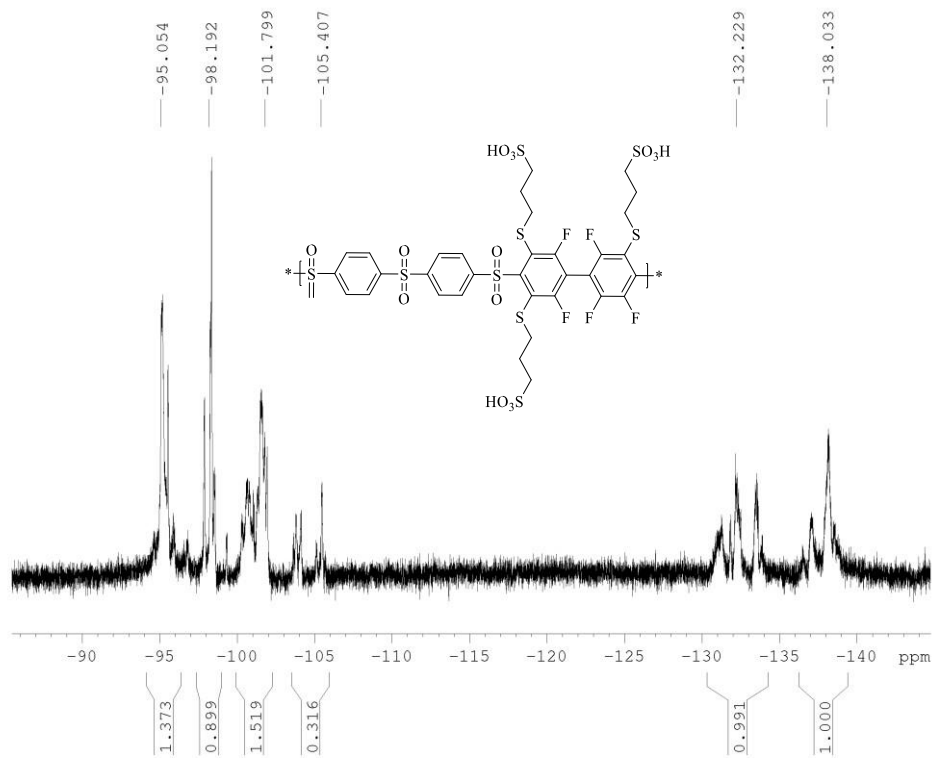


Figure III-47. ^{19}F NMR spectrum of partially sulfonated poly(phenylenesulfone)s using Sodium 3-Mercaptopropane-1-sulfonate.

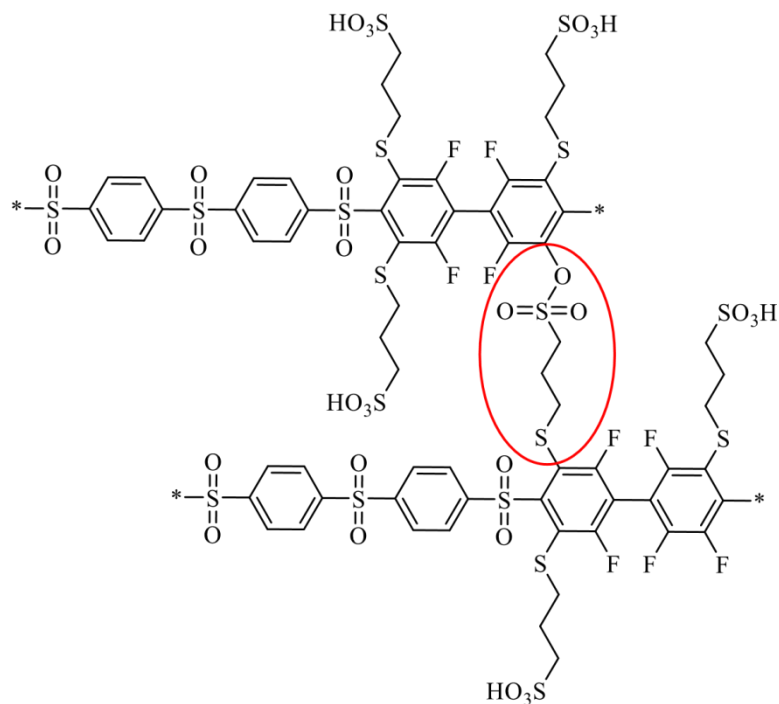


Figure III-48. Plausible interchain crosslinking between two neighbouring partially sulfonated chains.

As suspected by the hypothesis of the occurrence of some interchain crosslinking, this polymer was not easily dissolved in DMSO and no film could be obtained. It was concluded that a number of substitutions between 2 and 3 was obtained with the occurrence of crosslinking. Due to its insolubility it was not possible to measure the molecular weight and no more tests were done using fluorinated poly(phenylenesulfone)s as the backbone polymer.

g. Conclusion of sulfonation

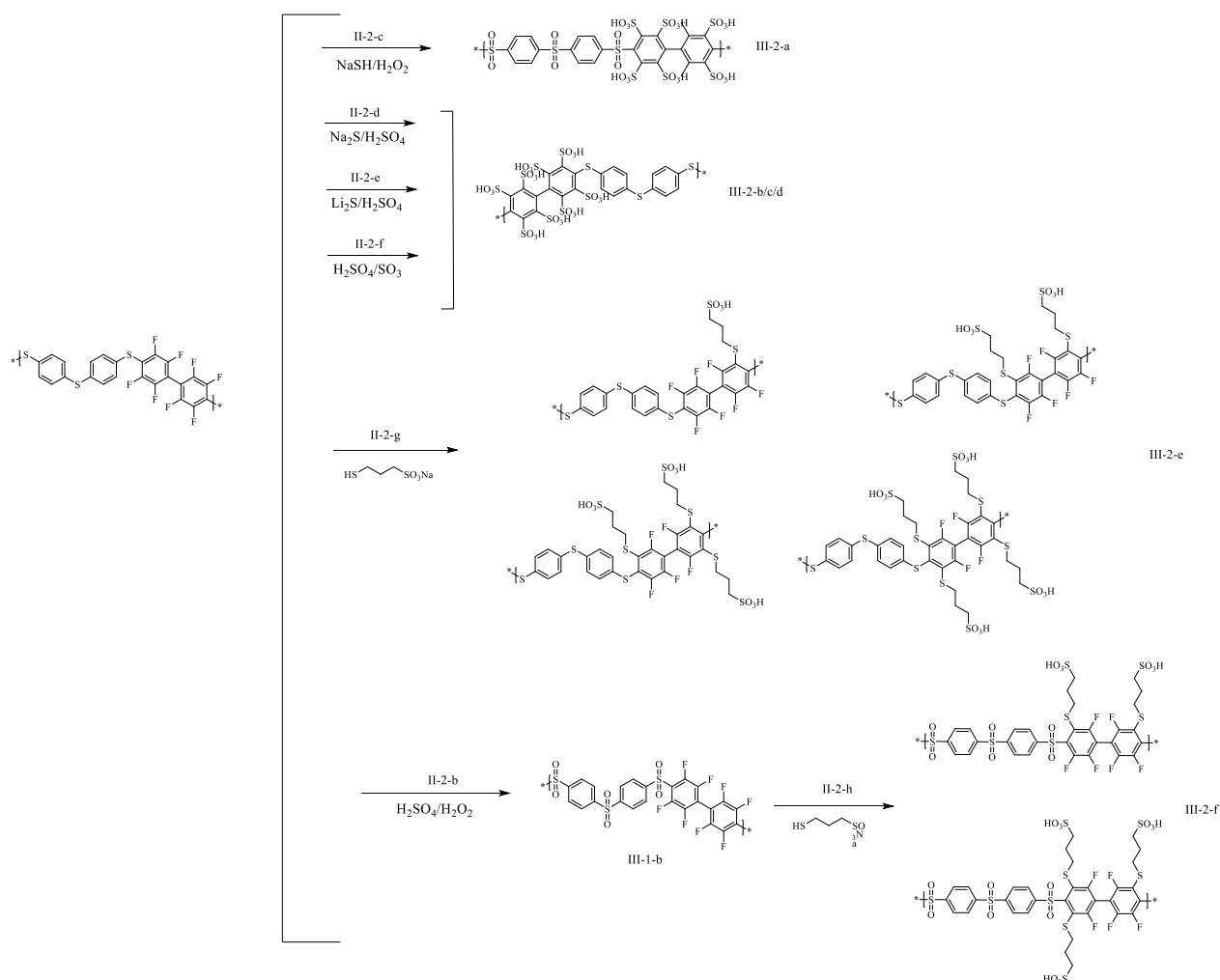


Figure III-49. Scheme of all sulfonation in *italic*, the paragraph number where the experimental protocol is described, above the arrows, the paragraph number where the polymerization is discussed.

The strategies II.2.c to II.2.f did not result in the synthesis of the targeted polymers. On the contrary, the products II.2.g with a degree of sulfonation from 1 to 4 were obtained with the optimization of the experimental conditions. When the degree of sulfonation is higher than 2, the polymer is soluble in water and therefore cannot be directly used to produce a membrane.

Physical crosslinking with another polymer, resulting in polymer blend, was investigated in chapter 4 so that a membrane could be processed. Films processed from the neat postfunctionalized polymers are most times of brittle and soluble in

water. The elaboration of the membranes requires a blending with another polymer that favours the film formation and keeps the conductivity at the same time. These membranes will be shown and discussed within Chapter 4.

The sulfonation of fluorinated poly(phenylenesulfone) was also successful, but the degree of sulfonation was a bit lower between 2 and 3. Because of the occurrence of probable crosslinking the solubility of organic solvent is low and should be considered to formulate the membrane to meet the requirements.

IV. Conclusions

Starting prepolymers were previously synthesised and described in chapter 2. Several functionalisation was attempted to obtain different proton conducting polymers. Even exhibiting low phosphonation efficiency, the phosphonation of the fluorinated poly(phenylenesulfide) gave a polymer that met the film forming requirement needed to be tested within the further step of membrane elaboration.

The phosphonation strategy has been followed by the sulfonation pathways to obtain another category of proton conducting polymers. Direct sulfonating groups were tried initially to substitute fluorides atoms with no success in obtaining a polymer that could be further used for a membrane. Even though sulfonation was observed, the harsh conditions of the reaction had cleavage the $-S-$ bond decreasing the molecular weight to a degree to where it was not anymore applicable for film production.

Best results were obtained when using milder conditions and sodium 3-mercapto propane-1-sulfonate as the sulfonating agent. The thiol from the 3-mercapto propane-1-sulfonate reacted with the fluorine at room temperature and several studies were done in this reaction. Well characterized polymers with different degrees of sulfonation were obtained. Several mercapto-propanesulfonic acid sidechains could be attached to the backbone, either fluorinated poly(phenylenesulfide) and poly(phenylenesulfone) polymer giving high conductivities (see chapter 4) while

keeping a M_w high enough to obtain films. These partially fluorinated/sulfonated poly(phenylene sulphide)s were further used for the processing of PEMs (chapter 4).

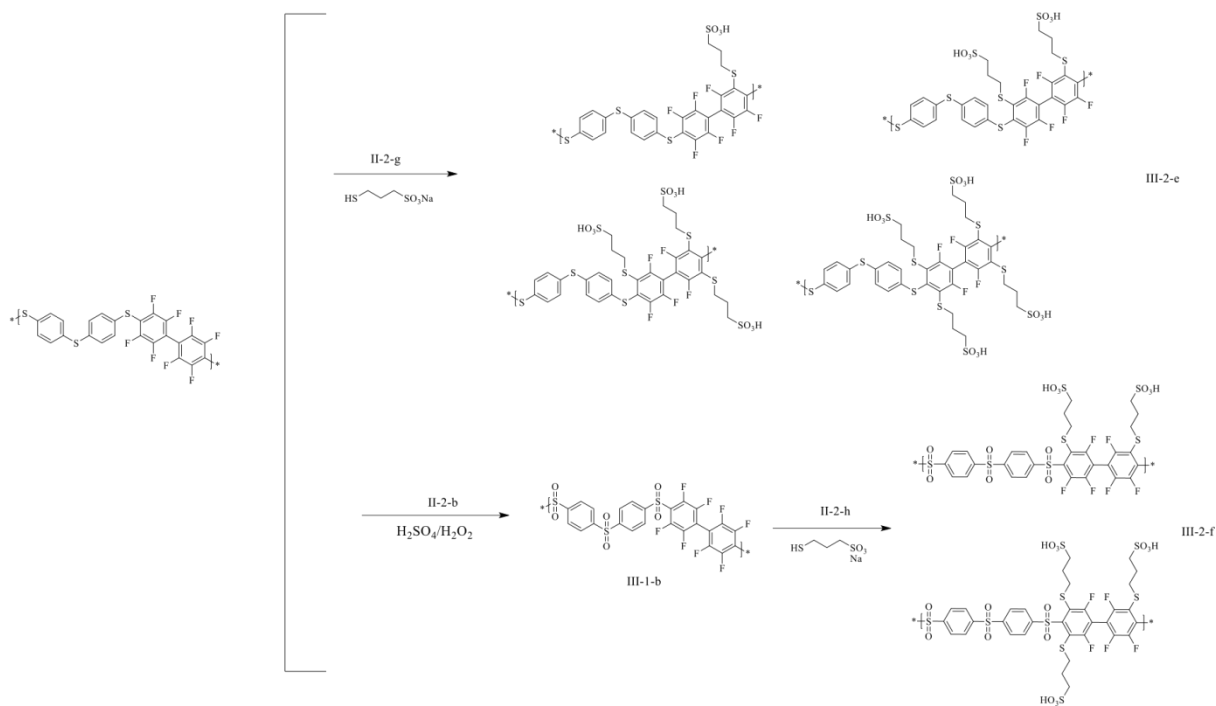


Figure III-51. Scheme of sulfonations with final products selected for the membrane elaboration.

In conclusion, a phosonated polymer and two sulfonated (III-2-e, III-2-f) polymers were selected for film preparation to be used as a PEM in the water electrolysing cell. The elaboration and processing of these membranes are discussed in chapter 4.

V. References

- ¹ Sun, Xinwei, Stian Christopher Simonsen, Truls Norby, and Athanasios Chatzitakis, *Composite Membranes for High Temperature PEM Fuel Cells and Electrolysers: A Critical Review*, 2019, *Membranes*, 9, 83 DOI: [10.3390/membranes9070083](https://doi.org/10.3390/membranes9070083)
- ² T. Bock, H. Möhwald, and R. Mülhaupt, *Arylphosphonic acid-functionalized polyelectrolytes as fuel cell membrane material*, 2007, *Macromol. Chem. Phys.*, vol. 208, no. 13, p.1324–1340 DOI: [10.1002/macp.200700193](https://doi.org/10.1002/macp.200700193)
- ³ G. V. E. and H. A. Tanner, *Intermediate Temperature Fuel Cells*, 1961, *Electrochem. Soc.*, vol. 108, no. 7, p.669 DOI: [10.1039/B612060C](https://doi.org/10.1039/B612060C)
- ⁴ M. Andújar and F. Segura, *Fuel cells, History and updating. A walk along two centuries*, 2009, *Renew. Sustain. Energy Rev.*, vol.13, no. 9, p.2309-2322 DOI: [10.1016/j.rser.2009.03.015](https://doi.org/10.1016/j.rser.2009.03.015)
- ⁵ S. J. Peighambardoust, S. Rowshanzamir, and M. Amjadi, *Review of the proton exchange membranes for fuel cell applications*, 2010, vol. 35, no. 17. Elsevier Ltd DOI:[10.1016/j.ijhydene.2010.05.017](https://doi.org/10.1016/j.ijhydene.2010.05.017)
- ⁶ Kang, N. R., Thanh H. P., Nederstedt H. and Jannasch P., *Durable and Highly Proton Conducting Poly(Arylene Perfluorophenylphosphonic Acid) Membranes*, November 2020 (2021), *Journal of Membrane Science*, 623., p.1190-74 DOI: [10.1016/j.memsci.2021.119074](https://doi.org/10.1016/j.memsci.2021.119074)
- ⁷ H. Pu, *Polymers for PEM fuel cells*, 2014, Wiley Series on Polymer Engineering and Technology, p. 61 DOI:[10.1002/9781118869345](https://doi.org/10.1002/9781118869345)
- ⁸ K. Z. Ekinçi, S. Ü. Çelik, and A. Bozkurt, *Enhancing the anhydrous proton conductivity of sulfonated polysulfone/polyvinyl phosphonic acid composite membranes with hexagonal boron nitride*, 2015, *Int. J. Polym. Mater. Polym. Biomater.*, vol. 64, no. 13, pp. 683–689 DOI:[10.1080/00914037.2014.1002094](https://doi.org/10.1080/00914037.2014.1002094)
- ⁹ S. Bano, Y. S. Negi, and K. Ramya, *Studies on new highly phosphonated poly (ether ether ketone) based promising proton conducting membranes for high temperature fuel cell*, 2019, *Int. J. Hydrogen Energy*, vol. 44, no. 54, pp. 28968–28983 DOI: [10.1016/j.ijhydene.2019.09.067](https://doi.org/10.1016/j.ijhydene.2019.09.067)
- ¹⁰ G. A. Ludueña, T. D. Kühne, and D. Sebastiani, *Mixed Grotthuss and vehicle transport mechanism in proton conducting polymers from Ab initio molecular dynamics simulations*, 2011, *Chem. Mater.*, vol. 23, no. 6, pp. 1424–1429 DOI: [10.1021/cm102674u](https://doi.org/10.1021/cm102674u)
- ¹¹ V. Atanasov, A. Lee, E.J. Park, S. Maurya, E.D. Baca, C. Fujimoto, M. Hibbs, I. Matanovic, J. Kerres and Y.S. Kim., *Synergistically integrated phosphonated poly(pentafluorostyrene)*

- for fuel cells, 2021, Nat. Mater., vol. 20, no. 3, pp. 370–377, 2021. DOI:[10.1038/s41563-020-00841-z](https://doi.org/10.1038/s41563-020-00841-z)
- ¹² V. Atanasov, A. Lee, E.J. Park, S. Maurya, E.D. Baca, C. Fujimoto, M. Hibbs, I. Matanovic, J. Kerres and Y.S. Kim, *Synergistically integrated phosphonated poly(pentafluorostyrene) for fuel cells*, 2021, Nat. Mater., vol. 20, no. 3, pp. 370–377 DOI:[10.1038/s41563-020-00841-z](https://doi.org/10.1038/s41563-020-00841-z)
- ¹³ J. M. Andújar and F. Segura, *Fuel cells: History and updating. A walk along two centuries*, 2009, Renew. Sustain. Energy Rev., vol. 13, no. 9, pp. 2309–2322 DOI:[10.1016/j.rser.2009.03.015](https://doi.org/10.1016/j.rser.2009.03.015)
- ¹⁴ R. Devanathan, *Recent developments in proton exchange membranes for fuel cells*, Energy Environ. 2008, Sci. 1, p.101-119. DOI: [10.1039/B808149M](https://doi.org/10.1039/B808149M)
- ¹⁵ J. Ran, L. Wu, Y. He, Z. Yang, Y. Wang, C. Jiang, L. Ge, E. Bakangura, T. Xu, *Ion Exchange Membranes: New Developments and Applications*, 2017, Journal of Membrane Science, 522, p. 267–91 DOI: [10.1016/j.memsci.2021.119584](https://doi.org/10.1016/j.memsci.2021.119584)
- ¹⁶ S. Takamuku, A. Wohlfarth, A. Manhart, P. Räder & P. Jannasch, *Hypersulfonated polyelectrolytes: Preparation, stability and conductivity*, 2015, Polymer Chemistry, 6(8), p.1267–1274 DOI: [10.1039/c4py01177e](https://doi.org/10.1039/c4py01177e)
- ¹⁷ A.Loupy, *Microwaves in organic synthesis*, (2006) 2nd edition, Wiley-VCH, p. 78 DOI:[10.1002/9783527619559](https://doi.org/10.1002/9783527619559)
- ¹⁸ Henyecz, Réka, *Microwave-Assisted Synthesis of Phosphonic and Phosphinic Esters and Phosphine Oxides by the Hirao Reaction, Phosphorus, Sulfur and Silicon and the Related Elements*, 194.4–6 (2019), 372–76 DOI:[10.1080/10426507.2018.1544983](https://doi.org/10.1080/10426507.2018.1544983)
- ¹⁹ M. Schuster, K. D. Kreuer, H. T. Andersen, and J. Maier, *Sulfonated poly(phenylene sulfone) polymers as hydrolytically and thermooxidatively stable proton conducting ionomers*, 2007,Macromolecules, vol. 40, no.3, p.598–607 DOI: [10.1039/b822069g](https://doi.org/10.1039/b822069g)
- ²⁰ A. Chromik, A. Katzfuss, K. Krajinovic, *Partially Fluorinated Sulfonated Poly(arylene sulfone)s Blended with Polybenzimidazole*, 2016, Eur. J., vol.17, no.1, p.36–42 DOI:[10.1002/pola.24624](https://doi.org/10.1002/pola.24624)
- ²¹ G. Titvinidze, K. Kreuer, M. Schuster, C. Araujo, J. Melchior and W. Meyer, *Proton Conducting Phase-separated Multiblock Copolymers with Sulfonated Poly(phenylene sulfone) blocks for electrochemical applications: preparation, morphology, hydration behaviour, and transport*, 2012, Adv. Functional Materials, Vol. 22, Issue 21, p. 4456-4470 DOI: [10.1002/adfm.201200811](https://doi.org/10.1002/adfm.201200811)
- ²² S. Takamuku, A. Wohlfarth, A. Manhart, P. Räder & P. Jannasch, *Hypersulfonated polyelectrolytes: Preparation, stability and conductivity*, 2015, Polymer Chemistry, 6(8), p.1267–1274 DOI: [10.1039/c4py01177e](https://doi.org/10.1039/c4py01177e)

- ²³ M. Ghanbari Kermanshahi & K. Bahrami, *Fe₃O₄@BNPs@SiO₂-SO₃H as a highly chemoselective heterogeneous magnetic nanocatalyst for the oxidation of sulfides to sulfoxides or sulfones*, 2019, RSC Advances, 9(62), p.36103–36112 DOI: [10.1039/C9RA06221A](https://doi.org/10.1039/C9RA06221A)
- ²⁴ M. Ghanbari Kermanshahi & K. Bahrami, *Fe₃O₄@BNPs@SiO₂-SO₃H as a highly chemoselective heterogeneous magnetic nanocatalyst for the oxidation of sulfides to sulfoxides or sulfones*, 2019, RSC Advances, 9(62), p.36103–36112 DOI: [10.1039/C9RA06221A](https://doi.org/10.1039/C9RA06221A)
- ²⁵ M. Horvat, G. Kodrič, M. Jereb & J. Iskra, *One pot synthesis of trifluoromethyl aryl sulfoxides by trifluoromethylthiolation of arenes and subsequent oxidation with hydrogen peroxide*, 2020, RSC Advances, 10(57), p.34534–34540 DOI: [10.1039/D0RA04621C](https://doi.org/10.1039/D0RA04621C)
- ²⁶ S. Takamuku, A. Wohlfarth, A. Manhart, P. Räder & P. Jannasch, *Hypersulfonated polyelectrolytes: Preparation, stability and conductivity*, 2015, Polymer Chemistry, 6(8), p.1267–1274 DOI: [10.1039/c4py01177e](https://doi.org/10.1039/c4py01177e)
- ²⁷ Atanasov, V., Oleynikov A., Xia J., Lyonnard S., and Kerres J., *Phosphonic Acid Functionalized Poly(Pentafluorostyrene) as Polyelectrolyte Membrane for Fuel Cell Application*, Journal of Power Sources, 343 (2017), 364–72 DOI: [10.1016/J.JPOWSOUR.2017.01.085](https://doi.org/10.1016/J.JPOWSOUR.2017.01.085)
- ²⁸ S. Takamuku, A. Wohlfarth, A. Manhart, P. Räder & P. Jannasch, *Hypersulfonated polyelectrolytes: Preparation, stability and conductivity*, 2015, Polymer Chemistry, 6(8), p.1267–1274 DOI: [10.1039/c4py01177e](https://doi.org/10.1039/c4py01177e)
- ²⁹ V. Braun, *Über cyclische Sulfide*, 1910, J. Ber. 43, p.3220 DOI: [10.1002/cber.19100430387](https://doi.org/10.1002/cber.19100430387)
- ³⁰ T. Taldone, P. D. Patel, H. J. Patel, and G. Chiosis, *About the reaction of aryl fluorides with sodium sulfide: Investigation into the selectivity of substitution of fluorobenzonitriles to yield mercaptobenzonitriles via S_NAr displacement of fluorine*, Tetrahedron Lett., vol. 53, no. 20, pp. 2548–2551, 2012. DOI: [10.1016/j.tetlet.2012.03.032](https://doi.org/10.1016/j.tetlet.2012.03.032)
- ³¹ F. Schönberger, A. Chromik, and J. Kerres, *Synthesis and characterization of novel (sulfonated) poly(arylene ether)s with pendent trifluoromethyl groups*, Polymer (Guildf.), vol. 50, no. 9, pp. 2010–2024, 2009. DOI: [10.1016/j.polymer.2009.02.043](https://doi.org/10.1016/j.polymer.2009.02.043)
- ³² M. K. Munshi et al., *1,8-Diazabicyclo[5.4.0]undec-7-ene (DBU): A highly efficient catalyst in glycerol carbonate synthesis*, J. Mol. Catal. A Chem., vol. 391, no. 1, pp. 144–149, 2014. DOI: [10.1016/j.molcata.2014.04.016](https://doi.org/10.1016/j.molcata.2014.04.016)
- ³³ G. J. Summers, M. G. Kasiama, and C. A. Summers, *Poly(ether ether sulfone)s and sulfonated poly(ether ether sulfone)s derived from functionalized 1,1-diphenylethylene derivatives*, Polym. Int., vol. 65, no. 7, pp. 798–810, 2016. DOI: [10.1002/PI.5135](https://doi.org/10.1002/PI.5135)

Chapter 4. Proton Exchange Membranes (PEMs)

I. Introduction.....	179
1. PEM state of the art.....	179
2. PEM process method.....	180
II. Materials and methods.....	181
1. Reagents.....	181
2. Experimental.....	182
a) Phosphonated membranes (P1PM).....	183
b) Sulfonated membranes (P1SM, P2SM, P4SM and P2SOM).....	183
3. Characterization.....	184
a) Water uptake.....	184
b) IEC.....	184
c) Proton Conductivity at room temperature.....	186
d) Catalyst-coated membrane (CCM).....	186
III. Results and discussion.....	186
1. Membrane processing.....	186
a) Main issues.....	187
b) Phosphonated Membranes.....	189
c) Sulfonated Membranes.....	189
2. PEM's properties.....	191
a) Properties at rt.....	191
b) Conductivity vs. temperature.....	193
c) Membrane surface.....	194

d) Electrochemical Impedance Spectroscopy (EIS).....	195
IV. Conclusion	199
VI. References.....	202

This chapter is dedicated to the final step of this research project: to produce proton conducting membranes starting from the polymers produced in the chapters 2 & 3. The prepared membranes were processed and characterized prior to be used in the electrolysis device mimic the artificial photosynthesis.

I. Introduction

1. PEM state of the art

Membranes are present in every single living organism; understanding how these thin layers worked in cells, plants, and other organisms helped elaborate synthetic membranes from synthetic materials in the twentieth century. The first PEM to be used in an operational system was built by General Electric Co. (a 1 KW power plant)¹ and relying on poly(styrene sulfonic acid) (PSSA), Figure IV-1:

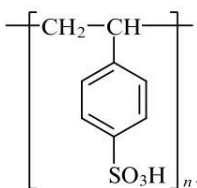


Figure IV-18. First operational PEM making use of poly(styrene sulfonic acid), PSSA².

The main drawback of this PEM was its limited lifetime due to its chemical degradation by radicals. The PEM concept for electrochemical cells was perfected by Grubbs in 1959 in electrochemical cells.³ At that time (already), competition was raging among top chemical companies were in competition and Walter Grot of DuPont de Nemours came up with a new membrane which is still the most used till date. It is known as Nafion[®] and one of its main advantages is its resilience, having a lifespan of up to 50000 hours. Optimized performance when it comes to conductivity (meaning a high conductivity) is obtained by Nafion membranes having a thickness in the ca. 20-300 μm range.⁴

Searching for surrogate to Nafion, the research has spread over a wide space of different macromolecular architectures, focusing mainly over the development of two specific families of interests:

- Sulfonated aromatic polymers

- Alkylsulfonated polymers

Even though in the last years several different polyelectrolytes have been synthesised to be used as membranes, their unfavourable cost/durability ratio did not allow further technological and commercial development. Therefore Nafion® and very similar membranes have remained the SoA membranes for commercial use.

Number of research groups are still working onto membrane formulation and within this thesis, the above-mentioned two research paths have been studied. Sulfonated aromatic polymers within Chapter 3 (III-2-a, III-2-b, III-2-c, III-2-d), followed by the synthesis of alkylsulfonated aromatic polymers still in Chapter 3 (III-2-e, III-2-f) while in this chapter the membrane elaboration starting from these polymers and the blending of these polymers with other polymers to increase their mechanical and thermal strengths.

2. PEM process method

There are different methods to process proton-exchange membranes, the two main consisting in casting and extrusion. The latter method is the most economical way to manufacture homogeneous polymer thin film in the industry and is commonly applied to thermoplastic, like polyolefins (e.g. poly(ethylene) and poly(propylene) and polyesters (e.g. poly(ethylene terephthalate)), to name a few. It involves pushing molten polymer through a circular or slot die. At the laboratory scale, the film-casting method is the easiest way to obtain samples with a thickness homogeneity that can be considered satisfactory even though it is questionable at the industrial scale on film with large surface areas.⁵

Being the common laboratory-scale method to obtain PEMs starting from SAPs (sulfonated aromatic polymers)⁶, it was the one we choose for casting PEMs. The casting method is thoroughly described by Francesco Galiano⁷. In this method, polymer and solvent are the main components of the processing medium considering that additives can be added to adjust the thin film casting process. The first important consideration is the choice of the solvent for the polymer. High boiling point aprotic solvents like N-methyl-2pyrrolidone (NMP), dimethyl sulfoxide (DMSO), dimethyl acetamide (DMAc) or dimethyl formaldehyde (DMF) are

commonly used for SAPs. If necessary, heating treatment is added to dissolve the polymer.

The steps followed in the casting method can be described as:

- Solubilize the polymer in the chosen solvent
- If necessary, add an additional polymer (e.g., polybenzimidazole (PBI)) to process a blend
- Cast the solution onto a clean and flat surface (e.g., glass/Teflon™)
- Dry it in an oven (preferably under vacuum to avoid bubble formation)
- Add some water/acid to detach the dried membrane from the substrate

II. Materials and methods

1. Reagents

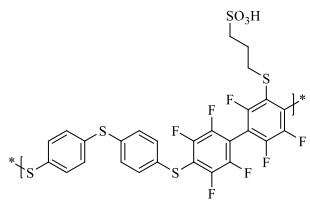
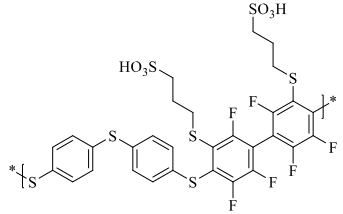
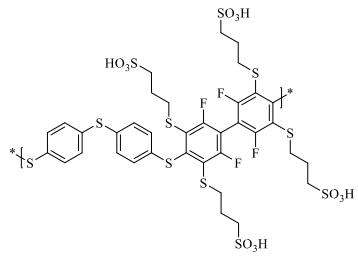
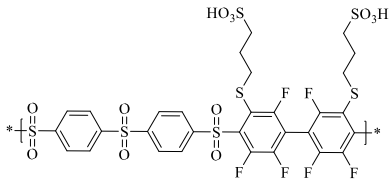
The solvents used for casting the PEMs (Dimethylsulfoxide DMSO, N-Methyl-2pyrrolidone, NMP) were of “anhydrous” quality (<0.005 % H₂O, ≥99.5 % purity, Sigma-Aldrich).

PBI-OO (poly-[(1-(4,4'-diphenylether)-5-oxybenzimidazole)-benzimidazole]) was supplied by Fumatech.

Proton-conducting polymers used within this chapter have been elaborated within this work, their synthesis and characterizations having been described and discussed in Chapters 2 & 3. Their references (in Chapter 3), names, and chemical structures (Polymer' repeating unit) are reported in the Table IV-1:

Table IV-1 Precursor polymers. First P refers to the poly(phenylenesulfide), the number stands for the degree of sulfonation, S refers to sulfonated, P to phosphonated and O to syntheses and characterizations of these polymers are detailed in chapter 3.

In chapter 3, referenced as:	Name	Chemical structure: Polymer' repeating unit
III-1-a	Phosphonated fluorinated poly(phenylene sulfide) (P1P)	

III-2e	Sulfonated fluorinated poly(phenylene sulfide) (P1S)	
	Sulfonated fluorinated poly(phenylene sulfide) (P2S)	
	Sulfonated fluorinated poly(phenylene sulfide) (P4S)	
III-2-f	Sulfonated fluorinated poly(phenylene sulfide) (P2SO)	

2. Experimental

The experimental protocols of the elaboration of the membranes are reported below. The success of the strategies are discussed within the section “results and discussion” together with the characterizations of the obtained PEMs.

The membranes with their names and formulation were elaborated and reported within Table IV-2, the experimental procedures are reported below.

Table IV-2. Membranes with the precursor polymers, the solvents used for the mixture with the additive and the additive to polymer ratio.

Precursor polymer	Solvent	Additive PBI-OO [PBI-OO]/[precursor polymer]	Membrane Name
P1P	DMSO	0	P1PM
P1S	DMSO	0	P1SM
P2S	DMSO	0.15	P2SM
P4S	DMSO	0.15	P4SM-a
		0.19	P4SM-b
		0.22	P4SM-c
P2SO	DMSO	0.07	P2SOM

a) Phosphonated membranes (P1PM)

As an illustrating example, the procedure is hereinafter described for the preparation of the membrane starting from P1P (chapter 3, p. 131), see Table IV-1.

In a 5 ml closed vial equipped with a magnetic stirrer, 0.065 g of P1P and 0.5 ml of DMSO were added in a vial. The mixture is stirred until complete solution of the polymer (4h). The solution was then poured within a petri dish and left for 12 hours at 80 °C, followed by an additional 2 hour-long period at 90°C under dynamic vacuum (base pressure of ca. 2×10^{-3} mbar) vacuum. Few drops of a 5 % HCl solution were deposited on the dried membrane thin film to peel it from the Teflon substrate.

b) Sulfonated membranes (P1SM, P2SM, P4SM and P2SOM)

The following procedure described the elaboration of the PEMs starting from P1S, P2S, P4S and P2SO (chapter 3, p. 149), see Table IV-1, and Poly-[(1-(4,4'-diphenylether)-5oxybenzimidazole)-benzimidazole] PBI-OO (figure IV-3).

In a 100 ml closed vial equipped with a magnetic stirrer, 1.5 g of P1S and 40 ml of DMSO (40 ml) were added in a vial. The mixture was stirred for 12 h. In the case of P2S, P4S and P2SO different quantities of PBI-OO were added to the solution and the solution was left stirring for another 12h. The solution was then poured on a Teflon™ squared mould (L x l x h =12 cm x 12 cm x 1 cm) and dried 12 hours at 80 °C followed by an additional 2 hour-long period at 90°C

under dynamic vacuum (base pressure of ca. 2×10^{-3} mbar) vacuum. Few drops of a 5 % HCl solution were deposited onto the dried membrane thin film to peel it from the Teflon substrate.

3. Characterization

a) Water uptake

Water uptake is calculated following equation IV-1:

$$\text{Water uptake (\%)} = \frac{W_f - W_i}{W_i} \times 100$$

Equation IV-1. Water uptake (%) calculation, being W_f = Final weight and W_i = Initial weight.

To calculate the water uptake, membranes were submerged in water during 6h, weighting them before (W_i) in their dry states and afterwards (W_f) in their wet states.

b) IEC

Theoretical (or calculated) Ionic Exchange Capacity is calculated by the following equation (IV2):

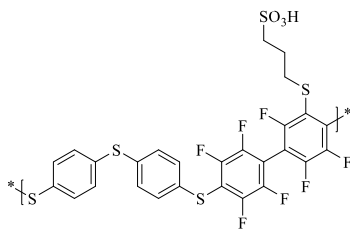
$$IEC_{calc.} = \frac{\text{number of } H^+ \text{ in } n \text{ unit of the polymer} \times 1000}{M_w(\text{Monomer Unit})}$$

IV-2. Ionic exchange capacity (IEC)..

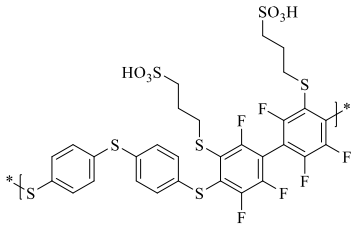
As an example, $IEC_{calc.}$ for P1S and P2S (Figure IV-4), our PPS-based functional polymers with respectively one vs. two side-chains ended by a SO_3H function per repeating unit would be:

$$IEC_{calc.} = \frac{1 \times 1000}{674.67} = 1.48 \qquad IEC_{calc.} = \frac{2 \times 1000}{804.83} = 2.49$$

With:



molecular mass (MM) of the repeating unit: 674.67 g/mol



molecular mass (MM) of the repeating unit: 804.83 g/mol

Figure IV-4. P1S and P2S, fluorinated sulfonated poly(phenylenesulfide).

When PBI-OO is added, $IEC_{Calc.}$ can be tuned by using the chosen quantity of PBI-OO. It is then calculated following the equation IV-3:

$$IEC_{Calc.} = \frac{IEC_{Pol.} \times W_{Pol.} - IEC_{PB100} \times W_{PB100}}{W_{PB100} - W_{Pol.}}$$

Equation IV-3. Ionic exchange capacity (IEC). With : $IEC_{Pol.}$ = IEC of the polymer calculated using Equation IV-2, $W_{Pol.}$ = Weight of polymer used for the membrane, IEC_{PB100} = IEC of PBI-OO calculated using Equation IV-2, W_{PB100} = Weight of PBI-OO used for the membrane.

Experimental IEC values were obtained using a titration method. Membranes were previously pre-treated by placing them in a 5 % HCl solution during 24h. They were then rinsed with bidistilled water (less than 1 μ S/cm) until the pH of the rinsing water became neutral. Afterwards the membranes were dried at 80 °C in a convection oven during 12h. They were then weighted and afterwards immersed in 50 ml of saturated NaCl water. The solution was stirred at room temperature for 24h. Titration was then done with 0.1N NaOH, using bromothymol blue indicator to pH 7.

The Experimental Ionic Exchange Capacity obtained by titration is called $IEC_{Titr.}$ and calculated from equation IV-4:

$$IEC_{Titr.} = \frac{C_{NAOH} \times V_{NAOH} - V_{NAOH} \times W_{PB100}}{W_{dry}} \times 1000 \text{ (meq g}^{-1}\text{)}$$

Equation IV-4. Ionic exchange capacity (IEC). $IEC_{Titr.}$ = IEC measured using titration method

c) Proton Conductivity at room temperature

A lab-made electrochemical work station was used to test for proton conductivity at room temperature. This electrochemical station measures initially Nafion® thin film membrane used as a reference and subsequently the membrane to be tested. Pre-treatment of the membranes tested with 0.5M HCl for 24 hours was carried on prior to conductivity measurements. Afterwards it was rinsed with bidistilled water. The membrane was placed between two Nafion layers and conductivity (R_M) was measured. It was then compared to the conductivity of the two Nafion (R_N) layers and divided by the thickness of the membrane to calculate its resistance. Proton conductivity was then obtained from the inverse of the resistance.

$$\text{Conductivity} = \frac{1}{R_{Sp}} = \frac{1}{(R_M - R_N)/L}$$

$$R_{Sp} = \frac{R_{\Omega} \times A}{L}$$

A = Area

L = Thickness

Equation IV-5. Conductivity measurements formulas.

d) Catalyst-coated membrane (CCM)

The preparation of the membrane for catalyst deposition was conducted in collaboration with Eindhoven University of Technology. A membrane was immersed in DI water for 1h prior to cutting 3 x 3 cm² squares. The cut squares were then immersed in 0.1 M H₂SO₄ for a week. Afterwards they were immersed in DI water to wash off excess H₂SO₄ then, dry at 60 °C between two metal plates to prevent wrinkling for 1h. The catalyst deposition was done with a solution containing 3.75 wt % catalyst and 1.25 wt % Nafion Ionomer in a 50:50 (vol/vol) Isopropanol/water solvent medium. It was then directly deposited onto the membrane and left at room temperature for the isopropanol/water processing medium to evaporate.

III. Results and discussion

1. Membrane processing

The elaborated membranes are based on phosphonated and sulfonated polymers. For the later, we have chosen to add polymer additive, triggering the formation of supramacromolecular complexes (through acid-base interactions of the two partners, leading to an ionic crosslinking) within the blend. The right choice of the polymer additive allows for an efficient mitigation strategy to fight against the deleterious solubilisation of the processed membranes in water. Discussed by J. Kerres⁸, this “blend” strategy has been successfully applied to elaborate membranes showing superior mechanical and thermal stability of the one based on the supramacromolecular complexes than from the one based on the sole polymers bearing SO₃H and PO(OH)₂ functional groups.

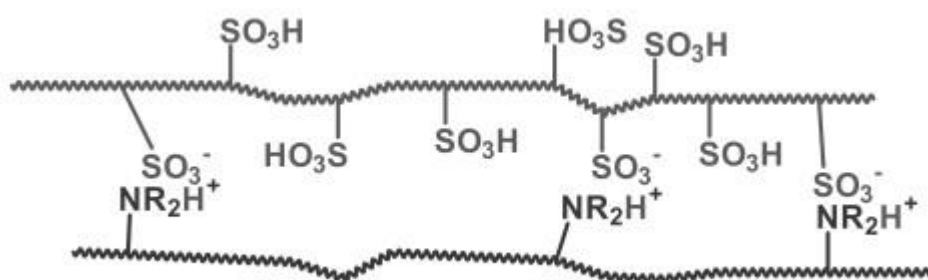


Figure IV-3. Scheme of ionically cross-linked acid-base blend membranes⁹.

a) Main issues

The elaboration of PEMs proved to be complex: there were several unsuccessful attempts and numerous issues to address. The initial problem was due to the solubility of the functional polymers in a suitable solvent. Some selected solvents were tried (NMP, DMAc, DMSO). DMSO was the solvent of choice, offering the best possible solubilities. The second main issue was that even when solubility could be reached after gentle heating and stirring, no continuous film was obtained after the evaporation of the solvent (figure IV-5), leaving thin films with cracks till powder with unsatisfactory film integrity and overall poor mechanical properties.



Figure IV-5. No film formation after evaporation of the solvent

The third problem encountered was that when applying the “blend approach” was the phase separation of the partnering polymers during the drying of the processing solvent illustrated in figure IV-5:



Figure IV-6. Film with phase separation after evaporation of the solvent.

At last, the water uptake of the membrane should be avoided as shown in (figure IV-7). It is especially critical with polymers carrying a high number of hydrophilic sulfonate groups.

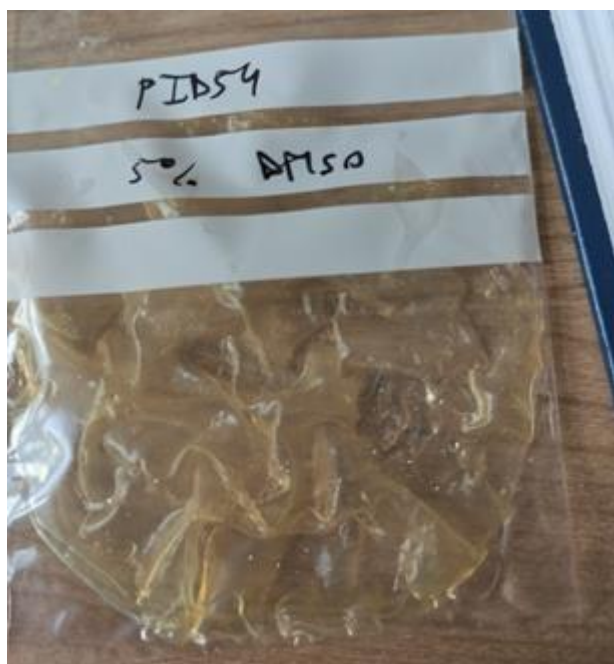


Figure IV-7. Swollen film with few ml of H₂O added to keep the membrane hydrated.

b) Phosphonated Membranes

In the case of the phosphonated membrane (P1PM, see Table IV-2), a brittle membrane was obtained. It was only possible to measure IEC and conductivity on small area (1 cm x 1 cm) samples. Higher Mw was required from the polymer forming this membrane to be mechanically stable. The membrane thickness was targeted to be of ca. 100 μ m from the polymer solution content and petri size area ($0.01 \text{ cm} \times \pi \times 4^2 \text{ cm}^2 \times 1.3 \text{ g/ml}$). Due to its low film-forming ability and the fact that IEC and conductivity tests did not reach acceptable values, no further membranes were made to elaborate membranes from the P1P phosphonated polymer.

c) Sulfonated Membranes

Different PEMs were elaborated starting from the sulfonated polymers (Table IV-1).

The first membrane (P1SM) was produced from P1S which has one SO₃H function per repeating unit. IEC calculated was 1.48 and the polymer was insoluble in water, therefore no mixing with PBI-OO was needed. With IEC values at 2, or higher, most polymers become water-soluble and therefore non-compatible with their uses as thin-film membranes within a PEMFC.

The membrane P2SM obtained from P2S (two SO₃H function per repeating unit) was proved to be water-soluble after its processing, requiring an optimization of its formulation for its use in a PEMFC. In such circumstances, one of the most used mitigating polymeric additive is poly(benzimidazole) (PBI)¹⁰ (Figure IV-8, up). However, in this case, a more flexible polymer given by the presence of two thioether bonds, the poly-[(1-(4,4'-diphenylether)-5-oxymethyl)-5-oxymethylbenzimidazole] (PBI-OO), was chosen (Figure IV-8, down).

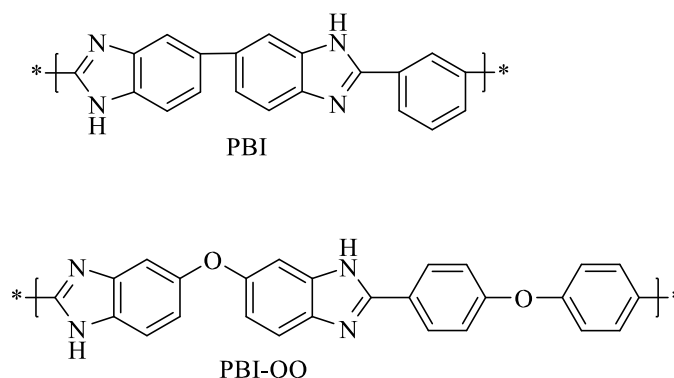


Figure IV-8. PBI and PBI-OO chemical formulas.

The membrane P2SM obtained with a ratio between the added PBI-OO and the sulfonated polymer of [PBI-OO]/[P2S]= 0.15 and up to 0.22 exhibits good mechanical properties thanks to its ionic crosslinking as reported within Figure IV-9. This cross-linking had been proposed in a paper using SPEEK sulfonated poly(ether ether ketone) and PBI-OO, pointing out how the imidazole groups of PBI-OO are protonated by –SO₃H groups¹¹.

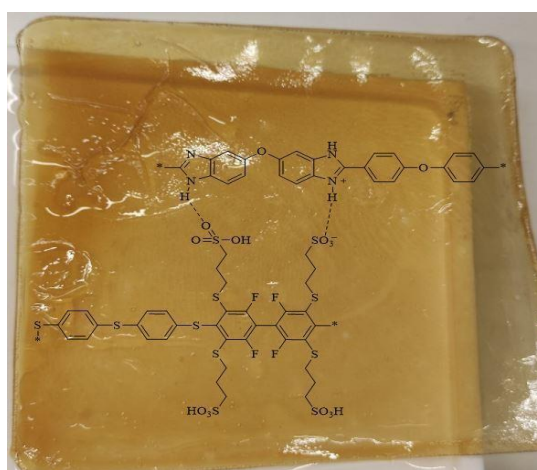


Figure IV-9. P4SM-a membrane.

Applying this mitigating “blend approach” resulted in film-forming and mechanically stable membranes based on P1S, P2S and P4S and PBI-OO, these membranes were further characterized and the results are described in the next section (chapter 4-III-2).

The membrane P2SOM was obtained from the P2SO (sulfone bridges), it proved to be too brittle (Figure IV-10. A 7 % of PBI-OO content was added with no success, another small sample using 15 % of PBI-OO was attempted with no further success. These membranes were not mechanically stable enough to be analysed and no further characterization was done.



Figure IV-10. P2SOM membrane.

2. PEM's properties

a) Properties at rt

The results of the characterization performed on the membranes are given within Table IV-3:

Table IV-3. Membranes characterization. First P refers to the poly(phenylenesulfide), number = degree of sulfonation, S refers to sulfonated, P to phosphonated and M to membrane. Finally a, b, c are membranes starting from the same polymer adding different quantities of PBI-OO.

Starting polymer	Membrane Name	PBI-OO (%)	IEC _{Calc.} (mEq/g)	IEC _{Tit.} (mEq/g)	Conductivity (mS/cm)	Water uptake (%)
P1P	P1PM	-	1.50	0.09	2	-
P1S	P1SM	-	1.48	1.57	135	-
P2S	P2SM	7	2.00	1.98	202	-
P4S	P4SM-a	15	2.50	1.09	179	57
P4S	P4SM-b	19	2.17	1.12	136	42
P4S	P4SM-c	22	1.90	1.13	64	30

- Membranes from phosphonated polymer :

Membranes from P1P could be obtained without adding PBI-OO. As expected from their low number of hydrophilic phosphonic groups per repeating unit, they showed a very small water uptake. Membrane was not completely homogenous but still usable to perform first tests. Experimental IEC was much below than the theoretical one calculated from its molecular formula, due to the fact that the phosphonation level was very low and no proton conducting channels could be formed. As for IEC, the conductivity value is considered to be very low, well below the targeted values (of ca. 100-200 mS/cm) envisioned for our project.

- Membranes from sulfonated polymers:

Water uptake is of great importance in the performance of a PEM. It swells the membrane and can turn it mechanically inappropriate in a device. While initially it was not deemed a problem as no swelling was observed this analysis was not done for P1S and P2S.

P1SM is the only sulfonated membrane obtained without PBI-OO being insoluble in water and having enough mechanical and chemical stability to be used in a PEMFC.

PBI-OO was needed to obtain P2SM (two SO₃H function per repeating unit) because of the water solubility of the precursor polymer P2S. While a pure P2SM (no PBI-OO added) has a theoretical IEC of 2.50 meq.g⁻¹, the presence of 7 % of PBI-OO turns it insoluble in water but at the same time, decreases the IEC value down to 2 meq/g. It is admitted that an IEC = 2 meq/g is the value below we should benefit from a membrane insoluble in water. P2SM is close to this threshold value, offering great potentials.

At last, P4SM (4 sulfonated units/polymer unit) was expected to have a higher conductivity than P2SM but the experimental results did not confirm the theoretical IEC values. This phenomenon could be linked to high degree of crosslinks that would induce a closure of the proton channels as suggested by Yue Zhouying *et al.* in their study on phosphoric acid-doped crosslinked sulfonated poly(imidebenzimidazole) for PEMFC applications¹². Different quantities of PBI-OO were added to benefit from the precursor polymer P4SM. While IEC values aren't much affected whatever is the PBI-OO content, the conductivity results are strongly impacted decreasing from 179 mS/cm to 64 mS/cm for membrane P4SM containing 15 and 22 % PBI-OO, respectively. Water uptake was also impacted by the content of PBI-OO

decreasing from 57 % (when using 15 % wt. PBI-OO) to 30 % when using a higher PBI-OO amount (22 % wt. PBI-OO)

b) Conductivity vs. temperature

Conductivity change vs. temperature was analyzed for P1SM, P2SM and P4SM and compared to Nafion® 212, chosen as a reference material for PEM. The conductivity values fall in the range of 14-90 mS/cm at 30 °C and 52-133 mS/cm when the temperature was increased up to 90 °C. P4SMa was chosen as having the highest conductivity at room temperature compared to P4SM-b and P4SM-c (179 vs. 136 and 64 mS/cm respectively). It was observed that the conductivity increases with the temperature and the best result is obtained for the membrane obtained from the highest substituted polymer P4S. P2SM has similar conductivity to Nafion® 212 while P1SM clearly exhibits a lower conductivity. P4SMa has an initial higher conductivity than Nafion® 212, but when measuring values from 90 °C to rt a decrease of conductivity under 70 °C is observed (Figure IV-11). This behavior is called hysteresis, it is due to the dependence of the properties of a system on its history, in this case the increase of temperature.

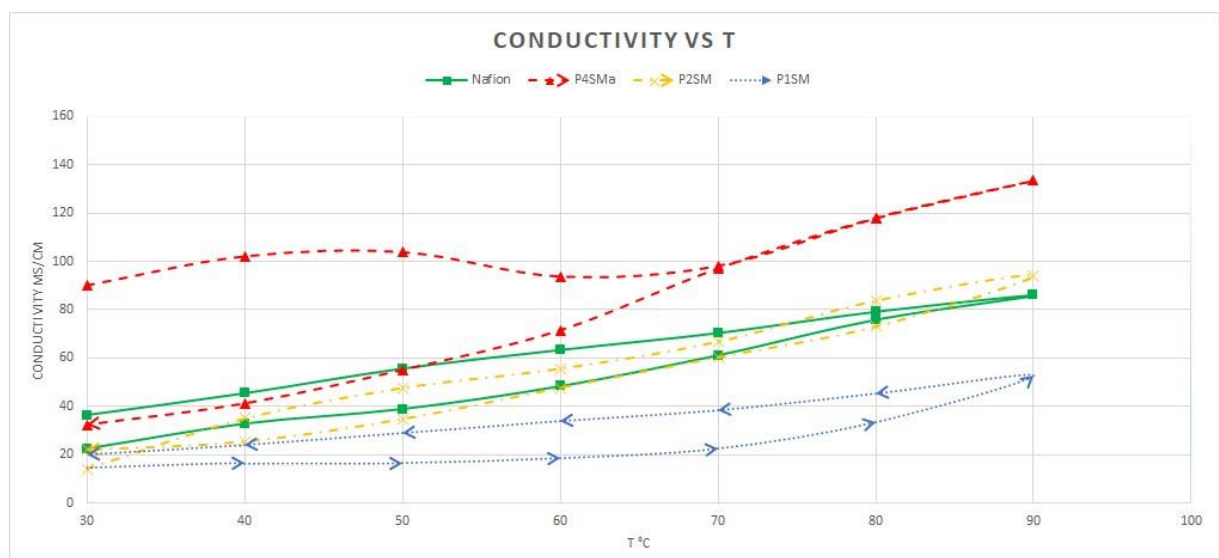


Figure IV-11. Membrane Conductivity vs. temperature.

Because of some time constrictions, further analysis could not be done but the study should be strengthened to evaluate the resilience of the membranes.

c) Membrane surface

The surfaces of the thin-film membrane surfaces were noticed by SEM (Scanning electron microscope) and differences were observed between the side in contact with the Teflon® substrate and the one in contact to the air, the later being the smoothest. (Figure IV-12). It is due to the imperfections in the Teflon® substrate, while the air side shows a smoother surface.

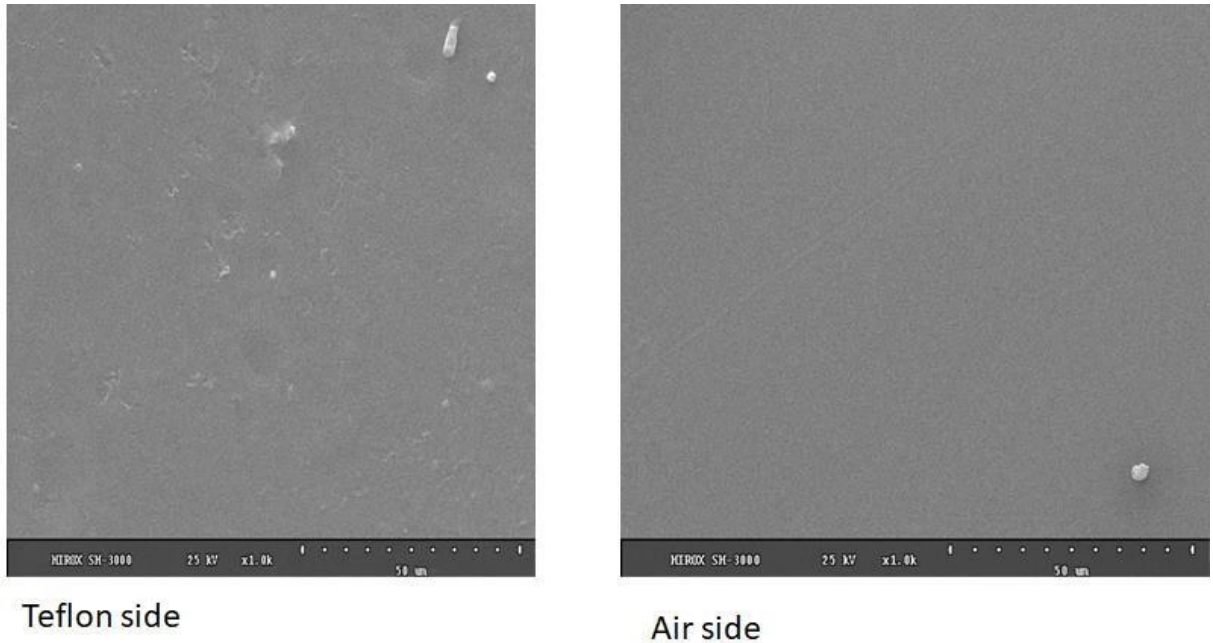


Figure IV-12. Membrane 12x12 cm². P4SMa SEM x 1K, Teflon® side (left), Air-side (right).

The cross-section of PEM thin films were also imaged by SEM too. The membrane thickness was measured to be 43 μm using SEM, lower than the one measured for conductivity measurements with a calliper gauge (61 μm). The difference is surely due to the analysis of a completely dried P4SM-a by SEM (Figure IV-13) whereas for conductivity the membrane was measured in a fully hydrated state.

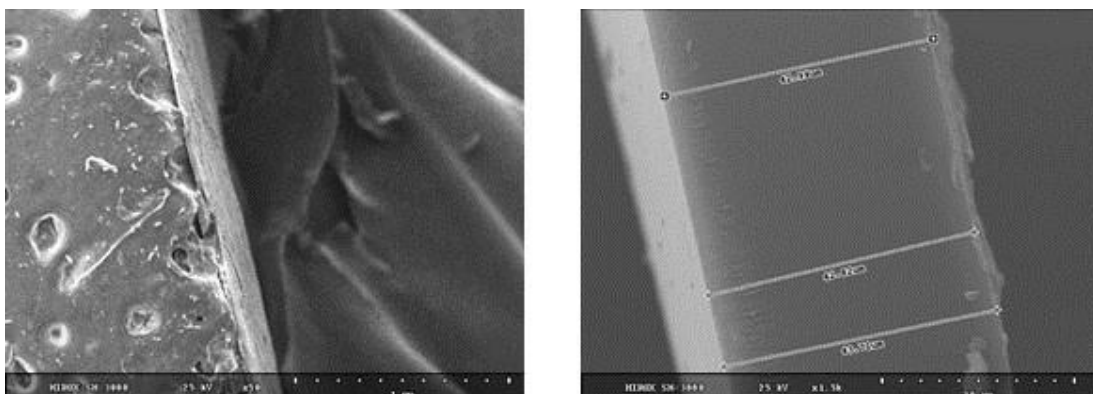


Figure IV-13. Membrane 12x12 cm. P4SM-a SEM x50. P4SM-a SEM x1.5k.

P4SM-a and P4SM-c were sent for analysis in the electrolysis cell. It was further analysed in the Technische Universiteit Eindhoven. (see chapter 4-II-d)

d) Electrochemical Impedance Spectroscopy (EIS)

Electrochemical Impedance Spectroscopy is a technique well-suited to study ionic transport properties of Ion-exchange membranes. As explained in J.S. Park *et al.*¹³ paper, EIS can be an alternative way to characterize quantitatively PEM systems, their experimental comparisons proved the analogy between impedance spectra and current-voltage curves.

Before carrying the EIS analysis the sample had to be prepared. Due to equipment constraints in Eindhoven, it was decided to focus on P4SM-a and P4SM-c, expecting to give distinct results. The preparation of the MEA (Membrane Electrode Assembly) was as follows, the example being given for membrane P4SM-c:

- The membrane was immersed in DI water for 1h prior to cutting 3 x 3 cm² squares
- Immerse the sample in 0.1 M H₂SO₄ for a week.
- Immerse in DI water to wash off excess H₂SO₄ then, dry at 60 °C between two metal plates to prevent wrinkling for 1h

Subsequently, the catalyst deposition was conducted as follows:

- Solution: 3.75 wt % Catalyst, 1.25 wt % Nafion ionomer in IPA : Water
- Casting onto the membrane
- Drying at room Temperature – slower evaporation avoids membrane breaking

The result of this MEA is shown in Figure IV-14. The membranes are renamed as P4SM-a_CCM and P4SM-c_CCM. Do note that CCM stands for Catalyst-Coated Membrane:



Figure IV-14. Membrane 3x3cm. P4SM-c_CCM after catalyst deposition.

The different steps of the electrochemical impedance spectroscopy characterization are defined as below:

1. OCP: 1h – Stabilize temperature and wetting of the membrane
2. Apply 10, 20, 40, 50, 100 mA.cm⁻²: 30 s each
3. 250 mA.cm⁻²: 30 min
4. OCP: 5 min
5. EIS at 10, 50 and 100 mA.cm⁻²
6. Polarization curve: 16 steps of 2 min, 5 curves, [1, 1500] mA.cm⁻²
7. EIS at 10, 50 and 100 mA.cm⁻²

Some delamination from the membrane surface was observed when preparing the device, probably due to the use of a different ionomer from the membrane (Figure IV-15):

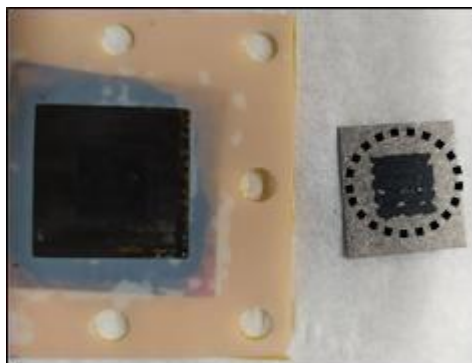


Figure IV-15. Delamination of the catalyst from the membrane surface in P4SM-c.

Therefore the preparation for P4SM-a was adapted and the new final device was named P4SM-a_CCS for Catalyst-Coated Surface, the procedure was as follows:

- Immerse in 0.5 M H₂SO₄ (overnight)
- Immerse in DI water to wash-off the excess H₂SO₄
- Membrane was cut into 3 x 3 cm² unitary sample

Afterwards catalyst composition was the same in terms of solution composition but it was deposited at the porous transport layer (PTL) at 85 °C and not directly onto the membrane.

PTLs were hot-pressed against the membrane at 80 °C, 5 Mpa, 5 min.

The protocol for testing includes the following steps:

1. OCP: 1h – Stabilize temperature and wetting of the membrane
2. Apply 10, 20, 40, 50, 100 mA.cm⁻²: 30 s each
3. 250 mA.cm⁻²: 30 min
4. OCP: 5 min
5. EIS at 10, 50 and 100 mA.cm⁻²
6. Polarization curve: 16 steps of 2 min, 5 curves, [1, 1500] mA.cm⁻²
7. EIS at 10, 50 and 100 mA.cm⁻²
8. Galvanostatic 18 h
9. Polarization curve: 16 steps of 2 min, 3 curves, [1, 1500] mA.cm⁻²
10. EIS at 10, 50 and 100 mA.cm⁻²
11. Galvanostatic <1 h for permeation experiment

P4SM-a_CCS and P4SM-c_CCM were measured at different current intensities and compared to Nafion® 112, the results being shown in Figure IV-16:

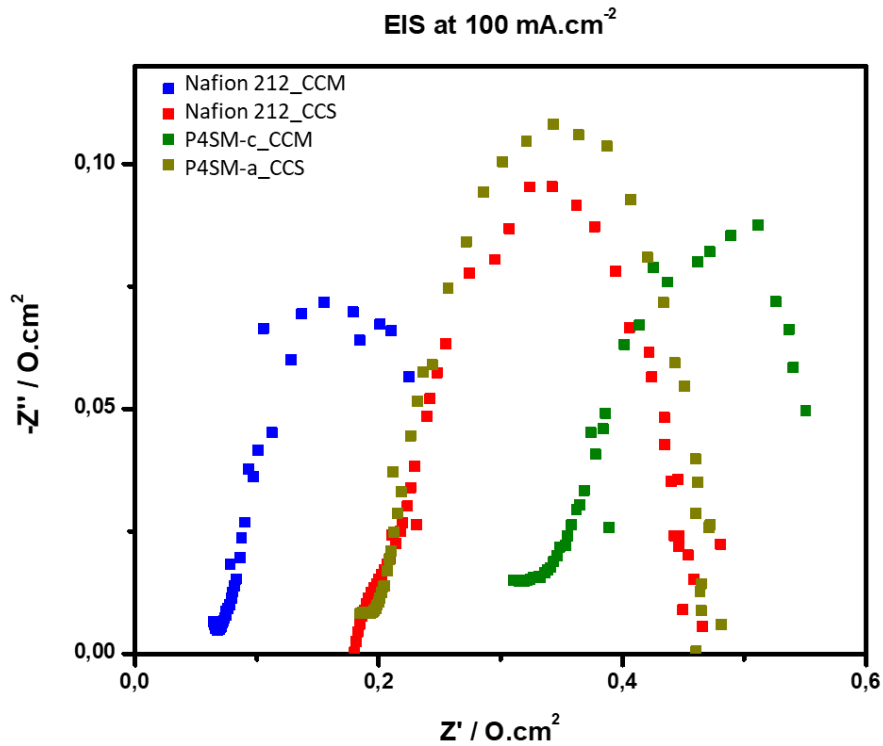


Figure IV-16. Electrochemical Impedance Spectroscopy (EIS) Nyquist plots.

In figure IV-16, it can be observed an important difference between Nafion 212_CCM and P4SM-c_CCM, nevertheless, this behaviour may be due to the high percentage of PBI-OO inside P4SM-c and to the occurrence of delamination that may affect the result.

On the other hand P4SM-a_CCS gave interesting and promising results : EIS gave similar values for Nafion 212_CCS and P4SM-a_CCS, meaning that the impedances are close.

The cell potential vs. the current density was also measured, results can be observed in Figure IV-17:

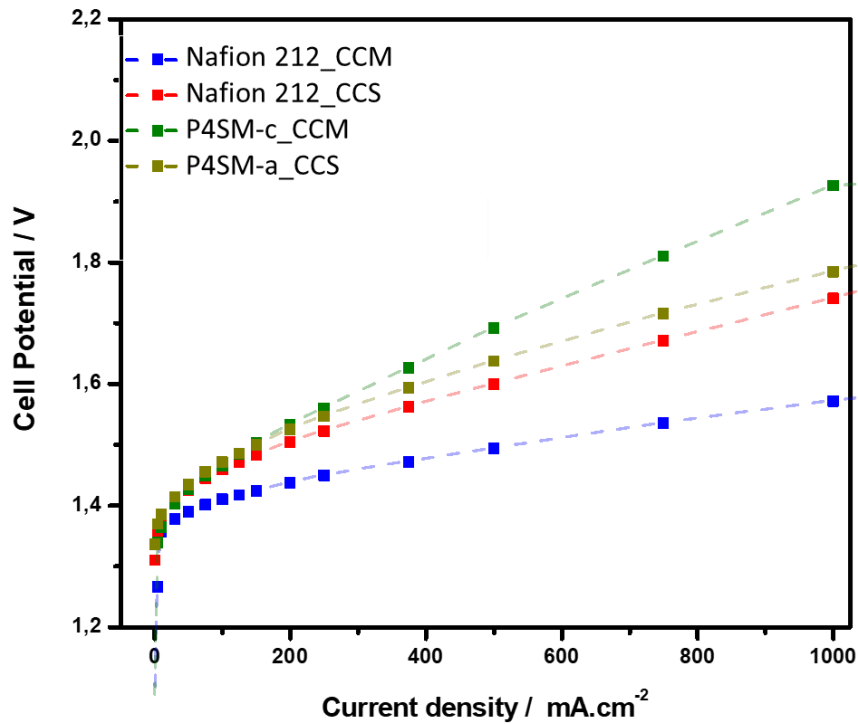


Figure IV-17. Cell Potential vs Current density.

In these results the same tendency as for EIS can be observed, while the difference for P4SMc_CCM and Nafion 212_CCM in cell potential increases with the increase of the current density, the results for P4SM-a_CCS are much closer to Nafion 212_CCS, not enhancing the spread as current density is increased.

IV. Conclusion

To conclude this chapter (see figure IV-2), the steps described before are depicted in four images for the process of elaborating a membrane:



Dried crude polymer



Polymer solution in teflon dish



Dried polymer with additives embedded



Membrane

V. *Figure IV-2. Process from dry polymer (P4S) to membrane (P4SM) after adding PBI-OO (poly-[(1-(4,4'-diphenylether)-5-oxybenzimidazole)-benzimidazole]) as additive.*

Several membranes were elaborated from the prepolymers synthesized in Chapter 2 and postfunctionalized into functional polymers for PEMFCs in Chapter 3. Best mechanically stable membranes have been elaborated starting from sulfonated polymers (table IV-1). PBI-OO was added as a multipurpose polymeric additive, enabling acceptable film-forming and mechanical properties, interesting proton conductivity and reduced water solubility. Two membranes from sulfonated polymers at two different contents of PBI-OO ($[PBI-OO]/[precursor\ polymer]=0.15$ and 0.22) were further characterized by Electrochemical Impedance Spectroscopy and compared to Nafion®212. Again, the preparation of the device has been optimized, and the best results are obtained with the lower content of PBI-OO and when the catalyst is deposited at the porous transport layer instead of being deposited directly onto the membrane. The preliminary results obtained from P4SM are close to those obtained for of Nafion®212, when following the same preparation protocol.

The sulfonated poly(phenylene sulfide)s (P4S) proton conducting materials appears to be promising. It offered a conductivity of 135 mS/cm at 90 °C with water uptake of 42 %. Further analysis should be done to optimize the formulation and the preparation.

VI. References

- ¹ T. A. Zawodzinski, C. Derouin, S. Radzinski, R. J. Sherman, U. T. Smith, T. E. Springer, S. Gottesfeld, *Water uptake by and transport through Nafion(R) 117 membranes*, 1993, J. Electrochem. Soc. 140, p. 1041 DOI: [10.1149/1.2056194](https://doi.org/10.1149/1.2056194)
- ² A. L. Rusanov, D. Y. Likhatchev, and K. Mu, *Proton-conducting electrolyte membranes based on aromatic condensation polymers*, 2002, Russian Chemical Reviews 71 (9), Vol. 761, p. 761774 DOI: [10.1070/RC2002v071n09ABEH000740](https://doi.org/10.1070/RC2002v071n09ABEH000740)
- ³ W. T. Grubb, L. W. Niedrach, *Batteries with Solid Ion-Exchange Membrane Electrolytes*, 1959, Journal of the electrochemical society, Vol. 107, No. 2, p. 131-135 DOI: [10.1149/1.2427329](https://doi.org/10.1149/1.2427329)
- ⁴ M. Carmo, D. L. Fritz, J. Mergel and D. Stolten, *A comprehensive review on PEM water electrolysis*, 2013, vol. 8, issue 1, International Journal of Hydrogen energy 38, p. 4901-4934 DOI: [10.1016/j.ijhydene.2013.01.151](https://doi.org/10.1016/j.ijhydene.2013.01.151)
- ⁵ Y. Molmeret, F. Chabert, N. El Kissi, C. Iojoiu, R. Mercier and JY. Sanchez, *Towards extrusion of ionomers to process fuel cell membranes*, 2011, Polymers, vol. 3, p.1126-1150 DOI: [10.3390/polym3031126](https://doi.org/10.3390/polym3031126)
- ⁶ P. Khomein, W. Ketelaars, T. Lap, and G. Liu, *Sulfonated aromatic polymer as a future proton exchange membrane: A review of sulfonation and crosslinking methods*, 2021, Renew. Sustain. Energy Rev., vol. 137, no. 110471 DOI: [10.1016/j.rser.2020.110471](https://doi.org/10.1016/j.rser.2020.110471)
- ⁷ F. Galiano, *Casting Solution*, no. 2009, p. 40872, 2014. DOI: [10.1007/978-3-642-40872-4_1870-3](https://doi.org/10.1007/978-3-642-40872-4_1870-3)
- ⁸ J. A. Kerres, *Blended and cross-linked ionomer membranes for applications in membrane fuel cells, fuel cells*, 2005, vol. 5, n. 2, p. 230-247 DOI: [10.1002/fuce.200400079](https://doi.org/10.1002/fuce.200400079)
- ⁹ J. A. Kerres, *Blended and cross-linked ionomer membranes for applications in membrane fuel cells, fuel cells*, 2005, vol. 5, n. 2, p. 230-247 DOI: [10.1002/fuce.200400079](https://doi.org/10.1002/fuce.200400079)
- ¹⁰ Sun, X., Simonsen, S. C., Norby, T., & Chatzitakis, A. *Composite Membranes for high Temperature PEM Fuel Cells and Electrolysers: A Critical Review*, 2019, Membranes, 9(7), p.83 DOI: [10.3390/membranes9070083](https://doi.org/10.3390/membranes9070083)
- ¹¹ A. Katzfuss, K. Krajcinovic, A. Chromik and J. Kerres, *Partially Fluorinated Sulfonated Poly(arylene sulfone)s Blended with Polybenzimidazole*, 2011, Journal of Polymer Science Part A: Polymer Chemistry, Vol. 49, p. 1919-1927 DOI: [10.1002/POLA.24624](https://doi.org/10.1002/POLA.24624)
- ¹² I. M. Tkachenko, N. A. Belov, Y. Yakovlev, P. V. Vakuliuk, O. V. Shekera, Y. P. Yampolskii, Shevchenko, *Synthesis, gas transport and dielectric properties of fluorinated poly(arylene ether)s based on decafluorobiphenyl*, Materials Chemistry and Physics 2016. DOI: [10.1016/j.matchemphys.2016.08.028](https://doi.org/10.1016/j.matchemphys.2016.08.028)

¹³J.S. Park, J.H. Choi, J.J. Woo and S.H. Moon, *An electrical impedance spectroscopic (EIS) study on transport characteristics of ion-exchange membrane systems*, Journal of Colloid and Interface Science 2006, vol. 300, p. 655-662 DOI: [10.1016/j.jcis.2006.04.040](https://doi.org/10.1016/j.jcis.2006.04.040)

Chapter 5. General Discussion and Conclusions

V. General Discussion	205
VI. General Conclusions	210
VII. Outlook	211
VIII. References	213

I. General Discussion

This work reported the synthesis of new polymers to elaborate proton exchange membranes (PEMs) from the (macro)molecular engineering and syntheses of these functional polymers, through the elaboration process of PEMs till the characterization of their properties as thin film membranes as well as within Proton-Exchange-Membrane Fuel Cells (PEMFCs). The first main discussion deals with the choice of (co)monomers for obtaining high performance functional polymers showing both high and long-lasting proton conductivity and mechanical stability. As shown in Figure V-1, the landscape of polymeric materials developed and used till date as PEMs for low-temperature PEMFC is vast, with many different families.

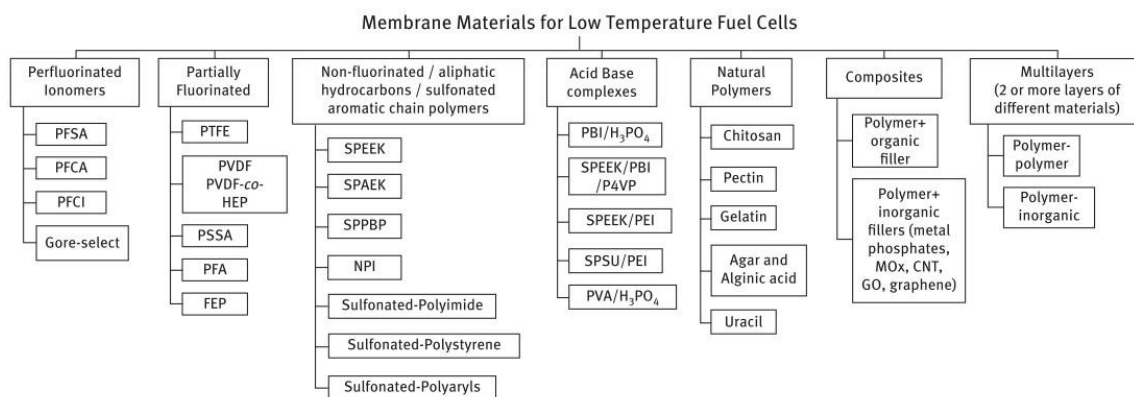


Figure V-1. Different materials used for PEMs (CNT: carbon nanotubes; FEP: poly(fluoroethylene-co-hexafluoropropylene); GO: graphene oxide; HEP: hexafluoropropylene; NPI: naphthalenic polyimide; P4VP: poly(4-vinylpyrrolidone); PBI: poly(benzimidazole); PEI: poly(etherimide); PFA: poly(tetrafluoroethylene-co-perfluorovinyl ether); PFCA: perfluorocycloalkene; PFCI: perfluorocarboxylated ionomer; PFSA: perfluorosulfonic acid; PSSA: poly(styrene sulfonic acid); PTFE: poly(tetrafluoroethylene); PVA: poly(vinyl alcohol); PVDF: poly(vinylidene fluoride); SPAEK: sulfonated poly(arylether ketone); SPEEK: sulfonated poly(ether ether ketone); SPPBP: Sulfonated poly(phenoxy benzoyl phenylene); and SPSU: sulfonated poly(sulfone)).¹

It is always hard to decide which path to take when you face such a vast field. A hand full of cutting-edge scientific articles are continuously being published as the need for cleaner energy and the need to decrease the dependency on gas and oil resources becomes urgent. Y. Zou *et al.*² explain why a sulfonated aromatic polymer can be seen as a (quasi) ideal materials platform owing to its ease of synthesis from industrial monomers and the possibility to fine-tune its physicochemical properties by adjusting its chain microstructure or by postfunctionalizing its macromolecular backbone. Following this research line, Simari *et al.*³

have reported the synthesis of a sulfonated poly(ethersulfone), abbreviated as PES, but the degree of sulfonation in a non-fluorinated aromatic ring is low and therefore conductivity is also not as high as desired (min. 100mS/cm) but it shows a mechanical stability that serves for the purpose of producing a membrane. Therefore, it was chosen to introduce a large number of acidic groups within the repeating unit of polymers aiming at generating high performance PEMs, a decafluorobiphenyl unit can be additionally chosen ^{4,5} as a comonomer for its ability to be post-functionalized.

Several strategies have been therefore implemented into this thesis:

We have first developed a polycondensation route to generate alternated copolymers relying on decafluorobiphenyl (DFBP) and four different dithiolated sub-units. Beyond the impact of the later comonomer, the polymerization conditions have been thoroughly studied toward their optimizations.

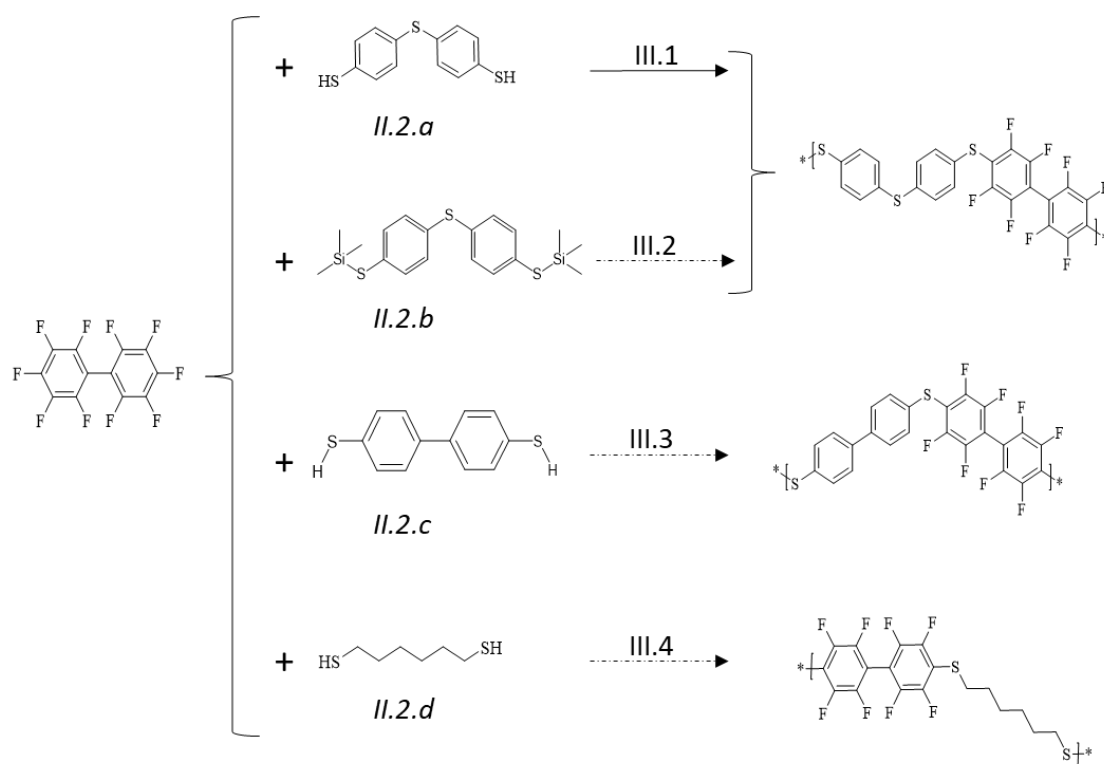


Figure V-2. Scheme of polymerizations starting with decafluorobiphenyl

The synthetic route using DFBP and 4,4-thiobisbenzenethiol, abbreviated as DBBT, (see II.2.a) proved to be the most promising in terms of reproducibility and polymer properties (high quantities were obtained, chemically and thermally stable (up to 400 °C) and high Mw up to

ca. $3 \cdot 10^5$ g/mol. The 3 other routes of this first implemented strategy only lead to oligomers, with little hope for generating the materials required for efficient PEMs. The use of less hindered co-monomers even with the alkyl thiol (II.2.d) leads to an oligomer of low molecular weight and with low thermal stability.

In an alternative (second) implementation of the polycondensation route (Figure V-3, lower part), the DBBT unit was copolymerized with two prefunctionalized unit incorporating SO_3H and $\text{PO}(\text{OH})_2$ functional groups. The polymer III.5 was obtained, with extremely low yield while the second pathway (III.6) led to a crosslinked polymer. If successful, this all-in-one approach would elegantly avoid the mandatory postfunctionalization step required to transform prepolymers obtained under the first polycondensation route into sulfonic acid and phosphonic acid-containing polymers for PEMs. Due to the lack of time, further optimization and trials were not attempted and could be the objective of future works. Several polycondensations of already functionalized monomers can be found in the literature, C. Liu *et al.*⁶ discussing a polycondensation route 2 relying on the disodium 3,3'-disulfonate-4,4'-dichlorodiphenylsulfone monomer.

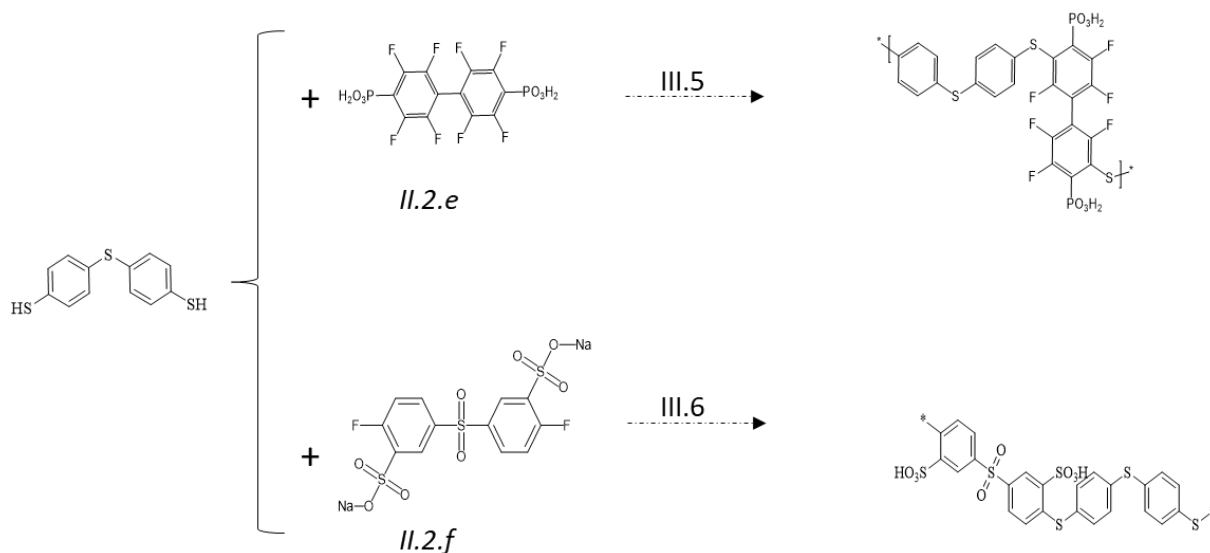


Figure V-3. Scheme of polymerizations starting with 4,4-thiobisbenzenthionol and prefunctionalized monomers.

The postfunctionalization of the prepolymers previously obtained via the pathway III.1 (Figure V-3) was optimized to obtain proton conducting polymers.

The first postfunctionalization involves phosphonation schemes (Figure V-4).

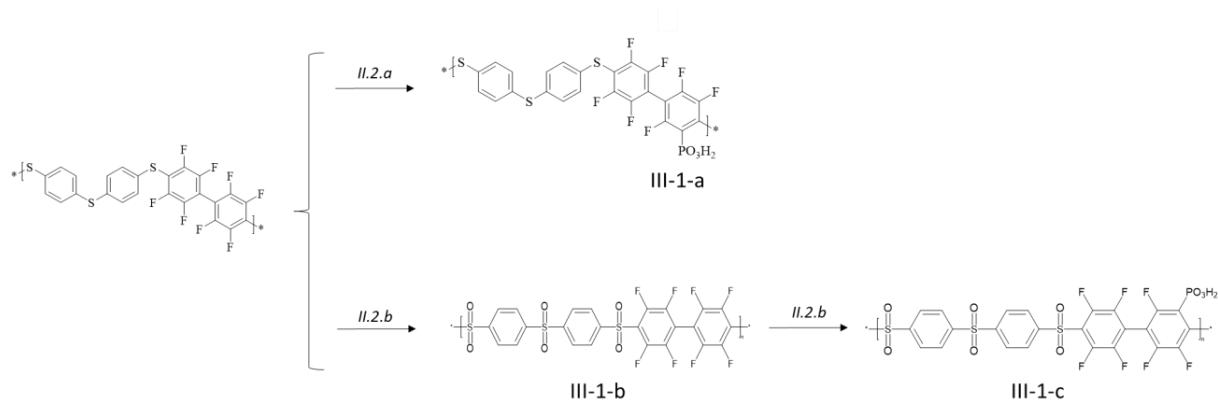


Figure V-4. Scheme of all phosphonation in italic, the paragraph number where the experimental protocol is described, above the arrows, the paragraph number where the polymerization is discussed.

The best phosphonation has been accomplished using TSMP (route II.2.a). Deceptively, a lower phosphonation yield than expected was obtained. The phosphonation of fluorinated poly(phenylene sulfone)s yielded a higher degree of phosphonation but this polymer was not kept for the elaboration of PEMs due to its extremely low solubility in organic solvents.

Cast from 10 % w. solution in DMSO, a PEM membrane was obtained with II-1a but both its conductivity and IEC values proved to be low, discarding this PEM for further study under a PEMFC configuration. A higher degree of phosphonation should be envisioned to obtain better membranes but it seems that direct phosphonation on the fluorines does not work well.

A second postfunctionalization approach relying on the sulfonation of the prepolymers has been developed and is schematically rationalized within Figure V-5.

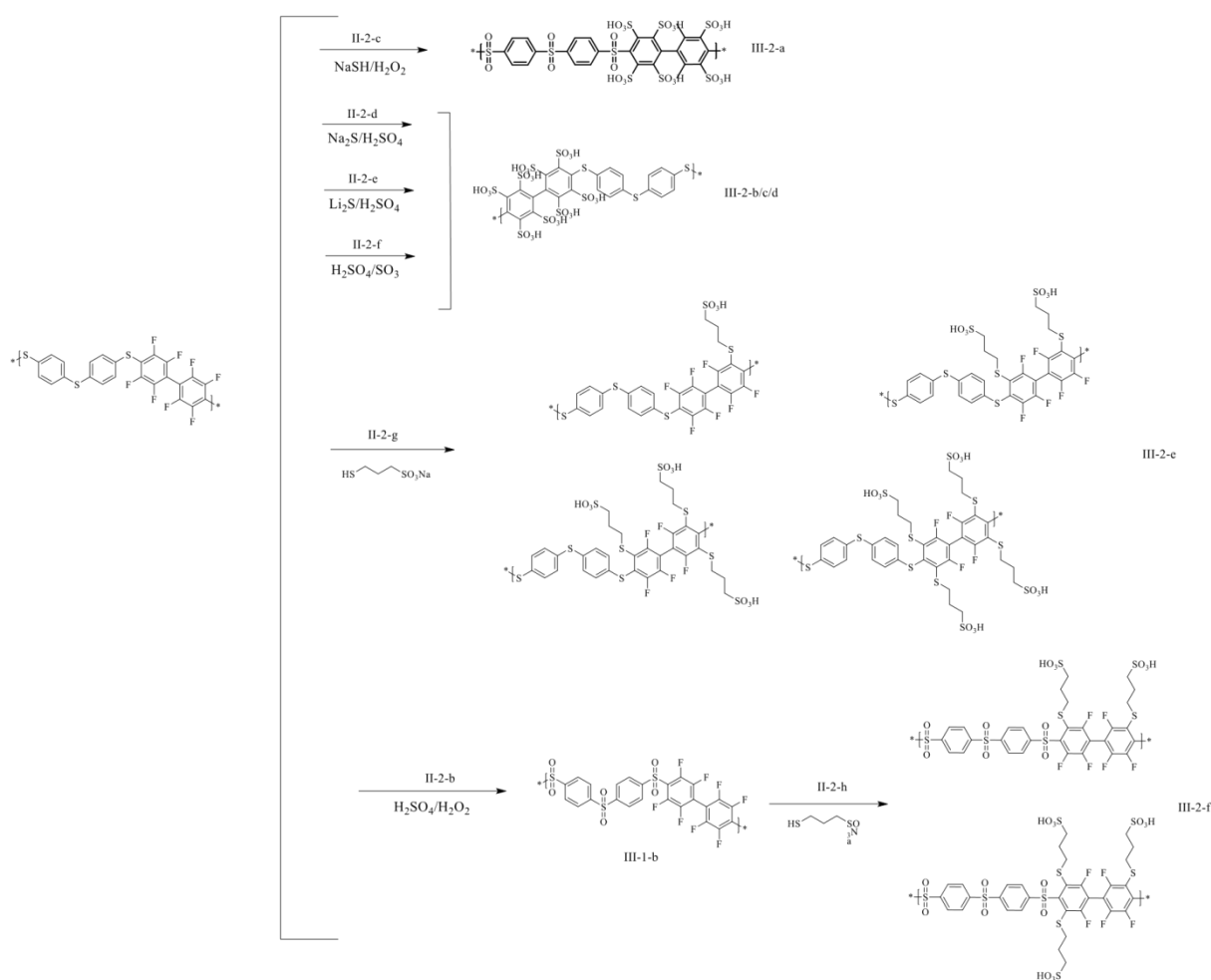


Figure V-5. Scheme of sulfonations

Direct sulfonation route (i.e., the strategies denoted II.2.a, b, c, and d) lead to a massive decreased of the polymers Mw, discarding them for PEM' elaboration due to their inherently moderate mechanical and thermal thermal properties.

The use of milder sulfonation conditions through the action (Aromatic nucleophilic substitution (S_NAr) reaction of the sodium 3-mercaptopropane-1-sulfonate agent onto the fluorine atoms of the DFBP sub-unit fortunately gave the targeted results. Depending on the experimental conditions, polymers with different sulfonation degrees were obtained, ranging from 1 to 4 sidechains ended with a SO₃H function grafted per DFBP sub-unit 1 to 4 (see Figure V-5, product III-2-e). On further clean step to obtain these polymers would be a one pot polymerization using DBU as the base followed by the sulfonation using the sodium 3-mercaptopropane-1-sulfonate. It would be a direct obtention of a suitable for PEM sulfonated polymer. The functionalization degree has a great effect onto the water solubility. Being water soluble, the polymers with a sulfonation degree equal to or higher than 2 should undergo to a specific formulation optimization during the

elaboration of the membrane to be usable in a cell with water. As pointed out by J. Kim et al.⁷ there is a trade-off between the increase in conductivity and the mechanical and chemical properties. A trade-off in between these key-enabling properties can be reached by formulating a blend in which the functional polymer is ionically crosslinked with a well-chosen partnering polymer.

Several membranes with these polymers were synthesised obtaining the highest conductivity at 90 °C for the polymer with the highest degree of sulfonation (4) (see Figure V-5, product III2-e) and the lowest % of PBI-OO used (15 %). While a higher degree of sulfonation increased the conductivity, higher % of PBI-OO decreased it, as expected, through combined diluting and crosslinking effects. PBI-OO-based blend membranes resulted in PEMs with the required mechanical stability and largely insoluble in H₂O but at the expense of reducing their protonic conductivity.

The mild sulfonation conditions (relying on sodium 3-Mercapto propane-1-sulfonate) successfully applied to the fluorinated poly(phenylene sulfide)s also worked in the case of the fluorinated poly(phenylene sulfone) prepolymers. The degree of sulfonation did not reach 4 (figure V-5, III-2-f) with this prepolymer, the sulfonated polymer lacking moreover of an appropriate solubility in organic solvent. While the elaboration of the PEM took these parameters into account and even though membranes were cast, no good mechanical stability was obtained using this polymer.

II. General Conclusions

As a conclusion, the most promising PEM using our best functional polymer has been obtained when using sodium 3Mercapto propane-1-sulfonate as the sulfonating agent and having the highest possible degree of sulfonation (4 per DFBP sub-unit). Their electrochemical characterizations revealed conductivity values higher than the ones displayed by membranes of Nafion®112 at 90 °C. However, when sent for their insertion within a PEMFC at the Eindhoven University of Technology, some issues emerged, the catalyst delaminating from the membrane surface. Still here also, these preliminary results were shown to compare favourably with respect to the ones obtained with Nafion©112.

As a first perspective, the polymerization and postfunctionalization of the prepolymers seem to work fine and good proton conductive polymers have been obtained using relatively mild conditions. A next worth-it postfunctionalization route could consist in developing the grafting *n*-alkylphosphonic side (through the use of an ad hoc functionalizing agent) onto the DFBP subunit, in order to provide fluorinated poly(phenylene sulfide)s with a higher content of PO(OH)₂ functional groups. This would interestingly pave the way to a comparison of the impact of SO₃H vs. PO(OH)₂ groups, when grafted onto the same polymer backbone, onto the performance of PEMs.

A second membrane and fuel cells-oriented perspective concerns additional work to perform onto the elaboration of PEMs, in particular with the evaluation of different solvents and (polymeric)additives. Sulfonated polymers obtained (figure III-49, III-2-e) have showed all the characteristics (conductivity, thermos and chemical stability) required to be the base of a good PEM starting from two relatively cheap monomers.

III. Outlook

It is hard to predict the future but it is quite clear that the transition to renewable energies is inevitable: it can be speed up or slow down, but there is no turning back. Hydrogen is one of the possible solutions to store energy and therefore water electrolysis development will probably accelerate in the years to come. PEM water electrolyzers have a higher rate of adoption than alkaline water electrolyzers due to their higher current density and lower gas permeability.⁸ Several PEMs have already been discussed and a high amount of time and money is being currently used to develop new PEMs that can improve the current ones. In the review by F. Kathib *et al.*⁹ the main points being worked on are further explained like reinforcing materials e.g. polymer fibbers for the production of the membrane to reduce the degradation of the membrane; the coating of the bipolar flow plate that could improve the embrittlement and corrosion of the membrane and the use of cheaper materials to make the production of hydrogen economically viable. Other interesting new methodologies can be the one done by C. Ru *et al.*¹⁰ which included introducing a MOF (Metal-organic-framework) with Ionic Liquid (IL) in a cross-linked sulfonated poly(arylene ether ketone). The inclusion of this IL

showed an improvement in conductivity and a reduction in the swelling ratio. Several authors have proposed the incorporation of hygroscopic inorganic materials like ZrO_2 , TiO_2 , $TiSiO_4$, and silica as fillers in the polymer matrix that result in high water retention enabling the membrane to maintain the proton conductivity over a broad range of temperatures.^{11,12} Another improvement when it comes to durability was proposed by Yoon *et al.*¹³ who proposed mussel-inspired polydopamine-treated composite membranes with self-supported CeO_x radical scavengers which increased the binding among PEM constituents. In Y. Wang¹⁴ review on PEM fuel cells all these issues are addressed and some solutions for humidification problems are proposed like the use of graphene oxide (GO) as nanoparticles that contain both hydrophilic and hydrophobic functional groups, carbon nanotube (CNT) being another promising filler creating one-dimensional water nanowires.

To conclude, there are a vast number of improvements being currently worked at in many different aspects of PEMs. The addition of small improvements in every part of the PEM production will give us in the future a PEM that can be produced from cheap and available materials that will have a better conductivity, durability and therefore will be economically viable for considering scaling up the PEMFC technology, helping very much mankind to accompany the energetic transition.

IV. References

- ¹ S. Sharma, *Membranes for low temperature fuel cells, Proton-conduction membranes: requirements, challenges and materials*, 2019, p. 13-38 <https://doi.org/10.1515/9783110647327>
- ² Y. Zou, M. Yang, G. Liu, and C. Xu, *Sulfonated poly (fluorenyl ether ketone nitrile) membranes used for high temperature PEM fuel cell*, 2020, *Heliyon*, vol. 6, no. 9, p. e04855 DOI:[10.1016/j.heliyon.2020.e04855](https://doi.org/10.1016/j.heliyon.2020.e04855)
- ³ C. Simari, C. Lo Vecchio, A. Enotiadis, M. Davoli, V. Baglio, and I. Nicotera, *Toward optimization of a robust low-cost sulfonated-polyethersulfone containing layered double hydroxide for PEM fuel cells*, 2019, *J. Appl. Polym. Sci.*, vol. 136, no. 34, pp. 1–10 DOI:[10.1002/APP.47884](https://doi.org/10.1002/APP.47884)
- ⁴ E. Quartarone, S. Angioni and P. Mustarelli, *Polymer and Composite Membranes for Proton Conducting, High-Temperature Fuel Cells: A Critical Review*, 2017, *Materials*, vol. 10, pp. 687 DOI:[10.3390/ma10070687](https://doi.org/10.3390/ma10070687)
- ⁵ P. Taylor, X. Li, and A. S. Hay, *Synthesis of High Molecular Weight Fluorinated Poly(phthalazinone ether)s by Self -Condensation of an AB-Type Monomer and by Condensation of AA Monomers with Decafluorobiphenyl*, 2007, *Journal of Macromolecular Science: Part A: Pure and Applied Chemistry*, no. 44, pp. 249-258 DOI: [10.1021/ma702039a](https://doi.org/10.1021/ma702039a)
- ⁶ C. Liu, X. Wang, J. Xu, C. Wang, H. Chen, W. Liu, Z. Chen, X. Du, S. Wang, Z. Wang, *PEMs with high proton conductivity and excellent methanol resistance based on sulfonated poly (aryl ether ketone sulfone) containing comb-shaped structures for DMFCs applications*, 2020, *Int. J. Hydrogen Energy*, vol. 45, no. 1, pp. 945–957 DOI: [10.1016/j.ijhydene.2019.10.166](https://doi.org/10.1016/j.ijhydene.2019.10.166)
- ⁷ J. D. Kim, A. Ohira, and H. Nakao, *Chemically crosslinked sulfonated polyphenylsulfone (CSPPSU) membranes for PEM fuel cells*, 2020, *Membranes (Basel)*, vol. 10, 31, no. 2 DOI: [10.3390/membranes10020031](https://doi.org/10.3390/membranes10020031)
- ⁸ Ito H, Maeda T, Nakano A, Kato A, Yoshida T. *Influence of pore structural properties of current collectors on the performance of proton exchange membrane electrolyzer*, 2013, *Electrochem Acta*, 100(30), pp.242–48. DOI: [10.1016/j.electacta.2012.05.068](https://doi.org/10.1016/j.electacta.2012.05.068)
- ⁹ F. N. Khatib, T. Wilberforce, O. Ijaodola, E. Ogungbemi, Z. El-Hassan, A. Durrant, J. Thompson, A.G. Olabi, *Material degradation of components in polymer electrolyte membrane (PEM)electrolytic cell and mitigation mechanisms: A review*, 2019, *Renew. Sustain. Energy Rev.*, vol. 111, no. May, pp. 1–14 DOI:[10.1016/J.RSER.2019.05.007](https://doi.org/10.1016/J.RSER.2019.05.007)
- ¹⁰ C. Ru, Y. Gu, H. Na, H. Li, and C. Zhao, *Preparation of a Cross-Linked Sulfonated Poly(arylene ether ketone) Proton Exchange Membrane with Enhanced Proton Conductivity and Methanol Resistance by Introducing an Ionic Liquid-Impregnated Metal Organic Framework*, 2019, *ACS Appl. Mater. Interfaces*, vol. 11, no. 35, pp. 31899–31908 DOI:[10.1021/acsami.9b09183](https://doi.org/10.1021/acsami.9b09183)

- ¹¹ N.H. Jalani, K. Dunn, R. Datta, *Synthesis and characterization of Nafion –MO₂ (M=Zr, Si, Ti) nanocomposite membranes for higher temperature PEM fuel cells*, 2005, *Electrochim. Acta* 51 (3), pp.553–560. DOI: [10.1016/j.electacta.2005.05.016](https://doi.org/10.1016/j.electacta.2005.05.016)
- ¹² E. Quartarone, S. Angioni, P. Mustarelli, *Polymer and Composite Membranes for Proton-Conducting, High-Temperature Fuel Cells: A critical review*, 2017, *Materials* 10 (7), p.687 DOI:[10.3390/ma10070687](https://doi.org/10.3390/ma10070687)
- ¹³ K.R. Yoon, K.A. Lee, S. Jo, S.H. Yook, K. Y. Lee, I. Kim, J.Y. Kim, *Mussel-Inspired Polydopamine-treated reinforced Composite Membranes with self-supported CeO_x Radical Scavengers for highly stable PEM Fuel Cells*, 2019, *Adv. Funct. Mater.* 29 (3), 1806929. DOI:[10.1002/adfm.201806929](https://doi.org/10.1002/adfm.201806929)
- ¹⁴ Y. Wang, D. F. Ruiz Diaz, K. S. Chen, Z. Wang, and X. C. Adroher, *Materials, technological status, and fundamentals of PEM fuel cells – A review*, 2020, *Mater. Today*, vol. 32, no. Jan.Feb., pp. 178–203 DOI:[10.1016/j.mattod.2019.06.005](https://doi.org/10.1016/j.mattod.2019.06.005)